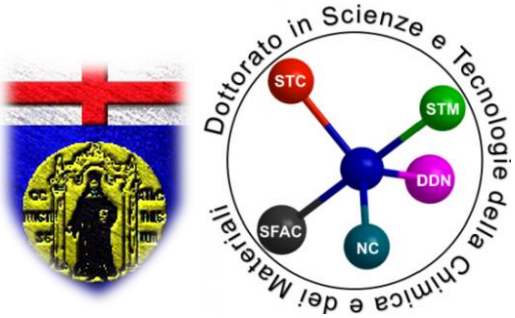

Doctoral thesis

Presented to Department of Pharmacy

University of Genoa

Synthesis of Amphiphilic and Hydrophilic Non-PAMAM Dendrimers Nanoparticles for Biomedical Applications and Realization of Water-soluble DDSs of two Triterpenoid Acids.

By

Taptue Gaby Brice

Supervisor: Prof. Alfei Silvana

TABLE OF CONTENTS

BACKGROUND

Carriers-mediated Drug Delivery emerged as a powerful strategy for the treatment of various pathologies. Many newly developed drugs are rejected by the pharmaceutical industry and will never benefit a patient because of poor bioavailability due to low water solubility and/or cell membrane permeability. Therefore, the development of new delivery technologies could help to overcome this challenge via the increase of specificity due to targeting of drugs to a particular tissue, cell or intracellular compartment, the control over release kinetics, the protection of the active agent or a combination of the above. For years, nanoparticles were proposed as drug carriers, and now are of eminent interest in biomedical applications mainly due to their stability and high drug-loading capabilities as well as permitting an easy control over their physicochemical properties. Among the various nanoparticles successfully tested as delivery tools systems dendrimers represent the most prospective drug delivery systems thanks to their inimitable characteristics including the exact molecular weight, the tree-like structure, poly-fuctionality, the spherical shapes as well as having a low index of polydispersion.

The first part of this thesis focuses on the design, preparation and characterization of not cytotoxic amphiphilic polyester-based dendrimers obtained from the 2,2-bis(hydroxymethyl)propanoic acid and functionalized with positive charged amino acids as nanostructures for Drug Delivery applications. While the second part discusses the encapsulation of Ursolic and Oleanolic acids in hydrophilic arginine dendrimers.These acids are two triterpenoids acids from plants kingdom endowed with several pharmacological activities but unfortunately not exploitable because of restrictions such as very poor solubility and consequently low bioavailability.

LA STORIA

La consegna di farmaci mediata dai vettori è emersa come una potente strategia per il trattamento di varie patologie. Molti farmaci di nuova concezione vengono rifiutati dall'industria farmaceutica e/o non potranno mai beneficiare un paziente a causa della scarsa biodisponibilità dovuta alla bassa solubilità in acqua e/o alla bassa capacità di attraversare la membrana cellulare. Pertanto, lo sviluppo di nuove tecnologie per veicolare i farmaci e preparare formulazioni idrosolubili, potrebbe aiutare a superare questa sfida. Sono neccessari l'aumento della specificità per un particolare compartimento tissutale, cellulare o intracellulare, del controllo sulla cinetica di rilascio, della protezione dell'agente attivo o una combinazione di soprattutto ciò. Per anni, le nanoparticelle sono state proposte come trasportatori di farmaci, e ora hanno un interesse eminente nelle applicazioni biomediche principalmente grazie alla loro stabilità e alle loro elevate capacità di carico di farmaci, oltre a consentire un facile controllo sulle loro proprietà fisico-chimiche. Tra le varie nanoparticelle testate con successo come sistemi di strumenti di somministrazione i dendrimeri rappresentano i sistemi di somministrazione di farmaci più prospettici grazie alle loro inimitabili caratteristiche tra cui l'esatto peso molecolare, la struttura ad albero, la polifunzionalità, le forme sferiche oltre ad avere un basso indice di polidispersione.

La prima parte di questa tesi si concentra sulla progettazione, preparazione e caratterizzazione di dendrimeri anfifilici di tipo poliestereo, non citotossici, ottenuti a partire dall'acido 2,2-bis (idrossimetil)propanoico, funzionalizzati con amminoacidi cationici, da utilizzare come nanostrutture per applicazioni in drug delivery. Mentre la seconda parte discute l'incapsulamento degli acidi Ursolico e Oleanolico in dendrimeri idrofilici contenenti arginina. Questi acidi sono due triterpenoidi appartenenti al regno vegetale, dotati di diverse attività farmacologiche, sfortunatamente non sfruttabili a causa di restrizioni quali la scarsa solubilità e conseguentemente la bassa biodisponibilità.

CHAPTER 1

GENERAL INTRODUCTION

1.1. Nanotechnology in biomedical field

According to the definition from NNI (*National Nanotechnology Initiative*), Nanotechnology is a research and technology development at the atomic, molecular, or macromolecular scale leading to the controlled creation and use of structures, devices, systems called nanoparticles characterized of sizes ranging from 1 to 100 nm (Figure 1).

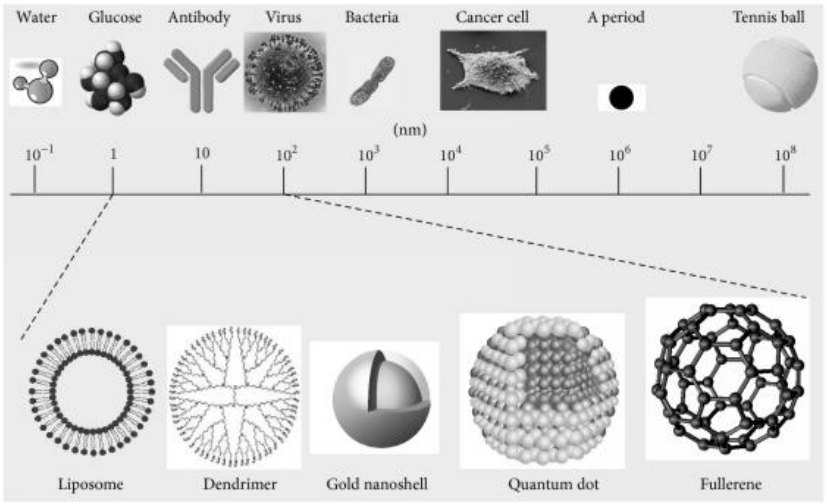

Figure 1. Examples of nanotechnology platformed used in drug development.[1]

Application of nanotechnology to medicine led to the emergence of a new area called "*nano*medicine". Nanomedecine refers to the application of nanotechnologies to the biomedical field for controlled drug delivery as well as for diagnostic purposes. In the last century, Nanomedecine has witnessed substantial growth and has completely revolutionated the delivery of biologically active compounds. Thus, many reviews aimed to analyze and to discuss the impact of nanotechnology in pharmacology to improve treatments of various diseases considered as the major health threats (cancer, infections, metabolic diseases, etc.) have been published.[2, 3, 4] Traditional therapeutics, usually present a number of unique problems including poor specificity, high toxicity for healthy tissues, the occurrence of dramatic side effects, and induction of drug resistance.

At present, several nanosized carriers, made of various materials such as lipids, polymers, metals, inorganic materials have been proposed for therapeutic and diagnostic agents as well as advancement of drug delivery. They have provided the scientific community with a platform that has the capacity and potential to evolve with the expanding knowledge and understanding of diseases.

In drug delivery technologies, nanocarriers have to be biocompatible i.e. able to integrate with a biological system without eliciting immune response or any negative effects and non toxic i.e. harmless to a given biological system. They are designed (i) to protect a drug from *in vivo* degradation; (ii) to improve solubility and stability, controlled release and site-specific delivery of therapeutic agents; (iii) to improve pharmacokinetics and biodistribution profile; (iv) to decrease toxicities. Furthermore, the surface modification of pharmaceutical can be used to control their biological fate and to use them simultaneously as therapeutic or diagnostic platform (theranostics). The most important results of such modification include an increased stability and half-life of nanocarriers in the circulation, passive or active targeting into the required pathological zone, and responsiveness to local physiological stimuli such as pathology-associated changes in local pH and/or temperature, and ability to serve as imaging/contrast agents for various imaging modalities.

Delivering therapeutic compound to the target site is a major problem in treatment of many diseases especially in cancer therapy. Each year, tens of millions of people are diagnosed with cancer around the world, and more than half of the patients eventually die from it. [5] Cancer is known to develop via a multistep carcinogenesis process entailing numerous cellular physiological systems, such as cell signaling and apoptosis, making it a highly incomprehensible and complex disease.[6, 7] The fact that several significant achievements towards the treatment of this disease have failed to profoundly impact patient survival. The last century saw the evolution of chemotherapy as a feasable, complementary therapeutic modality for the treatment of cancer. An enhanced understanding of the underlying mechanisms of tumor genesis busted the discovery and development of highly specific agents capable of exerting their effects on individual proteins or pathways either overexpressed or aberrant within tumors. Despite many advances in conventional treatment options such as chemotherapy, surgery and radiation, cancer therapy is still far from optimal because it is plagued by some drawbacks. Frequent challenges encountered by current cancer therapies include non specific systemic distribution of antitumor agents, inadequate drug concentrations reaching the tumor site, limited ability to monitor therapeutic responses and development of multiple drug resistance (MDR). These sobering facts indicate that to make further progress, it is necessary to put an emphasis on other existing but still under appreciated therapeutic

approaches. An increased interest is being focused on nanotechnological approaches in cancer treatment based on the concept that pharmacokinetics of an anticancer drug can be usefully altered in the body to promote drug accumulation predominantly in pathological sites.[8, 9] Such a strategy is aimed to improve the treatment ability to target and to kill cells of diseased tissues/organs while affecting as few healthy cells as possible. Several reviews, indeed, have focused on the potential of nanotechnology in cancer and discussed how different nanoparticulate drug delivery systems perform in this field.[10, 11, 12]

The therapeutic effects of many anticancer drugs could be significantly improved if delivery of the drug occurs specifically to tumors (cancer cells) or preferably inside specific organelles inside cells and reduction of drug toxic side effects is achieved. In so doing, a multifunctional construct based on novel nanomaterials can be delivered directly to the tumor site and eradicate cancer cells selectively. An appropriate design allows nanoconstruct to improve drug efficacy (activity at lower doses) as compared with the free-drug treatment, which in turn gives a wider therapeutic window and lower side effects. Furthermore, nanoparticle carriers are also capable of addressing several drug delivery problems, which could not be effectively solved in the past and include overcoming Multi drug resistance (MDR) phenomenon and penetrating cellular barriers that may limit device accessibility to intended targets, such as the blood–brain barrier, among others. There has been intense interest in identifying nanoparticle characteristics that are best suited for oncology applications. Pharmacokinetics of the nanoparticles (NPs) is crucial and depends on several physiochemical characteristics of the carrier such as size, surface charge, shape, nature and density of coating, composition, stability, steric stabilization, deformability, dose and route of administration.[13, 14] Regarding their composition and structure, nanocarrier platforms for cancer can be categorized as organic-based, inorganic-based or a hybrid combination of the aforementioned. Organic nanoplatforms include polymeric nanocarriers, lipid-based nanocarriers (e.g., liposomes and nanoemulsions), dendrimers, and carbon-based nanocarriers (e.g., fullerenes and carbon nanotubes). Inorganic nanoplatforms include metallic nanostructures, silica NPs, and QDs.

1.2. Nanoparticles as drug delivery systems

Over the past few decades, several nanocarriers have been developed as effective drug delivery devices. The drug of interest is dissolved, entrapped, adsorbed, covalently attached or encapsulated in the nanocarrier ready for the administration. Once in systemic circulation, particle-protein interaction is the first phenomenon taking place before distribution into various organs.[15, 16] Absorption from the blood capillaries allows the lymphatic system to

further distribute and eliminate the particles. This system has three main functions, two of which pertain to drug delivery. The first, fluid recovery, involves the filtering of fluids by the lymphatic system from blood capillaries. The second encompasses immunity, as the system recovers excess fluid; it also picks up foreign cells and chemicals from the tissues. As the fluids are filtered back into the blood, the lymph nodes detect any foreign matter passing through.[17] If something is recognized as foreign, macrophage will engulf and clear it from the body. This tends to be the struggle with nanoparticle based drug delivery; so in order to be effectively delivered towards the target tissues, carriers should be able to remain in the blood circulation for adequate duration of time.

The shape and size of nanoparticle affects their distribution, toxicity and targeting ability. Most importantly, nanoparticles can cross the blood-brain barrier (BBB) providing sustained delivery of medication for diseases that were previously difficult to treat.[18] It is reported that as particles size get smaller, their surface area to volume ratio gets larger. This would imply that more of the drug is closer to the surface of the particle compared to a larger molecule. Being at or near the surface would lead to faster drug release.[19] The manipulation of surface characteristics is an opportunity to generate the ideal system.[20] In order to create an optimum nanoparticle drug delivery system, the incorporation of appropriate targeting ligands, surface curvature and reactivity is important to address the prevention of aggregation, stability, and receptor binding and subsequent pharmacological effects of the drug.[21] Moreover, the drug needs to be released from the nanoparticle matrix. The release of drug from the nanoparticle-based formulation depends on many factors including, pH, temperature, drug solubility, desorption of the surface-bound or adsorbed drug, drug diffusion through the nanoparticle matrix, nanoparticle matrix swelling and erosion, and the combination of erosion and diffusion processes.[22, 23, 24] Depending on the type of nanoparticle being used, the release of drug will differ.

1.2.1. Solid lipid nanoparticles (SLNs)

Developed in early 1990s, SLNs or solid lipid nanospheres are nanosized colloidal drug carriers in the size range of 50-1000 nm (Figure 2).

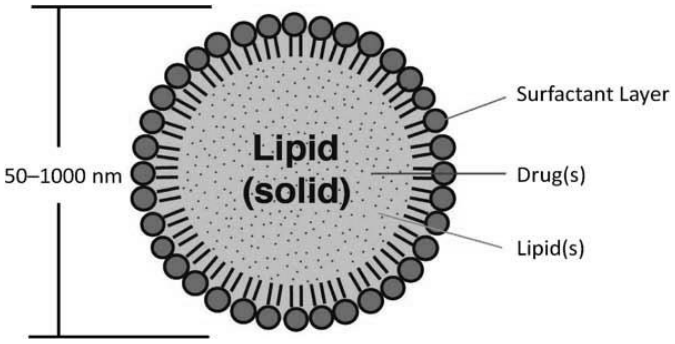

Figure 2. Structure of solid lipid nanoparticles[25]

They are particles made of lipid that are solid at room temperature including mono-, di- and triacylglycerols, free fatty acids, free fatty alcohols, waxes, steroids and combination of these materials[26]. SLNs are prepared by dispersing melted solid lipids in water, whereas emulsifiers are used to stabilize the dispersion. The two most commonly used methods for preparing SLNs are high pressure homogenization and microemulsification[27]. SLNs provide a highly lipophilic lipid matrix for drugs to be dispersed or dissolved. The main characteristics SLNs include a good tolerability, controlled drug release, lack of biotoxicity, high drug payload, an improved bioavailability of poorly water-soluble drugs, better stability and easy as well as economical large-scale production[28]. Additionally, some disadvantages have been observed, such as low loading capacity limited by the solubility of drug in the lipid and the structure and polymorphic state of the lipid matrix, physical and chemical properties of lipid or mixture of lipids, crystalline properties of lipids in biological temperature, and a relatively high water content of the dispersions[29].

Since their development, SLNs have been extensively used as a carrier to overcome or at least minimize the drawbacks of conventional chemotherapy. For example, SLNs systems have been utilized for the delivery of anticancer drugs such as docetaxel[30], doxorubicin[31], paclitaxel[32], methotrexate[33] and 5-fluorouracil[34] (5-FU).

Various models have been proposed to incorporate drugs into SLNs. Depending upon the composition of SLNs and production conditions; drug can be dispersed homogeneously in lipid matrix of SLNs, incorporated into the shell surrounding the lipid core or incorporated into the core surrounded by a lipid shell. In order to expand the applicability of lipid based carriers, NLC (nanostructured lipid carriers) and LDC (lipid drug conjugates) have been developed.[35, 36]

1.2.2. Liposomes

Liposomes were the first to be investigated as drug carriers. They are nanosized spherical vesicles ranging from 20 nm to micrometer with an aqueous core and a vesicle shell (Figure 3).

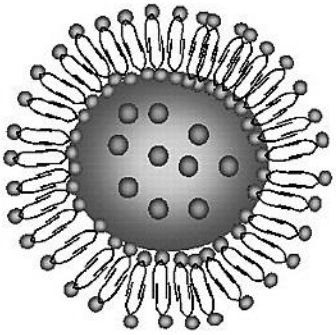

Figure 3. Structure of liposomes[37]

On the basis of their size and number of bilayers, liposomes can be classified into one of two categories: multilamellar vesicles (MLV) and unilamellar vesicles. Unilamellar vesicles can also be classified into two categories: large unilamellar vesicles (LUV) and small unilamellar vesicles (SUV) (Figure 4).

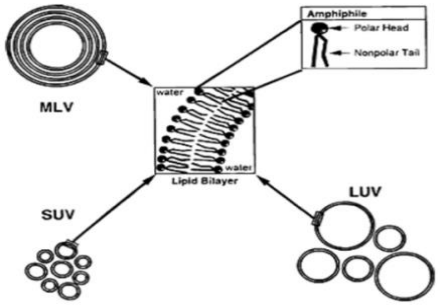

Figure 4. Types of liposomes[38]

In unilamellar liposomes, the vesicle has a single phospholipid bilayer sphere enclosing the aqueous solution. In multilamellar liposomes, vesicles have an onion structure.

Liposomes have many advantages: firstly they are biocompatible, biodegradable, non-toxic and non immunogenic. Secondly they are suitable for the delivery of hydrophobic, amphiphatic and hydrophilic drugs improving their stability. Additionally, liposomes reduce the toxicity of the encapsulated agents and help reduce the exposure of sensitive tissues to toxic drugs. They vary with respect to composition, size, surface charge and method of

preparation. They can be covered with polymers such as polyethylene glycol (PEG; PEGylated or stealth liposomes) to exhibit prolonged half-life in blood circulation[39].

Liposomes are the most clinically approved nanocarriers for chemotherapeutics. Doxorubicin (Doxil), Daunorubicin (DaunoXome), Cytarabine (DepoCyt), Mifamurtide (Mepact) Vincristine (Marqibo), and Irinotecan (Onivyde) are few marketed anticancer liposomal products[40]. Other liposomes-based products have been used for fungal infections, pain management, viral infections and for photodynamic therapy.

1.2.3. Polymeric nanoparticles (PNPs)

PNPs are solid, nanosized (10-1000 nm) colloidal particles made up of biodegradable polymers[41, 42] (Figure 5). In the last few decades, polymers have gained much attention in the area of drug delivery since they offer a number of attractive features in nanomedecine. They can either be classified as nanospheres (matrix type) or nanocapsules (reservoir type).

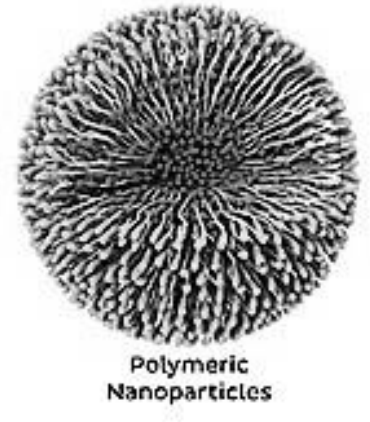

Figure 5. Structure of polymeric nanoparticles[43]

Depending on the methods used for preparation of polymeric carriers, drugs could be entrapped within the polymer or attached to the carrier matrix leading to the formation of nano/microcapsules and nano/microspheres, respectively[44]. Polymers used as drug conjugates can be divided into two groups of natural and synthetic polymers. Several natural polymers such as chitosan[45], albumin[46], gelatin[47], and heparin[48] have been extensively explored as matrix-based nanoparticles for developing delivery system for clinical therapeutics owing to their inherent properties, including biocompatibility, degradability and ease of surface modifications. Albumin and gelatin are the two most widely studied systems. Albumin is a small versatile globular protein with high aqueous solubility and stability, multiple binding sites and reactive surface functional groups, which make it an attractive nanocarrier for drug delivery. Additionally, albumin due to its higher half life in blood circulation had favorable

pharmacokinetics and was an interesting drug carrier for passive targeting[49]. Abraxane, an albumin-bound nanoparticulate formulation of paclitaxel is a marketed product in the fight against cancer[50]. It is highly soluble in water and accumulates in tumours using mechanisms that include the enhanced permeation and retention (EPR) effect, as well as the albumin transport pathway.

Polyethylenimines (**PEIs**) are one of the most promising examples of synthetic polymers and are considered the gold standard for nanotechnology applications. Linear, branched PEI (hetero and homofunctional) can be prepared according to Schemes 1B [51] and 1A[52] respectively.

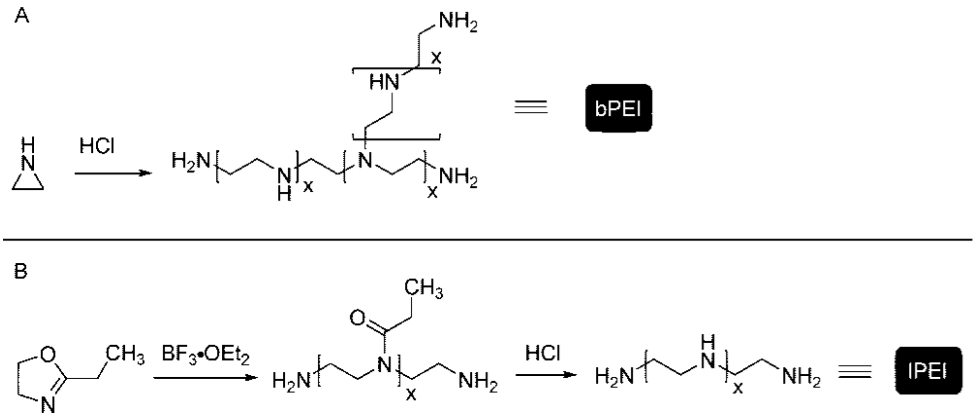

Scheme 1. Synthesis of Branched PEI (A) and Linear PEI (B)

The molecular weight (5 and 25 KDa) [53], the type of structure, linear or branched, the number and types of nitrogen determine the ability to condense drugs or DNA. PEIs are an excellent proton sponges[54], as they contain different types of protonable nitrogen atoms and therefore enjoy a high buffer capacity[55]. This prerogative allows PEI-drug polyplexes to cause lysis of the endosome and to avoid lysosomal trafficking which would lead to their degradation[55-57].

The transfection capacity of PEIs increases by increasing molecular weight[58, 59], but at the same time there is an increased cytotoxicity, caused by the aggregation of the polymeric complexes leading to the initiation of necrotic processes.

Typically, it was seen that the branched PEI (*b*PEI) better compact DNA and is the more stable the higher the content in primary amino groups, resulting more efficient as carriers for gene transfer[60-62].

In order to solve the problem of PEI's high toxicity and poor biodegradability, PEIs having imino bonds in their skeleton, sensitive to the endosomal acid environment and then hydrolysable to low molecular weight[63, 64] oligomers have been synthesized.

To combine the advantages offered by PEI and cationic lipids, lipopolymers have been synthesized, like for example lipopolymers based on PEI and cholesterol (*PEI-Chol*), resulting less toxic and potentially usable as vectors[63, 65], while the PEGylation reduces both the tendency to self aggregation of free PEIs and their interactions with plasma proteins and erythrocytes.

The Hydrophilic-Lipophilic Balance (Hydrophilic-Lipophilic Balance HLB), unfavorable in unmodified PEI, was improved by introducing amino acids such as alanine and valine and alkyl chains by alkylation of primary amine groups of PEIs with dodecyl and hexadecyl halides obtaining positive results in *test* only for alanine derivatives.

Others commonly used synthetic polymers include polylactic acid (PLA), polyglycolic acid (PGA), PLGA, PEG, polycaprolactone (PCL), N-(2-hydroxypropyl) methacrylamide copolymer, polyaspartic acid (PAA) and polyglutamic acid. These polymers offer potential in controlling the drug release profile and minimizing toxicity owing to the biodegradability and biocompatibility of the matrix. They have been used for various anticancer drug combinations.

1.2.4. Polymeric Micelles (PMs)

Polymeric micelles are spherical and nanosized particles (10-100 nm) made of amphiphilic di- or tri-block copolymers having hydrophobic and hydrophilic blocks in aqueous medium[66]. The hydrophobic core serves as a reservoir and allows the entrapment of hydrophobic drugs, whereas the hydrophilic shell serves to stabilize the core, ensures the PMs' solubility in the aqueous medium and controls in vivo pharmacokinetics.[67] One of the most important parameters of micelle formation is the critical micelle concentration (CMC), the concentration beyond which the polymeric chains associate to minimize the free energy of the system. CMC is directly related to the stability of the self-assembled structures, and a high CMC will imply disassembly upon dilution in biological fluids. PMs allow hydrophobic anticancer drugs to be entrapped into their cores, thus significantly increasing their water solubility.[68]A few commonly used block copolymers for PMs are *poloxamers, PEGylated polylactic acid (PEG-PLA), PEGylated polyaspartic acid (PEG-PAA), PEGylated polyglutamic acid, PEGylated polycaprolactone (PEG-PCL) and PEGylated poly(lactic-co-glycoli acid) (PEG-PLGA).* Many chemotherapeutic agents for cancer, including Methotrexate[69], Cisplatin[70], Paclitaxel[71], Docetaxel[72] and Doxorubicin[73], have successfully been formulated in PMs.

1.2.5. Dendrimers

Dendrimers are highly branched synthetic polymers; monodisperse with a spherical globular structure, a well defined and very regular architecture characterized by high symmetry and nanometric dimensions. These structural characteristics make them molecules of great interest for applications in nanomedicine. They are globular macromolecules characterized by three domains: a central core, the ramifications that branch off from it and which generate internal cavities and the functional groups at the surface that determine its chemical-physical properties. Their three main properties are (i) nanoscale container properties (i.e. encapsulation of a drug), (ii) nano-scaffolding properties (i.e. surface adsorption or attachment of a drug), and (iii) biocompatibility.[74, 75, 76, 77, 78, 79, 80] The degree of complexity of the dendrimal structure is directly proportional to the number of generations. Figure 6 schematically shows the structures of a second generation (a) and fifth generation dendrimer (b) highlighting the domains.

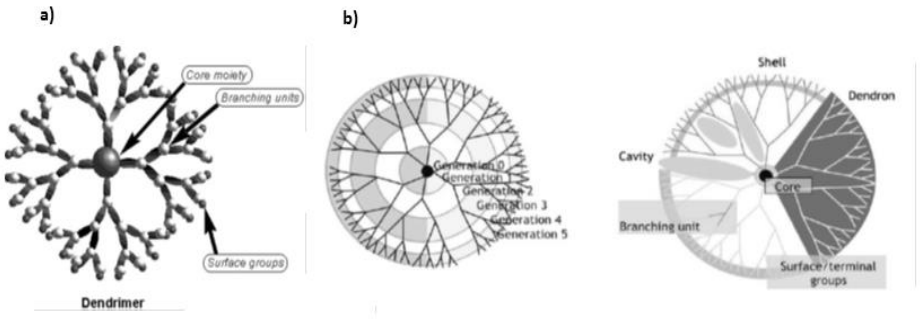

Figure 6. Second generation (a) and fifth generation (b) dendrimer structure

If the dendrimers are equipped with protonable amino groups or suitably functionalized with basic groups able to protect themselves at physiological pH values, they become polycationic materials able to conjugate to the phosphate groups of the genetic material or negative charges of drugs resulting attractive and promising nanocarriers[81]; moreover, targeting ligands can be attached to transform the surface functionalities in order to obtain specific objectives, which usually implicate precise contact at cell walls and biologically active sites. The ability to tailor dendrimer properties to therapeutic needs makes them ideal carriers for small molecule drugs and biomolecules.

Polyamidoamine (PAMAM) dendrimers are the most widely studied as scaffold for biomedical applications principally as carriers for anticancer therapy. PAMAM are commercially available and widely used dendrimers as carriers of genetic material or drugs.

Their synthesis dates back to Tomalia in the'80s and is an addition (similar to Michael addition) of a nucleophile core such as ammonia or ethylenediamine to methyl methacrylate, followed by amidation of the resulting ester with a suitable functional amine and so on that allows to obtain structurally diverse PAMAMs at low production cost (Scheme 2). [82]

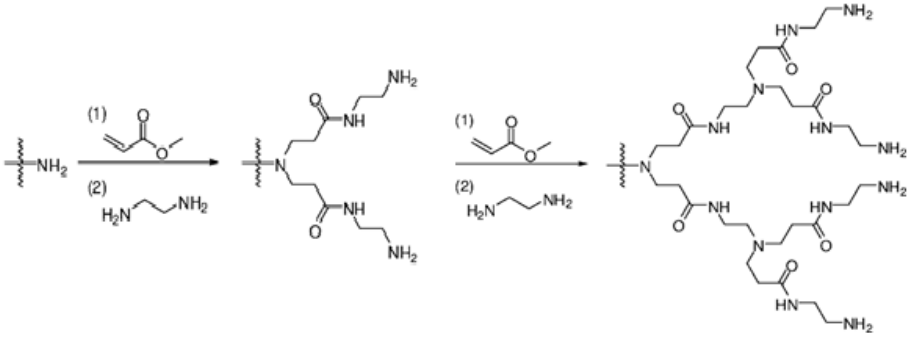

Scheme 2. Synthesis of a PAMAM dendrimer from a nitrogen core, methyl methacrylate and ethylenediamine

The PAMAMs of high generations (G5-G10) have shown to possess a high capacity of transfecting different cell lines [83-85] according to the charge density of drug-dendrimer complex linked to the N/P ratio (r). [86]

However, the main problem of PAMAM remains their high cytotoxicity, which was sought to remedy by chemical transformations. PAMAMs containing quaternary amino groups within the structure and hydroxyl groups at the periphery[87] were then synthesized, reducing not only the cytotoxicity but also the transfection efficiency. To improve transfection of fifth generation PAMAMs, they were partially functionalized with PEG chains. The dendrimers obtained have shown poor cytotoxicity and the ability of transfecting in an excellent way, probably because of the presence of PEG on one side makes the Drug-dendrimer interaction less strong while on the other it acts as a screen protecting the *dendriplex* from the endonuclease attack. PAMAM PEGylate and N-acetylated were found to be optimal carriers for the targeted delivery of anticancer drugs such as Doxorubicin (DOX) embedded in the dendrimer cavities. A three-block copolymer was also synthesized consisting of a PEG nucleus with two PAMAM substructures on both ends having a low cytotoxicity and a high transfection efficiency compared to PEI.[88]

PAMAM insertion of cyclic oligosaccharides containing a hydrophobic nucleus and a hydrophilic outer portion, such as α- and β-cyclodextrins generally used to increase the

stability, solubility and bioavailability of drugs, (Figure 7) promotes the outbreak endosomal and transfective capacity but lead to an increase in hemolytic processes.

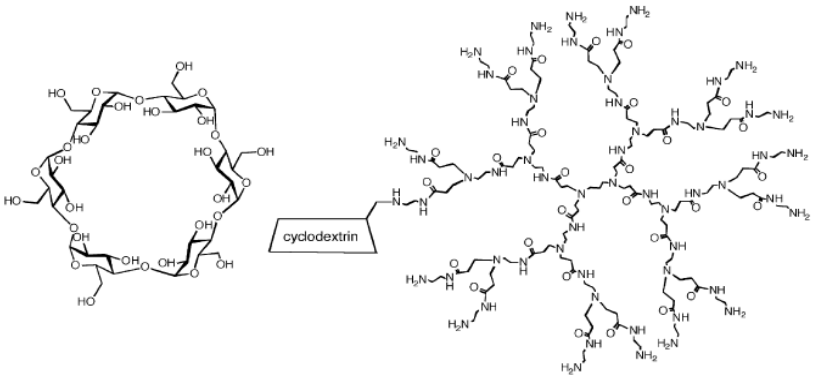

Figure 7. Functionalization of PAMAM with cyclodextrins.

PAMAM degraded by heat[89] (trade name of *Superfect*), have shown a greater efficiency of transfection probably because they are characterized by more flexible structures but still able to form compacted complexes with drugs that after swelling are able to release it from the *dendriplex* and nowadays they represent the main standard for the transfection efficiency studies of other types of dendriplesses. The introduction of *L*-arginine[90-91] residues led to an increase in cellular uptake and the location of the complex in the nucleus. This has further highlighted the importance of the expansion of the buffer capacity of the carriers conferred by functionalizing amino acids, in fact both the arginine residues and those containing lysine have pKa values of the basic function in the side chain (12.5 and 10.1 respectively) on average higher than those of the amine residues belonging to the amidoamino surface of the PAMAM (pKa = 8-10) not functionalized.

The introduction on PAMAM of phenylalanine[92] or the incorporation of lipid chains on the periphery of PAMAM dendrons, have provided promising results making it easier to be internalized[93] while PAMAM carrying leucine have proved to be much less effective vectors.

The structure of a dendrimer, its diameter and its conformation and ultimately its effectiveness as a carrier of genetic material also depend on the structure of the *core*[94].

PAMAM were synthesized with different *cores*, such as trimesyl core (Figure 8a), pentaerythritol (Figure 8b) and inositol (Figure 8c), characterized by similar chemical compositions, but different architecture.

In case of cores based on inositol and pentaerythritol, the minimum generation to obtain an effective transfection was the fifth, while in case of trimesyl the sixth. Studies on PAMAM with pentaerythitol core have shown greater efficiency and less cytotoxicity compared to the classic fifth and seventh generation PAMAM[95, 96].

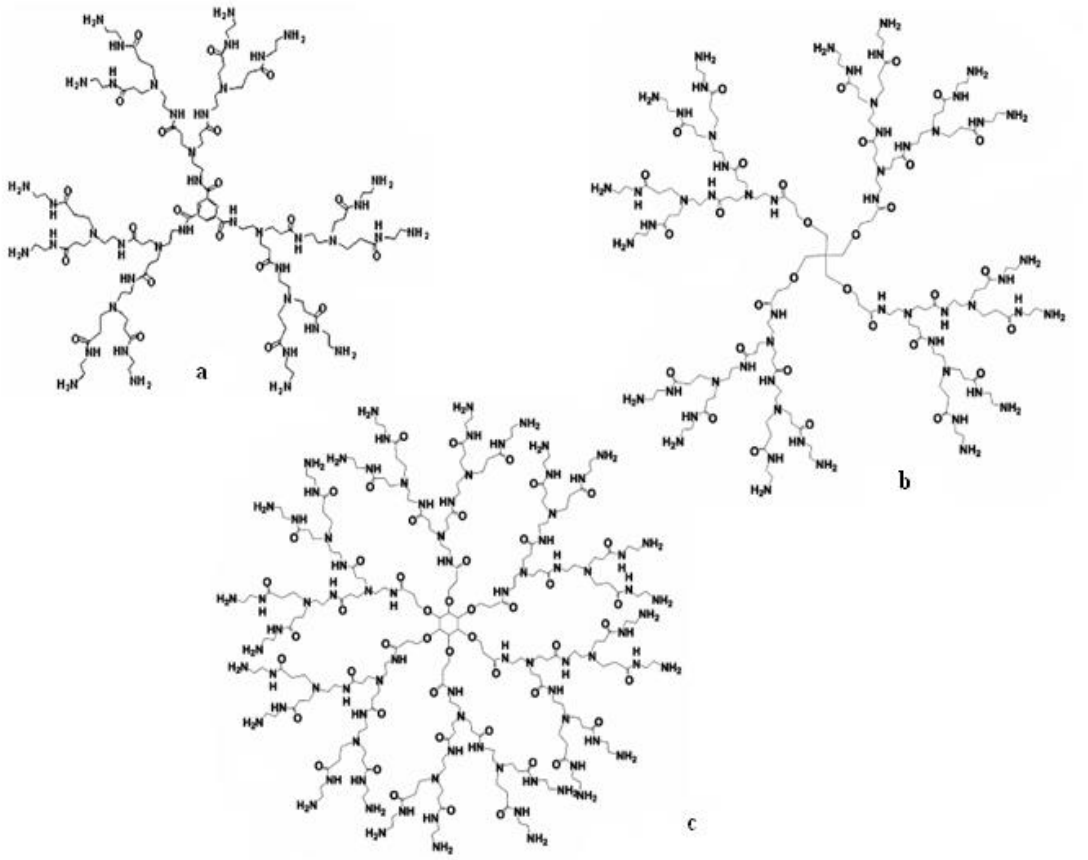

Figure 8. Example of dendrimers with a trimesyl core (a), pentaerythritol (b) and inositol (c)

Then there are several examples of PAMAM appropriately modified and functionalized on the outskirts used both as targeted prodrugs and as selective epigenetic therapeutic in anticancer therapy. PAMAMs having an ethylenediamine core and carboxyl groups in the periphery (G4.5-COOH) were conjugated with antigen molecules recognized by tumor cells such as the tripeptide Arginine-Glycine-Aspartate (RDG) or monoclonal antibodies (IL-6)[97] and then physically charged with DOX with the aim of obtaining selective prodrugs for the treatment of cervical cancer[98]. The conjugated IL-6 system compared to the conjugated RDG system has shown higher transfective capacity, more efficiency in drug delivery and greater toxicity to diseased cells (*HeLa cells*).

PAMAM of fifth generation (G5) covalently functionalized with residues of Folic Acid (FA) and Methotrexate (MTX) [99, 100] have been shown to have marked selectivity for skin tumor cells equipped with folate receptors (FR) with increased tumoricide activity compared to to that of the MTX alone. Subsequently, a simpler promising prodrug for the selective

treatment of the FR-shaped tumors was obtained with PAMAM of low generational grade (G3) endowed with peripheral hydroxyls following reaction with *D-glucoeptono-1,4-lactone* and functionalized with MTX also without FA residues[101]. The preparation of a prodrug that exploits the antitumor efficacy of a natural molecule such as Ursolic Acid (UA) was described in 2015 by Yu Gao et al.[102] The functionalization of third and fifth generation PAMAM (G3, 5) equipped with peripheral hydroxyls following reaction with *Glycidol*, FA and UA through a labile ester bond in an acidic environment has allowed to obtain selective prodrugs for the treatment of tumor cells expressing the folate receptors increasing the antitumor activity of the UA alone limited by its low solubility in water, poor bioavailability and nonspecific distribution. In 2015, instead, Hong Zong et al.[103] described the preparation of fifth generation *PAMAM* (G5) containing or not FA residues, functionalized with a *histone Deacetylase Inhibitor* (HDACi) capable of altering the epigenetic state of tumor cells by killing them. The conjugates obtained through ester binding made HDACi inactive until its release from the dendrimer with the result of reducing the numerous and harmful off-target effects associated with the use of HDACi alone, besides they did not show resistance to the drug in a different way than HDACi alone.

Polypropylenimmine (PPI) is another class of explored dendrimers used for drug delivery. Vögtle et al.[104] by a repeated sequence of additions of Michael of a primary amine to acrylonitrile followed by reduction with sodium boron hydride and cobalt were the first to prepare PPI with low yields but the use of Co-Raney as active reducing agent under more subsidiaries enabled the large-scale synthesis of PPIs and their commercialization (Scheme 3).

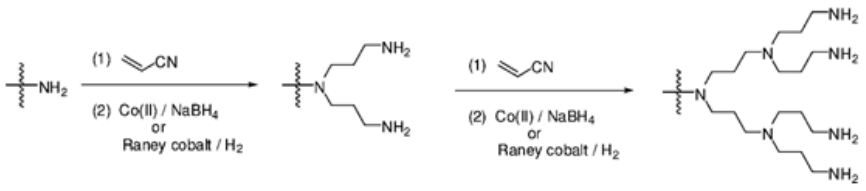

Scheme 3. PPI synthesis

Thanks to a large number of basic amino functions in the periphery (pKa 9-11) and a more acidic internal structure (pKa 5-8), consisting of tertiary amine groups that behave like " proton sponges " within the endosome, PPI of high generations lead to water-soluble cationic dendriplesses, and are therefore suitable for biomedical applications. However there are also PPI-DNA/Drug complexes of low generations that have shown less toxicity[105] and can also be used in nanotechnology.

Dendrimers based on polylysine (PLD) units represent another class of agents presently being explored as carriers for antiangiogenic therapy. They were synthesized in order to combine the advantages of dendrimeric structures with those of polypeptide vectors (Figure 9).

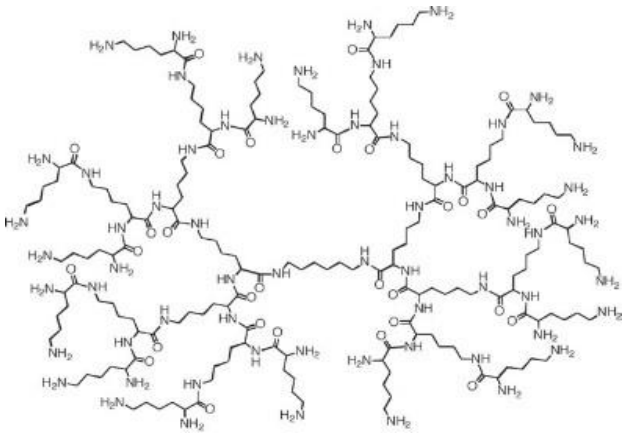

Figure 9. Fourth generation polylisinic dendrimer

The PLD, which are prepared using a divergent growth approach, starting from an asymmetric bidirectional core that allows to obtain a first generation PLD able to undergo additional coupling steps to give higher generation structures[106], are born with the aim of reducing the high toxicity of the PLL linear. To improve the transfective efficiency, the *L*-lysine terminal residues of the PLD were replaced with *L*-arginine or *L*-histidine[107]. Arginine derivatives, different from those histidine, ineffective, showed a significant ability to bind DNA and a transfection capacity of 3 to 12 times greater than that of unmodified PLDs. A successful example of the product obtained from the rational design of supramolecular nanovescicles capable of carrying out the controlled transport and release of both genetic and small hydrophilic drugs is shown in Figure 10.[108] Tris (2-aminoethyl) amine residues attached to hyperamified polyglycerol and terminating with β-cyclodextrine (CD-HPG-TAEA) and linear adamanthane bonded to a hydrocarbon chain of 18 carbon atoms (C18-AD) gave rise to an amphiphilic supramolecular conjugate capable of assembling into nanovescicles. These, rich in amino groups, were able to trap in their DOX • HCl cavity and simultaneously to bind the negativity of plasmid DNA through the positive charges, transport them and then release them within the cell with high efficacy. The presence of the drug also resulted in an improvement in transfection efficiency and in the internalization of the genetic material in the nucleus. This multitasking carrier also demonstrated serum-tolerant transgenic capacity and

lower toxicity compared to PEI, which is the standard of comparison for genetic material carriers.

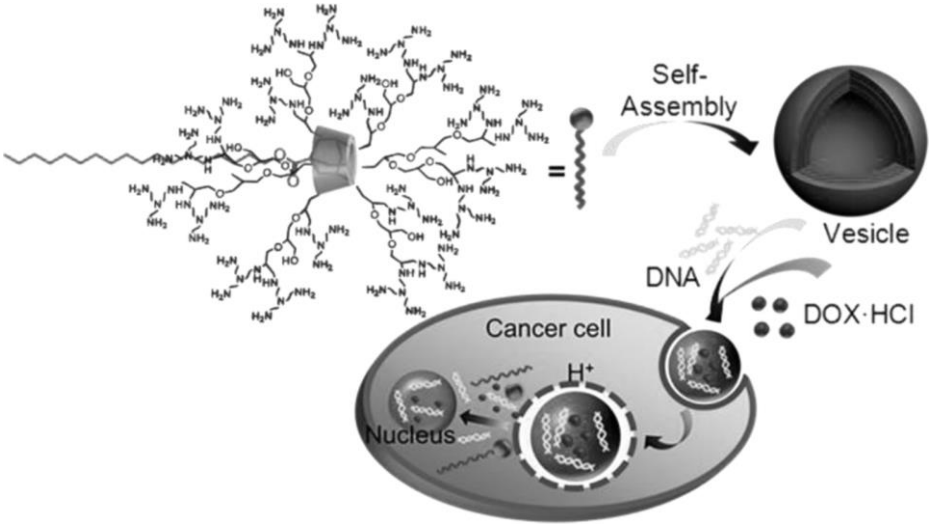

Figure 10. Example of amphiphilic supramolecular conjugate for *drug* and *gene delivery*.

1.2.6. Magnetic nanoparticles (MNPs)

Magnetic nanoparticles have a wide range of attributes that make them very promising drug delivery carriers. These are: easy handling using an external magnetic force, the ability to use passive and active drug delivery strategies, the visualization ability in Magnetic Resonance Imaging (MRI) and improved tissue absorption leading to effective treatment at therapeutically optimum doses. [109] MNPs tend to add to larger clusters, loosing the specific properties associated with their small dimensions and making physical handling difficult. In turn, magnetic force may not be strong enough to overcome the blood flow force and accumulate magnetic drugs at the target location only. [110] Therefore, designing magnetic drug delivery systems requires taking into consideration many factors, such as magnetic properties and size of particles, strength of magnetic field, drug loading capacity, the place of accessibility of target tissue, or the rate of blood flow.

Depending on magnetic properties, MNPs can be divided into pure metals such as cobalt, nickel, manganese and iron, their alloys and oxides. Iron oxide (Fe_3O_4) nanocarriers exhibit the favorable features, for clinical use. Covalent binding, electrostatic interactions, adsorption or encapsulation processes can be used to connect a drug to MNP. Therapeutic activity of ciprofloxacin[111], gemcitabine[112], doxorubicin[113], 5-fluorouracil[114], paclitaxel[115]

incorporated into iron oxide nanocarriers have been tested and reported. Concomitant use of magnetic resonance or magnetofluorescent imaging and targeted therapy can enhance the effectiveness of cancer therapy.

1.2.7. Gold nanoparticles

Gold nanoparticles are consisted of a core of gold atoms that could be functionalized through the addition of monolayer of thiol (SH)-containing groups.[116] They have been long considered as potential delivery vehicles for diagnostic and therapeutic purposes. The potential benefits for employing gold nanoparticles for drug delivery include the ability to image and diagnose diseases sites, the selectivity of drug targeting, the capacity of sensitizing the cells to anticancer drugs, as well as the possibility of monitoring and guiding surgical procedures[117]. Their ease functionalization provides a versatile platform for nanobiological assemblies with oligonucleotides, antibodies, and proteins. Gold nanoparticles prepared with antitumour drugs like doxorubicin[118], camptothecin[119], 5-fluorouracil[120] and irinotecan[121] are reported for targeted delivery in chemotherapy.

1.2.8. Silica materials

Silica materials used in controlled drug delivery systems are classified as xerogels and mesoporous silica nanoparticles (MSNs). Silica xerogels possess an amorphous structure with high porosity and enormous surface area. A porous structure (shape and pore dimensions) depends on synthesis parameters.[122] Phenytoin[123], Doxorubicin[124], Cisplatin[125], Metronidazole[126], Nifedipine[127], Diclofenac[128], and Heparin[129] are examples of drugs which have been loaded into xerogels. MSNs in comparison with xerogels possess several attractive features such as good biocompatibility, large specific surface area and pore volume, high loading capacity, controllable pore diameters ranging from 2 to 50 nm with narrow pore size distribution, good thermal and chemical stability and versatility of loading drugs with hydrophilic and lipophilic characteristics, which make them promising nanoscale drug carriers.[130, 131] In addition, ease of surface functionalization for controlled and targeted drug delivery enables MSNs to enhance therapeutic efficacy and reduce the toxicity of drugs[132]. The best known types of mesoporous silica nanomaterials are (i) MCM-41 (Mobil Composition of matter) with a hexagonal arrangement of the mesopores that can be easily adjusted and (ii) SBA-15 (Santa Barbara Amorphous type material) with a well-ordered hexagonal connected system of pores.[133] Diverse types of drugs, including anticancer drugs[134], antibiotics[135], and heart disease drugs[136], have been embedded into MNSs.

1.2.9. Carbon nanomaterials

Carbon nanocarriers used in DDS are differentiated into nanotubes (CNTs) and nanohorns (CNH). Carbon nanotubes (CNTs) are nanosized, hollow, tube-like assemblies of carbon atoms discovered by Iijima[137] in 1991. They belong to the family of fullerenes (a third allotropic form of carbon) and are formed by rolling up of grapheme sheet into a tube-like structure.[138] CNTs are classified as single-walled carbon nanotubes (SWCNTs) formed by rolling up a single grapheme sheet or multi-walled carbon nanotubes (MWCNTs) formed by rolling up several concentric grapheme sheets into a tube-like assembly (Figure 11). CNTs have cross-sectional dimensions in nanometer range and length, the SWNTs have a diameter about 0.5 – 1.5 nm and length of 20 -100 nm, while MWNTs are larger in size with a diameter in the range of 1.4 – 100 nm and length from 1 to several μm.

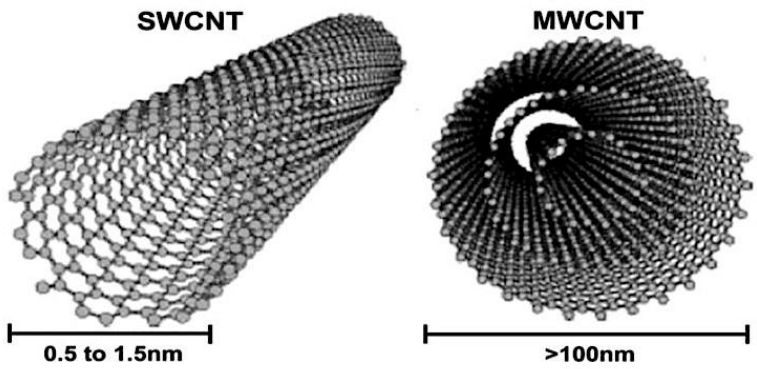

Figure 11. Schematic representation of single walled carbon nanotube (SWNT) and multi walled carbon nanotube (MWNT). [139]

CNTs possess some distinctive physiochemical and biological characteristics that make them a promising carrier for drug delivery. Some of these characteristics include nanoneedle shape, hollow monolithic structure, high aspect ratio (length: diameter >200:1), ultrahigh surface area, ultralight weight, high mechanical strength, high electrical and thermal conductivities and their ability for surface modifications.[140, 141] The needle-like shape of CNTs allows them to cross the cell membrane via endocytosis or "needle-like penetration" and subsequently enter into the cell.[142] The major problems with CNTs as a drug carrier are their poor water solubility and toxicity. However, nanotubes can be functionalized by covalent anchoring of PAMAM dendrimers, amphiphilic diblock copolymers or PEG layers on their surface which render them water soluble, biocompatible, not / less toxic and as a serum-stable carrier.[143] In the past 2 decades, CNTs have been studied as a carrier for anticancer drug

delivery. Anticancer drugs can either be encapsulated in the inner cavity of CNTs or can be attached, either covalently or noncovalently, to the surface of CNTs.

Nanohorns (CNH), a type of the only single-wall nanotubes exhibit similar properties to nanotubes. Their formation process does not require a metal catalyst, thus, they can be easily prepared with very low cost and are of high purity.[144]

1.2.10. Viral nanoparticles (VNPs)

Virus-based nanoparticles (Figure 12) are nanosized particles with diameters approximately < 100 nm, self-assembled robust protein cages having uniform nanostructures and well-defined geometry.[145]

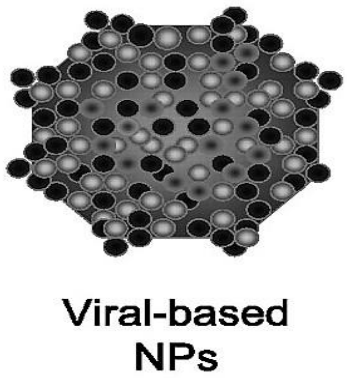

Figure 12. Viral-based nanoparticles[146]

They have been widely explored for nanotechnological purposes, including Drug Delivery, Gene Therapy, vaccination, imaging and targeting. A variety of viruses from different sources including plant viruses like *cowpeas cloroticmottle virus* (CCMV), *cowpea mosaic virus* (CPMV), *red clover necrotic mosaic virus* (RCNMV), *tobacco mosaic virus* (TMV), *insect viruses* (flock house virus), bacterial viruses or bacteriophages (MS2, M13, Qβ) and animal viruses (adenovirus, polyomavirus) have been developed for biomedical and drug delivery applications.[146, 147] Viral nanoparticles offer several attractive features including morphological uniformity, biocompatibility, easy surface functionalization and availability in a variety of sizes and shapes.[148] The basic structure of viral carriers could be manipulated in such a way that its internal cavity filled with drug molecules or imaging reagents, whereas the external surface could be decorated with targeting ligands.[149] Several ligands or antibodies including transferring, folic acid and single chain antibodies have been conjugated to viruses for specific tumor targeting *in vivo*. Additionally, PEGylating the surface of VNPs can improve their circulation time in the host.

For Drug delivery applications, drugs can either be physically entrapped in viral nanoparticles or chemically attached to the surface. In that way, in various studies VNPs loaded with chemotherapeutic agents have been investigated for tumor targeting. [150, 151]

1.3. Types of targeted Drug Delivery

As we have seen prreviously, most of the nanoparticles investigated have been principally used for the formulation of anticancer drugs. Ideally, for anticancer drugs to be effective in cancer treatment, they need to first (after administration) be able to reach the desired tumor tissues via the penetration of barriers in the body with minimum loss of activity in the bloodstream. Second, after reaching the tumor tissue, drugs should have the ability to selectively kill tumor cells without affecting normal cells and extend their effect along time.[146] These two basic strategies are also associated with improvements in patient survival and quality of life, by simultaneously increasing the intracellular concentration of drugs and reducing dose-limiting toxicities. In principle, NP delivery of anticancer drugs to tumor tissues can be achieved by either passive or active targeting (Figure 13).

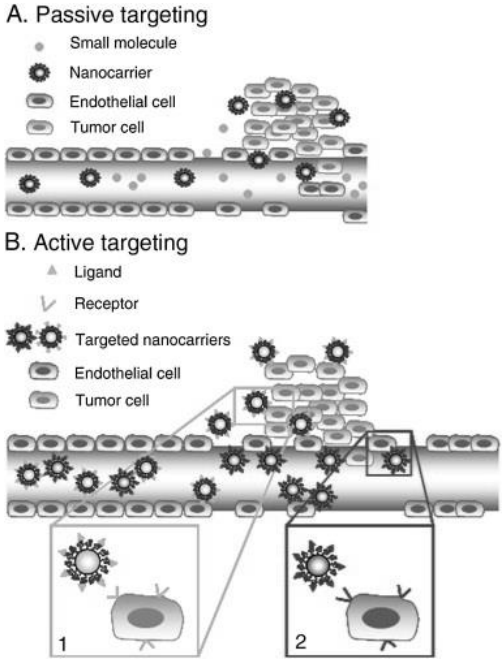

Figure 13. Passive (A) and active (B) tumor targeting of nanoparticles[152]

1.3.1 Passive Targeting

Nanoparticles that satisfy the size and surface characteristics requirements have the ability to circulate for longer time in the bloodstream and a greater chance of reaching the targeted tumor tissues.Passive targeting refers to the accumulation of a drug or a drug carrier

system at a desired site owing to physic-chemical or pharmacological factors of the disease. It takes adavantage of tumor vasculature and microenvironment. The unique pathophysiologic characteristics of tumour vessels enable macromolecules, including nanoparticles, to selectively accumulate in tumor tissues.[153] Fast-growing cancer cells need to form new blood vessels, via angiogenesis process, in order to obtain nutrients and oxygen. The newly formed tumor blood vessels present the same abnormal architecture, including defective endothelial cells with wide fenestrations, irregular vascular alignment, and lack of a smooth muscle layer or innervations. The resulting imbalance of angiogenic regulators such as growth factors makes tumor vessels highly disorganized and dilated with numerous pores showing enlarge gap junctions between endothelial cells and compromised lymphatic drainage system; thus, an inadequate circulatory repossession of the extravasated molecules occurs leading to the assemblage of nanocarriers at the tumor location. This is called Enhanced permeability and retention effect (EPR effect) [154] which constitutes a great approach in effective tumor targeting (Figure 14).

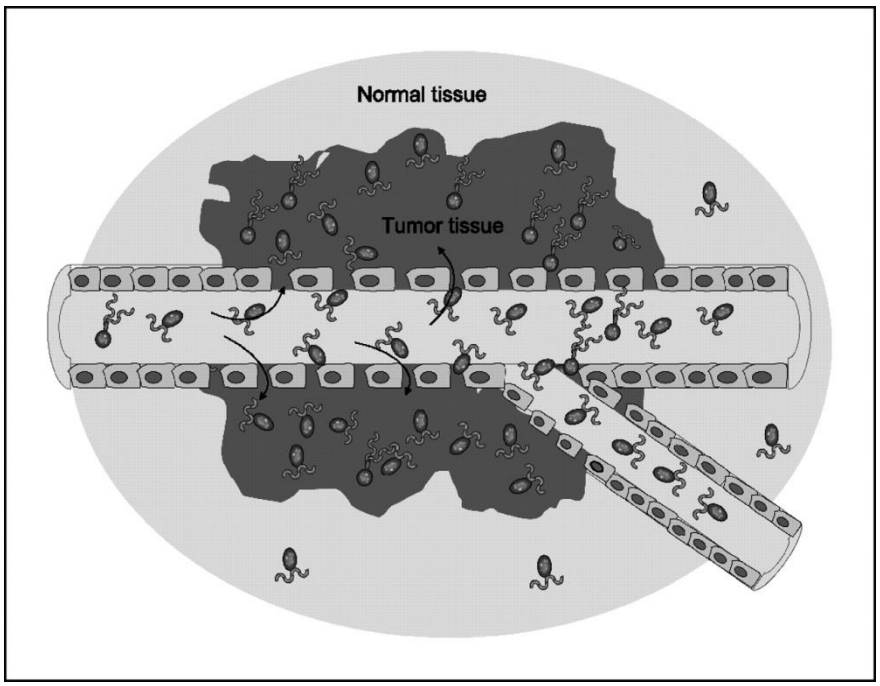

Figure 14. Passive tumor targeting of nanoparticles by enhanced permeability and retention[146]

The pore size of tumor vessel varies from 100 nm to almost 1 mm in diameter, depending upon the anatomic location of the tumors and the stage of tumor growth. In comparison , the tight endothelial junctions of normal vessels are tipically of 5-10 nm in size.

The leaky and defective architecture of tumor vasculature might be due to elevated levels of vascular mediators such as bradykinins, nitric oxide, VEGF, basic fibroblast growth factor, prostaglandins and so on. Moreover, solid tumors are also characterized by an impaired and lack lymphatic network that decreases the clearance of macromolecules giving, consequently, extended retention times in the tumor interstitium[155, 156]. Normal tissues contain linear blood vessels maintained by pericytes. Collagen fibres, fibroblasts and macrophages are in the extracellular matrix and lymph vessels are present. Tumor tissues contain defective blood vessels with many sac-like formations and fenestrations. The extracellular matrix contains more collagen fibres, fibroblasts and macrophages than in normal tissue. Lymph vessels are lacking.

Another contributor to passive targeting is the fact that the microenvironment adjacent to tumor cells is different from that of normal cells. Fast-growing, hyperproliferative cancer cells show a high metabolic rate and the supply of oxygen and nutrients is usually not sufficient for them to maintain this. Therefore, tumor cells use glycosis to obtain extra energy, resulting in an acidic environment.[157] For example, the pH-sensitive liposomes are designed to be stable at physiologic pH of 7.4, but degraded to release active drug in target tissues in which the pH is less than physiologic values, such as in the acidic environment of tumor cells.[158]

1.3.2 Active Targeting

Active targeting of specific tumor tissues is accomplished by surface modification of nanocarriers with site-specific targeting ligand. The targeting ligands have the capability of binding to specific receptors exclusively overexpressed by tumor cells or tumour vasculature.[152] The targeting agents commonly used to increase the site specificity of nanocarriers include small molecules, antibodies and antibody fragments, peptides (arginylglycylaspartic [RGD]), glycoproteins (transferrin), vitamins (folic acid), growth factors and nucleic acids.[159] A high surface area to volume ratio of nanocarriers allows them to effectively attach multiple targeting moieties, thereby achieving better targeting of specific tumor cell types. Active tumor targeting is utilized not only to reduce the off-target delivery of chemotherapeutic agents but also to avoid the drawbacks of passive tumor targeting and overcome the multiple drug resistance.[160] For the effective utilization of active targeting strategy, the desired target receptor must be homogeneously expressed in all target cells and the selected targeting moiety must exclusively bind to a receptor overexpressed by tumor cells only. Active targeting is designed either to direct the ligand-decorated nanocarrier to target the tumor cells or tumor microenvironment/vasculature.[161] In the field of active targeting, both of these cellular targets have gained considerable attention in the recent past to improve the

efficacy of chemotherapeutic agents and to reduce their adverse effects. Active targeting of tumor cells involves the targeting of overexpressed cell surface receptors with ligand-anchored nanocarrier via ligand-receptor interactions.[162] The subsequent receptor-mediated endocytosis (internalization) improves the uptake of nanocarriers by cancer cells, thereby increasing intracellular drug concentration with no or only little increase in tumor accumulation.[163] Most commonly targeted cell surface receptors overexpressed on tumor cells in many types of tumors include folate receptor (FR), TfR, epidermal growth factor receptor (EGFR) and cell surface glycoproteins.

1.4. Administration route of Nanoparticles

Nanoparticles provide massive advantages regarding drug targeting, delivery and release, and with their additional potential to combine diagnosis and therapy, emerge as one of the major tools in nanomedicine. The main goals are to improve their stability in the biological environment, to mediate the bio-distribution of active compounds, improve drug loading, targeting, transport, release, and interaction with the multiple biological barriers.[164]

The various routes of administration of a drug into the body can be generally classified into (i) direct entry into the body, (ii) entry into the body by overcoming the skin, (iii) entry into the body by overcoming mucosal membranes. Oral delivery is the most widely used and most readily accepted form of drug administration. Despite its potential advantanges, oral formulations face several common problems such as poor stability in the gastric environment, low solubility or bioavailability and require an intact intestinal mucosa for the nanoparticles uptake.[165] These limitations are particularly important for peptides and proteins. Drugs can be administered directly into the body, though injection or infusion, this form of drug administration is called parenteral drug delivery. Depending on the site of administration into the body one can differentiate between intravenous, intramuscular, subcutaneous, intradermal and intraperitoneal administration. This route has plethora of advantages for patients who cannot take drug orally and require rapid onset of action i.e. in case of unconscious patients. Despite these many benefits, parenteral formulations are more expensive and costly than conventional formulations.[166] Drug can also be administrated by pulmonary route; pulmonary drug delivery offers several advantages in the treatment of respiratory diseases over other routes of administration. Inhalation therapy enables the direct application of a drug within the lungs. It is a non-invase and avoids the first-pass metabolism in the liver. One example of this kind of formulation is iloprost (Ventavis®), a worldwide approved therapeutic agent for treatment of pulmonary arterial hypertension (PAH).[167] Another route that can be used to

administrated drugs is the transdermal delivery onto the skin to enter into the body. Transdermal systems are non-invasive and can be self-administered. They can provide release for long periods of time (up to one week). They also improve patient compliance and the systems are generally inexpensive. However the greatest challenge for transdermal delivery is that only a limited number of drugs are amenable to administration by this route.[168]

CHAPTER 2

2.1. 2, 2-bis (hydroxymethyl) propanoic acid in the dendritic architectures

Dendrimers are currently a very large class of structures that includes different types of molecular architectures, all with great prospects of being used in various fields, from optics to biology but all characterized by being monodisperse polymers with a high degree of symmetry and nanostructured with wide application potential in Nanomedicine in particular for gene therapy or for targeted drug delivery. Their preparation requires the application of "robust" chemical reactions and accurate isolation and purification procedures, as well as a characterization that requires sophisticated techniques and expensive equipment, usually not available in common laboratories. Therefore, especially for application purposes, the researcher's interest has focused on a limited number of dendrimeric scaffolds. In general, the molecular structure of a dendrimer starts from a polyfunctional core (di-, tri- or tetra-functional) from which the successive generations branch off to grow, leading to a progressive increase in peripheral functions through reactions of monomers, in their turn, ramified of the type AB_n with $n \geq 2$. Figure 15 shows, as an example, the structures of a monomer of the AB_n type with n = 2, of the fourth generation *dendron* that can derive from it and the structure of the fourth generation *dendrimer* obtainable by "assembly" of the dendronic unit on a trifunctional core.

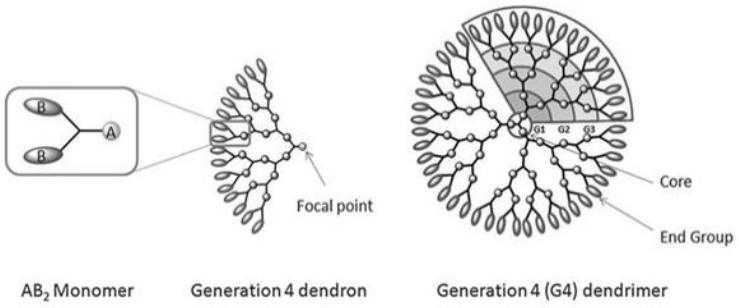

Figure 15. Dendron and fourth generation dendrimer's structures obtained from the monomer AB_2.[169]

The 2,2-*bis* (hydroxymethyl) propanoic acid (*bis*-HMPA) (Figure 16) is a trifunctional, pro-chiral aliphatic molecule characterized by having two primary alcoholic groups and a carboxylic group and is commercially available at low costs. Its derivative anhydrides have the hydroxyl functions of *bis*-HMPA in protected form and the third carboxylic function in activated form and can provide two units of *bis*-HMPA in synthesis

techniques of dendrimeric structures containing *bis*-HMPA which in macromolecular chemistry is classifiable as a monomer type AB_2.

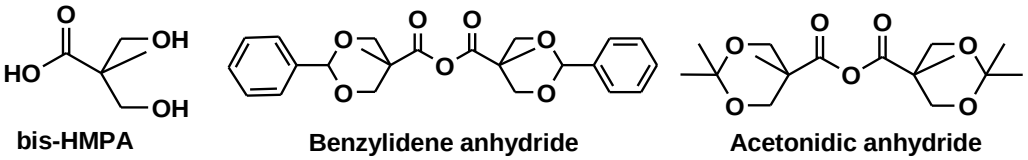

Figure 16. Structures of the bis-HMPA monomer and of its benzylidene and acetonidic anhydrides.

The bis-HMPA can be used to prepare a wide variety of polyester dendritic[170] molecular architectures with good biocompatibility[171], low cytotoxicity and therefore can be used in the biomedical field. Figure 17 shows various types of monodisperse or polydisperse dendritic structures derived from the bis-HMPA.

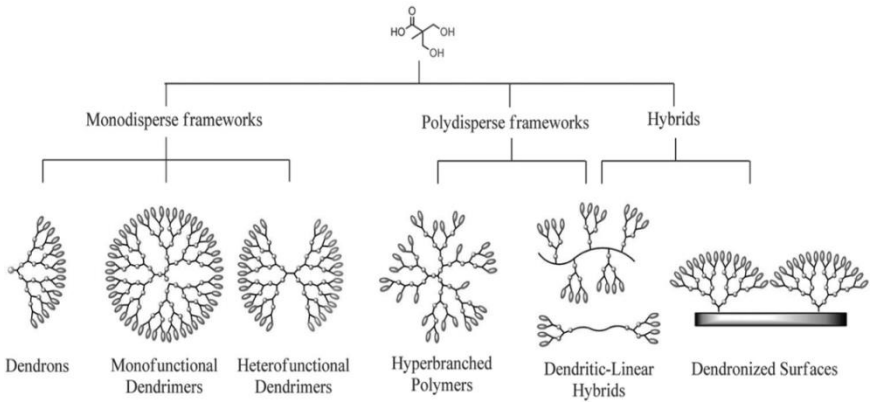

Figure 17. Overview of the main types of bis-HMPA dendrimers.[170]

2.2. Strategies for the synthesis of dendritic systems starting from HMPA

In general, for the synthesis of dendrimers, several conventional strategies (divergent and convergent growth approaches) and unconventional approaches i.e. revisited approaches known as accelerated syntheses. In both types of approach, synthesis is based on growth and activation/deactivation of the AB_n monomeric units and it is important that the reactions used proceed effectively and with high yield as the generations increase.

2.2.1. Conventional approaches

❖ *Divergent growth*

This approach is also called *Inside-Out*. It starts from a multifunctional core B_n ($n \geq 2$) and uses a monomer of the AB*n* type ($n \geq 2$) where A is an activated group while B is a deactivated / protected group to allow the controlled growth. In a study carried out by Fréchet et al.[172] the partially activated and protected benzylidene anhydride was coupled to a triphenolic core (B_3).

The subsequent deprotection reactions of the benzylidene groups by hydrogenolysis, esterification to increase the generations, followed by further deprotections of the external benzylidene groups and so on led to the obtainment of a fifth generation G5 *dendrimer* with a yield of 52%.

The final deprotection freed up 96 peripheral hydroxyls further functionalizable according to requirements. (Scheme 4)

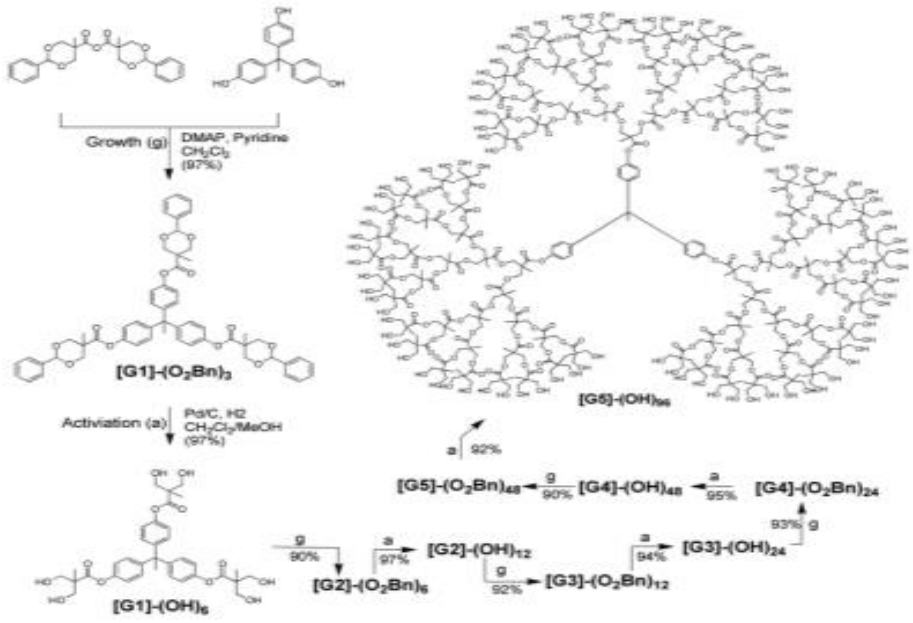

Scheme 4. Divergent growth approach for the construction of a bis-HMPA dendrimer with 96 hydroxyls at the periphery[172]

A synthetic improvement following the same strategy was obtained by Hult et al.[173] using the acetonidic anhydride of the bis-HMPA in the synthesis of a fourth generation G4 dendrimer in 8 consecutive steps. An inconvenient of this strategy is the risk of constructing dendrimers with structural defects that are difficult to separate from the good dendrimers

deriving from incomplete functionalization of the peripheral groups caused by phenomena of steric dimensions directly proportional to the generational degree.

❖ *Convergent growth*

In the 90s the first alternative steps were taken in the preparation of *dendrimers* using convergent growth[174], which first provides the preparation of perfectly branched *dendrons* of the desired generational degree protected to peripheral functions such as acetonides starting from the usual bis-HMPA, activation of their focal point (carboxylic group) and then their coupling with the triphenolic polyfunctional central core B_3 (Scheme 5).[175] The subsequent functionalization of the peripheral groups then provides a phase of deprotection of the hydroxylic functions which will be reacted with suitable activated molecules. Monitoring the generative growth of *dendrons* is simpler and their purification from parasitic products, such as the monomeric anhydrides used and their N-isoacilureic derivatives are less laborious due to the greater structural diversification of reagents and products.

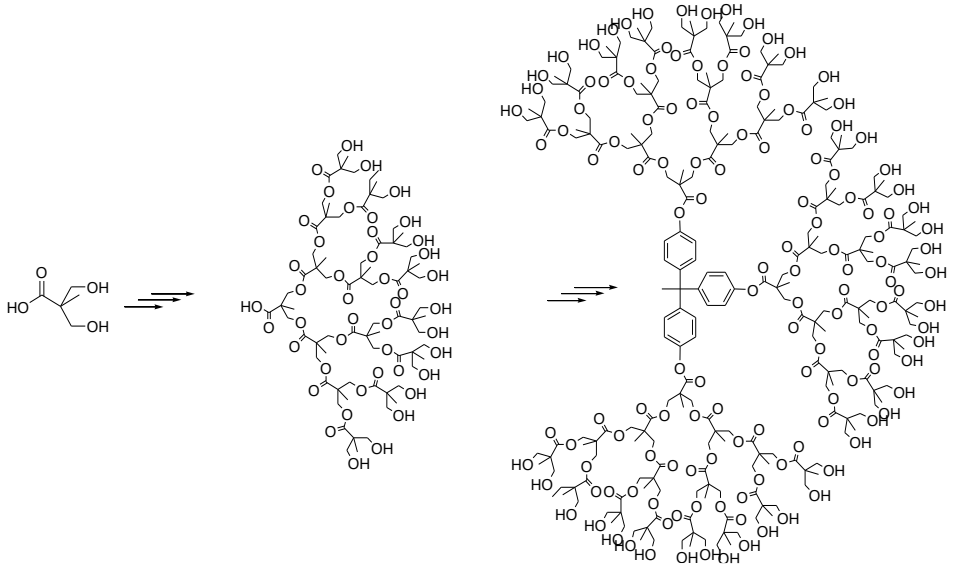

Scheme 5. Example of convergent synthesis of bis-HMPA[175]

In any case, the control of the growth of *dendrons* and *dendrimers* is easily achievable by proton NMR spectroscopy which presents absolutely simple traces to be interpreted when they have a high degree of symmetry; mass spectrometry in its MALDI-TOF version, even if very expensive, remains the main investigative tool for the confirmation of the final dendrimeric structure.

2.2.2. Accelerated approaches

The two conventional approaches just described are "weighed down" by a large number of synthetic steps and therefore by many laborious purification operations of the intermediates, a high probability of obtaining defective *dendrimers* or *dendrons* to get rid of, need for increasing excess reagents to ensure complete replacement of all reactive groups. Therefore, even if with demanding synthetic efforts by researchers in the field, they have been designed a synthetic effort, the so-called accelerated strategies have been designed, investigated and developed to overcome or minimize these problems. Figure 18 shows the Hypermonomer Strategy (Frèchet et al. [176]) which uses more functionalized monomers (Hypermonomers) than the traditional AB_2 monomer on which to construct the dendrimeric structure by halving the number of steps necessary to obtain dendrimers of the same generational degree, even if the only synthesis of Hypermonomer is however laborious and multistage.

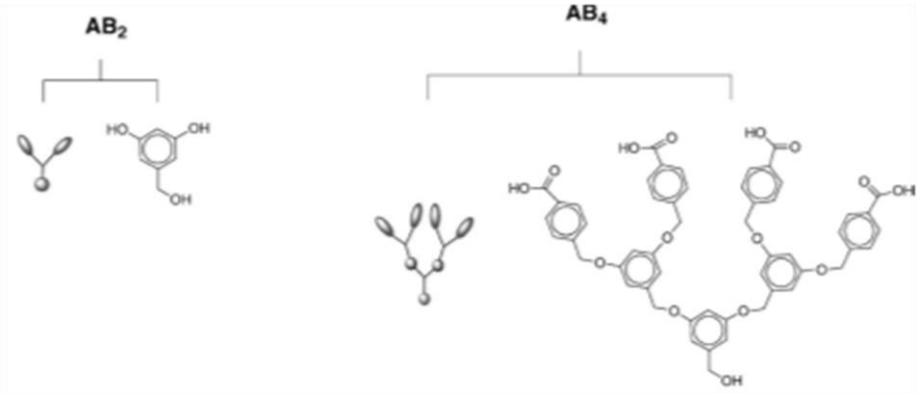

Figure 18. Examples of a conventional monomer of the AB_2 type and an AB_4 type hypermonomer for the synthesis of the dendrimers[169]

Instead, Moore et al.[177] exploiting as an accelerated approach the *Double Stage Convergent Growth*, which realizes the generational growth through the functionalization of a low-generation dendrimer (*Hypercore*) with also low generation *dendrons*, have succeeded in synthesizing the fourth generation G4 phenylacetylen dendrimers by coupling a second generation *dendron* D2 with a second generation G2 dendrimer. The final dendrimers are obtained in one step, but the preparation of the *dendrons* and the *hypercore* requires four synthetic steps each, so the final dendrimer is still obtained in a total of nine steps. This method is therefore useful only to prepare dendrimerswhich cannot be obtained by conventional methods.

The *Double Exponential Growth* involves the preparation of protected or deactivated low generation *dendrons* which, after being activated at their focal point or at the periphery, reacted with each other. Following this approach, a fourth generation G4 *dendrimer* of *bis*-HMPA containing 48 hydroxylic groups at the periphery was synthesized (Scheme 6).[178]

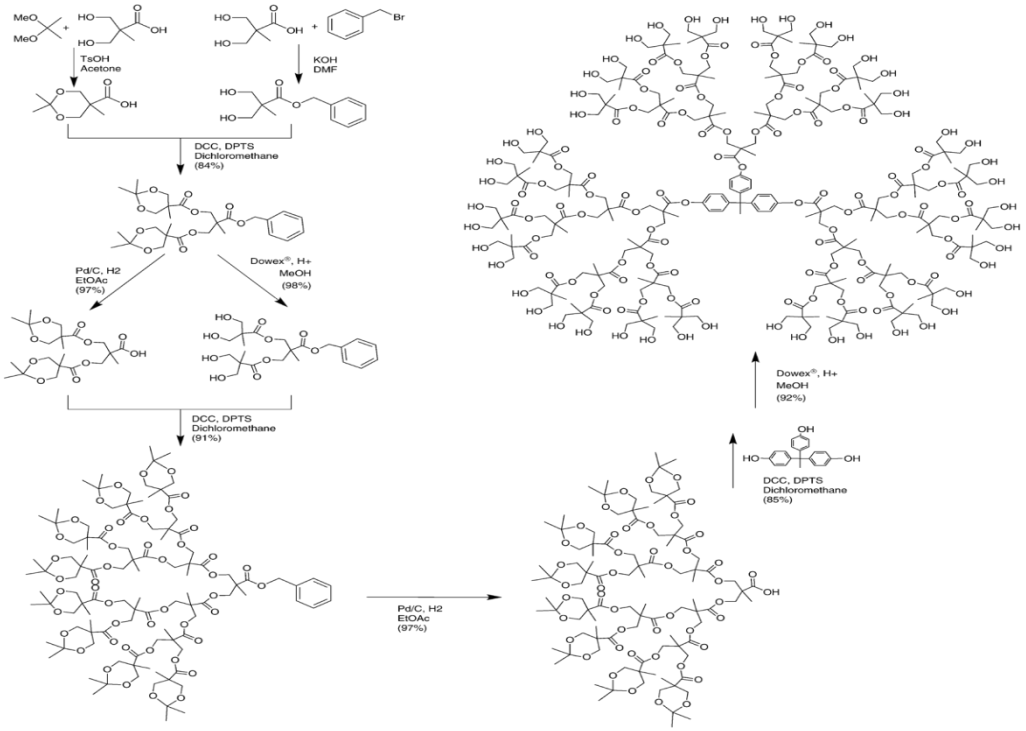

Scheme 6. Fourth generation G4 dendrimer's synthesis through double exponential approach[178]

2.2.3. Procedures via Click Chemistry

In the last decade the new types of organic reactions known as *Click Chemistry* allowed the accelerated synthesis to make a significant step for the preparation of *dendrimers* with greater synthetic efficiency. The term *Click Chemistry*, coined by Sharpless[179] in 2001, indicates all the coupling reactions characterized by a high " thermodynamic thrust ", such as the alkino-azide cycloaddition catalyzed by copper (CuAAC), the Diels-Alder reaction (DA), or the thiolo-alchene coupling (TEC) (Scheme 7).

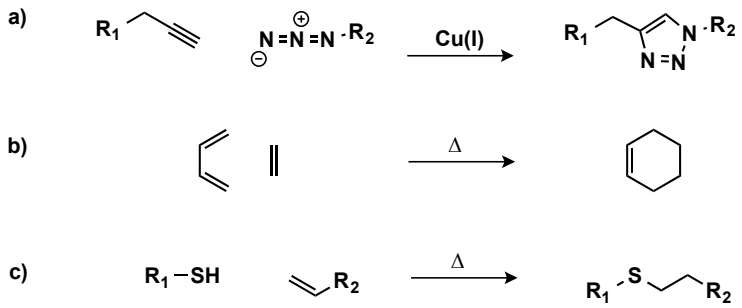

Scheme 7. Examples of Click Reactions: a) alkino-azide cycloaddition catalyzed by copper (CuAAC); b) Diels-Alder reaction (DA); c) thiolo-alchene coupling (TEC)

The construction conditions (room temperature and wide availability of solvents including water), simple purification steps such as extraction or filtration, high selectivity and yields (100%) and compatibility with a large number of functional groups, made *Click Reactions* very interesting both in the eyes of Hawker, Fréchet and Sharpless,[180] which showed that the 1,3-dipolar azide-alkino cycloaddition catalyzed by Cu (I) (CuAAC) could provide a triazole product and could be a synthesis method very suitable for the preparation of dendrimeric structures. Always using the catalytic system (CuAAC) Antoni et al.[181]synthesized a fourth generation G4 dendrimer starting from monomeric units of the AB_2 and CD_2 type and from a triphenolic core in only 4 steps (Figure 19 and 20).[182]

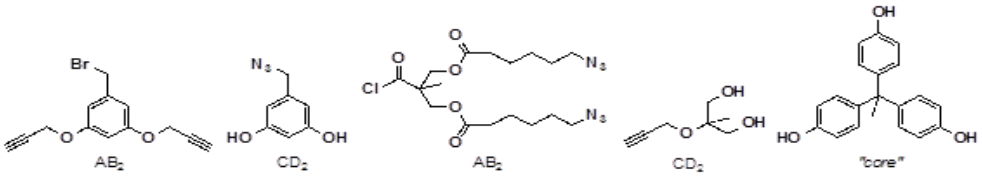

Figure 19. Examples of AB_2/CD_2 monomer pairs and triphenolic core used in accelerated dendrimers synthesis via Click Chemistry[182]

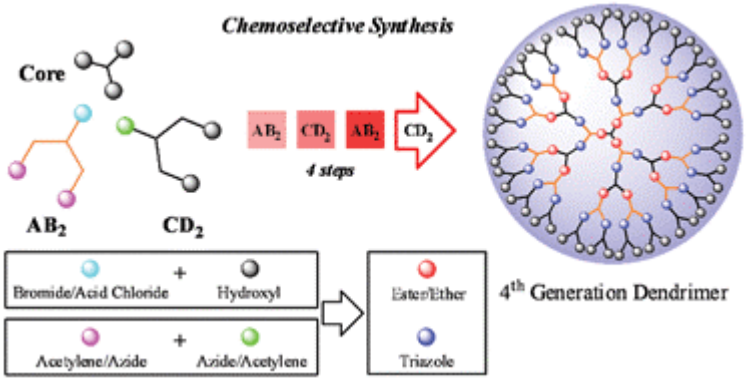

Figure 20. Construction of a fourth generation dendrimer containing 48 free hydroxyls using *Click reactions*.[182]

2.3. Heterofunctional dendrimeric systems

The term *Heterofunctional Dendrimers* or HFD refers to more complex, advanced and sophisticated structured *dendrimers* having more than one type of peripheral function. Several synthetic approaches have been devised and realized to obtain heterofunctional dendrimers[169, 183, 184] that present different functions also arranged in different positions within the same dendritic architecture and not only peripheral (Scheme 8). The big synthetic complications to deal with to get HFD strongly limit their accessibility.

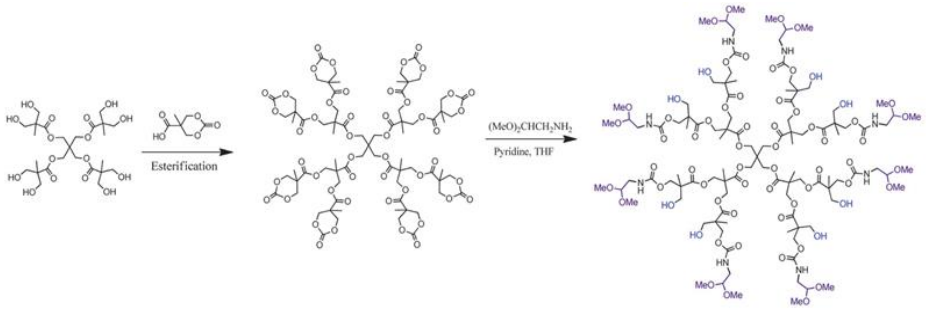

Scheme 8. Simplified strategy for the synthesis of a second generation HFD of bis-HMPA bearing two different alternate external functions[184]

2.4. Hybrid dendritic systems

Since the 1990s,[185-187] combining the knowledge of expert chemists in both organic chemistry and macromolecular chemistry and addressing complex processes of synthesis, purification and characterization, it was possible to prepare hybrid systems containing both linear polymers and *dendrimers* in the same molecular structure. The products obtained thanks to new properties, both in solution and in solid state still continue to arouse great interest in the world. Figure 21 shows in a pictorial way some hybrid structures where the linear and dendrimeric polymeric parts are visually recognizable.

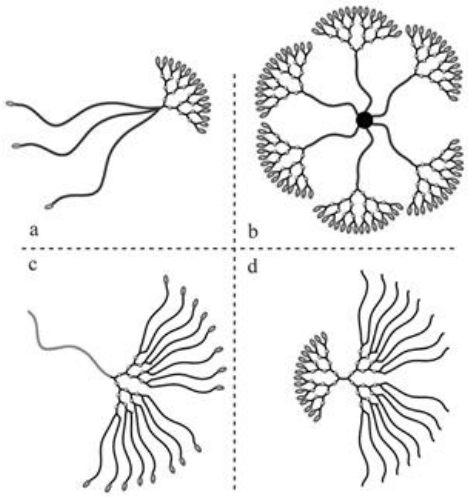

Figure 21. Hybrid linear polymer-dendrimer structures.[163] (a),[188, 189] (b),[190] (c),[191] (d)[183]

Figure 22 shows the two processes used to bind bis-HMPA to the polymeric chain by means of ester or amide link (*graft from*) and to grow the dendrimeric structures using the two terminal hydroxyl groups, or to bind dendrons preformed to the polymer chain as long as it has suitable reactive functions (process known as *graftto*).

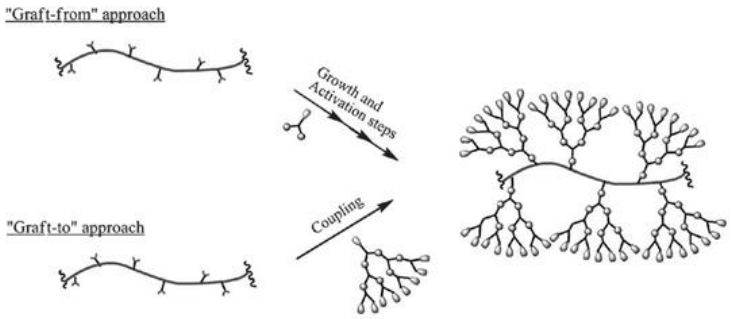

Figure 22. *Graft from* and *graft to* method for the obtainment of hybrid linear polymer-*dendrimer* systems[182]

An example of application of the *graft from* is the preparation of a linear dendritic copolymer containing units of *bis*-HMPA inserted using its acetonidic anhydride and subsequently functionalized with retinoic acid (PEG-G3-3A_8) to be used as carrier for the embedding and targeted release of Paclitaxel (PEG-G3-3A_8 / PTX), which provided a promising breast cancer care prodrug (Scheme 9, Figure 23).[192]

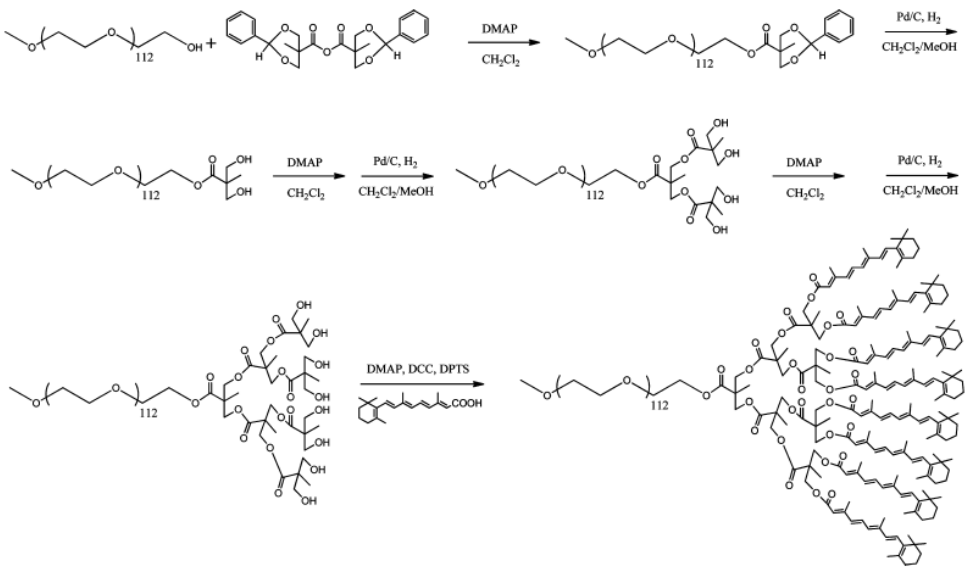

Scheme 9. Synthetic route for the preparation of PEG-G3-3A8

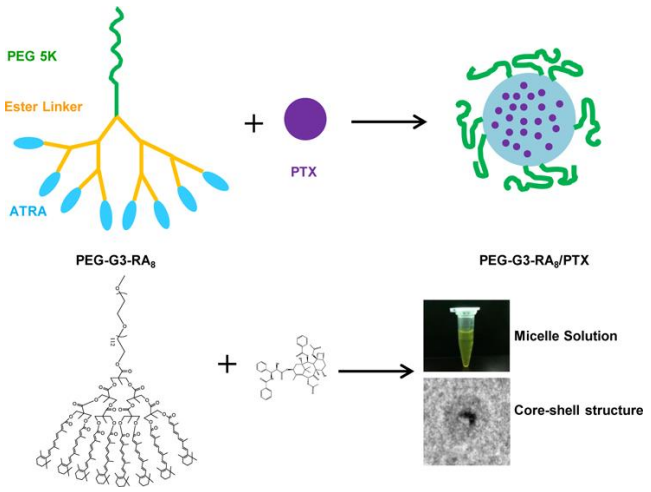

Figure 23. Incorporation of PTX on the linear dendritic copolymer and its micelle organization

Another way to obtain polymer-*dendrimer* hybrid systems involves the polymerization of dendritic macromonomers. The preferred polymerization techniques are the cationic and anionic processes, the ring-opening metathesis (ROMP) polymerizations, the radical transfer atom polymerization (ATRP) and the reversible chain transfer (RAFT), which guarantee a control on the degree of polymerization and therefore the tendency to monodispersion (Figure 24).[193]

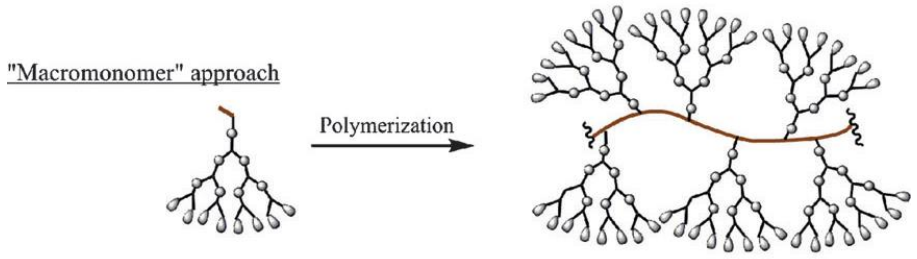

Figure 24. Macromonomer method for the obtainment of hybrid linear polymer-dendrimer systems[193]

Another and different type of hybrid system is represented by *star-like systems* (star hybrid systems) in which a pre-packaged dendrimer plays the role of polymerization macroinitiator (*core first* approach) or support for the coupling of preformed polymers (*arm first* approach), giving both approaches to a star-like structure where the number of arms is determined by the number of peripheral functional groups of the initial dendritic structure. Hybrid star systems have been prepared by exploiting in a core first approach the hydroxyl groups at the periphery of dendrimers of 1 (G1-G4) to promote ring opening polymerizations (ROP) of ε-caprolactone (ε-CL), acid lactic acid (L-LA), (Hedrick et al.[194]) or of both monomers ε-CL and L-LA in a polymerization at 110 ° C using as catalyst $Sn(Oct)_2$.[195]

The *arm first* was instead taken into consideration by Nyström et al.[196] who achieved a direct coupling by esterification between the carboxylic function of PEG polymers (molecular weight of 5 or 10 KDa) and commercial *dendrimers* of *bis*-HMPA, Boltorn H30 and H40 (Figure 25).

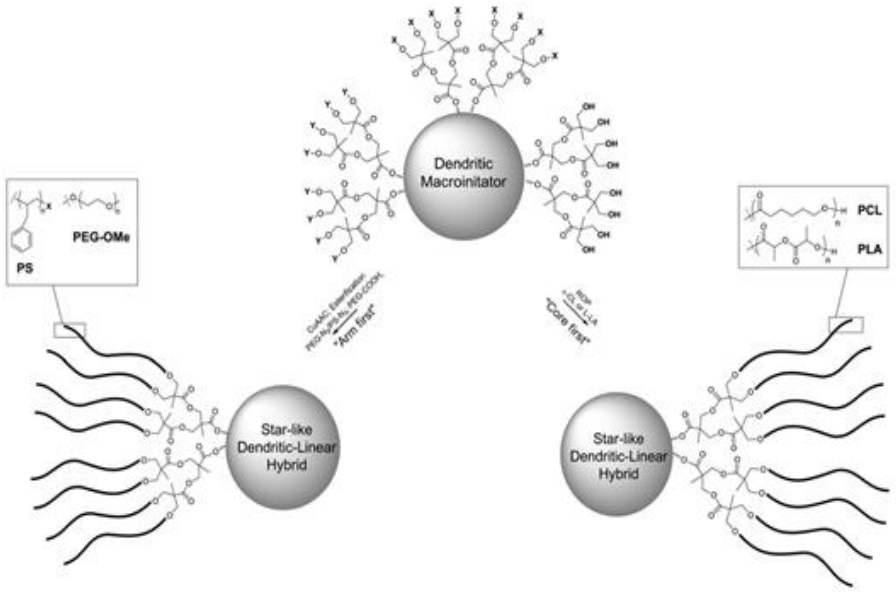

Figure 25. Examples of *core first* and *arm first* approaches for the construction of *star-like* dendrimers based on *bis*-HMPA[170]

Other hybrid dendritic systems consist of linear dendritic block copolymers[172] (Scheme 10).[197]

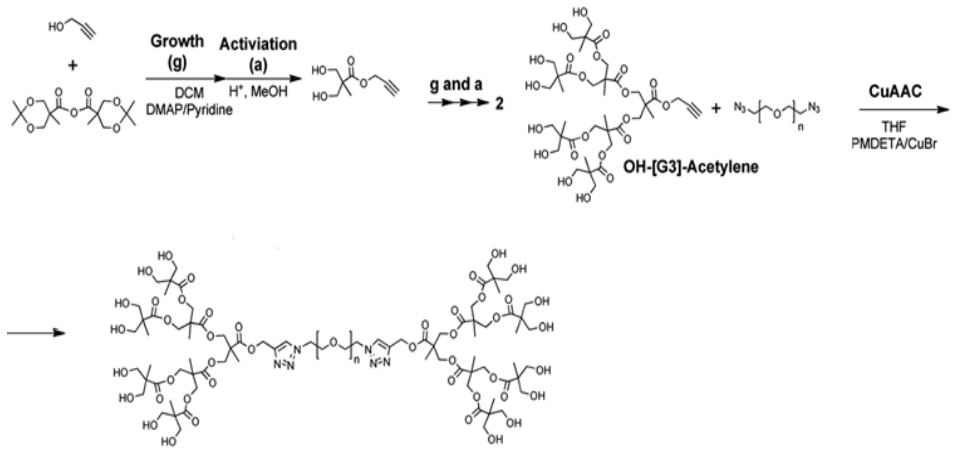

Scheme 10. Synthesis of a block copolymer of the ABA type based on CuAAC[197]

2.5. Dendronized surfaces

By immobilizing dendritic structures using simple absorption or by creating a covalent bond on solid surfaces, the so-called "dendronized surfaces" are obtained. Scheme 11 shows the realization of Malkoch et al.[198] who dendronized activated cellulose surfaces with azide function with acetylenic *dendrons* of bis-HMPA up to the fifth generation. Their hydroxylic

groups were further functionalized by a *graft from* approach with an AB_2C monomer and the resulting surface was finally functionalized with residues of carbohydrates, antibiotics, dyes and glycolic chains.

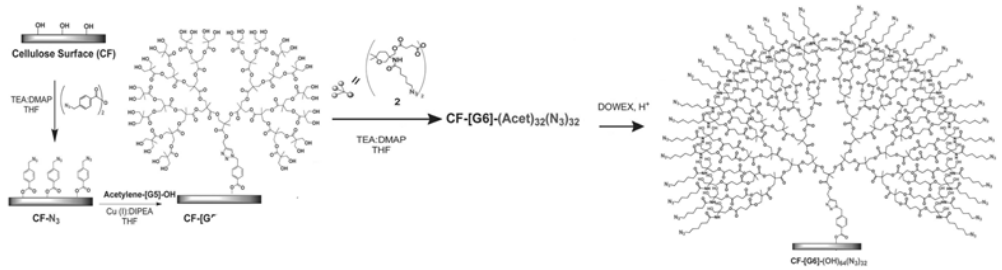

Scheme 11. Dendronized cellulose surface with sixth generation G6 *bis*-HMPA dendrimers obtained by combination of *graft to* and *graft from* approaches[170]

Other examples of dendronized surfaces with *bis*-HMPA were silanized silicon oxide,[199] clay,[200] and calcium carbonate.[201] To conclude this chapter, we report the dendronization of gold surfaces with bis-HMPA dendrons (Scheme 12).[202, 203]

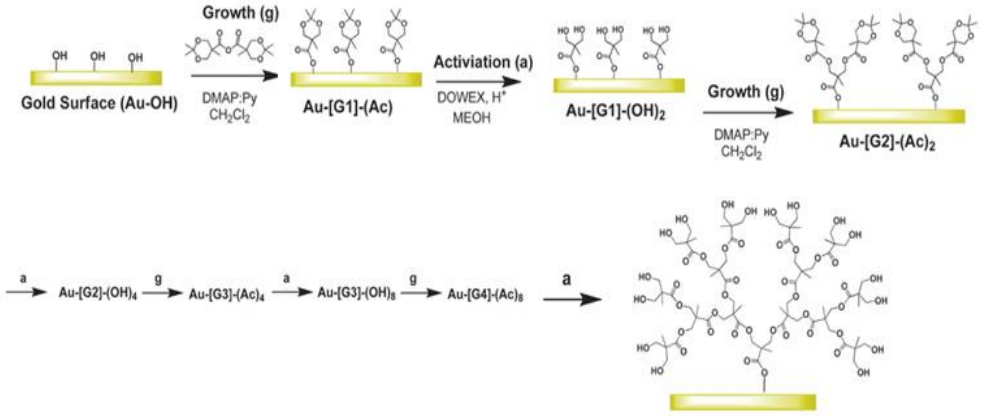

Scheme 12.*Graft from* approach used for the realization of a fourth generation dendronized gold surface[202, 203]

CHAPTER 3

3.1. Synthesis and Characterization of Amphiphilic Polyester-based Dendrimers peripherally decorated with positive charged amino acids as New Drug Carriers.

As a premise, it should be noted that generally in the field of dendrimeric structures, and so in this work, with the term *dendrone* indicates the molecules of various generations without the core, while the term *dendrimer* indicates the structures obtained by assembling the dendron on the polyfunctional core.

As illustrated in Chapter 2, the 2,2-bis (hydroxymethyl) propanoic acid is a very versatile monomer widely used for the construction of polyester-based dendrimeric systems. The structural variety, combined with biocompatibility, places these systems in first positions among the materials suitable for applications in the biomedical field.

In light of these considerations, in our laboratory a research activity is currently underway aimed to prepare dendrimeric structures with internal polyester and biodegradable matrix derived from the bis-HMPA, and polyoxydrilated periphery exploited for further esterification with amino acids, natural or not, to explore their effectiveness as carriers for the targeted delivery of drugs.

We chose to decorate the surface of our dendrimers with amino acids as biocompatible and protonable to the amine groups of different nature and therefore able to give materials that contain them an adequate density of positive charges necessary to interact with the negativity of the membrane lipids and an adequate buffer capacity at the physiological pH (pH = 4.5-7.5), fundamental parameter for the release of materials transported inside the cells in the cytosol. The first two steps involved the preparation of samples classifiable as non-arginine dendrimers and dendrimers containing arginine.

Non-arginine samples are fourth, fifth and sixth generation polyester dendrimeric materials obtained from the fourth generation dendrimer (G4OH) derived from bis-HMPA having 48 free hydroxyls at the surface which has been functionalized either directly with amino acids, or with dendrons already esterified with amino acids (Figure 26).

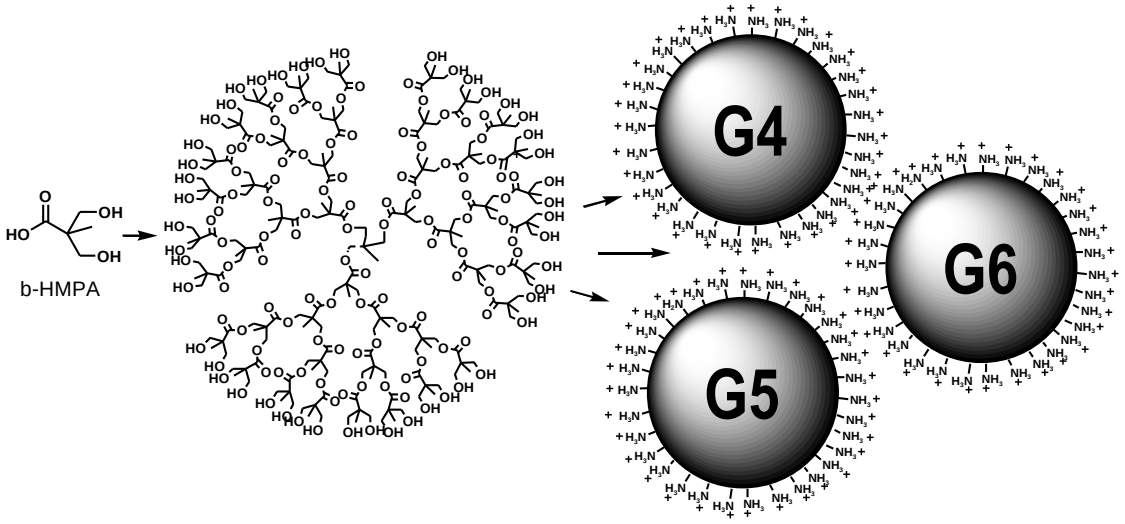

Figure 26. Structure of the first prepared dendrimeric materials.[204]

These samples surface have 48 to 384 protonated amino groups, an optimal buffer capacity, were much less cytotoxic compared to commercial PEIs (Table 1) and bind well DNA (Figure 27), but have shown unsatisfactory transfective efficiency.

Table 1. Cytotoxicity of some of our dendrimers compared to that of PEI

Code	Dendrimer	MW	Mortality*
PEI25	PEI	22000	28.6
A6	G5LysHis	30592	2.5
A7	G5His	29141	2.5
A8	G5Lys	28966	2.6
A9	G4lys	15503	2.1
***% of dead cells**			

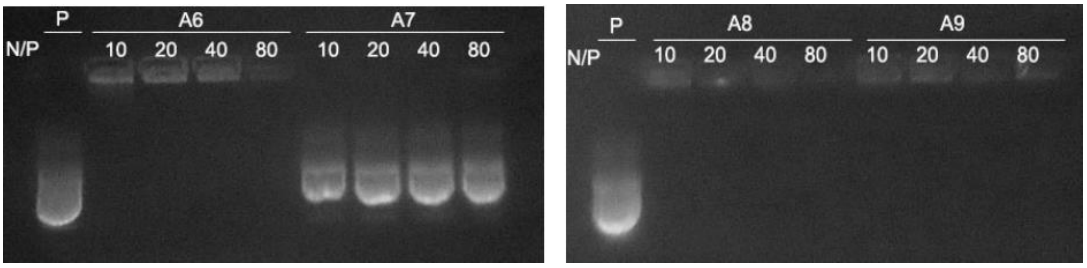

Figure 27. Plasmid DNA binding test of a selection of non-arginine vectors

Hence the decision to prepare dendrimers containing *L*-arginine.[205] It is well known that arginine-rich peptides are widely used as nucleic acid [206] and siRNA vectors, [207] there are also examples of arginine-containing dendrimers that have been shown to improve the cellular uptake) of siRNA[208, 209]and transfection efficiency.[210, 211] In addition to the synthesis of homodendrimers, also heterodendrimers were synthesized which, in addition to the arginine residues, also present lysine and methoxytirosinic residues, the latter designed to give the dendrimer the greatest hydrophobia that could benefit from the interaction with the cell membrane (Figure 28) .[205]

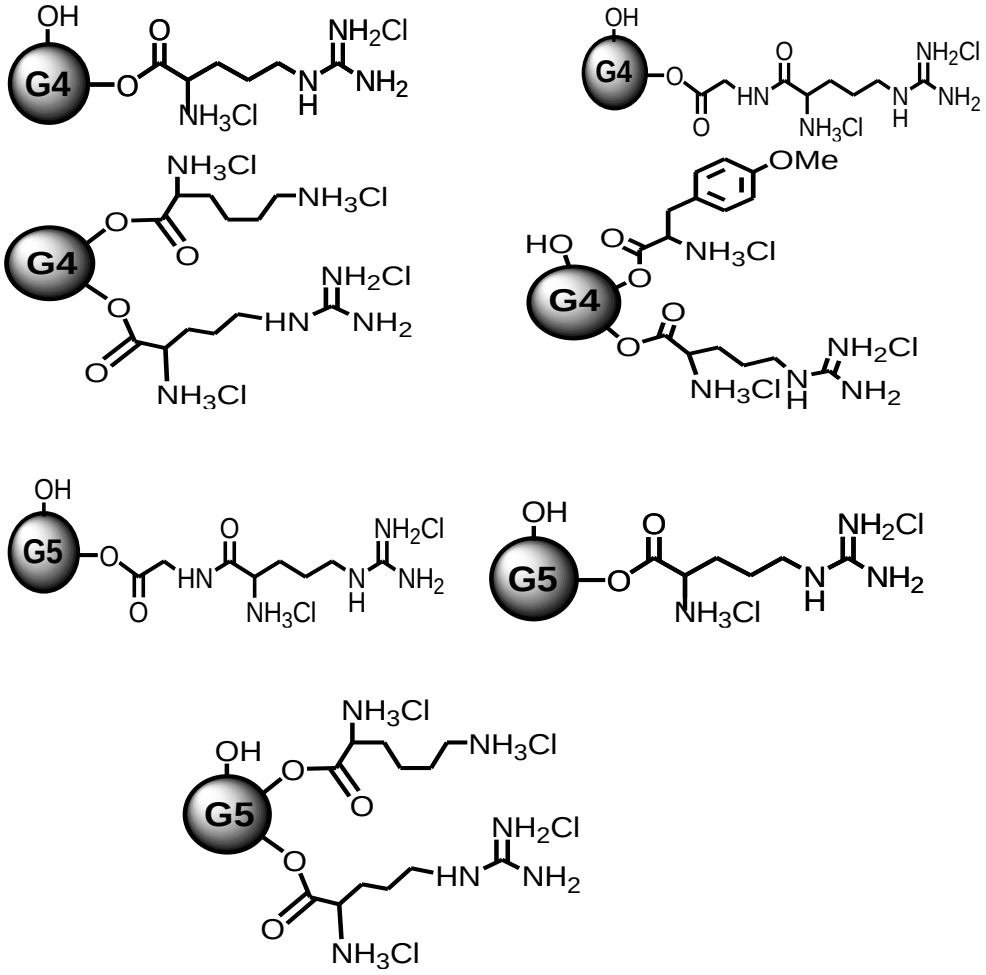

Figure 28. Arginine dendrimers prepared.[205]

As it can be seen from Figure 28, except in one case, the new arginine dendrimers contained non-esterified hydroxyls. It was therefore thought that the presence of residual OH groups could confer excessive hydrophilia on the new samples, hindering their passage through the cell membranes and opposing the transfection again. Therefore, the need of re-establishing a favorable Hydrophilic-Lipophilic Balance (Hydrophilic-Lipophilic Balance HLB) and the idea of achieving this intent by inserting a hydrophobic residue at some level of the synthesis of our carriers. This chapter shows the results obtained from the multi-step synthesis of a new type of dendrimeric structures always derived from the bis-HMPA having as polyfunctional stones the molecules **1 or 2** (Figure 29) and containing in addition a hydrocarbon chain of 18 carbon atoms as hydrophobic residue to promote the interaction with the apolar tails of membrane lipids, facilitate the crossing of cellular barriers, improve cellular up-take and transfective power.

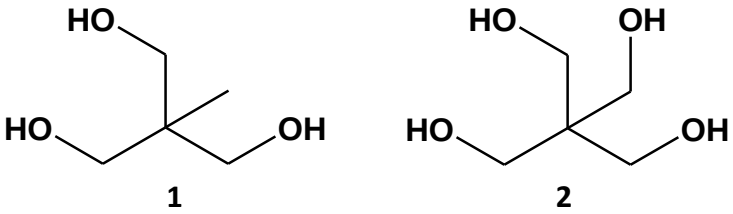

Figure 29. trifunctional (**1**) and tetrafunctional core (**2**)

3.2. Preparation of 2,2-*bis*(hydroxymethyl)propan-1-ol mono-stearate (4) and 2,2-*bis*(hydroxylmethyl)-1,3-propanediol mono-stearate (5)

We have thought to insert a chain of 18 carbon atoms directly on the stones making them react according to a slightly modified literature procedure[212] with the acyl chloride of stearic acid **3**. This has been prepared in our laboratory from commercial stearic acid and always according to a variant of a literature procedure. [213, 214] Stearic acid was added to an excess of thionyl chloride in absence of solvent at 0°C and then was kept under stirring at reflux for about two hours (Scheme 13).

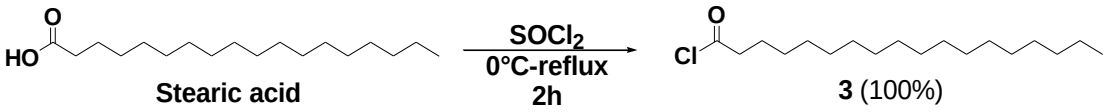

Scheme 13

The reaction was monitored by FTIR spectroscopy on a drop of the reaction mixture. The disappearance of the band relative to the C = O of the acid at 1702 cm^{-1} was observed, and the appearance instead of the one at 1802 cm^{-1} of the chloride (Figure 30).

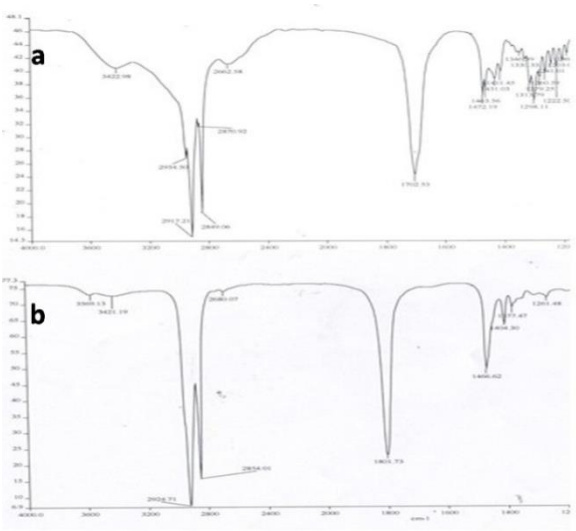

Figure 30. Comparison between the FTIR spectrum of **3** (b) and that of commercial stearic acid (a)

Compound **3** was isolated by evaporation under vacuum of the thionyl chloride excess and was stored in a flammed test tube in a nitrogen stream and in the freezer as very unstable and susceptible to hydrolysis.

The purity of **3** was verified by ^{1}H NMR and ^{13}C NMR spectroscopies and provided data in agreement with those of literature.[215]

The esterification reactions of the three functional 2,2-bis(hydroxymethyl)propan-1-ol (**1)** and the 2,2-bis(hydroxymethyl)-1,3-propanediol (**2)** were performed according to a slightly modified literature protocol.[215] The acyl chloride **3**, previously prepared, was reacted with **1** or **2** gaining in both cases very complex crudes (Scheme 14 and 15).

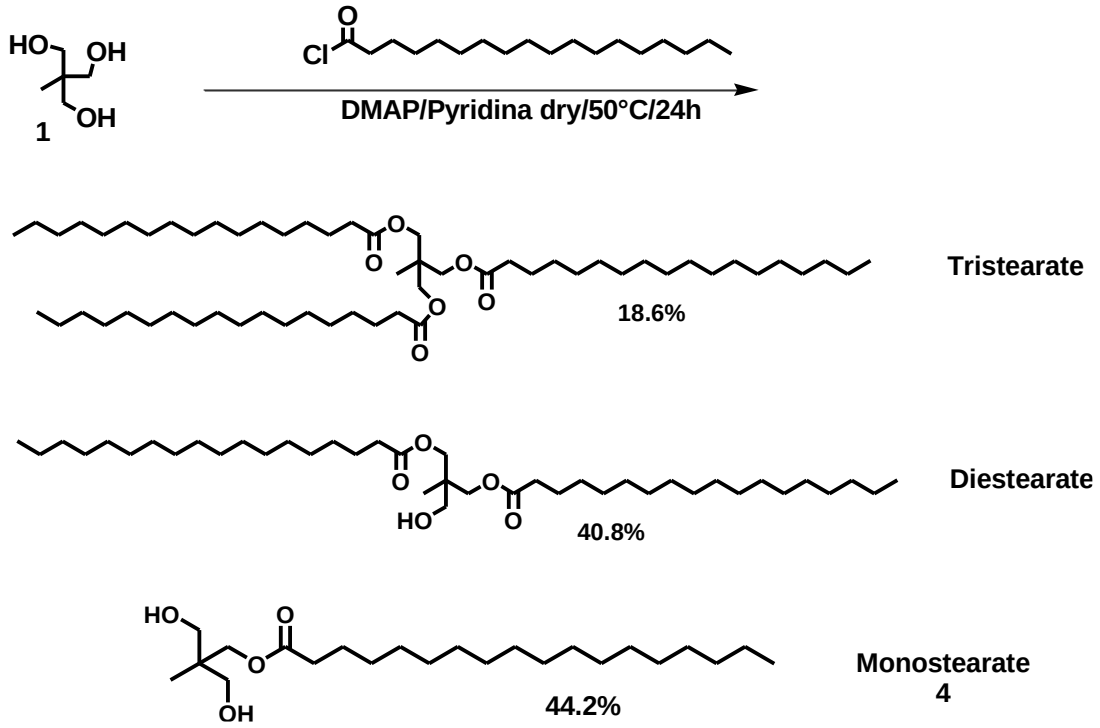
HO
OH
OH
1
Cl
O
DMAP/Pyridina dry/50°C/24h
Tristearate
18.6%
Diestearate
HO
40.8%
HO
Monostearate
4
44.2%

Scheme 14

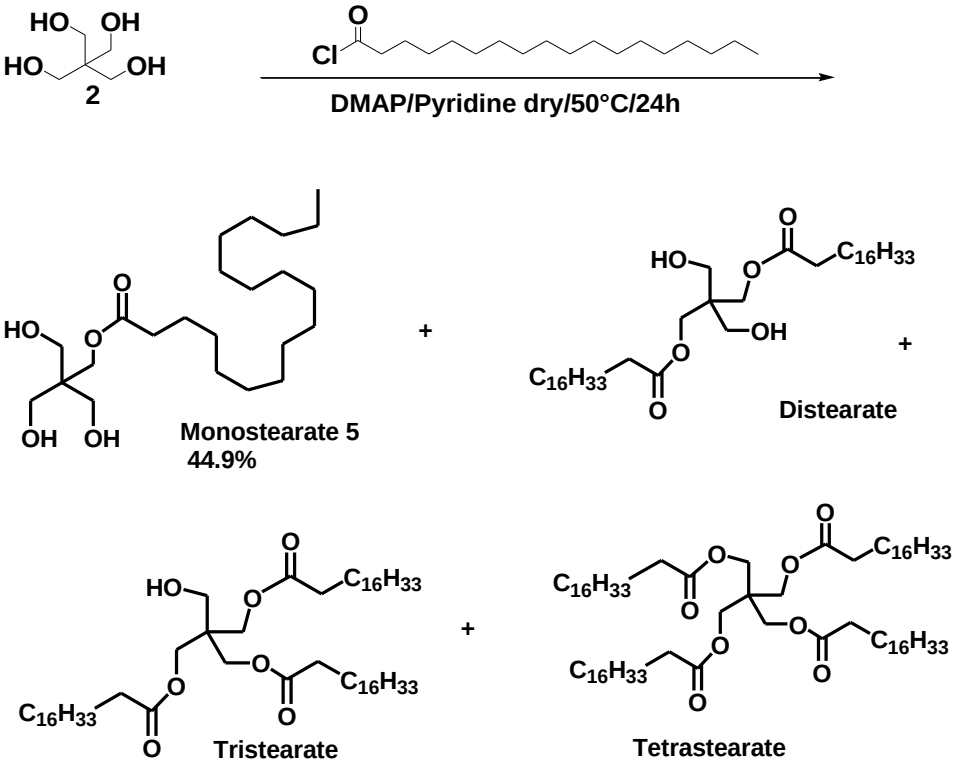

Scheme 15

In both cases the crude was subjected to silica gel column chromatography[216] (petroleum ether/Et_2O/MeOH). Regarding the crude obtained from esterification reaction of **1**, a single column allowed the separation of the tri-ester (petroleum ether / Et_2O = 1:1; 19%), of the di-ester (Et_2O = 100%; 41%) and of the desired mono-ester **4** (Et_2O / MeOH = 95:5; 44%). The three compounds were characterized by FTIR, ^1H and ^{13}C NMR techniques and Elemental analysis.

For example, in the FTIR spectra of all three stearates there was an ester peak at 1722-1736 cm^{-1} but, in the monostearate spectrum, two bands related to the two OH groups at 3412 and 3271 cm^{-1} were appreciated and in the single spectrum band at 3431 cm^{-1}, in the spectrum of the triester this band was totally absent.

However, it was mainly the ^1H NMR spectra that allowed us to confirm the three structures (Figure 31). The monostearate spectrum showed OH signal as a triplet at 2.70 ppm. This signal, which can be integrated for two protons, disappeared in a subsequent deuteration experiment. With the same value of integrals the singlet of CH_2OC = O, the triplet of CH_2C = O and the multiplet of CH_2CH_2C = O respectively 4.21, 2.36 and 1.63 ppm were visible;

between 3.48 and 3.60 ppm one could appreciate the copolymer of the diastereotopic methylenes of the two CH_2OH, a signal that became a simple quartet with a marked roof effect following deuteration, since the coupling with hydroxyls was no longer necessary. The very intense peak of all hydrocarbon chain methylenes with 28 protons integral fell to 1.26 ppm, while the CH_3 triplet of the stearate and the CH_3 singlet of the core in a 1:1 ratio were respectively at 0.88 and 0.84 ppm (Figure 31a). The diester spectrum presented mostly analogous signals for δ values, but less complicated and with different integral ratios. It was not possible to determine the single hydroxyl signal, but the singlet of the CH_2OH group was integrable for two protons at 3.39 ppm, while double integration was obtained for the singlet of the $CH_2OC = O$, the triplet of the $CH_2C = O$ and the multiplet of $CH_2CH_2C =$ or respectively at 4.03, 2.33 and 1.62 ppm. The peak of the methylenes of the hydrocarbon chains with integral of 56 protons fell to 1.25 ppm, while the triplet of the CH_3 of the stearate and the singlet of the CH_3 of the core in a 2:1 ratio between them stood at 0.88 and 0.96 ppm respectively (Figure 31b). Finally, in the triester spectrum, the peak of the CH_2OH group was obviously absent; the singlet of the $CH_2OC = O$, the triplet of the $CH_2C = O$ and the multiplet of the $CH_2CH_2C = O$ integrable each for six protons were respectively 3.93, 2.24 and 1.54 ppm; the peak of all the methylenes of the three hydrocarbon chains with integral of 84 protons fell to 1.19 ppm while the CH_3 triplet of the stearates and the CH_3 singlet of the core in a 3:1 ratio were respectively at 0.81 and 0.94 ppm (Figure 31c).

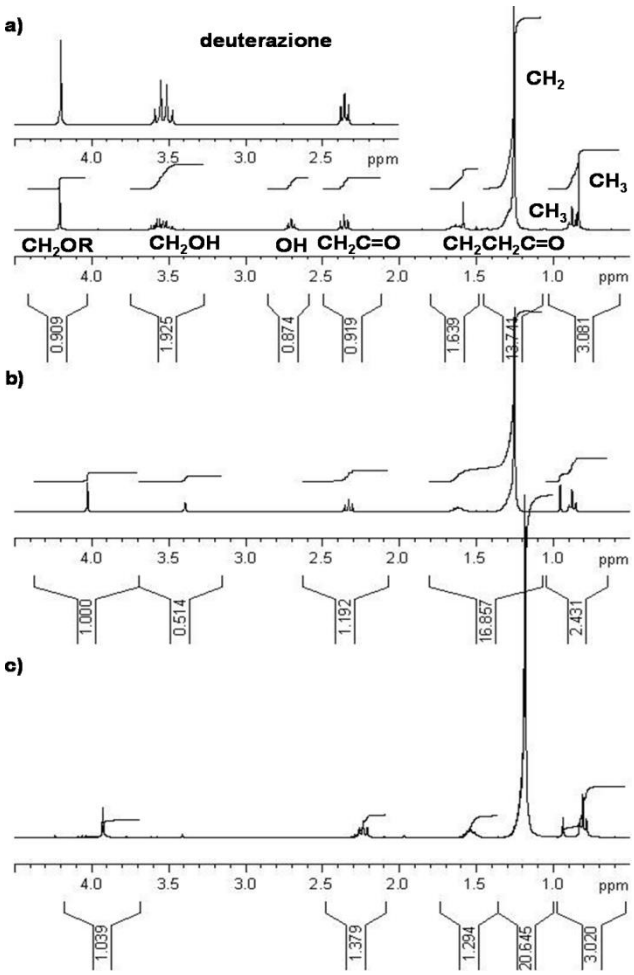

Figure 31. Comparison between ^{1}H NMR spectra of monostearate (a), distearate (b) and tristearate (c).

In order to avoid this laborious chromatographic work and therefore reduce preparation times and costs, aspiring also to increase the yield, we have tried to prepare the monoester **4** also according to another procedure.[217, 218] This initially provided for the protection of **1** at one to two of the hydroxyls as benzylidene through a common reaction of formation of cyclic acetals starting from 1,2- or 1,3-diols, then the esterification of the residual hydroxyl with the chloride **3** and finally the deprotection of the compound obtained to free the OH groups and obtain **4**. To implement this protocol, **1** in anhydrous THF was treated with benzaldehyde added dropwise in presence of p-toluenesulfonic acid as a catalyst[219] (Scheme 16).

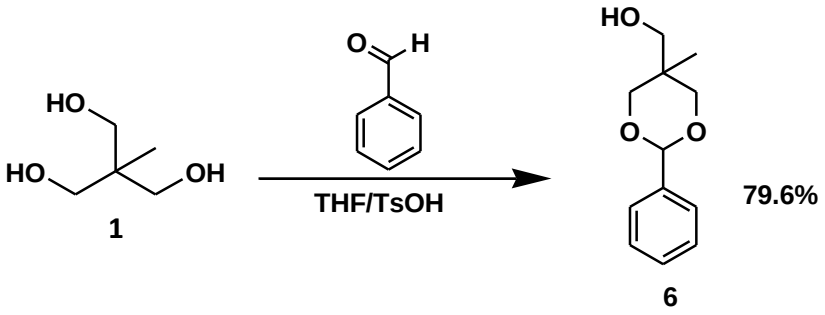

Scheme 16

After one night at r.t. the reaction mixture was then treated with aqueous ammonia and after evaporation, dissolution in DCM, washing with water, drying of the organic phases on $MgSO_4$ and elimination of solvents under reduced pressure, **6** was obtained as pyridine smelling oil and was crystallized from toluene / n-hexane to obtain the (5-methyl-2-phenyl- [1,3] dioxane-5-yl) -methanol **6** as a white crystalline solid with an 80% yield. This compound was analyzed by FTIR and NMR techniques which gave results in perfect agreement with the data present in the literature and confirmed its structure. **6** was then used in the subsequent esterification reaction with **3** followed by deprotection of the hydroxyls[234] (Scheme 17).

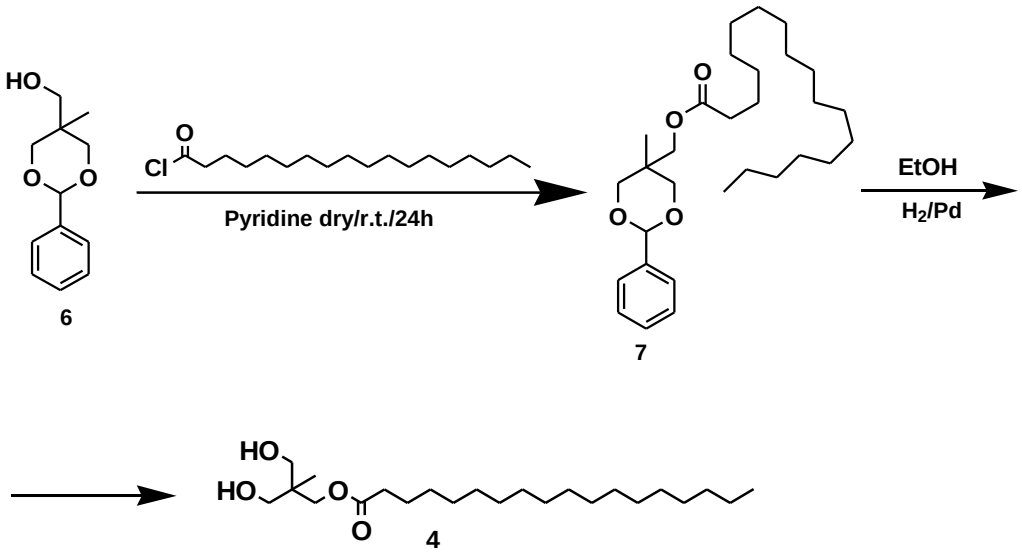

Scheme 17

The (5-methyl-2-phenyl- [1,3] dioxane-5-yl)-methanol dissolved in anhydrous pyridine was treated with **3** added dropwise at 0 ° C, so it was left to r.t. for 1h 30 '. The FTIR performed on a drop of solution had shown the total absence of the chloride band at 1802 cm^{-1}

and the presence of the ester band at 1736 cm^{-1}, then the reaction was interrupted and the crude product obtained as oil orange has been crystallized with petroleum ether. The obtained solid was then filtered, washed with water to remove the residual pyridine and then recrystallized from MeOH to obtain **7** as a dark crystalline solid from a weakly colored with a yield of 73%. After the FTIR and NMR spectra had confirmed the structure, **7** was subjected to deprotection by catalytic hydrogenation (Pd/C 10%) with H_2 at 1.5 atm in 100% EtOH at r.t. After filtration of the catalyst on silica plug and removal of the solvent, a colorless oil was obtained which solidified by cooling to a waxy solid. This material was subjected to recrystallization tests from EtOH / H_2O and subsequently from 100% EtOH obtaining a white crystalline solid whose FTIR and NMR spectra were unfortunately identical to those of the precursor **6**, highlighting the unforeseen deprotection. Even subsequent attempts to deprive of **6** with acid resins, a procedure known to us and widely used to deprotegate dendrons and dendrimers in the form of acetone to free the hydroxyls, have been unsuccessful, even leading to total degradation of the structure of the precursor. In light of these facts, no other reactions have been tried, thus preferring the direct esterification procedure of **1** previously described.

In the case of the esterification of **2**, in order to obtain the monoester **5** sufficiently pure in order to be used in esterification reactions with the dendrons, two column purifications were necessary. Attempts to recrystallize the product obtained after a first chromatographic separation from both MeOH and acetone did not lead to acceptable results. The first chromatographic column allowed the mixture separation of the tetrasubstituted compound, of the triester and of a large part of the diester in the fractions eluted with petroleum ether/Et_2O mixtures with increasing gradient of Et_2O and with MeOH increasing gradient Et_2O/MeOH mixtures, while from the fractions eluted with 100% Et_2O, the monoester **5** still polluted with traces of diester (328.9 mg) was obtained. The second column was necessary to separate the distearate in the fractions of the head and obtain the monoester (45%) from the tail fractions. The NMR spectra confirmed its structure and in particular in the ^1H NMR spectrum the signals in 3:1 ratio of the protons of CH_2OH to 3.64 ppm and of $CH_2OC=O$ to 4.17 ppm were clearly visible. At lower values than δ the signals of all the methylenes are instead found: the methylene triplet near the C = O at 2.34 ppm, the next methylene signal in the form of a multiplet at 1.62 ppm and the very intense signal of all the others CH_2 at 1.25 ppm. Finally at 0.90 ppm the signal of the only CH_3 that closes the hydrocarbon chain (Figure 32) is visible.

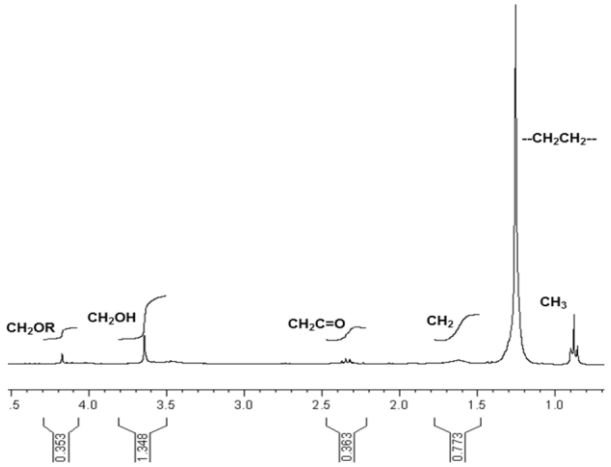

Figure 32.[1]H NMR of **5**

3.3. Synthesis of Dendrons

The structure of the monomer bis-HMPA and dendrons **8**, **11** necessary for the functionalization of compounds **4**, **5** and the intermediates **9** and **10** were shown in Figure 33.

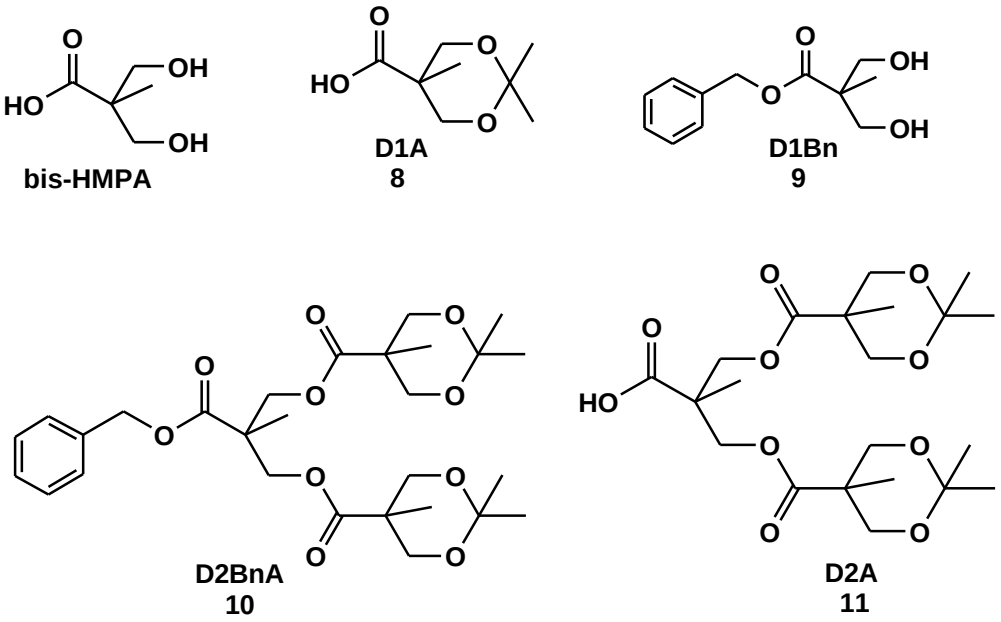

Figure 33. Structure of bis-HMPA and its dendrons derivatives **8-11**

Dendrons **8-11** were prepared starting from the *bis*-HMPA according to Ihre and Hult[178] procedure which has already been used extensively in the preparation of the previous dendrimers. This involves the combination of two divergent and convergent synthetic approaches through a series of selective activation / protection reactions at focal points of the bis-HMPA. The monomer bis-HMPA was reacted with 2,2-dimethoxypropane in anhydrous acetone in presence of p-toluenesulfonic acid (TsOH) as a catalyst to give the acetonidic dendron D1A **(8)** in the form of carboxylic acid as a white solid and degree of satisfactory purity without further purification.

The bis-HMPA was then reacted with benzyl bromide in DMF anhydrous, in a basic environment, to give the benzyl dendron D1Bn **(9)** as oil and subsequently crystallized as a white solid (Scheme 18).

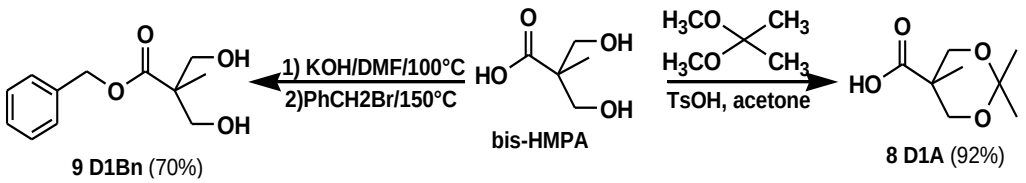

Scheme 18

Since dendrons **8** and **9** are the fundamental units that will give rise to the next more complex second generation dendron, the interpretation of their NMR spectra is very important.

The ^{1}H NMR spectrum of **8** (Figure 34) shows the methyl signal in α to the group carboxylic acid at 1.20 ppm, the methyl signals on acetal carbon at 1.42 and 1.45 ppm and the methylene protons signals of the 1,3-dioxane system at 3.68 and 4.20 ppm, each in the form of doublets with J of 12 Hz.

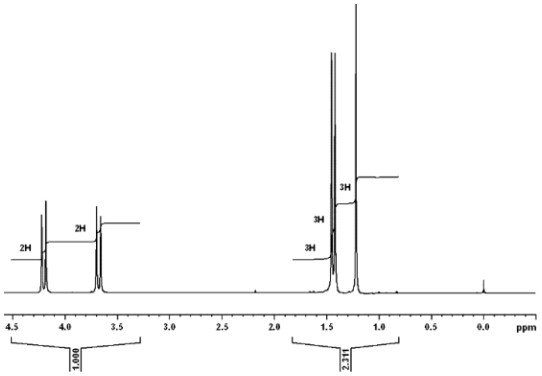

Figure 34. ^{1}H NMR spectrum of **8**

The ^{13}C NMR spectrum contains the signals of all seven carbons of **8** (Figure 35). Note the three distinct methyl signals on the 1,3-dioxane system: at 21.96 and 25.12 ppm those on acetalic carbon and at 18.39 ppm that in α to the carboxylic group.

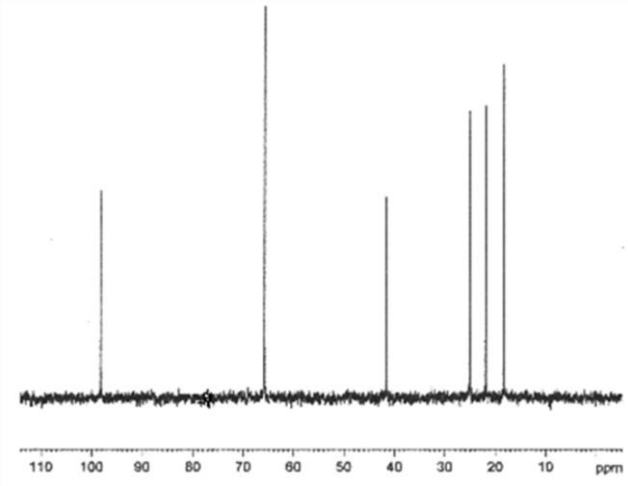

Figure 35. ^{13}C NMR spectrum of **8**

The ^{1}H NMR spectrum of **7** (Figure 36) shows a single singlet signal for the methyl in α to the carboxyl at 1.09 ppm, the signals in the form of doublets of the methylenes bound to the hydroxyls at 3.72 and 3.92 ppm in analogy with the spectrum of **8**, with respect to which the benzene methylene singlet at 5.19 ppm is enriched, of the aromatic system multiplex at 7.35 ppm and of the singlet relative to the two OH at 3.00 ppm.

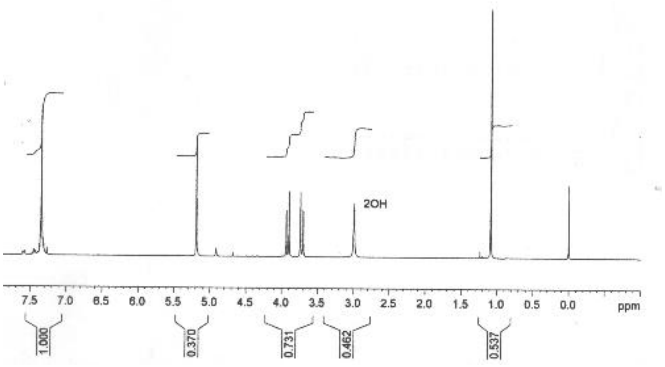

Figure 36. ^{1}H NMR spectrum of **7**

Also the ^{13}C NMR spectrum of **9** (Figure 37) is simplified between 10 and 30 ppm where only the methyl signal in α to the carboxylic group appears at 17.16 ppm and around 100 ppm where the acetonide quaternary carbon signal is no longer present, but the 66.63 ppm signal of benzene methylene and the four distinct signals between 127.66 and 133.30 ppm of the aromatic carbons are enriched.

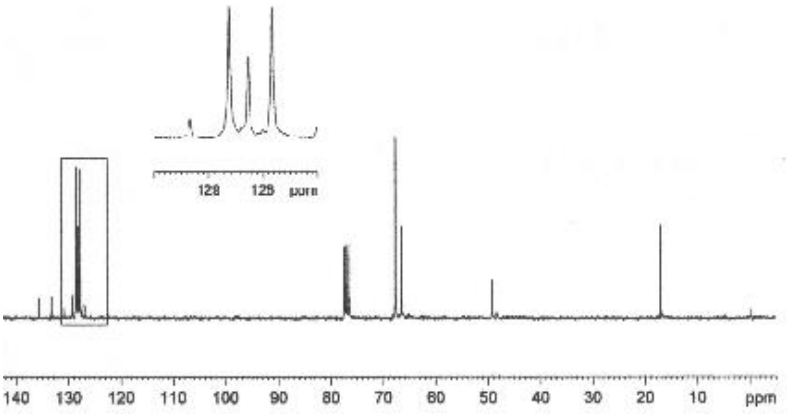

Figure 37. ^{13}C NMR spectrum of **9**

First generation dendrons **8** and **9** were subsequently used in the synthesis of the totally protected second generation Dendron D2BnA **(10)** obtained by esterification in dichloromethane in the presence of *N, N'*-dicyclohexylcarbodimide (DCC) and of the salt *p*-toluenesulfonate of 4- (*N, N'*-dimethylamino) pyridinium (DPTS) as a catalyst.

The dendron **10** was then deprotected to the carboxyl group by hydrogenolysis reaction with H_2 in presence of 10% Pd/C as a catalyst in AcOEt, to obtain the debenzylated derivative D2A **(11)** in the form of viscous oil (Scheme 19).

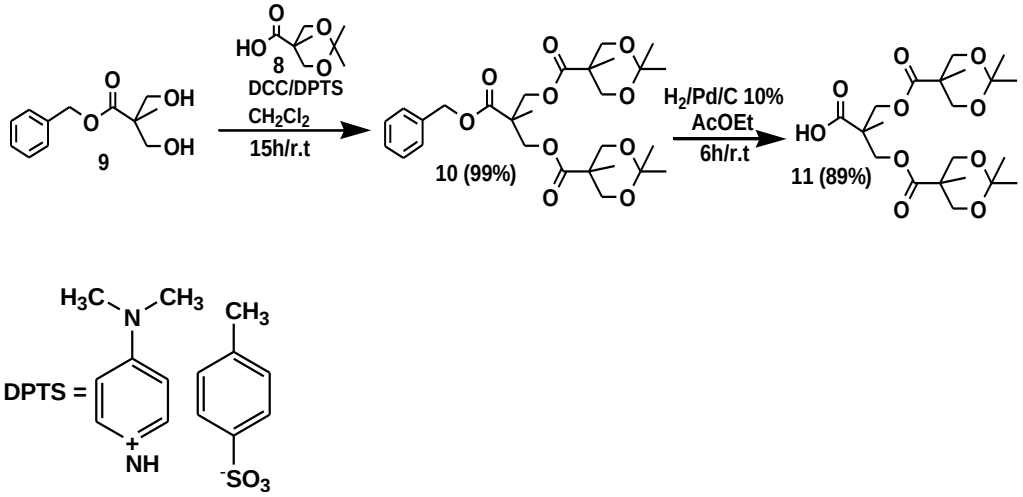

Scheme 19

DPTS[221] was prepared by reaction of the TsOH, anhydrified by azeotropic distillation in benzene, with 4- (*N, N'*-dimethylamino) pyridine (DMAP) and subsequent crystallization of the crude salt using the solvent/non-solvent pair $CHCl_3/CCl_4$ and was preferred to 4- (*N, N'*-

dimethylamino)-pyridine (DMAP) as it limits the formation of significant amounts of N-acylureic adduct of **8** (Scheme 20, A). In fact, the preparation of **10** involves the formation of by-products including precisely (A) resulting from a rearrangement reaction of the activation product of **8** with DCC (O-isoacylurea) and/or its anhydride (Scheme 20, B). For these reasons the purification of **10** has involved the use of a chromatographic column on silica gel using a petroleum ether/AcOEt mixture as eluent to eliminate such by-products, in addition to the unreacted DCC, which are collected in the fractions of the head.

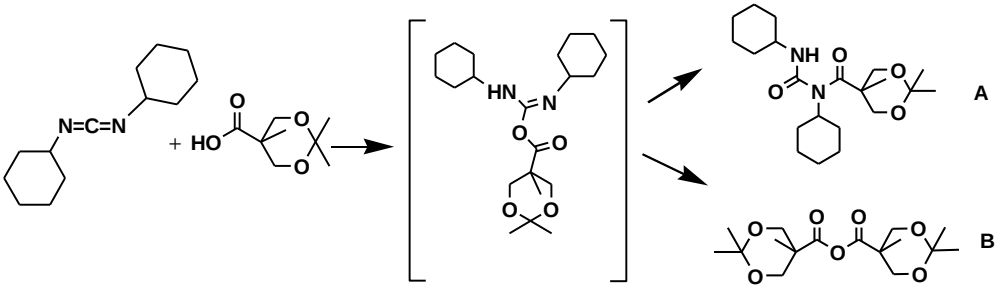

Scheme 20

The commercial DCC, which has the purpose of activating the carboxyl group to promote the esterification reaction, is added lastly by noting the immediate formation of a suspension due to dicyclohexylurea (DCU), which precipitates as a white solid.

Having grown one generation, in the ^{1}H NMR spectrum of **10** the peaks of CH_3 acetonide continue to remain two, but double the value of their integral, while the zones of CH_3C and CH_2O are enriched both by a singlet integrable for 6 and for 8 protons. **11** or in sequence before **8** and then **11** have been used in esterification reactions of monostearate **4** obtaining two types of new amphiphilic dendrimers which, as regards their two-fan dendrimal portion, can be classified second and third generation. Using both **8** and **11** in successive esterification reactions of **5**, a third generation fan-shaped dendrimal frame portion was constructed obtaining a third new amphiphilic dendrimeric scaffold.

3.4. Esterification of 2,2-bis(hydroxymethyl)propan-1-ol mono-stearate (4)

4 was esterified with an excess 2:1 of **11** in presence of DCC, DPTS in DCM at room temperature for 24h obtaining after chromatographic column (petroleum ether/AcOEt) from the fractions eluted with petroleum ether/AcOEt 1:1 the compound **12** in the acetonide form (98%). After deprotection with acidic resins in methanol, **12** provided the new second generation amphiphilic hydrid dendrimer **(13)** having a hydrophobic hydrocarburic chain of 18 carbon atoms and further functionalizable peripheral hydroxyls (Scheme 21).

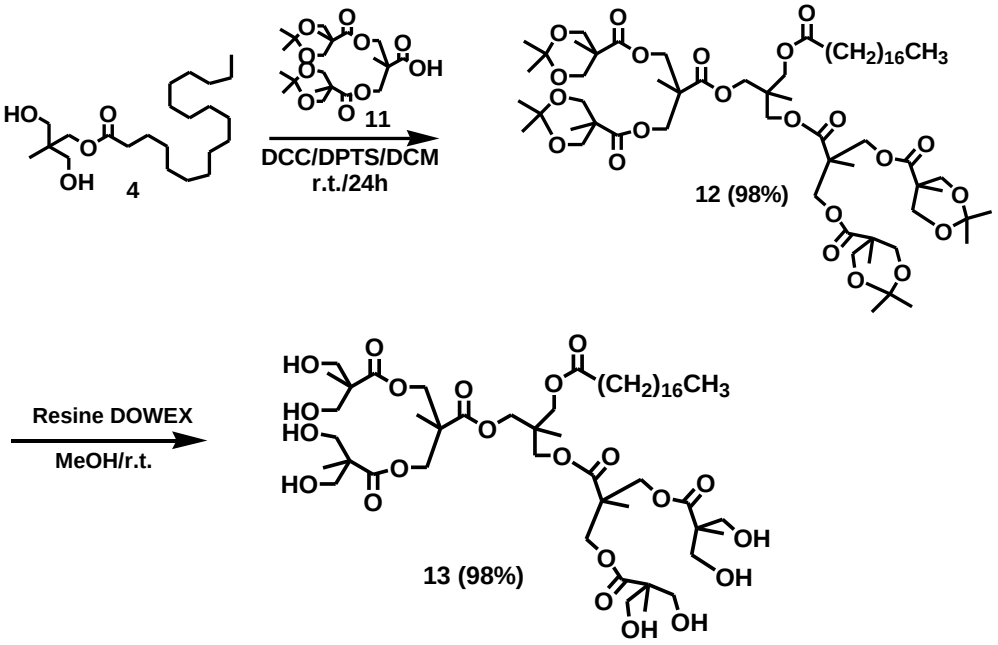

Scheme 21

In another preparation **4** was reacted under the same conditions (DCC/DPTS/DCM) with an excess 2:1 of the first generation dendron **8**. The product **14** obtained after column (petroleum ether/AcOEt 4:2 and 3:2) with 87.4% yield was deprotected with acid resins to obtain the intermediate **15** having 4 free hydroxyls. These were exploited in a subsequent esterification reaction with **11** always using DCC/DPTS. After purification by chromatographic column (petroleum ether/AcOEt 1:1 and AcOEt 100%) **16** was obtained and was subsequently deprotected to the acetonides in the usual conditions providing the second type of new hybrid amphiphilic dendrimer (**17**) this time of third generation and having as many as 16 functionalizable hydroxyls in the periphery (Scheme 22).

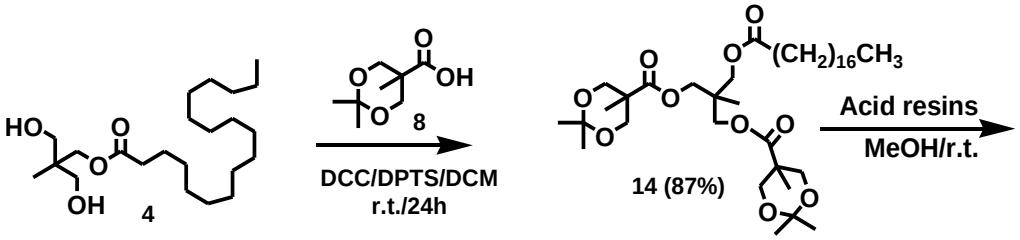

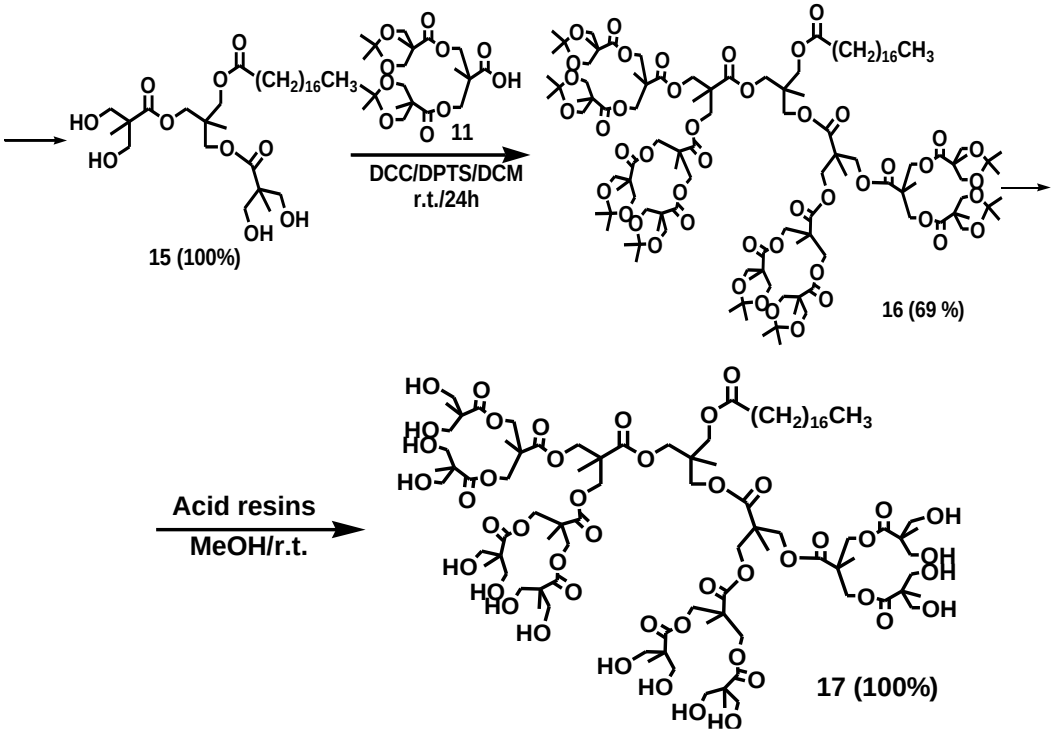

Scheme 22

3.5. Esterification of 2,2-bis(hydroxymethyl)-1,3-propanediol mono-stearate (5)

5 was esterified to the three free hydroxyls with an excess 3:1 of **8** in presence of DCC, DPTS in DCM at room temperature for 24 h. The crude was subjected to a chromatographic column eluent with a petroleum ether/AcOEt mixtures with increasing gradient of AcOEt and from the eluted fractions with the combined 3:2 and 1:1 mixtures, and the dendrimer **18** was obtained (65%). **18** was then deprotected with acid resins in MeOH for 24h at room temperature obtaining the compound **19** having 6 free hydroxyls in almost quantitative yield (95%). The hydroxyls of **19** were then again esterified with **11** (ratio 6:1) under the usual conditions, but using a mixture 27:1 of DCM/DMF in order to obtain a homogeneous solution of **19** not completely soluble in dichloromethane alone. The crude was again chromatographed on a column obtaining from the fractions eluted with 100% ethyl acetate the third generation dendrimer **20** (35%) in the acetonide form and after its deprotection in the usual acid conditions provided, the third generation amphiphilic dendrimer **21** (100%) with 24 free hydroxyls exploitable in future functionalizations with amino acids (Scheme 23).

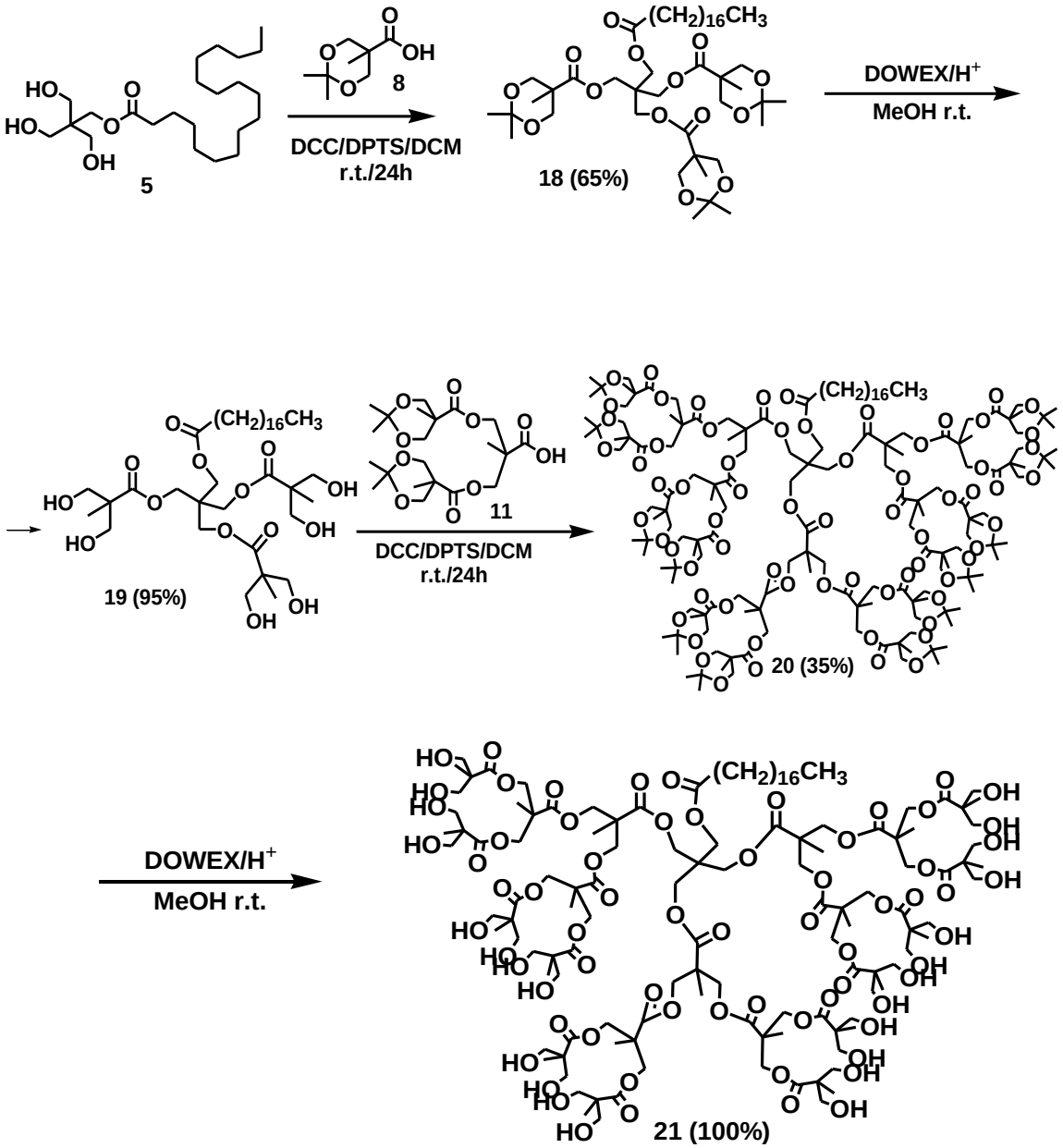

Scheme 23

All the steps of esterifications of **4** or **5** were monitored by FTIR and NMR techniques. The ^{1}H NMR spectra performed for all the compounds obtained were very useful to verify the correct behavior of the reactions and to confirm the structures of intermediates and products. By way of example Figure 38 shows how the spectrum of monostearate **4 (a)** is modified when it is esterified with the dendron D1A obtaining **14 (b)** and how the spectrum of the product obtained in turn changes after deprotection to the acetonides **15 (c)**. In particular, esterification leads to the disappearance of the CH_2OH multiplet (δ = 3.48-3.60 ppm) and of the hydroxyl triplet (δ = 2.70 ppm), while next to the CH_2O signal esterified with the C18 chain (δ = 4.12 ppm) the signals of the $CH_2OC = O$ of the core appear (δ = 4.04-4.07 ppm)

bringing the value of the integral from 2 to 6, and the two doublets with J of 12 Hz of the CH_2O of the 1,3-dioxane rings integrable for 4 appear + 4 protons (δ = 3.65 and 4.18 ppm). At high spectrum fields are then visible the new two singlets of CH_3 acetonide integrable for 6 + 6 protons (δ = 1.36 and 1.42 ppm) and the split singlet probably due to the stiffness of the CH_3 molecule of D1 integrable for 6 protons (δ = 1.19 and 1.20 ppm). Obviously, these characteristic signals of the cyclical acetal return to disappear in the spectrum of the deprotected compound, where we find instead the multiplet of the CH_2OH groups that can be integrated by eight protons (δ = 3.77 ppm).

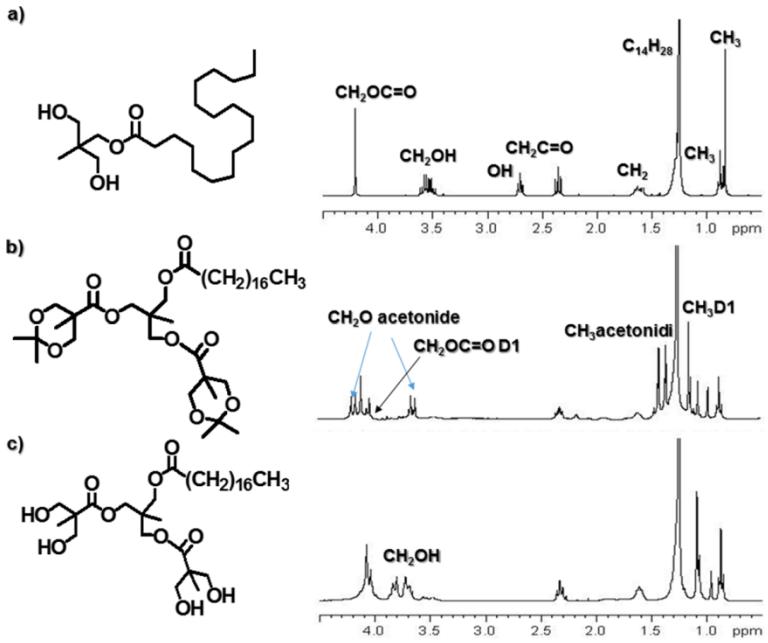

Figure 38.spectra of **4** (a), **14** (b), and **15** (c)

Figure 39 instead shows the changes that occur when **15** (a) where the signal of CH_2OH integrable for eight protons is present (δ = 3.77 ppm) is again esterified with **11** to give **16** (b) in whose spectrum reappear the signals of both CH_3 that of the acetalic CH_2O and subsequently shows the disappearance of such signals and the reappearance of the CH_2OH signal in the spectrum of its deprotection product (**17**) (c). Similar changes are observable in the spectra of **12** and **13**.

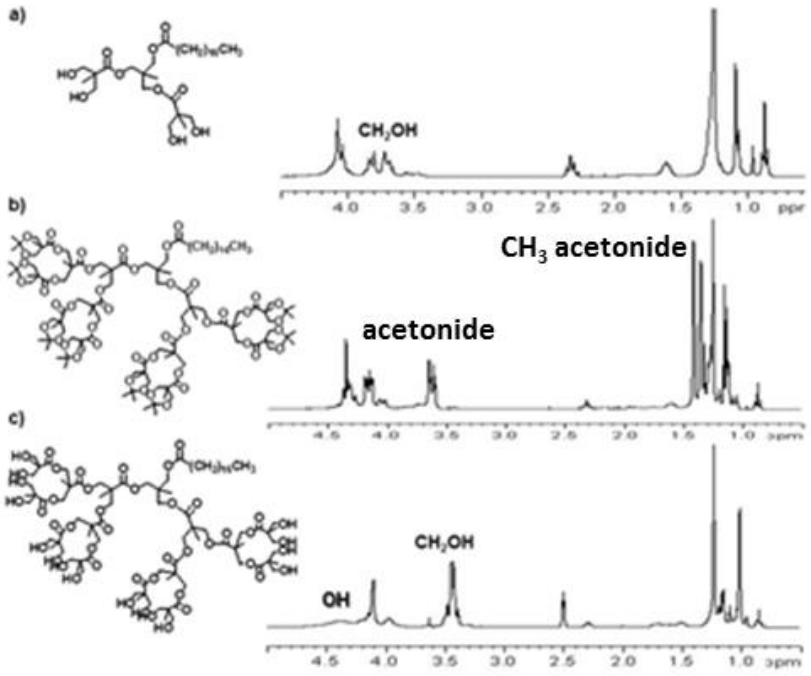

Figure 39.[1]H NMR spectra of **15** (a), **16** (b) and **17** (c)

Figures 40 and 41 show how similarly the spectra of **5** are modified to give **18**, and of **18** if it is deprotected at **19**, of **19** when it is esterified at **20** and of the latter when it is deprotected to the final dendrimer **21**.

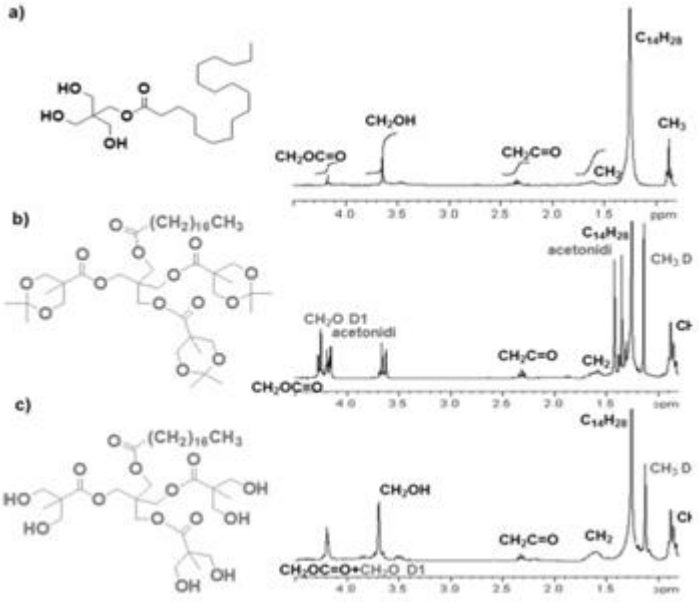

Figure 40. [1]H NMRSpectra of **5** (a), **18** (b) and **19** (c)

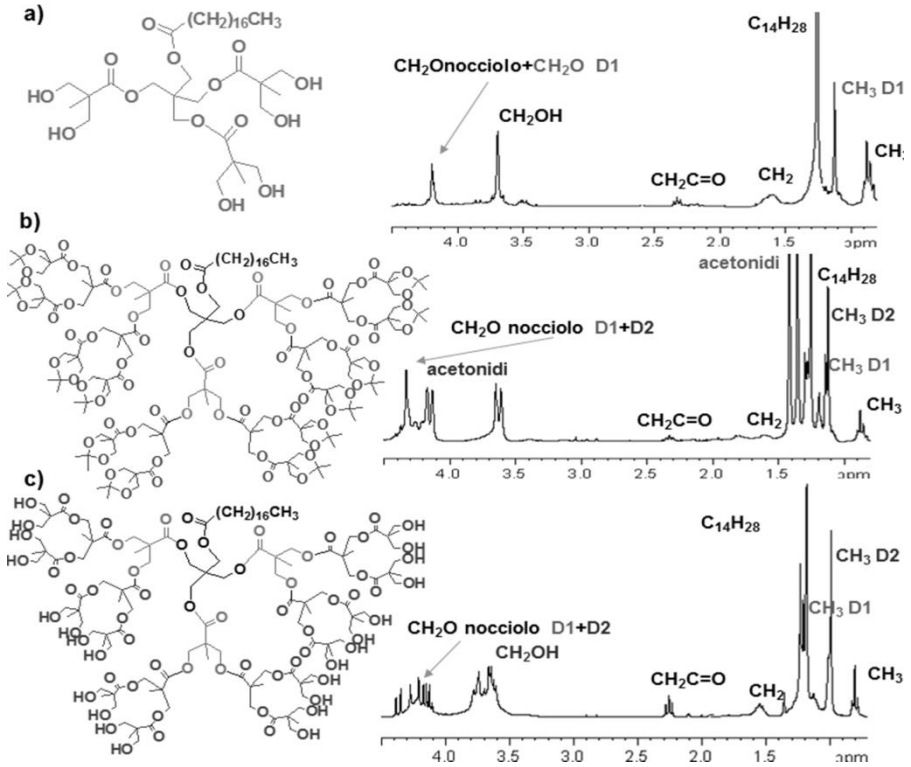

Figure 41.[1]H NMR Spectra of **19** (a), **20** (b), and **21** (c)

3.6. Functionalization reactions of amphiphilic dendrimer scaffolds with amino acids

At this point, the subsequent step was the functionalization of the new amphiphilic dendrimers on their periphery with amino acids arginine, lysine or a mixture of amino acids. So we needed to conceptualize and optimize a synthetic and versatile procedure allowing the functionalization by esterification reactions our polyester scaffolds with several peripheral hydroxyls on one side with *L*-arginine and *L*-lysine and on other side with a mixture of four amino acids appropriately selected (*L*-arginine, *L*-lysine, *N,N'*-dimethylglycine, *N*-methylglycine). The four amino acids (Figure 42) were selected to insert onto the not charged polyester scaffold, differently protonable basic residues, and *L*-arginine guanidine group, in order to promote electrostatic interactions with genetic materials, drugs and membrane lipids and in order to obtain a good buffer capacity with the result of an increased transfection activity and residence time. Except for DMG, the amino acids were used in their protected forms to the basic nitrogen atoms to avoid unpleasant interfering side reactions.

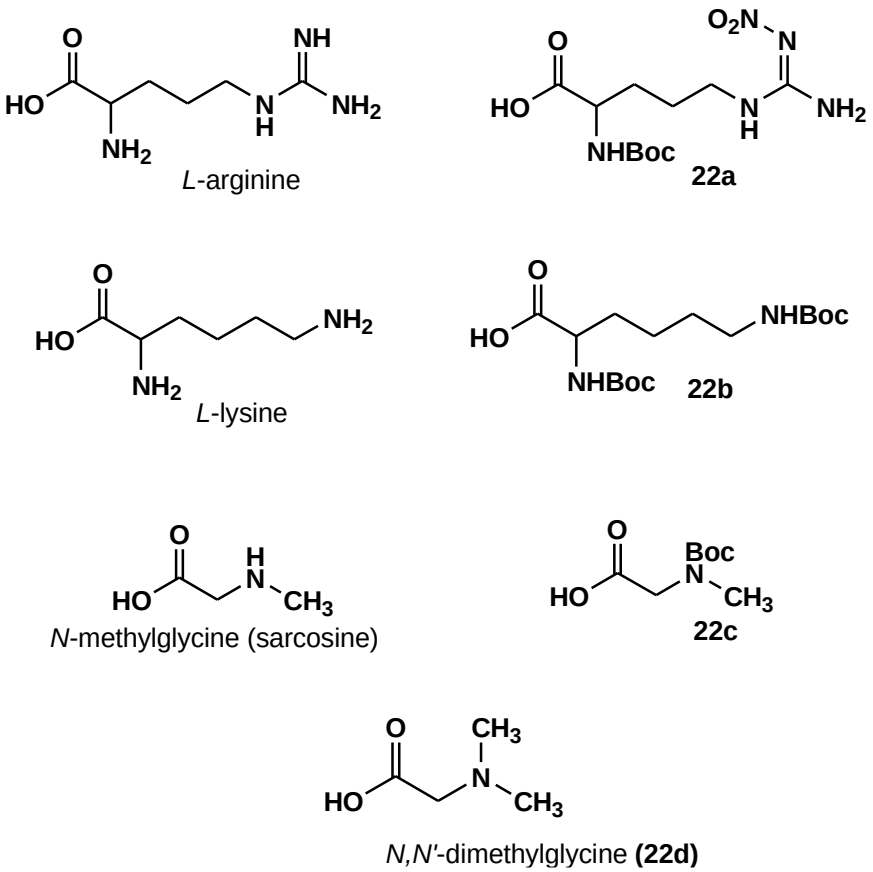

Figure 42. Amino acids for the functionalization

The fourth generation dendrimer **G4OH** prepared according to a reported procedure[204] and having 48 peripheral hydroxyls (Figure 43) was chosen as dendrimer scaffold. Before subjecting this dendrimer to the delicate functionalization reactions, the MALDI-TOF spectrum was acquired in order to have more certainties on its structure. From the performed experiments, two were the successful and optimized methods which allowed us to obtain the desired materials.

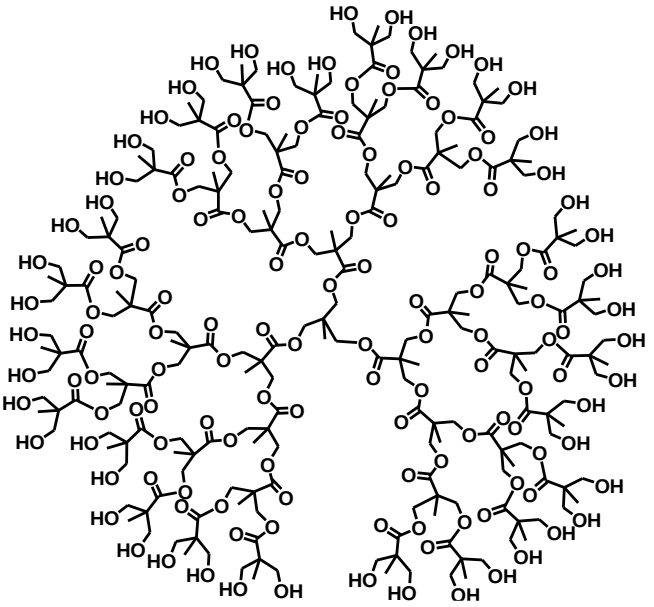

Figure 43. Structure of G4OH

3.6.1. Method 1

Past experiences made during the first stage of this research line had revealed us the complete inertia of DMG in esterification reactions of polyester dendrimers or more simple structures as first generation dendrons both using the EDC/DMAP/DMF system and the DCC/DMAP/DMF one.

On the other hand, it is known that the efficiency of transfection of a delivery system depends, on an adequate buffer capacity of the polycationic polymer or dendrimer.[222] Thanks to its buffering power, the synthetic carrier, once inside the endosome, can act as a "proton sponge" and causes its rupture. Commercial PEIs are characterized by very good transfection activity and are regarded as very efficient "proton sponges", because of the presence of several secondary and tertiary amino groups in their matrix.[223] Hence, the interest in decorating dendrimer scaffolds also with DMG and MG, never used by us to prepare hetero dendrimers, alongside *L*-lysine and *L*-arginine was born. If lysine and arginine contribute to provide three types of primary amine groups which favor electrostatic interactions and to supply the guanidine group whose importance is well known,[224] the addition of DM and DMG would have improved the buffer capacity and consequently the transfection efficiency.

An appealing strategy to overcome the obstacle of DMG's inertia was developed, and the "problematic" amino acid was built piece by piece on dendrimer architecture in a two-step reaction. This idea involved the esterification of **G4OH** with a studied amount of

α-bromoacetic acid (AcBrOH) and subsequently the bromine replacement with the dimethylamino group by reaction with N,N'-dimethylamine hydrochloride (DMA HCL). In such a way, the DMG residues have been attached to G4OH.

❖ *Functionalization of G4OH with α-bromoacetic acid **(23)**: preparation of AcBr-modified polyhydroxylated dendrimer **(24)***

To manage at esterifying **G4OH** having 48 peripheral hydroxyls with approximately 10 units of AcBr and to obtain a product with approximately 38 residual hydroxyls, the dendrimer was treated with 20% mol/OH free x 1.05 equiv. of AcBrOH **(23)**. AcBrOH was in turn obtained by treating a mixture of acetic acid (AcOH), acetic anhydride (Ac_2O), and pyridine with a Br_2 solution added drop-wise.[225a] Elemental analysis and spectral data, which were in agreement with the literature data, confirmed the structure.

The esterification reaction of **G4OH** was performed both with N-(3-dimethylaminopropyl)-N'-ethylcarbodiimide hydrochloride (EDC)/DMAP/DMF and DCC/DPTS/DCM/DMF (Scheme 24) systems, and **Table 2** shows the results obtained.

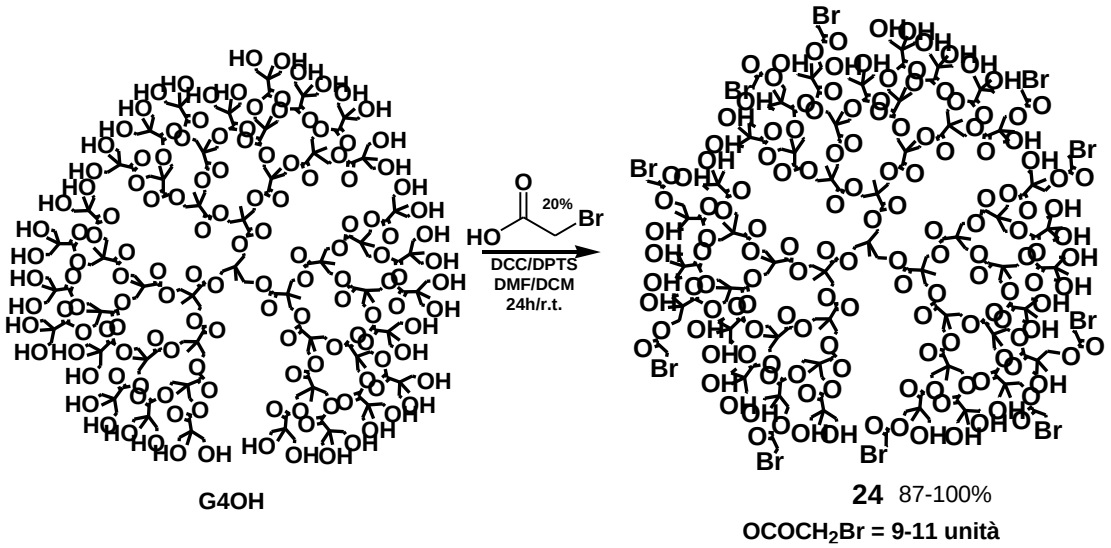

Scheme 24

Table 2. Results from esterification reactions of G4OH with AcBrOH (23) in different conditions.

G4OH [mg, mmol]	AcBrOH (23) [mg, mmol]	System [Time/°C]	24 [mg, mmol]	Yield [%]	AcBr Units[a]
101.4, 0.0190	26.6, 0.1910	EDC/DMAP/DMF 24 h/r.t	39.7, 0.0061	**32**	**10**
177.6, 0.0332	46.5, 0.3347	DCC/DPTS DCM/DMF 3/2 24h/r.t.	216.3, 0.0330	**99**	**10[b]**
213.2, 0.0399	55.9, 0.4020	DCC/DPTS DCM/DMF 3/2 24h/r.t.	231.2, 0.0340	**87**	**11**
226.3, 0.0423	59.3, 0.4267	DCC/DPTS DCM/DMF 3/2 24h/r.t.	280.4, 0.0420	**98**	**11**
233.8, 0.0437	61.3, 0.4409	DCC/DPTS DCM/DMF 3/2 24h/r.t.	276.7, 0.0430	**98**	**9**

[a]Estimated by ^{1}H NMR spectra
[b]Compounds employed in following reactions of bromine exchanged with DMA HCl

The last column of **Table 2** shows that the number of units of AcBrOH that entered onto the dendrimer was reproducible and respected the percentage of acid used and expectations (9-11 equiv. of AcBr moieties per dendrimer mole depending on preparation), while the yields of the product obtained with DCC/DPTS were much more higher than with EDC/DMAP.

Such results are attributed to the different way employed to isolate the crude from the reaction mixture. When basic EDC was used, as literature suggests, the hydrolysis with 10% $KHSO_4$ to eliminate all basic side products obtaining the sufficiently pure desired product without need of further purification was made. But, presumably, because the bromine group can act as a good outgoing group, the acidic aqueous environment was not suitable to **24**. The result was that **24** has hydrolyzed and mostly degraded. When DCC was used, hydrolysis did not occur and **24** did not deteriorate. The compound **24** was analyzed by FTIR and NMR techniques. In particular ^{1}H NMR ($CDCl_3$) analysis was useful to confirm the structure, to evaluate degree of purity, and to estimate its composition on the periphery. As Figure 44 shows, a peak (3.89 ppm) or sometimes two peaks (3.86 and 3.88 ppm) were detectable for the methylene of the AcBr units entered onto the substrate **G4OH**. The possibility of more than one signal for the same group derived from the fact that the distribution of AcBr residues on the 48 hydroxyls of **G4OH** occurred randomly and the product obtained was no longer symmetrical. The δ (ppm) values of these signals were

perfectly in agreement with the literature data for the CH_2Br signal of the ethyl ester of α-bromoacetic acid ($AcBrOCH_2CH_3$, δ = 3.9 ppm),[226] and the number of AcBr units that esterified G4OH was estimated by the integration of these peaks. The ^1H NMR spectrum showed also the constant presence of traces of DPTS as pollutant, but so small that they did not influence the result of elemental analysis. It was perfectly in accordance with that required by the molecular formula estimated by ^1H NMR spectrum and so confirmed the structure of **24**. DPTS traces were eliminated by aqueous hydrolysis after having exchanged bromine with the *N,N'*-dimethylammino group. Because this group is a very bad outgoing group and not susceptible to hydrolysis like bromine, compound **25** was more resistant to hydrolytic treatments. Obviously, no further experiences with EDC/DMAP were repeated.

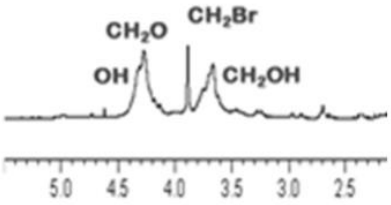

Figure 44. significant part of ^1H NMR spectrum of **24**

*Exchange reaction with N,N'-dimethylamine HCl: preparation of DMG-modified polyhydroxylated dendrimer **25***

A sample of **24** containing 10 AcBr residues (Table 2 second row) dissolved in acetone was treated with *N,N'*-dimethylamine (20.00 equiv.) dissolved in acetone and traces of water where it had been released from its hydrochloride salt for NaOH 1:1 treatment. The reaction occurred after 1 hour at room temperature and when three new bands at 1646, 1628, and 1576 cm^{-1} appeared in the FTIR spectrum (scheme 25).

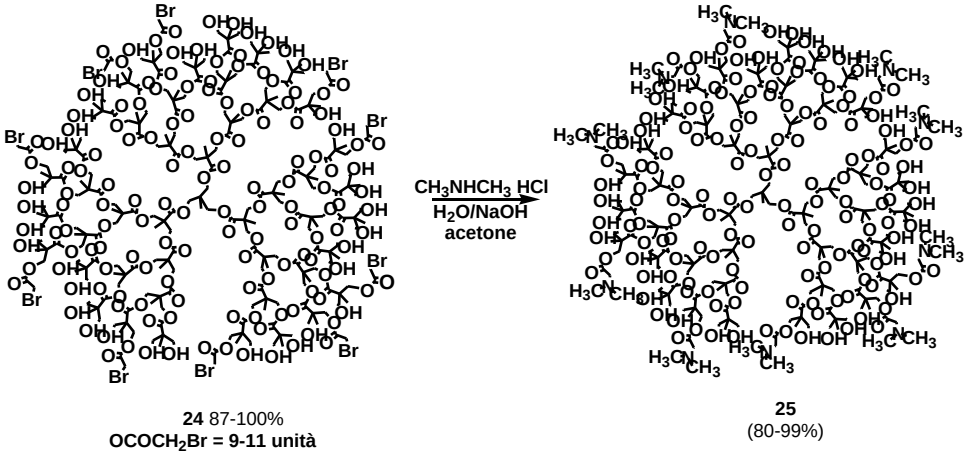

Scheme 25. Synthesis of DMG-modified dendrimer **25**

The compound **25** was obtained as white spongy solid (isolated yield 80-99%). The successful exchange and the structure of **25** were evaluated by ^{1}H NMR analysis which showed the disappearance of the peak at 3.89 ppm, the increase in intensity of the signals already formed in the previous reaction (new CH_2O of the dendrimer), and the appearance of signals around 4.13 ppm (CH_2N groups of the DMG) in such a way created. Furthermore, a new peak for the dimethylamino group (2.89 ppm) and signal sometimes hidden by the signals of DMF difficult to completely remove were appeared (Figure 45). The estimated structure was validated by elemental analysis.

For the good outcome of the exchange, it is recommended to minimize the amount of water used to dissolve the initial hydrochloride and the reaction times. Excessive water content provoked destruction by hydrolysis of the substrate **24** not allowing getting to product **25**.

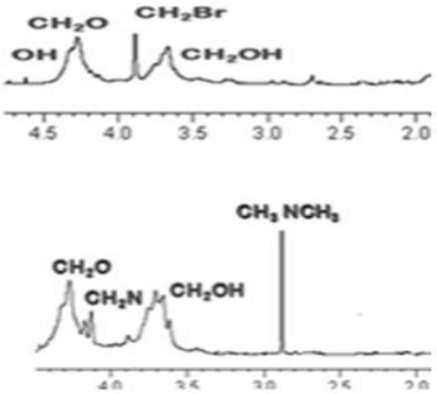

Figure 45. Comparison between significant portions of ^{1}H NMR spectra of **24** (spectrum above) and of **25** (spectrum underneath).

❖ *Functionalization of **25** with $^{\alpha}$N-BOC- $^{\omega}$N-nitro-L-arginine **(22a)**, $^{\alpha}$N,$^{\varepsilon}$N-diBOC-L-lysine **(22b)** and N-BOC-sarcosine **(22c)**: preparation of amino acids- modified dendrimer **26***

This first synthetic pathway designed to introduce the four amino acids on **G4OH** was accomplished in a single passage by reacting **25** having still 38 reactive hydroxyls with $^{\alpha}$N-BOC- $^{\omega}$N-nitro-*L*-arginine **(22a)**, $^{\alpha}$N,$^{\varepsilon}$N-diBOC-*L*-lysine **(22b)** and N-BOC- sarcosine **(22c)** in ratio 10:14:14 (1.05 equiv. in excess), at the same time. A first experiment with EDC/DMAP provided a very complex crude. The reaction was then carried out in the presence of DCC/DPTS system in DMF/DCM 2:3 for 24 hours at room temperature (scheme 26) with better results.

Compound **26** was obtained as glassy solid (48%). It was analyzed with FTIR and then with ^{1}H NMR to confirm definitively the presence of all three amino acids alongside the already present *N,N'*-dimethylglycine **(22d)** and to estimate their ratio.

The FTIR spectrum showed, near the signal at 1740 cm^{-1} (esters), two strong bands at 1712 and 1692 cm^{-1} of the carbamate C=O confirming the presence of the BOC groups, while in ^{1}H NMR spectrum were observable a series of singlet signals relative to the methyl groups of **22c** and **22d** (2.88-2.98 ppm), very broad signals between 3.0 and 3.2 ppm and between 3.2 and 3.5 ppm (CH_2NHBOC of *L*-lysine and CH_2NH of *L*-arginine), signals belonging to the CH_2N of **22c** (3.9-4.1 ppm) and signals relative to CH_2N of **22d** (4.1-4.2 ppm) partially covered by the very broad signal of all the CH_2O groups of **G4OH** (Figure 46).

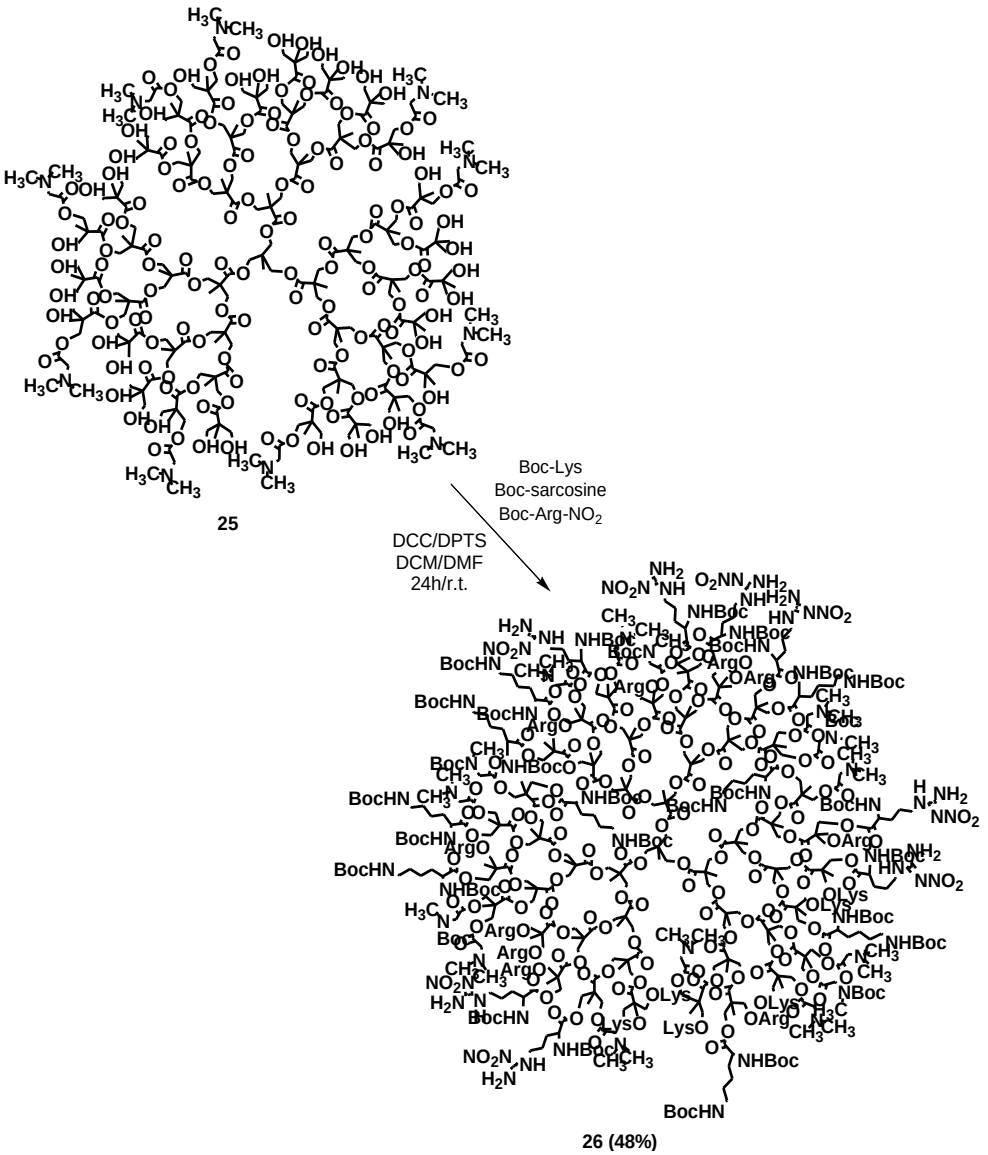

Scheme 26. Synthesis of DMG-modified dendrimer 26

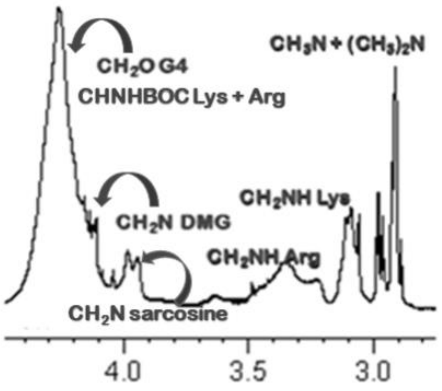

Figure 46. Significant portion of ^{1}H NMR spectrum of **26**

The peripheral amino acid composition of **26** estimated in 10 units of DMG, 5 of MG, 18 of *L*-arginine and 15 of *L*-lysine was deduced from the ratio of the integral values of cited signals. This composition, confirmed also by Elemental Analysis, revealed the greater reactivity of *L*-arginine and *L*-lysine with respect to sarcosine and led us to elaborate a second protocol that took into account this fact. The use of EDC/DMAP was not further investigated and abandoned again.

3.6.2. Method 2

This second procedure starts from **25**, and was designed to prevent the competition of sarcosine **(22c)** with *L*-arginine and *L*-lysine, which showed greater reactivity, with the hope of increasing the number of secondary amino groups of the final cationic compound according to literature suggestions.[223]

- *Functionalization of **25** with 26% N-BOC- sarcosine (**22c**): preparation of DMG and MG-modified polyhydroxylated dendrimer **27***

A sample of **25** containing an estimated number of DMG equal to 11 (Table 2, fourth row) was treated with *N*-BOC-sarcosine **(22c)** 26% (mol/free OH), in presence of EDC/DMAP, obtaining only a little amount (milligrams) of a product containing **22c**. The low yield of this procedure did not allow to make use of it in the subsequent reactions and to achieve the final product. The very low yield of this procedure can be rationally ascribed to the final acid hydrolysis again. In these conditions, the dendrimer basic residues of **22c, 22d** were protonated by $KHSO_4$ and transformed into the water soluble salts and the major

part of the product was confined in the aqueous phase where it was lost. The use of EDC/DMAP was not further investigated and abandoned again. Then, another sample of **25** obtained containing 9 DMG residues as estimated by NMR (Table 2, fifth row) was treated with *N*-BOC-sarcosine at 26% (mol/OH free, 1.05 equiv.) in presence of DCC/DPTS/DCM for 24 hours (Scheme 27).

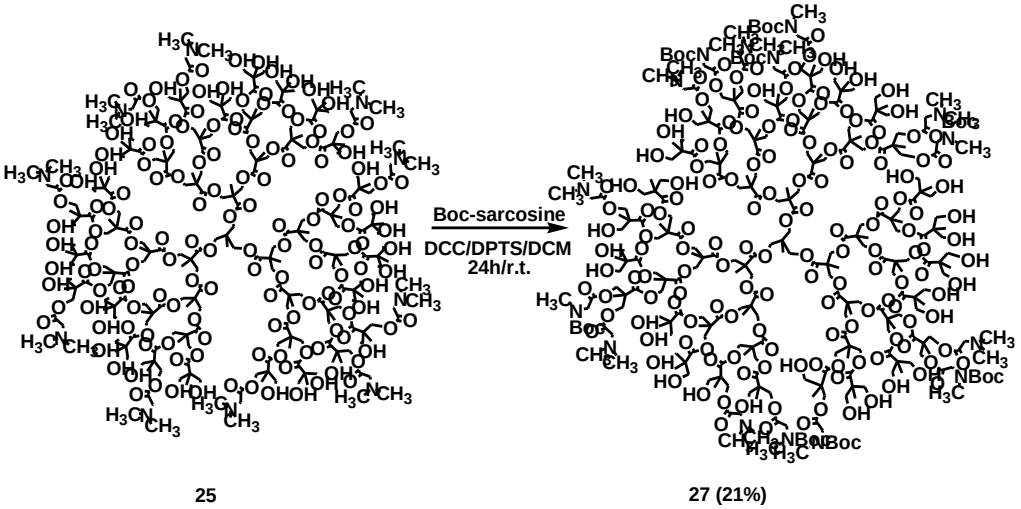

Scheme 27. Synthesis of DMG-MG-modified poly-hydroxylated dendrimer **27**

The crude **27** was obtained as white spongy solid and was treated several times with Et_2O to remove not dendrimer small molecules including a discrete amount of anhydride of **22c** which lowered significantly the yield of **27**, which was firstly investigated with FTIR. The characteristic carbamate band around 1700 $cm^{-1}$was not detectable but the ^1H NMR spectrum confirmed the presence of BOC-sarcosine **(22c).** The signals of CH_2N (3.97, 3.99 and 4.04 ppm) and CH_3N (2.95 and 2.99 ppm) groups of **22c** were clearly visible (Figure 47). By integrating the signals between 4.10 ppm and 5.00 ppm (CH_2N of *N,N'*-dimethylglycine and CH_2O of the dendrimer **G4OH**), between 3.97 and 4.04 (CH_2N of N-BOC-sarcosine) and the broad signal between 3.5 and 3.8 ppm (CH_2OH) it was possible to estimate sarcosine units (8) and to re-elaborate a more accurate estimate of the dimethylglycine **(22d)** units (7) and thus deducing that residual hydroxyls to be exploited in esterification reactions with *L*-lysine and *L*-arginine were 33. The structure of **27** was validated by Elemental Analysis.

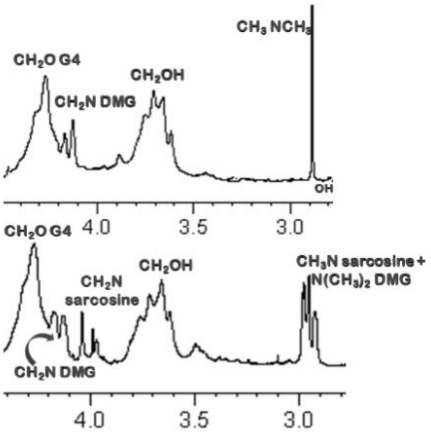

Figure 47. Comparison between significant portions of ^{1}H NMR spectra of **25** (above) and of **27** (underneath).

- *Functionalization of **27** with $^{\alpha}$N-BOC-$^{\omega'}$N-nitro-L-arginine (**22a**), $^{\alpha}$N,$^{\varepsilon}$N-di-BOC-L-lysine(22b): preparation of amino acids-modified mono-hydroxylated dendrimer **28***

L-arginine and *L*-lysine did not show significant differences in reactivity, so this second functionalization protocol was completed by introducing the two amino acids simultaneously. On the background of the results till now obtained, the EDC/DMAP system was immediately avoided and **27** was treated with **22a** and **22b** 1:1 (17.85 equiv.) under the usual conditions that were successful (Scheme 28).

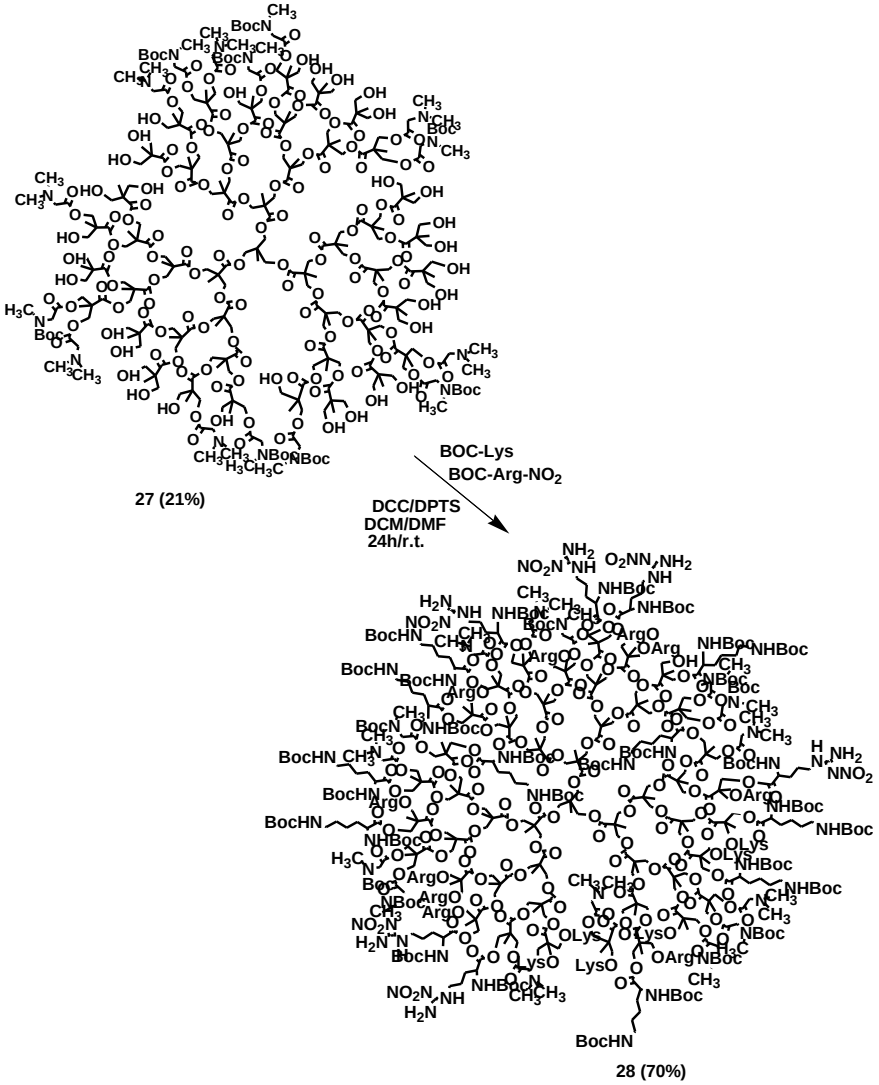

Scheme 28. Synthesis of aminoacids-modified monohydroxylated dendrimer **28**

In Figure 48 it can observe that between 3.0 and 3.2 ppm and between 3.2 and 3.5 ppm the broad signals of *L*-lysine $^{\varepsilon}CH_2NHBOC$ and of *L*-arginine $^{\delta}CH_2NH$ respectively and from the comparison between integrals of these signals it was possible to deduce that the Lys/Arg ratio was 1:1 in accordance with the stoichiometric ratios used for the reaction. Proceeding towards higher δ values a split signal that was interpreted as the CH_2N signal of **22c** switched to higher fields and coinciding with the usual area of the CH_2OH (3.55-3.70 ppm) signal, was detectable. Then at 4.10-4.20 ppm and partially covered by the very large signals of the CH_2O of dendrimer, the signal CH_2N of *N,N'*-dimethylglycine (**22d**) was observable.

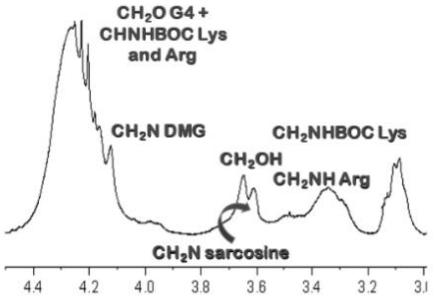

Figure 48. Significant portion of ^{1}H NMR spectrum of **28**.

From the integration of all these signals and by setting up appropriate equations that did not exclude the presence of OH residues, it was possible to estimate the composition of this second *hetero* dendrimer in 7 units of DMG, 8 of sarcosine, 16 of *L*-arginine, 16 of *L*-lysine and a residual free hydroxyl. The structure of **28** was also confirmed by Elemental Analysis.

3.7. Removal of protecting groups from 26 and 28

The removal of NO_2 and BOC groups was performed into two steps as described in Experimental Section. The intermediate till BOC-protected obtained as formic acid salt, was isolated as spongy solid and submitted without purification to the second step to remove BOC groups in acidic conditions. In order not to damage the polyester matrix, gaseous HCl was generated in situ by adding an excess of CH_3COCl to the methanol solution of BOC-protected dendrimer (Scheme 29 and Scheme 30).

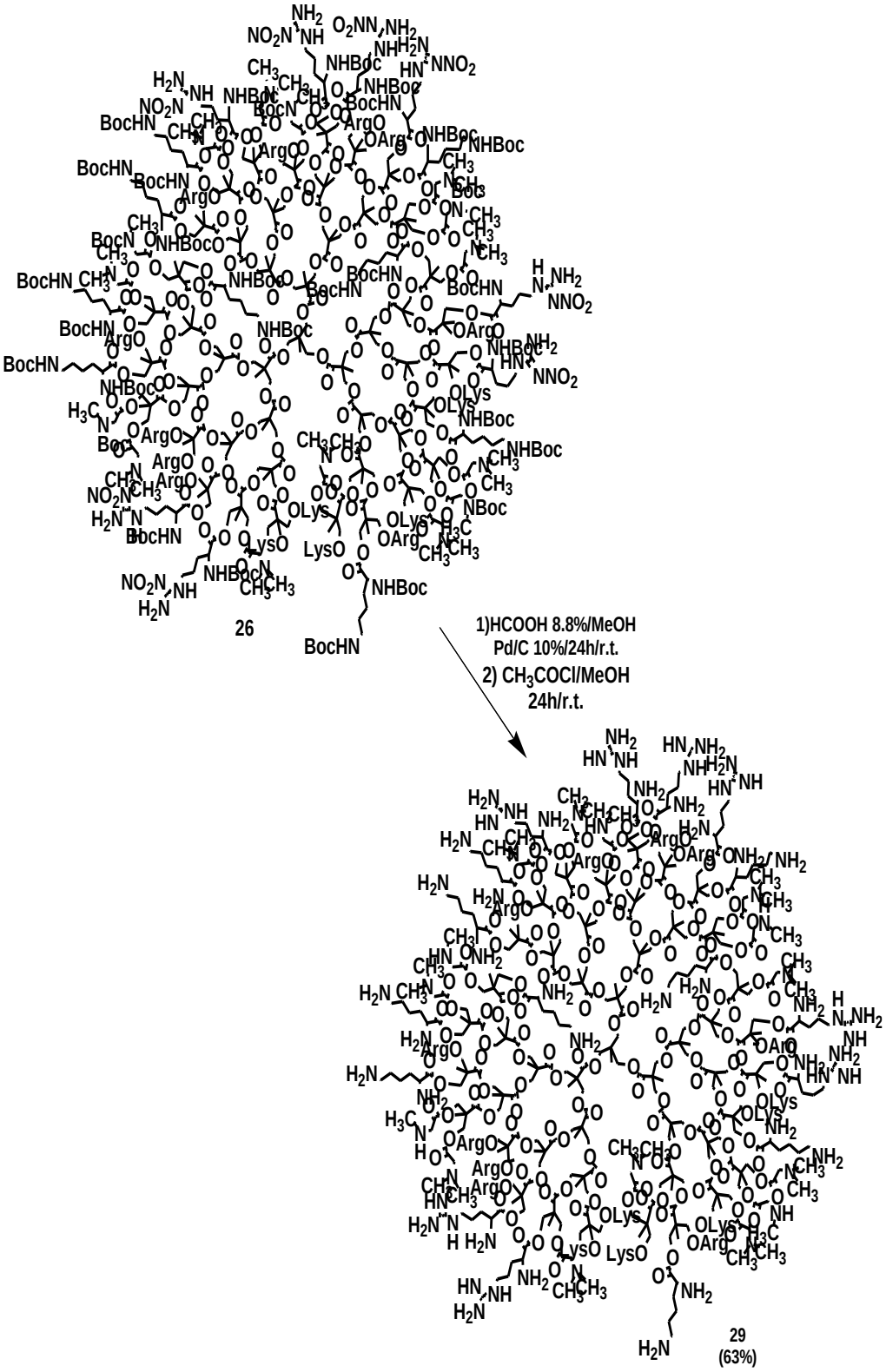

Scheme 29

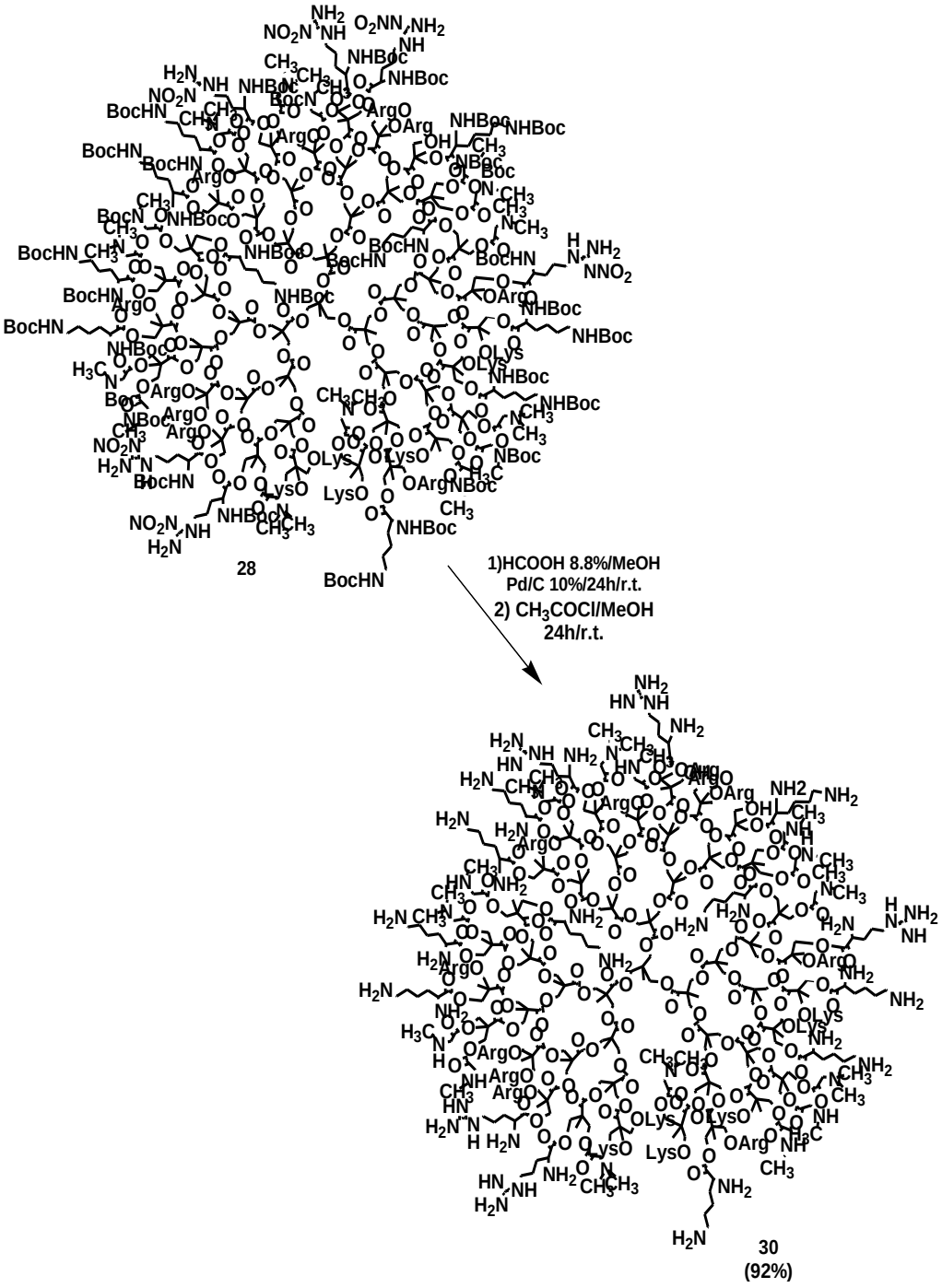

Scheme 30

This second step was monitored by FTIR evaluating the disappearance of the carbamate bands at 1712 and 1692 cm^{-1}. The dendrimers **29** (63%, overall yield) and **30** (92%, overall yield) were obtained as hydrochlorides and as lightly hygroscopic glassy solids. The ^{1}H NMR spectra of **29** and **30** confirmed the structure of the two hydrochlorides and reconfirmed their peripheral compositions. Elemental Analysis validated these results.

In particular for compound **29** in the range of δ between 7.5 ppm and 11.0 ppm, very intense peaks relative to protonated amine groups and flatting the NH and NH_2 groups of the guanidine groups of the *L*-arginine were detectable. The integral value was in accordance with 254 H and with 81 protonable nitrogen atoms (N = 81).

In a similar way the ^{1}H NMR spectrum of **30** in the range of δ between 7.8 ppm and 9.0 ppm, showed very intense peaks whose integral value was in accordance with 247 H and with 79 protonable nitrogen atoms (N = 79). As an example, in Figure 49 a comparison between ^{1}H NMR spectrum of BOC protected dendrimer **28** and of hydrochloride dendrimer **30** is a shown. Obviously the spectra of compounds **26** and **29** had a similar look.

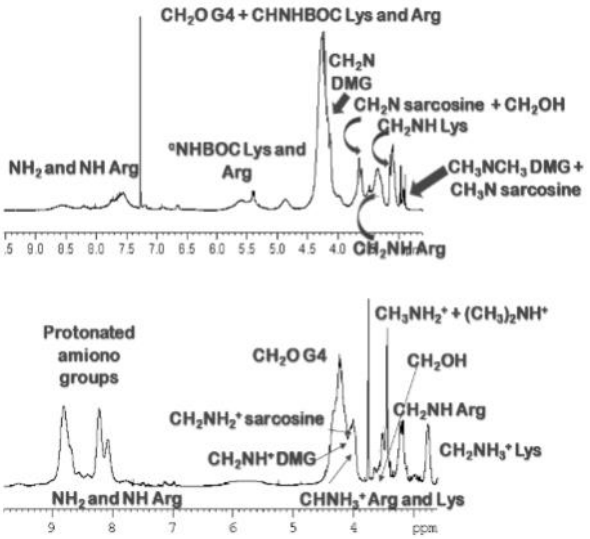

Figure 49. Comparison between ^{1}H NMR spectrum of BOC protected dendrimer **28** and of hydrochloride dendrimer **30**

3.8. Functionalization reactions of amphiphilic dendrimer scaffolds 33, 34, 37, 38 and 43 with amino acids

The second generation dendrimer **13** was functionalized only with $^{\alpha}$*N*-BOC-$^{\omega'}$*N*-nitro-*L*- arginine **(22a)** (Scheme 31) and the crude obtained as spongy solid was subjected to chromatographic column.

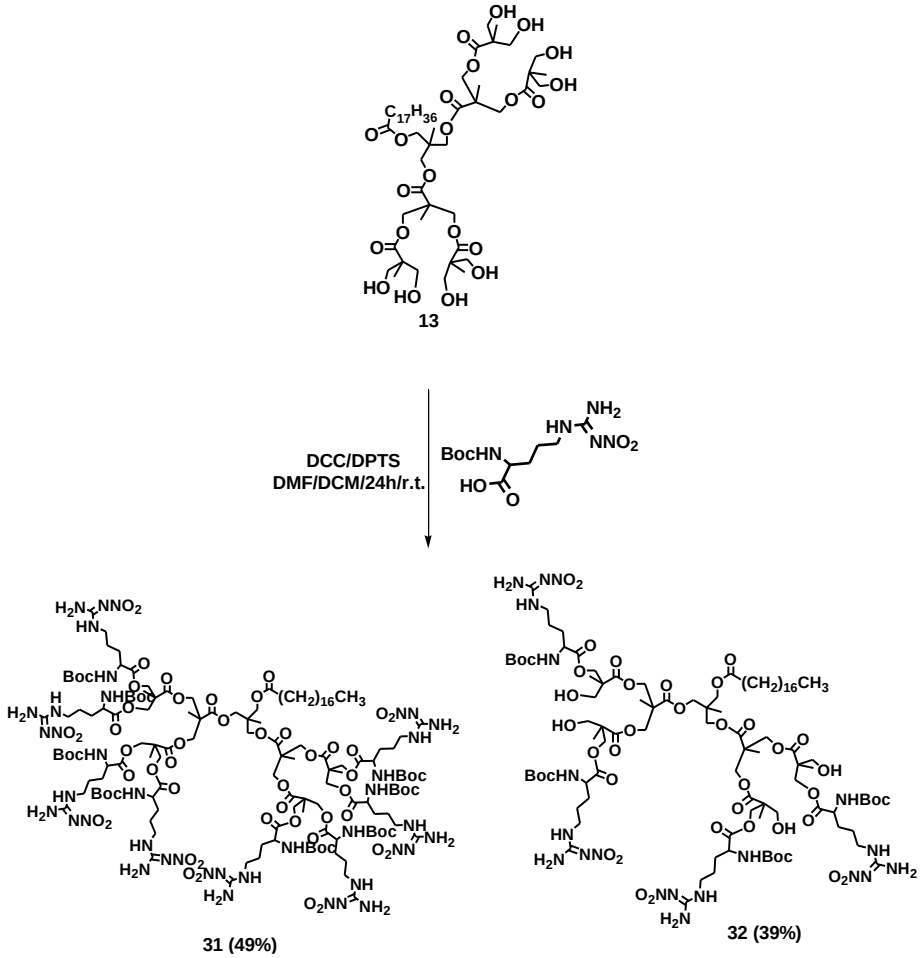

Scheme 31

In the head fractions the unreacted DCC and the *N*-isoacylureic derivative of **22a** were eluted. The arginine derivatives were isolated in fractions eluted with EtOAc/petroleum ether/MeOH = 93:93:14, then 47:47:18 and finally 35:35:30. Two arginine-modified products were obtained: the fully functionalized compound **31** and the half functionalized compound still having four residual hydroxyls **32**. The deprotection reactions of **31** and **32** provided the two cationic dendrimers **33** and **34** (Scheme 32 and 33) endowed with sixteen and eight protonated groups respectively.

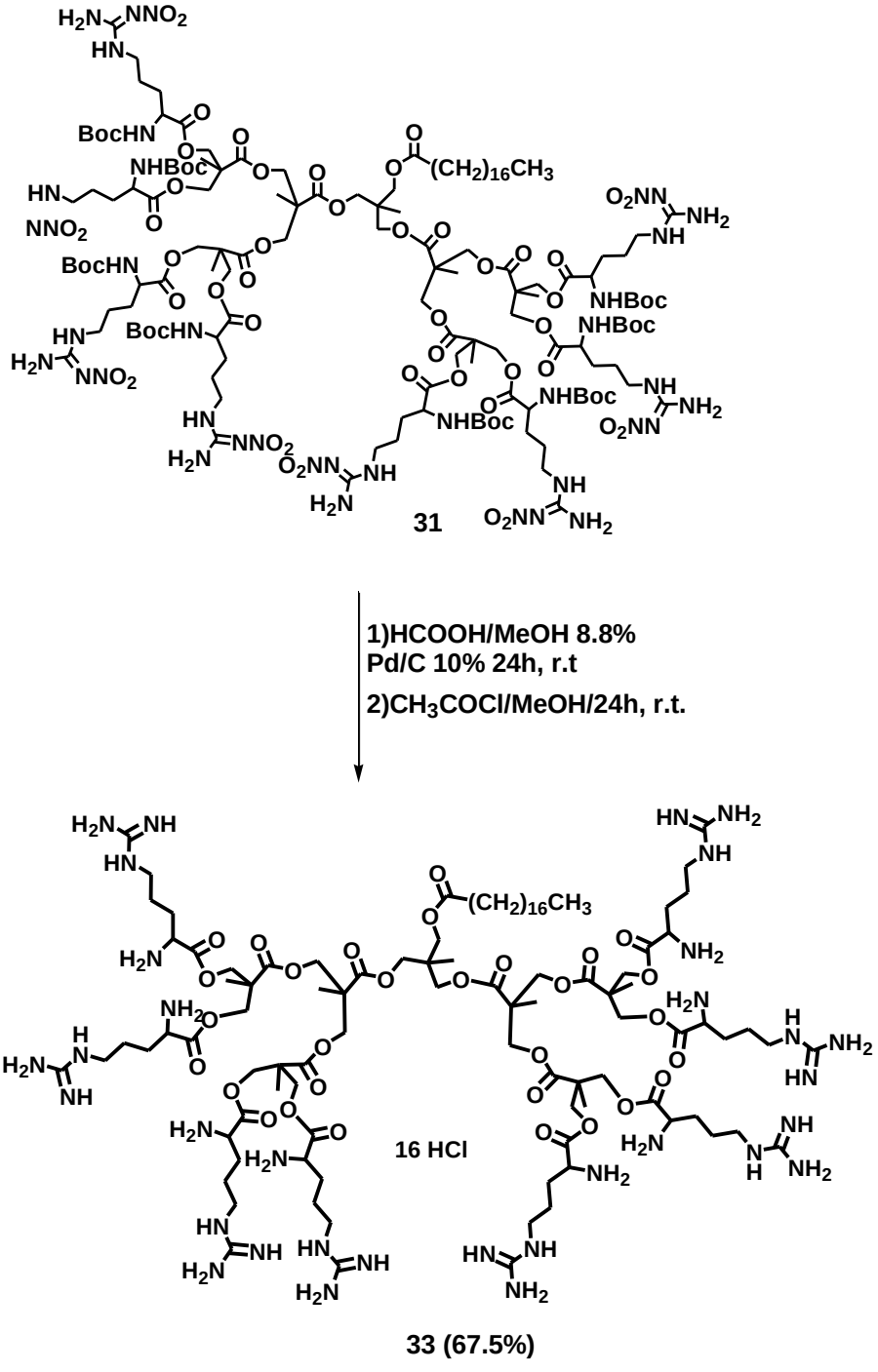
31
1)HCOOH/MeOH 8.8%
Pd/C 10% 24h, r.t
2)CH3COCl/MeOH/24h, r.t.
16 HCl
33 (67.5%)

Scheme 32

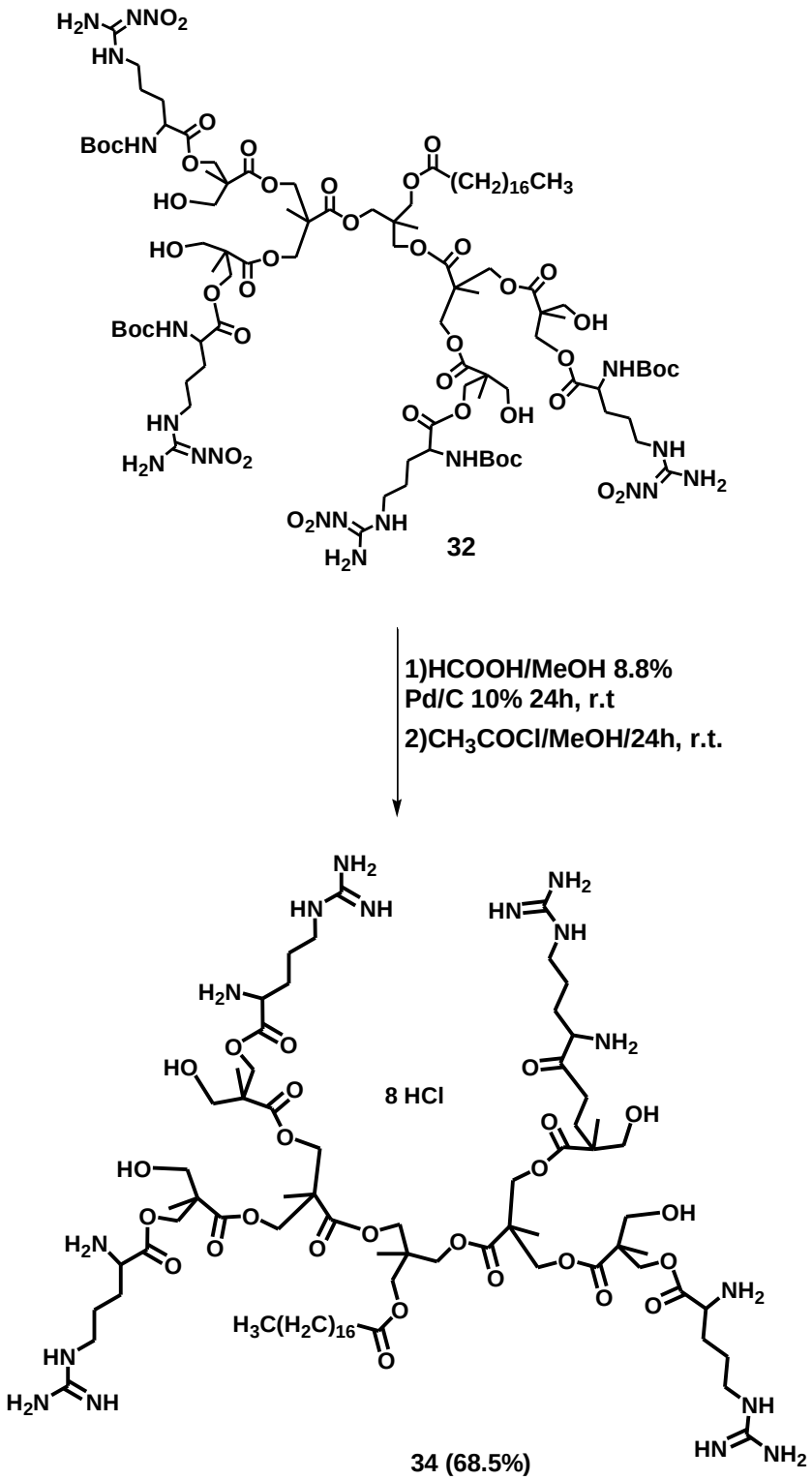

Scheme 33

The third generation dendrimer **17** was functionalized under the same conditions with a mixture 1:1 of $^{\alpha}N$-BOC-$^{\omega'}N$-nitro-*L*-arginine (**22a**) and $^{\alpha}N,^{\varepsilon}N$-di-BOC-*L*-lysine (**22b**) (Scheme 34). Since it was reported that protonated primary amino groups play a key role in

interactions with weak acids drug molecules, with the negatively charged DNA or RNA and with phospholipids and proteoglycans of biological membranes, thus helping the efficiency of transfection, *L*-lysine was added to *L*-arginine with the purpose of inserting a greater variety of protonable primary nitrogen atoms.

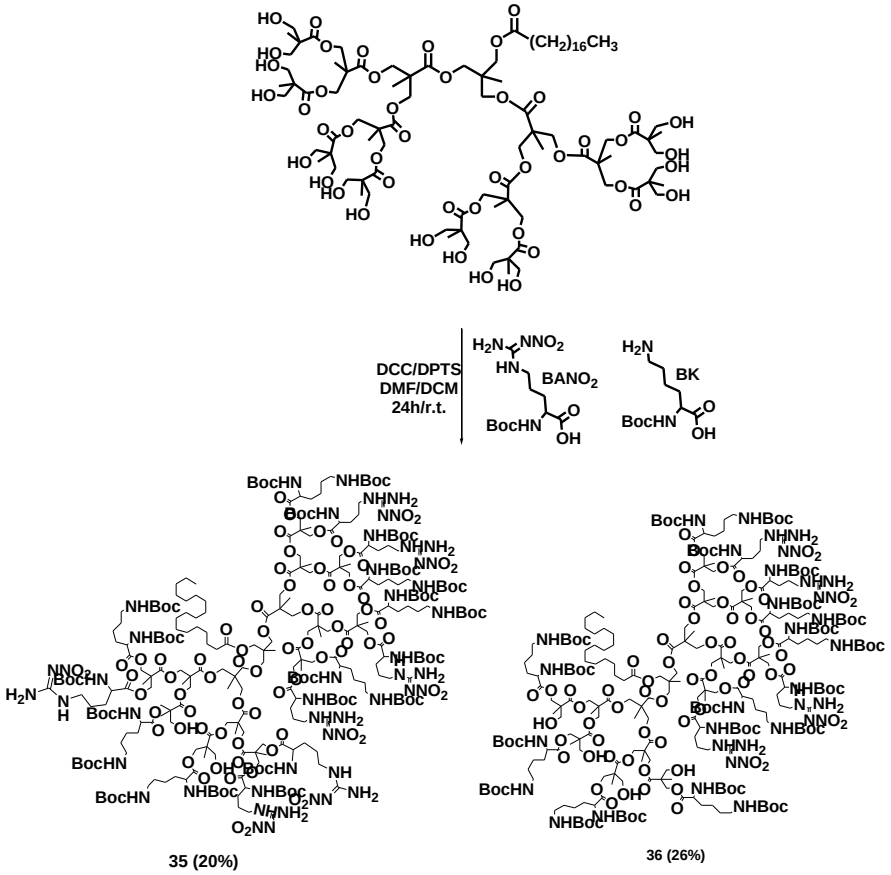

Scheme 34

Five amino acids-modified dendrimers were isolated from the complex crude, among which, **35** and **36** were the main products. Figure 50 shows the structure of the other three isolated and characterized dendrimers.

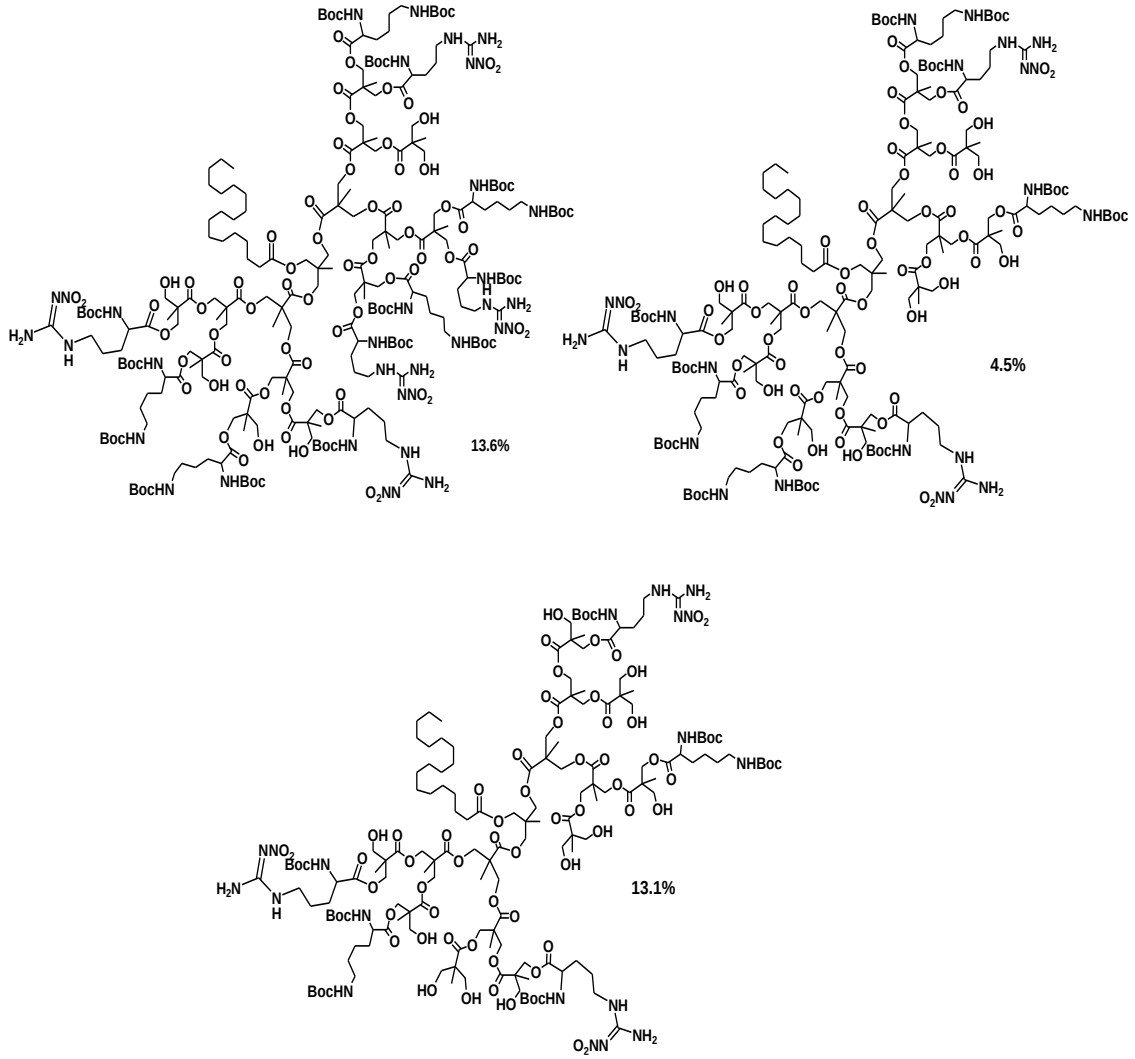

Figure 50. Minor compounds resulting from the esterification of **17** with protected *L*-arginine

The deprotection reactions of **35** and **36** performed as usual, provided the final samples **37** and **38** having respectively 28 and 24 protonated amine groups (Scheme 35 and 36).

^{1}H NMR spectra were very useful in determining the structures of dendrimers both in the protected forms and as hydrochlorides. They were decisive for estimating in a sufficiently accurate way the dendrimers peripheral composition in amino acids and free OH groups (if present) by comparing the integrals value of appropriate significant peaks. Once the structure and composition were known was possible to calculate the molecular weights of the products. Furthermore, for having greater security of the reliability of the estimated data, the structure of the protected dendrimers **31**, **32**, **35** and **36** were confirmed

also by Elemental analysis while that of hydrochlorides **33**, **34**, **37** and **38** by molecular weight obtained by volumetric titrations.

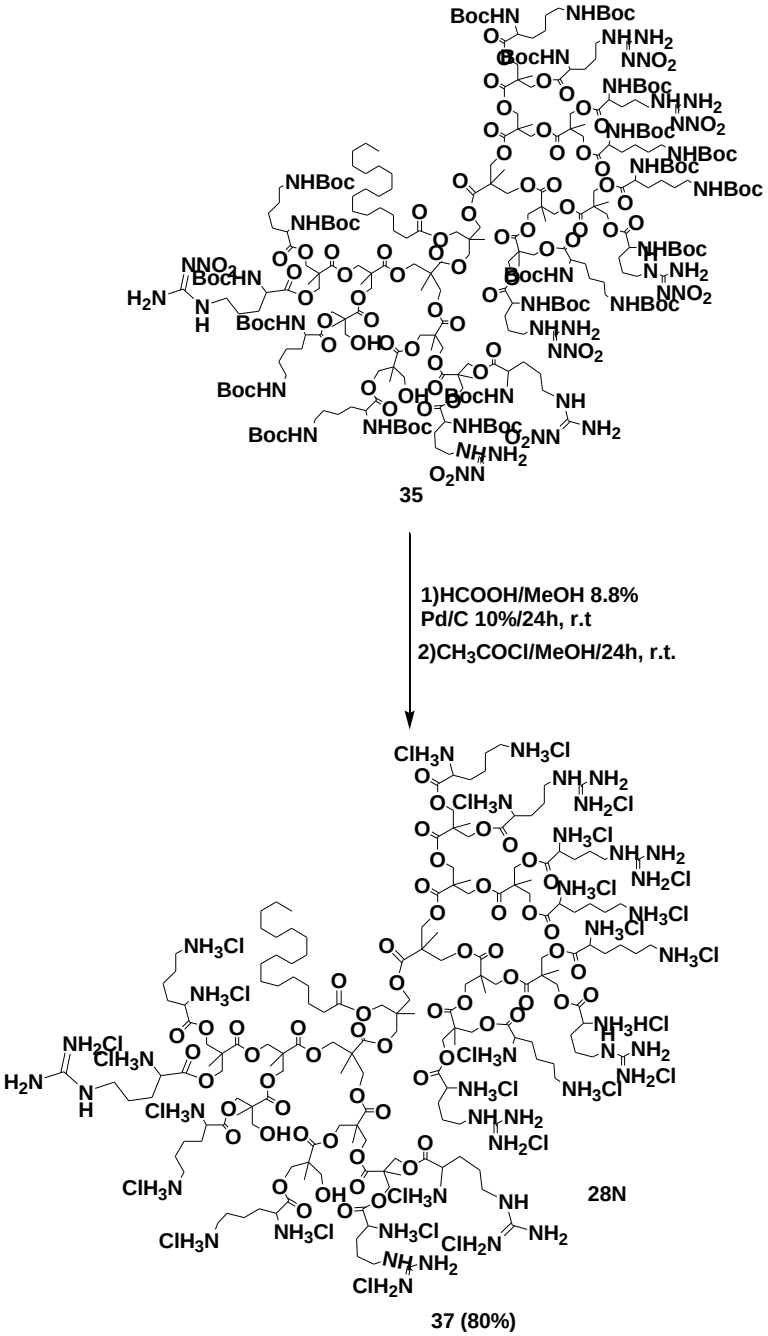

Scheme 35

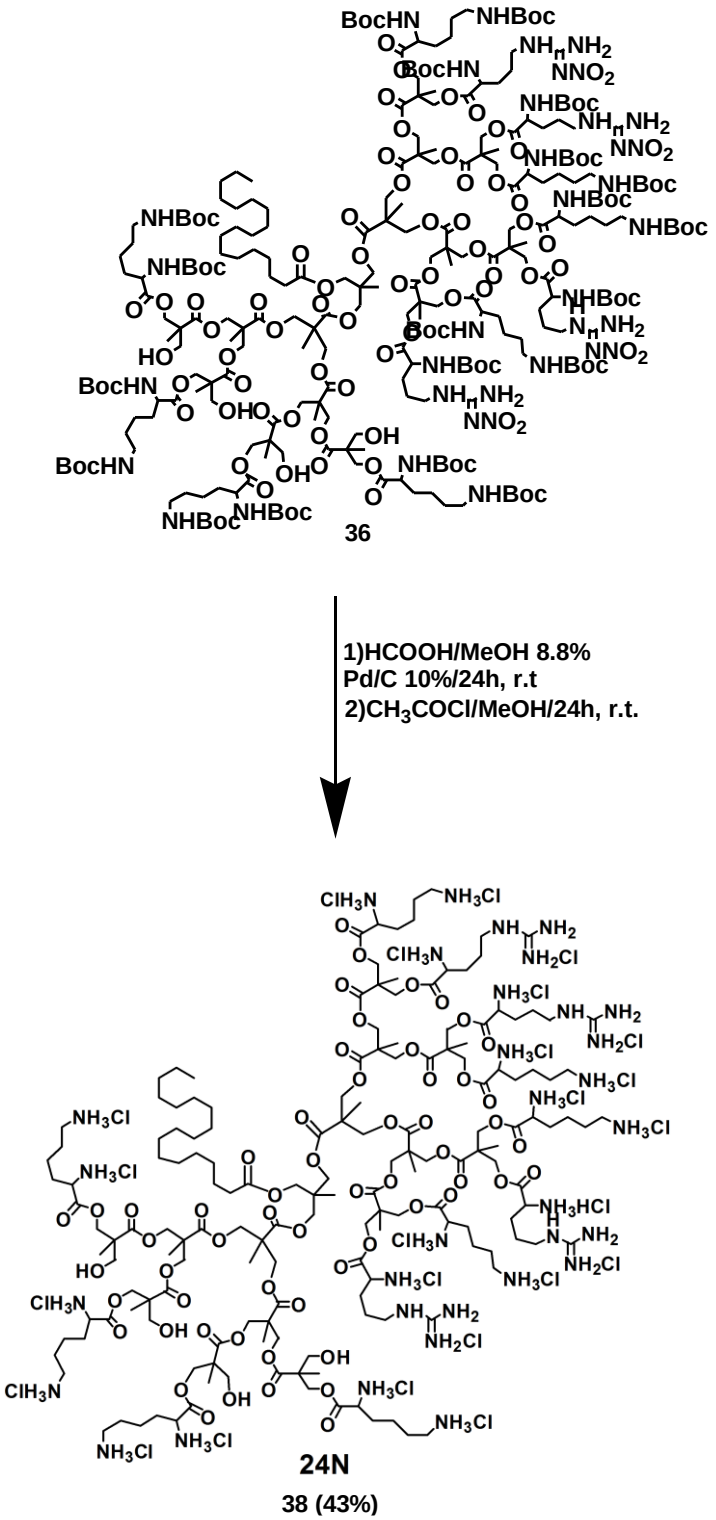

Scheme 36

As an example in Figure 51 it is possible to observe how the spectrum of **13**, having eight free OH groups (a), modified when esterified with $^{\alpha}$*N*-BOC-$^{\omega'}$*N*-nitro-*L*-

arginine (**22a**) to give the fully functionalized product **31** (b) and how the spectrum of **31** modified after total deprotection to provide **33**(c).

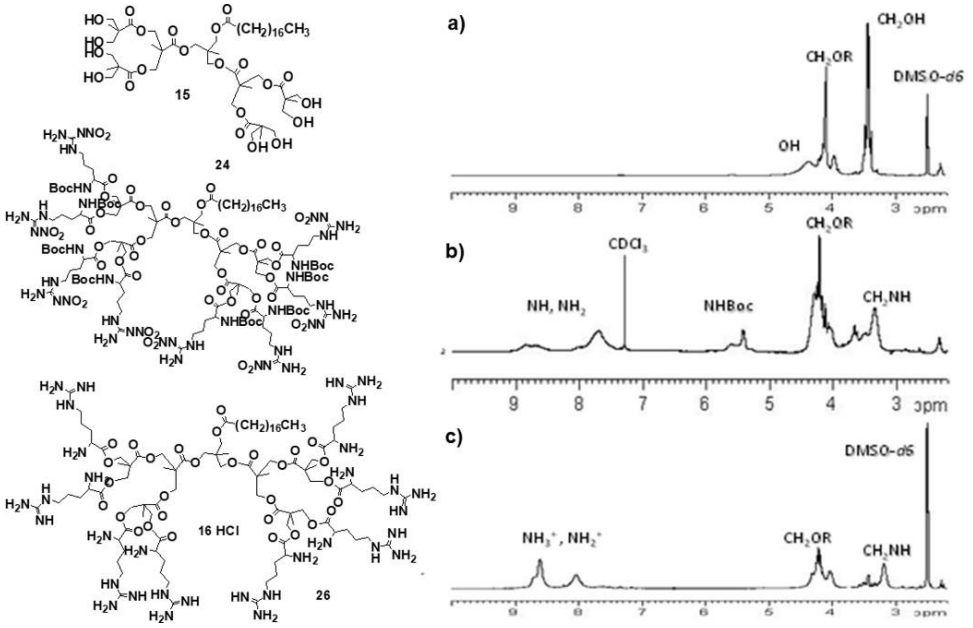

Figure 51. ^{1}H NMR Spectra of **13** (a), **31** (b), **33** (c)

The spectra acquired for samples containing both *L*-arginine and *L*-lysine were much more complex and difficult to be interpreted. However, they presented well separated signals for the $CH_2{}^{\delta}NH$ of *L*-arginine (3.34 ppm) and $CH_2{}^{\varepsilon}NHBOC$ of *L*-lysine (3.10 ppm), so it was possible to estimate their ratio by comparing the value of their integrals. Then by relating the value of *L*-arginine and *L*-lysine peak integrals with those of the peak of the $CH_2C{=}O$ of stearate at 2.38 ppm, it was possible to calculate the number of two amino acids moieties present on the dendrimer scaffold and therefore calculate the number of residual hydroxyls. The third generation dendrimer **21** was decorated with four different amino acids. *L*-arginine (**22a**) and *L*-lysine (**22b**) were selected again; *N*-methylglycine (MG, **22c**) and *N,N'*-dimethylglycine (DMG, **22d**) were also chosen in order to equip the final dendrimers with secondary and tertiary amine groups that are considered to be the main promoter of the so called "proton sponge" effect.[223] The so variegated cationic shell provided an optimal buffer capacity which is a fundamental property for a good delivery system.[222]

According to the two reliable and versatile protocols developed on **G4OH** for the step-wise synthesis of our acids-modified amphiphilic dendrimers. Dendrimer **21** was treated with α-bromoacetic acid **23**[225a] using DCC/DPTS/DCM system. The functionalization was successful and a number of AcBr units that respected the

stoichiometry used, randomly esterified the dendrimer **21**. Dendrimer **39** (scheme 37) was obtained as white spongy solid (yield = 95 %) and was analyzed by FTIR and NMR techniques to confirm the structure, degree of purity and peripheral composition. In particular, in the ^{1}H NMR spectrum acquired in $CDCl_3$ it was possible to appreciate the appearance of a peak (3.89 ppm) attesting the presence of the methylene of the AcBr units.[226] From the integration of this peak it was possible to estimate the number of AcBr units that esterified **21** in number of 4-5 depending on preparations. ^{1}H NMR spectrum also revealed the presence of traces of DPTS as a pollutant (minor than 9.9 % by weight), which were eliminated by aqueous hydrolysis in the subsequent passage. Deleting them through aqueous or basic washings on **39** or at the time of its isolation could be risky since the bromine could react to a substitution reaction.

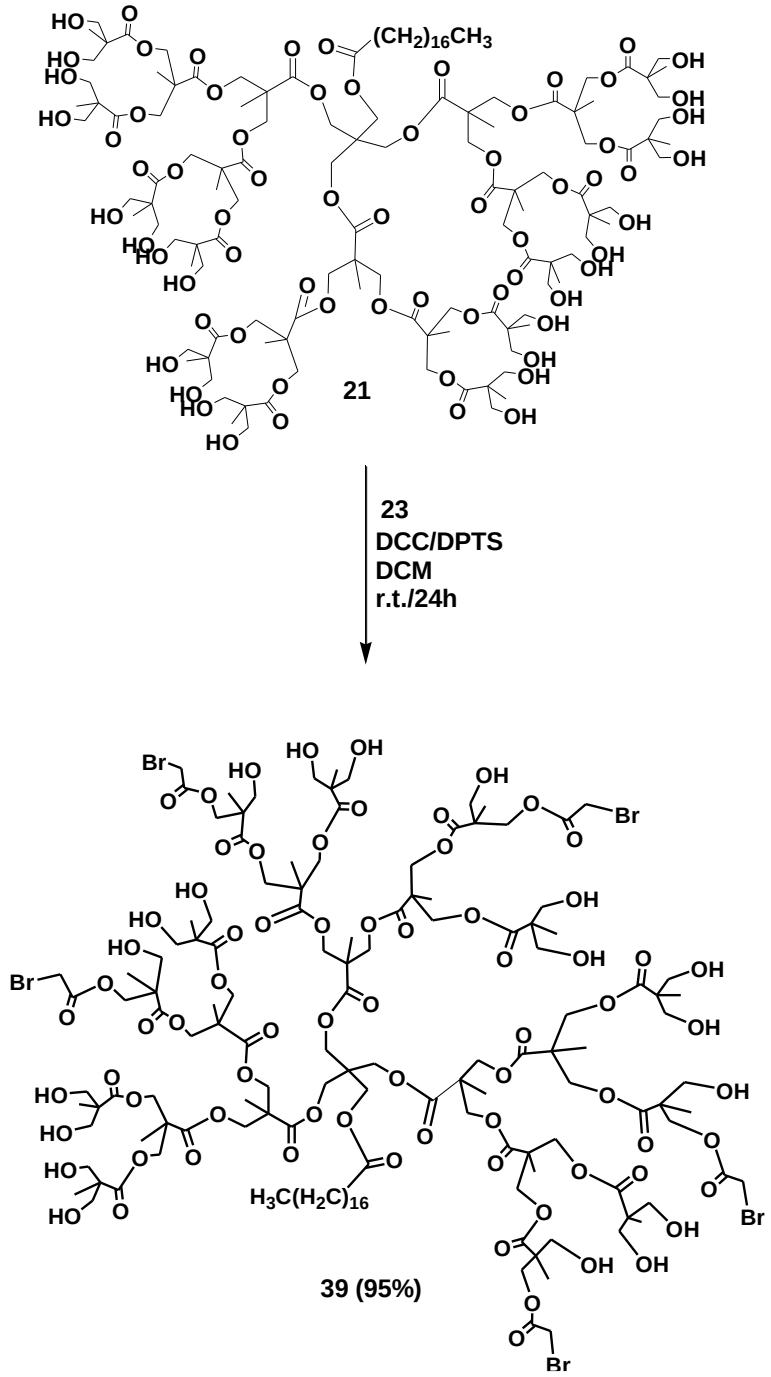

Scheme 37

A sample of **39** containing five AcBr residues dissolved in acetone was treated with a strong excess of *N,N'*-dimethylamine released *in situ* from its hydrochloride salt by its treatment with 1:1 NaOH solid (Scheme 38). The reaction was stirred for a long time, because the exchange was rather difficult probably due to the presence of the long hydrocarbon chain that made the substitution site not easily accessible. The reaction was monitored by ^{1}H NMR until the complete disappearance of the CH_2Br group signal that for

example was still present after 1h. Compound **40** was obtained as an off white spongy solid (yield = 80 %) and in its ^{1}H NMR spectrum the peak of CH_2Br disappeared, while new peaks around 3.00 ppm and near 4.00 ppm appeared for $(CH_3)_2N$ and CH_2N groups of DMG respectively. The presence of five units of DMG was confirmed.

After the introduction of DMG on the dendrimer scaffold, the residue hydroxyls were esterified with the other three amino acids in two successive steps to avoid competition between the less reactive MG and the more reactive *L*-lysine and *L*-arginine. Compound **41**(Scheme 39) was achieved from the first step as a spongy white solid in yield = 74 %. Its structure and peripheral amino acids composition that revealed additional four sarcosine units was estimated by ^{1}H NMR. Dendrimer **42** (scheme 40) was obtained from the second step as a white solid (yield = 99 %). The FTIR analysis confirmed the presence of BOC groups and the ^{1}H NMR spectrum confirmed the presence of both the new amino acids and allowed their quantification in seven units for each amino acid with consequently one residual hydroxyl free. Summarizing, this new hetero-dendrimer resulted in containing five DMG, four MG, seven *L*-arginine, seven *L*-lysine and a residual hydroxyl group. The removal of NO_2 and BOC groups was performed as already described and **43** was obtained in the form of hydrochloride (overall yield = 70 %) as a slightly hygroscopic glassy solid (scheme 41).

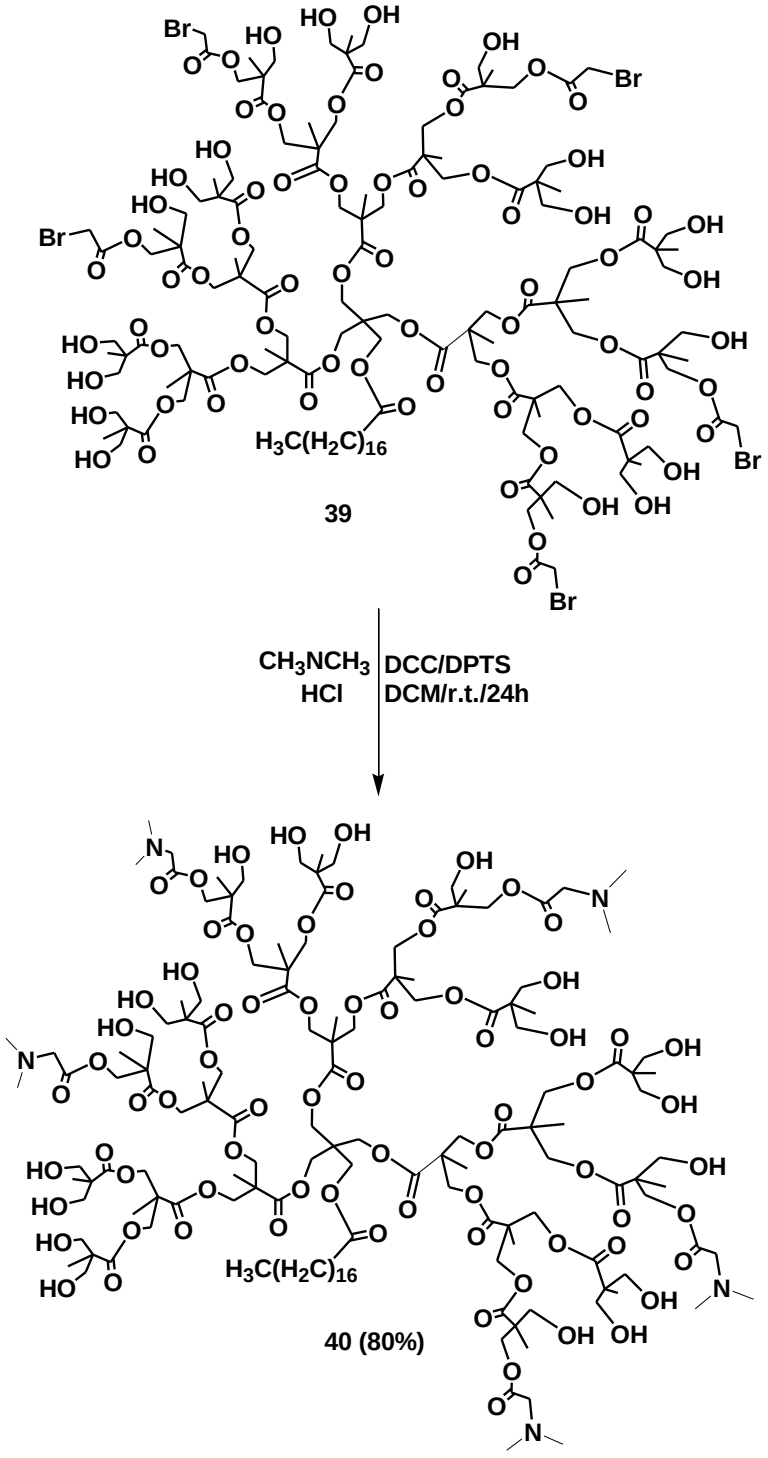

Scheme 38

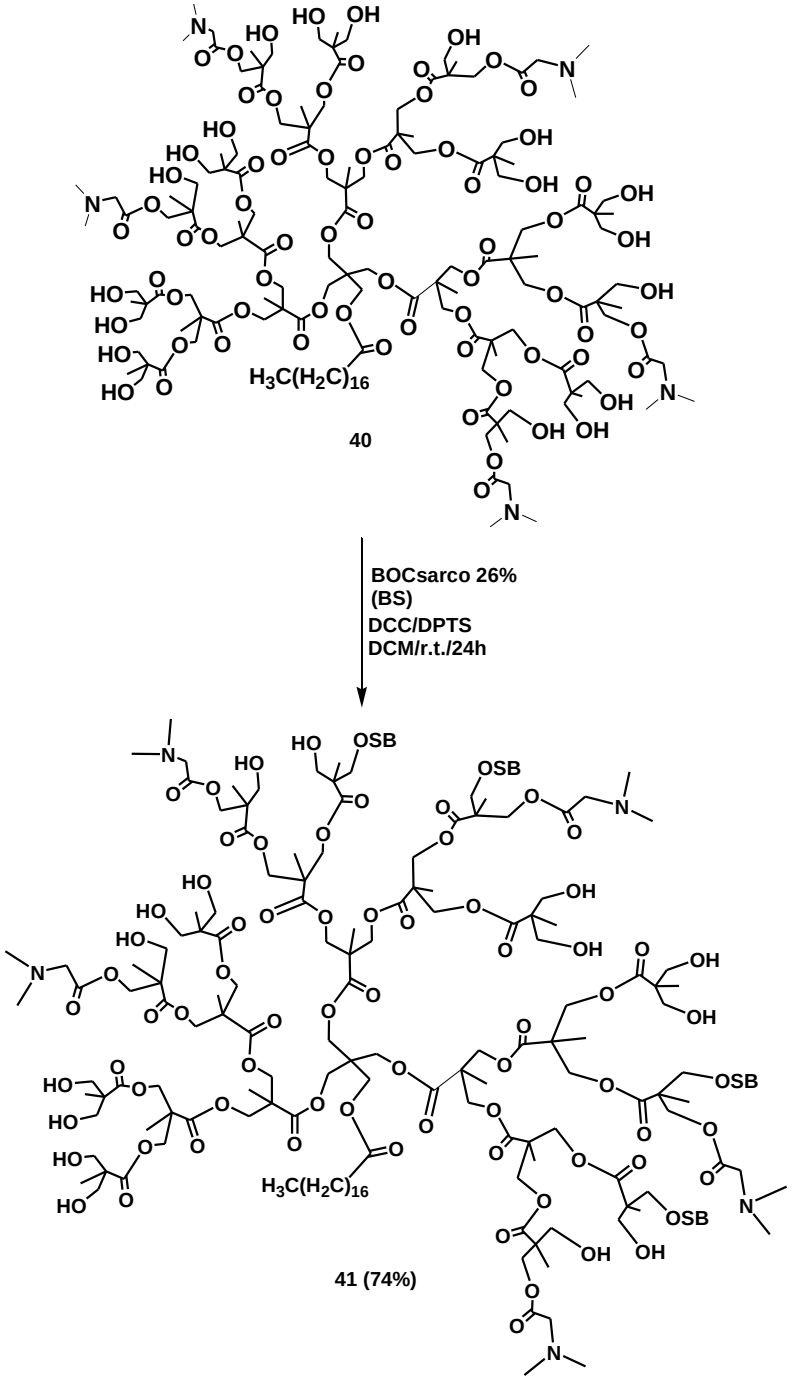

Scheme 39

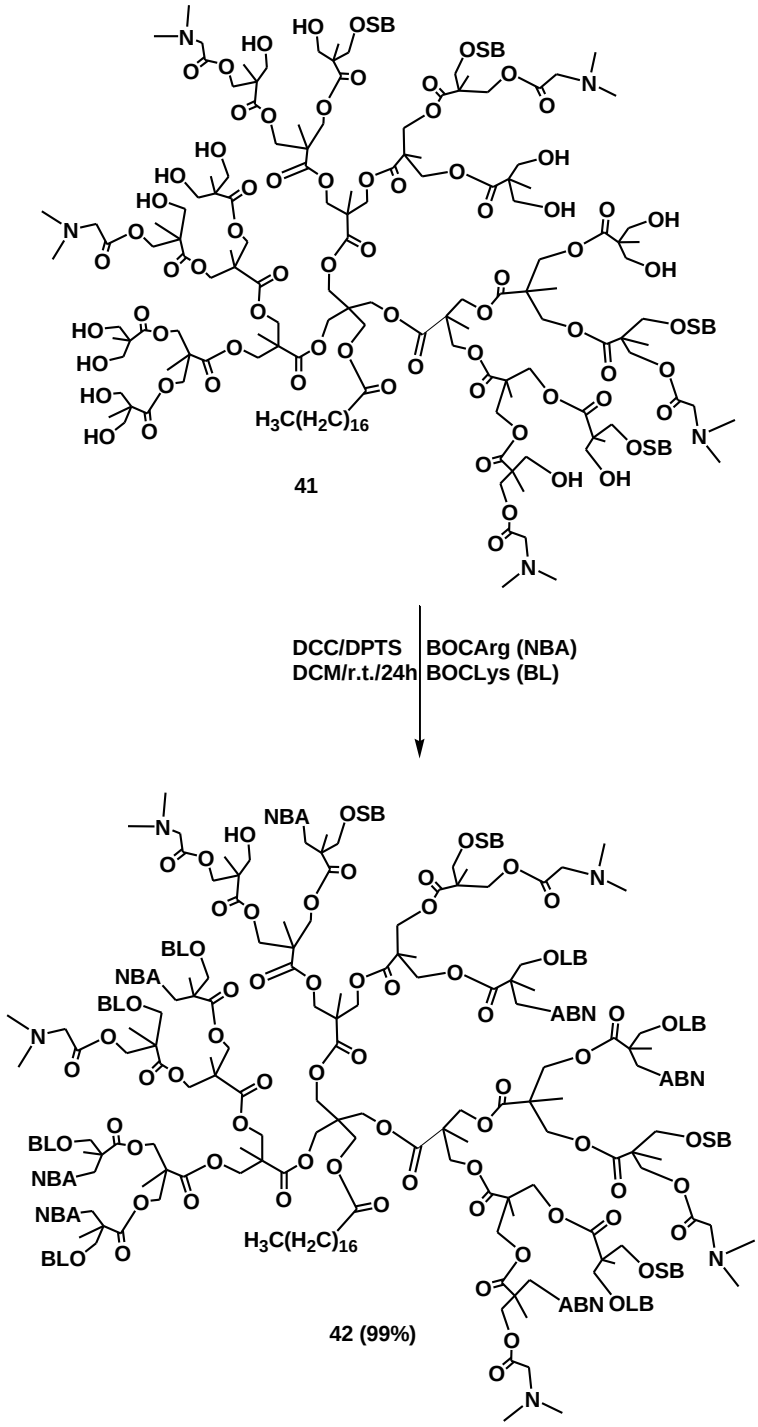

Scheme 40

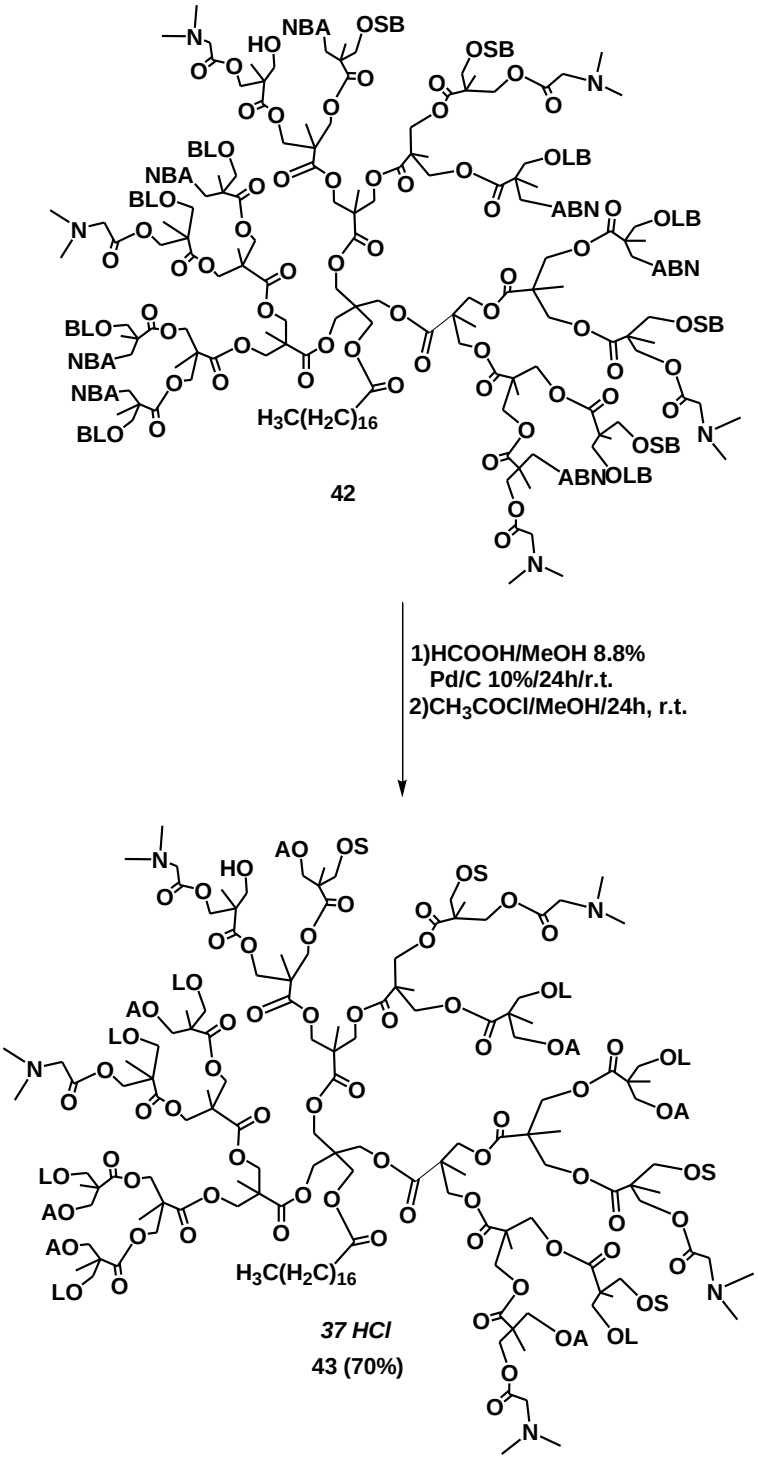

Scheme 41

3.9. Volumetric titrations of dendrimers

To complete the characterization of the prepared cationic dendrimers, having further confirmation of their composition on the periphery and to determine their molecular weight without having to resort the routine well-known but very expensive

techniques like MALDI-TOF, the titration of amine hydrochlorides with $HClO_4$ solutions in AcOH in the presence of mercuric acetate and quinaldine red as indicator[227] proved simple and affordable.

The accuracy of this method, already adopted by us to determine molecular weight of cationic amino acids-modified dendrimers previously prepared[204, 205], was secured by a sharp endpoint of titration, while its reliability has been demonstrated by the reproducibility of results. Table 3 shows the estimated peripheral composition of dendrimers prepared, the N value, and the molecular weight estimated by NMR spectra compared with the experimental one obtained from volumetric titrations [N (degree of freedom) = 5].

Table 3

Dendrimer DMG*/MG**/Arg/Lys/OH	N[£]	Computed MW[$]	Experimental MW[a,b]	Error [%]
26 **10/5/18/15/0**	81	14 239.03	13 686.52 ± 0.52	3.9
28 **7/8/16/16/1**	79	13 939.79	13 878.12 ± 0.44	0.4
33 **0/0/8/0/0**	16	2932.16	2946.53 ± 0.11	0.49
34 **0/0/4/0/4**	8	2015.73	2035.90 ± 0.10	1.00
37 **0/0/7/7/2**	28	5023.64	5468.54 ± 0.35	8.14
38 **0/0/4/8/4**	24	4417.30	3760.58 ± 0.23	14.8
43 **5/4/7/7/1**	37	6762.43	6728.79 ± 0.37	0.50

*****N,N-dimethylglycine ;**N-methylglicine; [£]N=number of peripheral protonable amine groups; $ estimated by ^{1}H NMR spectra; [a]obtained by volumetric titration; [b]degree of freedom = 5

The generally good and very good agreement of observed data with the calculated one confirmed the molecular structures of the prepared dendrimers and the soundness of the method.

3.10. Potentiometric titrations of the prepared dendrimers

It is generally accepted that carriers improve their efficacy of transfection of endowed with a proper buffer capacity and so with an average buffer capacity in the pH

range 4.5-7.5 suitable to make them escape from endosome compartments where pH is in the 5-6 range.[228] To have an estimate of the buffer capacity of the prepared dendrimers, potentiometric titrations of **26**, **28**, **33**, **34**, **37**, **38** and **43** were performed according to Benns et al. [229] Since PAMAM are considered to be a good reference in the field both of gene delivery and drug delivery literature data of three G4-PAMAM derivates[230] potentiometrically titrated with the same protocol were used to obtain their titration curve. Furthermore even if PEIs are not dendrimers but linear or branched polymers, since they are considered to be the gold standard for transfection efficiency too, a sample of commercial branched PEIK25 (b-PEI25K) was titrated by us under the same conditions. The β and β_{av} values of each synthetized sample, of G4-PAMAM derivatives and b-PEI were calculated from the titration data. Table 4 collects the β and β_{av} values recorded in the pH range 6-7 and 4.5-7.5 respectively.

Table 4

Cationic Vector	Buffer Capacity β [pH = 6.0-7.0]	Average Buffer Capacity β_{av}[pH = 4.5-7.5]
PEI25K*	0.0510,0.0530,0.0760	0.5170
PAMAMG4**	0.0014	0.0170
PAMAMG4Arg$^{£}$	0.0024	0.0180
PAMAMG4ArgHis$^{\$}$	0.0038	0.0410
26	0.0540, 0.0500, 0.0320	0.3500
28	0.1670, 0.1050, 0.0800	0.6400
33	0.02703	0.180
34	0.02105	0.183
37	0.0714, 0.0909, 0.10000	0.478
38	0.0112	0.128
43	0.077, 0.091, 0.056	0.480

*commercial PEI with molecular weight of 25000, **fourth generation PAMAM, $^{£}$G4-PAMAM containing arginine, $^{\$}$G4-PAMAM containing the His-His-Arg sequence

With great satisfaction, all the new samples resulted in having β and β_{av} values several times higher than those of PAMAMs and not too different from those of PEIs. In the case of **28**, **37** and **43**, the β values were also higher than those of PEIs and their average buffer capacities were in line with that of PEI25K.

3.11. Dynamic light scattering (DLS) and zeta potential

Particle hydrodynamic size (diameter) and Zeta potential of all prepared aminoacids-modified dendriemrs were measured and the obtained data together woth the deviation standard [N (degree of freedom) = 12] values are summarized in Table 5. Particle sized was determined by Dynamic Light Scattering (DLS) and was reported as the intensity-weighted average (Int-Peak), (Z-AVE, nm). Zeta potential (mV), which

provides a measure of the electrostatic potential at the surface of the electrical double layer and the bulk medium and which is related to the nanoparticle surface charge, was performed using zeta-sizer [N (degree of freedom) = 12].

As expected the mean diameters of the fourth generation two samples **26** and **28** were very similar to each other with decimal different supposedly depending on the slightly different composition on the periphery. In any case, they were within range 4 to 5 nm and comparable to the values reported for NH_2-PAMAMs of the same generations.[231-233] Their Z-potential values were in the range 32 to 34 mV; values very similar and in agreement with G4-PAMAM-NH_2 literature data.[232]

The mean diameters of the second generation samples were lower than those of the third generation ones, with decimal differences supposedly depending on the number and type of amino acids present on the periphery but in any case they were within the 3-4 nm range and comparable to the values reported for PAMAMs-NH_2 of the same generations.[231-233] Some differences were instead observed for the surface charge of the examined samples that were found within the 5.3-5.9 mV range. If Z-potential of samples **37**, **38** and **43** were sufficiently in agreement with G3-PAMAMs-NH_2 literature data[231], Z-potential of G2 samples **33** and **34** were significantly lower than G2PAMAMs-NH_2 literature data.[231] This, presumably due to the relatively low N value caused by the dendrimer structure formed by only two sails, to the presence of the hydrophobic hydrocarbon C-18 chain which mitigates the cationic character of the hydrophilic portion of the molecule and in the case of **34** for the low functionalization of the dendrimer scaffold. Obviously within the same generation of prepared dendrimers the zeta potential increases with the increase of N.

Table 5

Dendrimer DMG*/MG**/ Arg/Lys/OH	N[£]	Computed MW[$]	Experimental MW[a,b]	Z-potential (mV)[c]	Z-AVE size (nm)[c]
26 **10/5/18/15/0**	81	14 239.03	13 686.52 ± 0.52	33.4 ± 0.2	4.5 ± 0.1
28 **7/8/16/16/1**	79	13 939.79	13 878 ± 0.44	32.8 ± 0.3	4.6 ± 0.1
33 **0/0/8/0/0**	16	2932.16	2946.53 ± 0.11	5.4 ± 0.2	3.3 ± 0.1
34 **0/0/4/0/4**	8	2015.73	2035.90 ± 0.10	5.3 ± 0.9	3.2 ± 0.1
37 **0/0/7/7/2**	28	5023.64	5468.54 ± 0.35	5.7 ± 0.2	3.4 ± 0.1
38 **0/0/4/8/4**	24	4417.30	3760.58 ± 0.23	5.6 ± 0.1	3.3 ± 0.1
43 **5/4/7/7/1**	37	6762.43	6728.79 ± 037	5.9 ± 0.6	3.6 ± 0.1

*N,N-dimethylglycine, **N-methylglycine, [£]N= number of peripheral protonable amine groups, [$]estimated by ^{1}H NMR spectra, [a]obtained by volumetric titration, [b]degree of freedom = 5, [c]degree of freedom = 12

3.12. "*In Vitro*" cytotoxicity evaluation

To determine the potential of biomedical applications of amphiphilic amino acid modified dendrimers achieved, their cytotoxicity profile was investigated through in vitro tests on two model cell lines (B14 and BRL cells).

In order to determine the effect of dendrimers on cell viability, MTT assay, a method based on monitoring of NAD(P)H-dependent cellular oxidoreductase enzymes activity and is therefore related to inhibition of metabolic processes in mitochondria was performed. For comparison purposes, in order to verify whether the presence of the hydrophobic chain and a better HLB resulted in a reduction of cytotoxicity compared to hydrophobic compound, the same test was carried out on two hydrophilic hetero dendrimers (H1 and H2). Dendrimers concentrations used in MTT assay were in the range of 0.5-20 µM according to literature.[234] Regarding our dendrimers this range means concentration of 1.0-40.3 µg/mL for the amphiphilic dendrimer with lower MW (**34**) and of 3.4-135.2 µg/mL for the amphiphilic dendrimer with higher MW (**43**). Dendrimers H1 and H2 were consequently tested at concentrations in the range of 6.9-278.8 µg/mL and 7.1-284.8 µg/mL respectively. The results reported in Table 6 refer to the fixed concentration of 40.3 µg/mL selected because it is the higher possible concentration for dendrimer **34**. As reported in Table 6, all the amphiphilic compounds

only marginally effected cell growth, since viability percentage values were in the 79.9-111.7% range for B14 cells and in the 79.6-105.8% range for BRL cells and even if not extravagantly, they were less cytotoxic than dendrimers H1 and H2 not equipped with the C-18 chain. Furthermore the achieved amphiphilic dendrimers were found to be much less cytotoxic than PEI25K that at concentration 40 μg/mL determine the survival of only 30-40% of two cancer cell lines.[235]

Table 6		
	Cell viability (%)	
Cpd	**B14**	**BRL**
H1	106.7 ± 8.2	75.4 ± 7.0
H2	69.9 ± 3.1	84.2 ±1.7
33	84.3 ± 2.1	79.6 ± 0.4
34	80.1 ± 3.4	79.8 ± 0.8
37	111.7 ± 10.7	83.4 ± 2.2
38	79.9 ± 8.3	87.2 ± 5.2
43	109.2 ± 8.4	105.8 ± 3.3

CHAPTER 4

4.1. Synthesis of Water-soluble, Polyester-based Dendrimer Formulations of a mixture of two Triterpenoids Acids for Biomedical Applications

The target of this chapter was to obtain new efficient prodrugs of Ursolic and Oleanolic acids, two pentacyclic triterpenoids isomers extracted as a mixture from Salvia Corrugata Vahl[236] which are endowed with several pharmacological activities not exploitable above all because of their low water solubility. The strategy was to complex them with proper vectors which, unlike the prodrugs widely reported in the literature did not have a polyamidoamide highly cationic matrix but a hydrolysable ester-based one, in order to reduce or eliminate the risk of permanent damages to cellular membranes and toxicity to cells. The desired prodrugs should be water-soluble to authorize safe and effective administrations of the two triterpenoids thanks to increased bioavailability and pharmacokinetic and at the same time should be able to protect them from premature degradation and if possible to decrease their toxic side part. As vectors we chose to test six polycationic amino acids-modified polyester-based dendrimers of fourth and fifth generation previously prepared.[205] The hydrolysable inner matrix of the ester type assured low level of toxicity of the vector while the cationic peripheral character conferred by amino acids promoted the interaction with negatively charged lipids of membrane advancing the endocytotic cellular uptake. Furthermore the excellent buffer capacity of these materials guaranteed the escape from endosomal and from lysosomal attack thanks to the so-called *proton-sponge* effect when inside the cell thus allowing the release of the transported material into the cytosol. In literature is reported that in dendrimer/drug systems[237-239] such as PAMAM/weakly acidic drug moieties (ibuprofen, DOX, MTX), [240-242] hydrogen bonding and ionic interactions are among those mechanisms suggested to play a decisive part in dendrimer/drug complexation. So, we reasonably thought that the UOA mixture could be complexed by dendrimers **44**-**49** (Figure 52) thanks to the presence of several amino groups capable of establishing hydrogen bonds or electrostatically interacting with the triterpenoids acids as well as PAMAM with ibuprofen, DOX or MTX. On the other hand, attempts to covalently bind the two acids on the not cationic polyester and polyhydroxylated dendrimer G4OH[204,205], were no successful either with *N,N'*-dicyclohexylcarbodiimide (DCC), 1-ethyl-3-(3-dimethylaminopropyl)carbodiimide (EDC) or following the

procedure which uses 2-chloro-1-methyl-pyridinium iodide (CMPI)[243] as condensing agents.

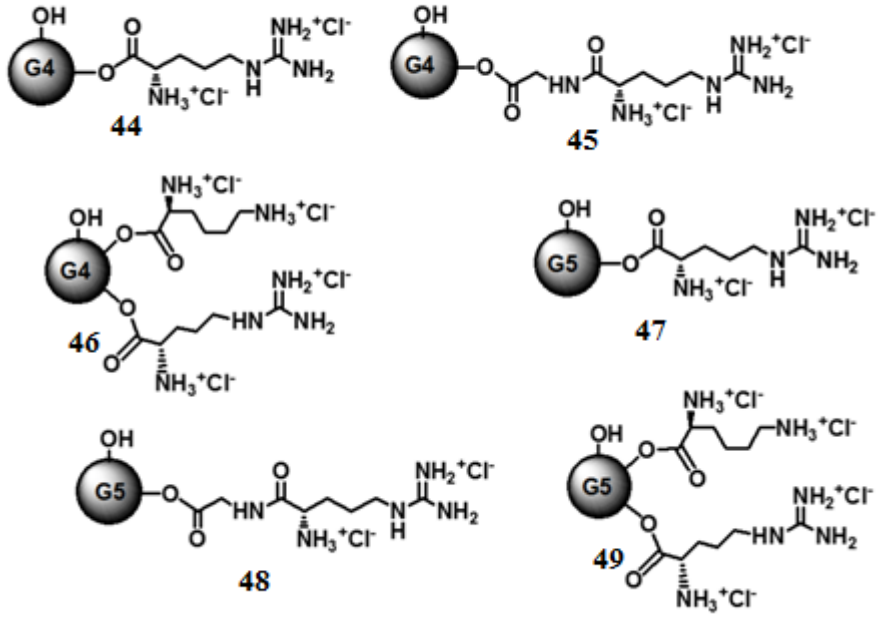

Figure 52. G4 and G5amino acids-modified dendrimers **44-49** used to encapsulate the UA and OA (UOA) mixture

4.1.1.Incorporation of Ursolic and Oleanolic acids Mixture (UOA) in dendrimers 44-49

Dendrimers **44-49**[205] were dissolved in methanol and subsequently, the UOA mixture extracted and isolated from Salvia Corrugata Vahl according to a described procedure[236] and whose ^{1}H-NMR spectrum is available in Figure 53 was added.

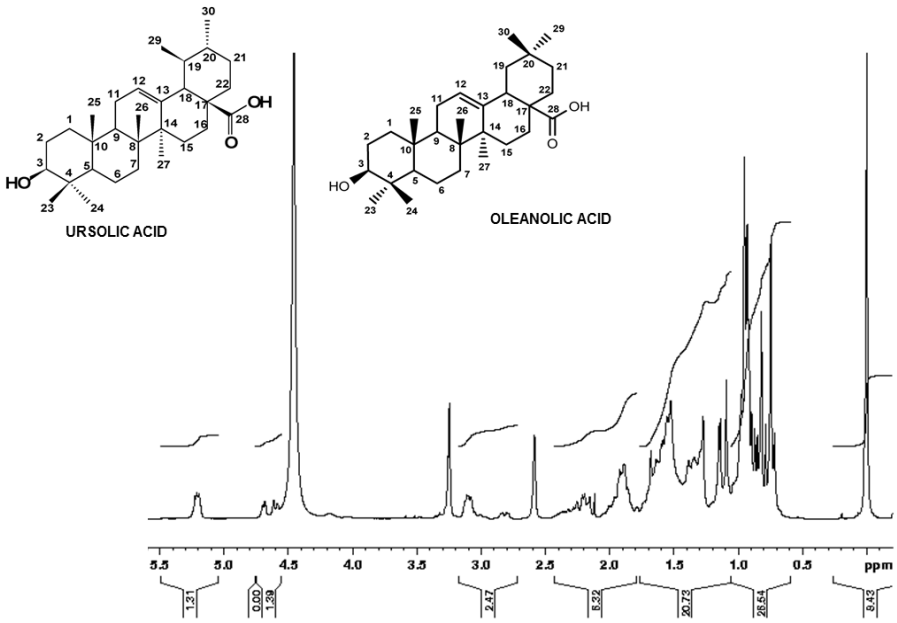

Figure 53. [1]HNMR spectrum of the Ursolic and Oleanolic acids mixture extracted by Salvia CorrugataVahl[236]

The reaction was vigourously stirred for 72h at room temperature in the dark (Scheme 42)**.** The methanol solution was evaporated at reduced pressure to remove the solvent. The residue solids were dried under vacuum in order to remove methanol completely. Then, DCM was added to extract the UA and OA not encapsulated, as UA and OA are soluble in DCM while complexes are not. They were water soluble as expected.

The solid complexes were further purified by dissolution in MeOH and precipitation in acetone and then recovered by centrifugation (3400 r/min, 15', twice). The UOA-dendrimer complexes were obtained in the form of white or yellowish slightly hygroscopic fluffy solids and stored on P_2O_5 in a dryer. FTIR was not significantly diagnostic to confirm the formation of the complexes but [1]H-NMR spectroscopy was useful to have both qualitative and quantitative information about the composition of the dendriplexes.

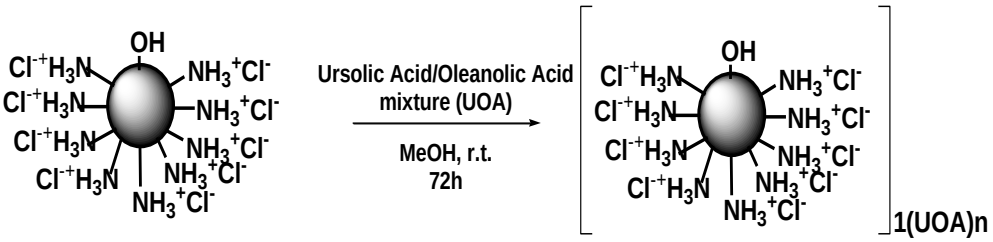

44 G4[Arg(36)OH(12)]
45 G4[ArgGly(29)OH(19)]
46 G4[Arg(16)Lys(19)OH(13)]
47 G5[Arg(66)OH(30)]
48 G5[ArgGly(52)OH(44)]
49 G5[Arg(38)Lys(30)OH(28)]

n=6, **50** G4[Arg(36)OH(12)UOA(6)]
n=7, **51** G4[ArgGly(29)OH(19)UOA(7)]
n=4, **52** G4[Arg(16)Lys(19)OH(13)UOA(4)]
n=3, **53** G5[Arg(66)OH(30)UOA(3)]
n=12, **54** G5[ArgGly(52)OH(44)UOA(12)]
n=8, **55** G5[Arg(38)Lys(30)OH(28)UOA(8)]

Scheme 42

In Figure 54 is shown the ^{1}H-NMR spectra of the all dendriplexes **50-55** with an expansion of the zone between 2.0 and 0.5 ppm (determining to confirm that the incorporation was successful) compared to ^{1}H-NMR spectra of UOA mixture and of the parent dendrimers **44-49**.

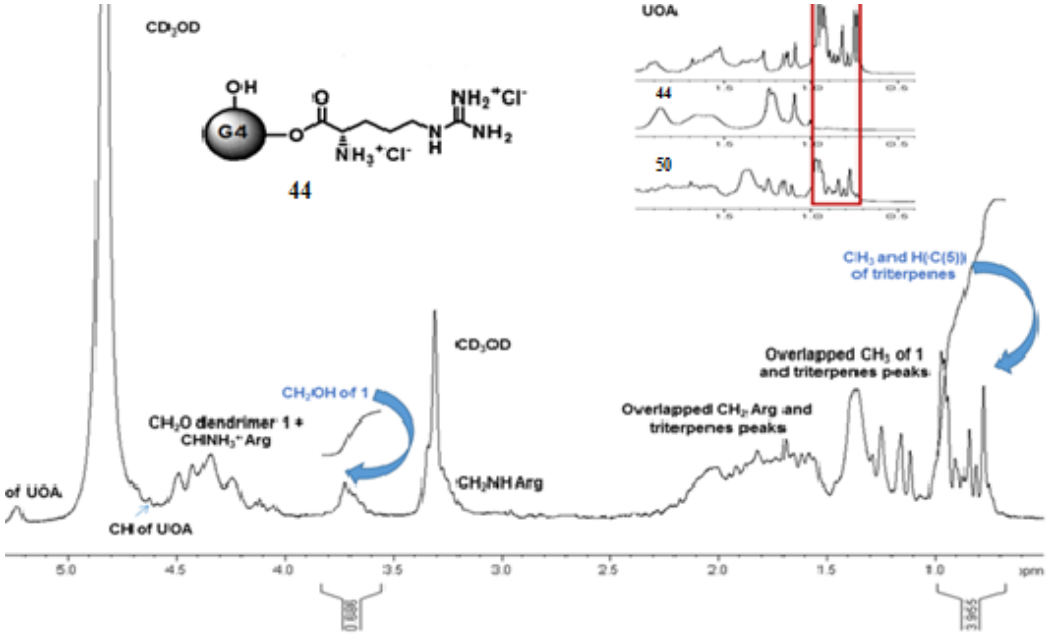

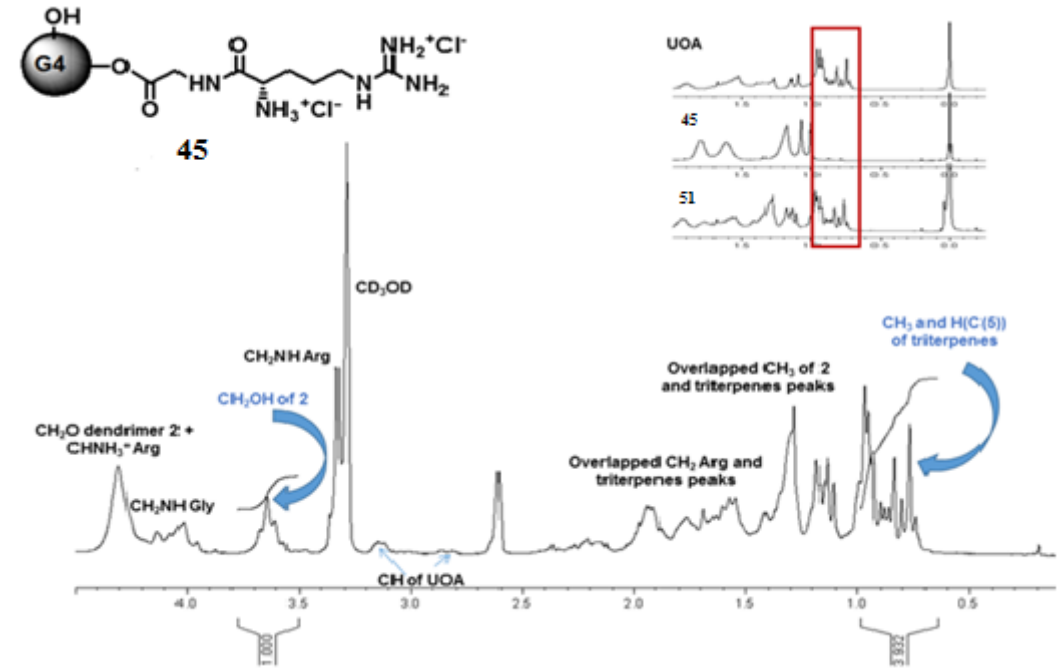
OH
G4
O
HN
NH2+Cl-
NH3+Cl-
N
H
NH2
45
UOA
45
51
CD3OD
CH2NH Arg
CH2OH of 2
CH2O dendrimer 2 + CHNH3+ Arg
CH2NH Gly
CH of UOA
Overlapped CH3 of 2 and triterpenes peaks
Overlapped CH2 Arg and triterpenes peaks
CH3 and H(C(5)) of triterpenes
4.0
3.5
3.0
2.5
2.0
1.5
1.0
0.5
1.000
3.922

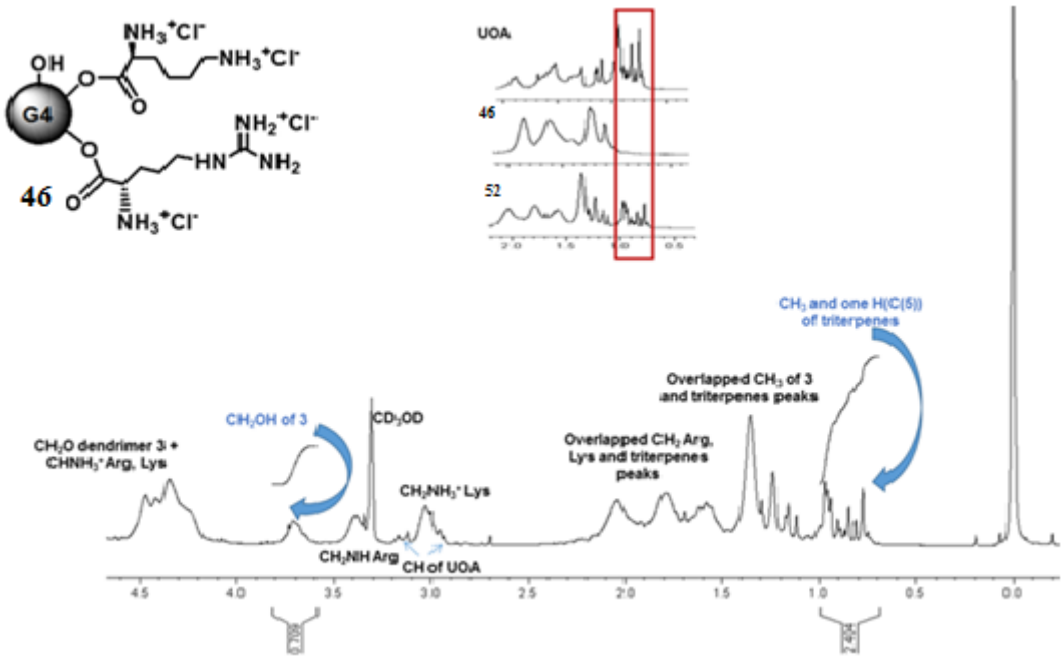
NH3+Cl-
NH3+Cl-
OH
G4
NH2+Cl-
HN
NH2
NH3+Cl-
46
UOA
46
52
CH3 and one H(C(5)) of triterpenes
Overlapped CH3 of 3 and triterpenes peaks
CH2OH of 3
CD3OD
CH2O dendrimer 3 + CHNH3+ Arg, Lys
Overlapped CH2 Arg, Lys and triterpenes peaks
CH2NH3+ Lys
CH2NH Arg
CH of UOA
4.5
4.0
3.5
3.0
2.5
2.0
1.5
1.0
0.5
0.0
2.000
7.494

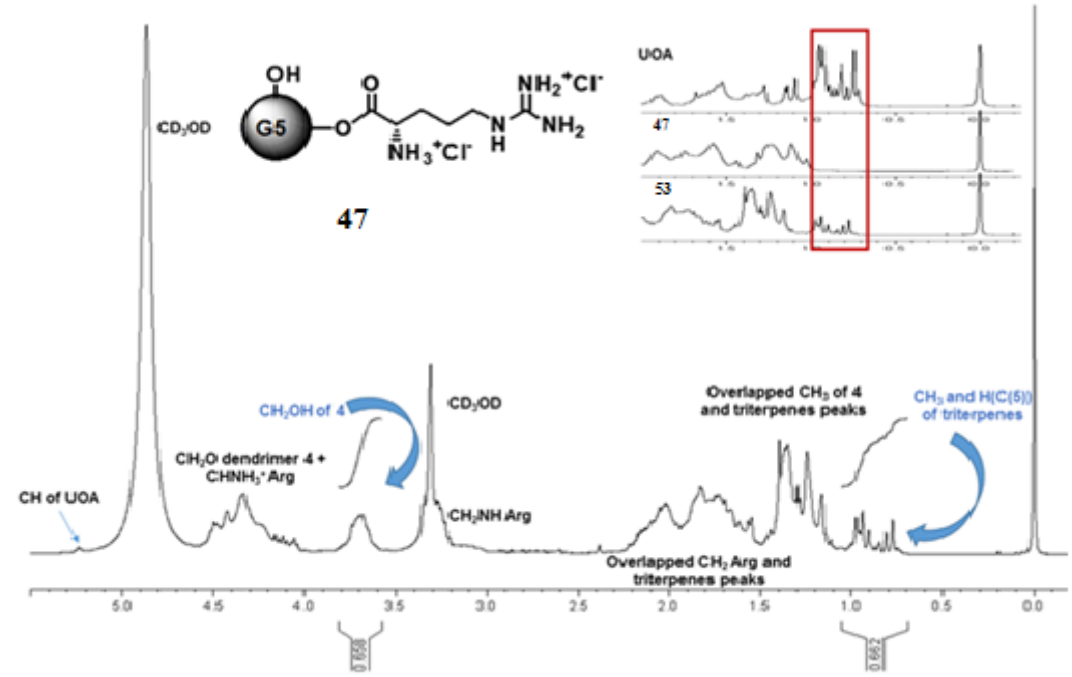
UOA
47
53
CD3OD
G5
47
CH2OH of 4
CD3OD
CH2O dendrimer 4 + CHNH3+ Arg
CH2NH Arg
CH of UOA
Overlapped CH3 of 4 and triterpenes peaks
CH3 and H(C(5)) of triterpenes
Overlapped CH2 Arg and triterpenes peaks

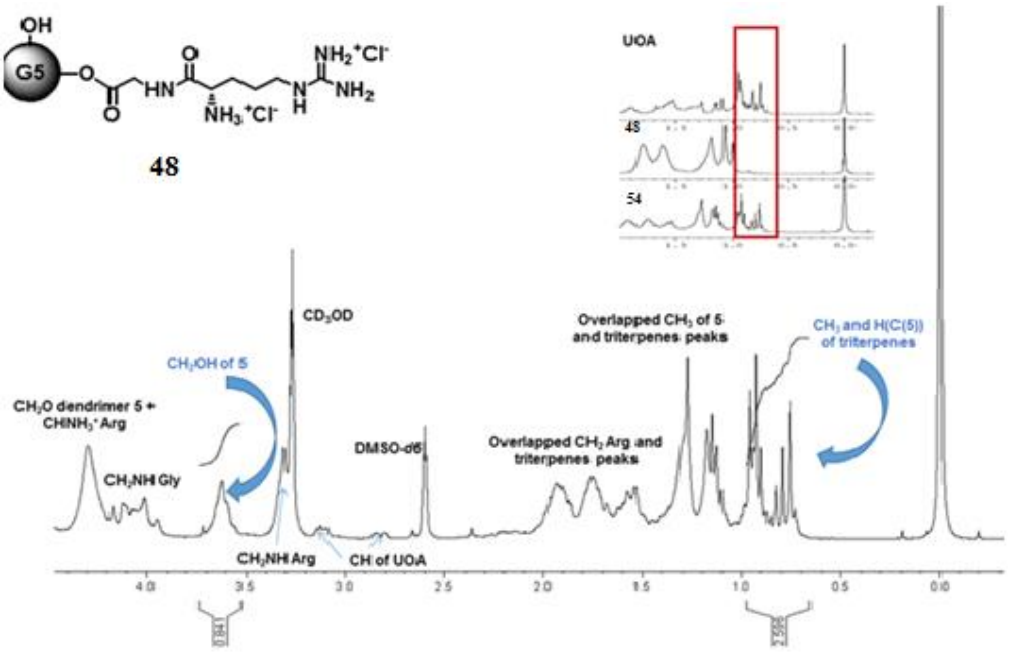
G5
48
UOA
48
54
CD3OD
CH2OH of 5
CH2O dendrimer 5 + CHNH3+ Arg
CH2NH Gly
CH2NH Arg
CH of UOA
DMSO-d6
Overlapped CH2 Arg and triterpenes peaks
Overlapped CH3 of 5 and triterpenes peaks
CH3 and H(C(5)) of triterpenes

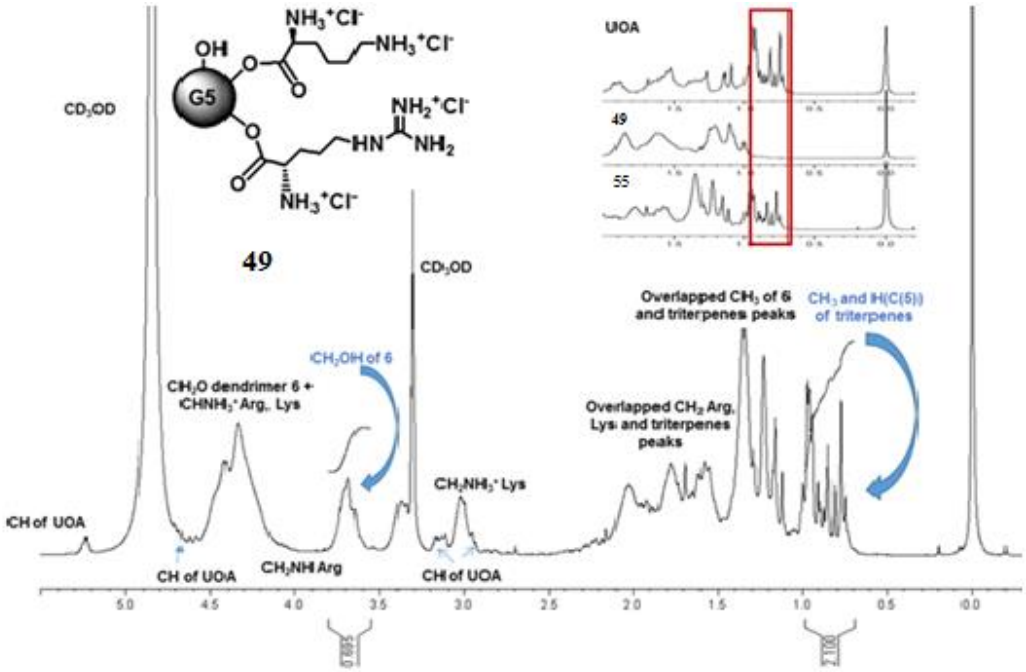

Figure 54. Comparison between ^{1}H-NMR spectra of the mixture UOA(CD_3OD/DMSO-*d6*, 300MHz),parent dendrimers **44-49** (DMSO-*d*6, 300 MHz) and dendriplexes (DPX) **50-55** (CD_3OD, 300 MHz)

It is clear that the peaks under 1.0 ppm not present in the parent dendrimers spectrum, but peculiar of UOA mixture and regarding seven CH_3 groups and H (C(5)) for a total of 22 H [244] were well detectable in the spectrum of the dendriplexes and very diagnostic to confirm that the encapsulation was successful and estimate the number of UOA units encapsulated per dendrimer mole.

As an example, Figure 55 shows the spectrum of **52** with in evidence the peaks and the integral values used to quantify the amounts of triterpenoid acids loaded per dendrimer mole. Briefly, for all dendriplexes, UOA units per complex mole were obtained comparing the integral value of CH_2OH at 3.6-3.8 ppm and the value of the integral of peaks between 0.72 and 0.98 ppm.

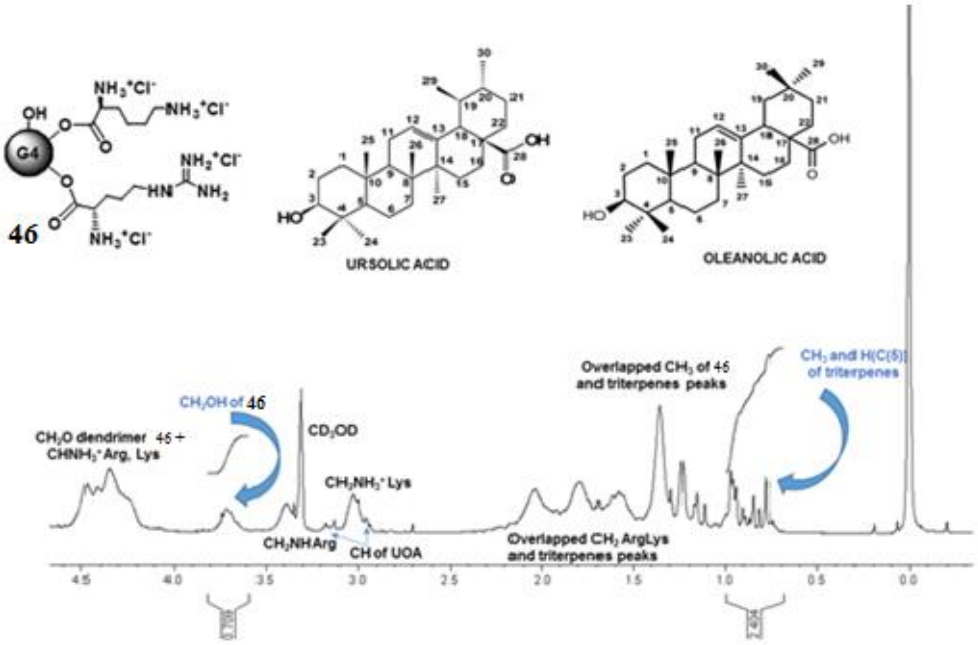

Figure 55. ^{1}H-NMR Spectrum of **52** (300MHz, CD_3OD)

Table 7 summarizes the principal data and results about the preparation of dendriplexes **50**-**55.**

Dendrimers of the fifth generation **48** and **49** decorated with dipeptide *L*-arginine –glycine and mixed *L*-arginine and *L*-lysine respectively, showed more efficiently in complexing UOA than the analogue dendrimers **51** and **52** of the fourth generation, which complexed half or almost of UOA per mole. Surprisingly, with dendrimers containing only *L*-arginine **50** and **53**, exactly the opposite happened; it was actually the fifth genereation dendrimer **53** that complexed the half amount of UOA in respect of **50**.

Table 7

Entry (mg/mmol)	N[a]	MW[b]	Dendriplex (mg)	Per dendrimer mole UOA units loaded[c] mg UOA/wt/wt %
44 47.6/0.0035	72	13593	**50** 51.4	6 8.6/16.8
45 21.7/0.0016	58	13644	**51** 12.5	7 2.4/19.0
46 31.5/0.0020	70	12831	**52** 27.0	4 3.4/12.5
47 41.2/0.0016	132	26040	**53** 44.2	3 2.2/5.0
48 24.0/0.0009	104	25799	**54** 16.1	12 2.8/16.1
49 29.0/0.0011	136	25661	**55** 20.5	8 2.6 /7.9

[a]Number of peripheral basic groups as determined by NMR;[b]Molecular Weights (MW) as determined by dendrimers composition estimate by NMR;[c]estimate by ^{1}H NMR spectra by integrating thesignals at 0.72-0.98 ppm [peaks of CH_3 groups of UOA and of H (C(5))] and at 3.6-3.8 ppm (CH_2OH group of parent dendrimer)

After having estimated the UOA units loaded per dendrimer mole it was possible to make an estimate of molecular weight of compounds **50-55** simply by summing the molecular weight of the forerunner dendrimer to the molecular weight of UOA multiplied by the number of complexed units as deduced by NMR spectra. Table 8 summarizes the obtained data.

Table 8 Calculated Molecular Weight of 50-55

Dendriplexes	Per dendrimer mole UOA units loaded[a] mg UOA/wt/wt %	MW
50	6 8.6/16.8	16334
51	7 2.4/19.0	16841
52	4 3.4/12.5	14658
53	3 2.2/5	27410
54	12 2.8/16.1	31280
55	8 2.6/7.9	29315

[a]Estimated by ^{1}H NMR spectra

4.1.2. Potentiometric Titrations of the Prepared Dendrimers

It is known that carriers improve their efficacy as delivery systems (DDSs) if endowed with a proper buffer capacity [$\beta = dc_{(HCl)}/(dpH)$][245]and so with an average buffer capacity [$\overline{\beta} = dV_{(HCl)}/d(pH)(1)$][246]in the pH range 4.5-7.5 suitable to make them escaping from endosomes compartments where pH is in the 5-6 range.[228] To have an estimate of the buffer capacity of the prepared dendriplexes, potentiometric titrations of **50-55** were performed according to Benns et al.[229] Since PAMAM are considered as good reference in the field both of gene delivery and of drug delivery literature data of three G4-PAMAM derivatives [230] potentiometrically titrated with the same protocol were used to obtain their titration curve. The β and $\overline{\beta}$ values of each prepared dendriplex and of G4-PAMAM derivatives were calculated from the titration data. Table 9 collects the β values recorded in the pH range 5-7 and Figures 56, 57 and 58 show all the titration and β curves and of the histogram of all the $\overline{\beta}$ calculated. As expected, considering the data about buffer capacity values of dendrimers **44-49**, all the dendriplexes prepared using them as vectors resulted in a β value higher than the G4-PAMAM derivatives taken as reference.

Table 9 Buffer capacity values of dendriplexes **50-55** and G4-PAMAMs in the pH range 6-7 from potentiometric titrations

Dendriplexes	pH	β
50	6.40	0.0833
51	6.00	0.0150
52	6.50	0.033
53	6.80	0.0426
54	6.10	0.0227
55	6.30	0.0180
G4-PAMAM[a]	7.00	0.0014
G4-PAMAM-Arg[b]	6.25	0.0024
G4-PAMAM-His-His-Arg[c]	6.20	0.0038

[a]Fourth generation PAMAM; [b]G4-PAMAM modified with arginine; cG4-PAMAM modified with the His- His-Arg sequence

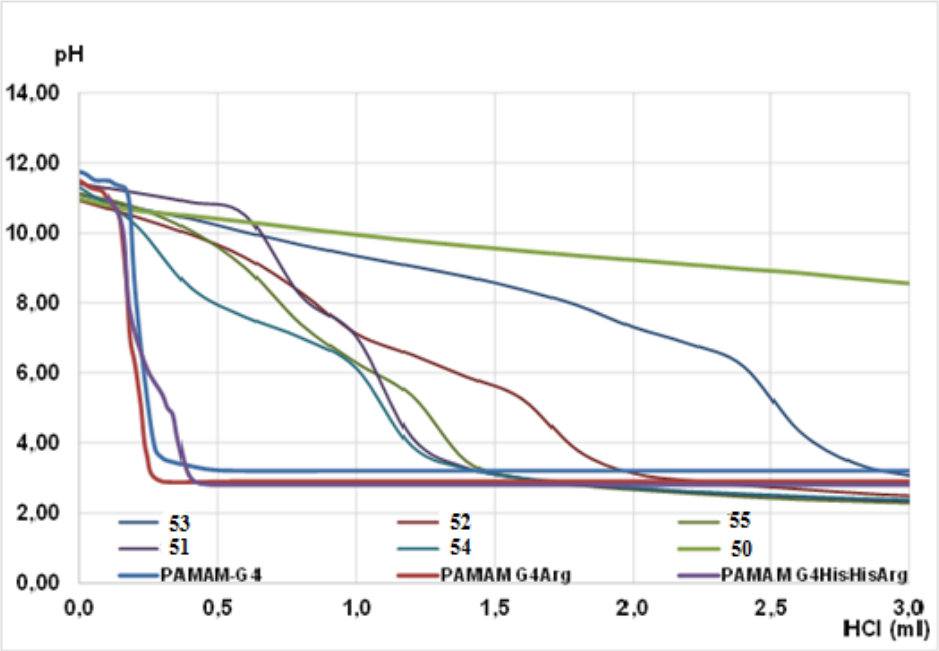

Figure 56. Potentiometric titration curves of prepared dendriplexes and of three G4-PAMAM derivatives

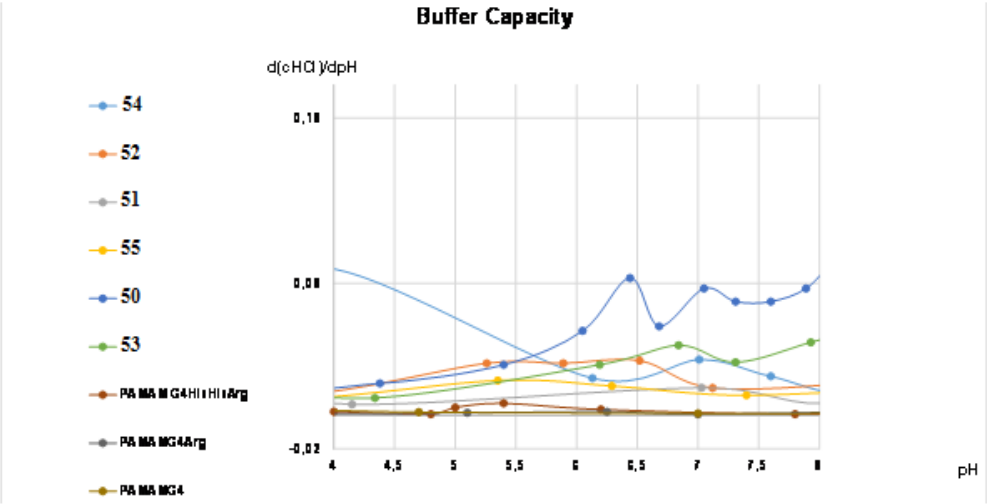

Figure 57. Graphic of the buffer capacity (β) of prepared dendriplexes and of three G4-PAMAM derivatives

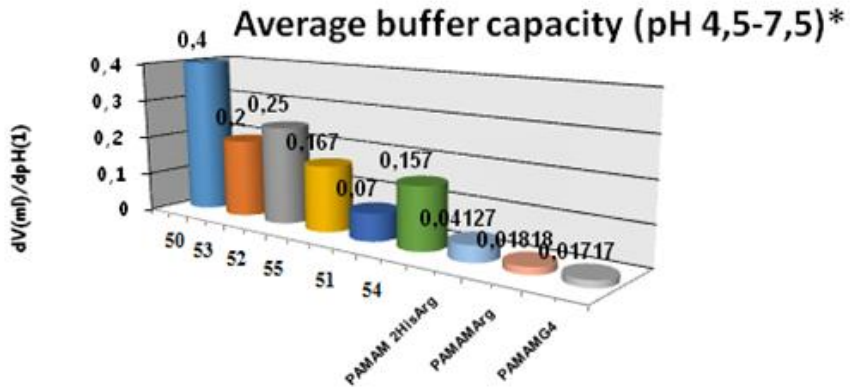

*calculated for three degrees of freedom

Figure 58. Histogram of average buffer capacity of prepared dendriplexes and of three G4-PAMAM derivatives (pH = 4.5-7.5)

4.1.3. Dynamic Light Scattering (DLS) and Zeta Potential

Particle hydrodynamic size (diameter) and Zeta Potential were measured and the obtained data together with the deviation standard (N=12) values are summarized in Table 10. Particle size was determined by Dynamic Light Scattering (DLS) and Z average diameter (Z-AVE, nm), derived from a cumulants analysis of the measured correlation curve, was reported as the intensity-weighted average (Int-Peak) hydrodynamic radius. Zeta potential (mV), which provides a measure of the electrostatic potential at the surface of the electrical double layer and the bulk medium and which is related to the nanoparticle surface charge, was performed using zeta-sizer (N=12). It is known that smaller particles more rapidly penetrate tumors compared to larger ones but extremely minute particles could easily undergo hepatobiliary and renal clearance. A balance between maximizing tumor penetration while minimizing both toxicity to normal tissue and clearance by the mononuclear phagocytic system (MPS) is the best solution and as reported, particles less than 100 nm and greater than 20 nm could be a good choice [247, 248]. As exposed in the Table 10 the mean particle size of G4,5 dendrimer/UOA complexes of the present paper was increased in comparison to parent dendrimers in function of the percentage wt/wt of UOA loaded.

Table 10 Summary of particles characterization: particles hydrodynamic size (DLS) and Zeta-Potential at 25°C of parent dendrimers **44-49** and of dendriplexes **50-55**

Dendrimer	N[a]	Z-Potential (mV)[b]	Z-AVE size (nm)[b,c]	Dendriplex UOA[d] wt/wt %	Z-Potential (mV)[b]	Z-AVE size (nm)[b,c]
44	72	31.2±0.1	4.4±0.1	**50** 6 16.8	22.2±0.1	30.6±3.1
45	58	21.5±0.6	4.7±0.1	**51** 7 19.0	15.5±0.6	36.3±3.4
46	70	34.8±0.2	4.6±0.1	**52** 4 12.5	24.8±0.2	24.9±1.1
47	132	50.0±0.6	5.1±0.1	**53** 3 5.0	34.0±0.6	16.1±2.1
48	104	43.7±0.7	5.4±0.1	**54** 12 16.1	30.7±0.7	35.9±2.8
49	136	51.8±0.1	5.3±0.1	**55** 8 7.9	31.8±0.1	20.3±3.1

[a]Number of peripheral basic groups as determined by NMR;[b]Degree of freedom = 12;[c]Derived from a cumulants analysis of the measured correlation curve and reported as the intensity-weighted average (Int-Peak)
hydrodynamic radius;[d]units of UOA complexed per dendrimer mole as estimated by ^{1}H NMR spectra

In any case the size was less than 100 nm, a value which assures that these prodrugs will not form the administration embolism and resulting promising for intravenously or intraperitoneally administration to the patient. Finally, except for sample **49**, the nanoparticles were all > 20 nm resulting suitable to be used as drugs vehicles with prolonged circulation time and efficient tumor penetration. The surface charge of the examined samples was slightly reduced compared to dendrimers **44-49** presumably due to interactions with the drugs moieties and was within range 15-35 mV with higher values for G5 samples than G4 and increasing at the increase of N.

4.1.4. Studies of the In Vitro Ursolic and Oleanolic acids release from Dendriplexes 50-55

As expected, the physical entrapping of the two triterpenoid acids in polyester-based, amino acids-modified dendrimers **44-49**, used as nanoparticle vectors, provided highly water-soluble prodrugs with expected enhanced bioavailability, but in order to explicate their pharmacological effects, ursolic and oleanolic acids need to be released from dendriplexes. Then, their in vitro release from the prodrugs was studied in buffer solutions at pH = 7.4, adding to the incubation medium (20% V/V with ethanol) to favour their solubility. Samples were taken out of the medium at fixed time points (1, 2, 5, 10, 24 and 48 h) and the released triterpenoids acids were quantified by HPLC. As data summarized in Table 11 all the profiles of the drugs released from the dendrimers prodrugs showed a three phase's pattern. The first phase resolved after the first hour of incubation at pH = 7.4, when the release was almost null. This presupposes that, after administration, only a minimum release of the drugs in the systemic circulation will occur and that the DDSs may have time to reach and enter the target cells where the bulk of the release should occur. Then a very fast release phase started while after five hours a sustained release phase took place. The amount of UOA released from G4-UOA dendriplexes was more than that released from G5-UOA ones and inside a generation, the release profile showed a dependence on N value. This may be rationally due to the stronger interactions of free UOA mixture with dendrimers having more cationic groups. This feature, that significantly differentiates the behaviour of our materials (at least in vitro), may be useful to modulate the amount of drug released over time and the total amount of drug that will be released, according to the therapeutic needs. In addition, to eliminate the effects of dialysis bag and release medium on the release rate, the release of free UA and OA mixture in the same release medium was also studied and reported as cumulative release (%) in the last row of Table 11.

Table 11 *In vitro* drugs release study results

UOA-loaded dendriplex (10 mg)	N[b]	Release of free UOA after different time (μg/10mg)[c]						
		0h	1h	2h	5h	10h	24h	48h
50	72	0	0.2	38.8	48.6	58.2	75.2	80.5
51	58	0	0.5	44.4	59.4	69.4	85.0	103.9
52	70	0	0.2	39.1	48.7	58.5	75.5	81.0
53	132	0	0	36.8	43.0	53.1	65.2	69.5
54	104	0	0	37.4	46.8	56.6	68.4	73.7
55	136	0	0	35.6	43.7	53.7	65.9	72.3
Release of free UOA (%)[a]	_	7.5	10.8	18.3	30.0	50.1	73.3	73.3

[a]Cumulative release percentage; [b]Number of peripheral basic groups as determined by NMR; [c]Weight of the free mixture UOA released from 10 mg of dendriplex.

EXPERIMENTAL

MATERIALS AND INSTRUMENTS

All the reagents and solvents were purchased from Aldrich or Merck and were used without further purifications. The solvents were dried and distilled according to standard procedures. Petroleum ether refers to the fraction with boiling point 40-60°C.

Melting points, determined on Leica Galen III hot stage apparatus or Mettler Toledo MP50 Melting Point System, are uncorrected. FTIR spectra were recorded as films or KBr pellets on a Perkin Elmer System 2000 spectrophotometer. ^{1}H and ^{13}C NMR spectra were acquired on a Bruker Avance DPX 300 Spectrometer at 300 and 75.5 MHz respectively and assigned through DEPT-135 and decoupling experiments. Coupling constant values were given in Hertz. Fully decoupled ^{13}C NMR spectra were reported. Chemical shifts were reported in δ [parts per million (ppm)] units relative to the internal standard tetramethylsilane (δ = 0.00 ppm) and the splitting patterns were described as follows: s (singlet), d (doublet), t (triplet), q (quartet), m (multiplet) and br (broad signal).

MALDI-TOF spectrum was acquired with a Brucker Reflex III MALDI instrument equipped with nitrogen laser (337 nm) using as matrix trans-3-indolacrylic acid or 2,5-dihydroxybenzoic acid.

Centrifugations were performed on an ALC 4236-V1D Centrifuge at 3400-3500 rpm. Dynamic Light Scattering (DLS) and Zeta Potential were performed on a Malvern Zetasizer Nano ZS instrument (Southborough, MA). pH measurements were performed with Mettler Toledo Four pH meter MP225 Real Panel after calibration with buffer pH = 4 and pH = 7. Elemental analysis were performed with an EA1110 Elemental Analyser (Fison-Instruments).Thin layer chromatography (TLC) system for routine monitoring the course of reactions and confirming the purity of analytical samples employed aluminium-backed silica gel plates (Merck DC-Alufolien Kieselgel 60 F254) and detection of spots was made by UV light and/or by ninhydrin solution 0.2% in ethanol and heating in stove at 100°C. Flash chromatography (FC) was performed on Merck Silica gel (0.040-0.063 mm). Organic solutions were dried over anhydrous sodium sulphate and were evaporated using a rotatory evaporator operating at reduced pressure of about 1.3-2.7 KPa. Polycationic amino acids-modified dendrimers of fourth (**44**-**46**) and fifth (**47**-**49**) generation were prepared according with a previously reported procedure.[205]

PLANT MATERIAL AND METHODS[236]

Fresh aerial parts of Salvia Corrugata Vahl were obtained from the Istituto Sperimentale per la Floricoltura (Sanremo,Italy) and Centro Regionale di Sperimentazione ed Assistenza Agricola(Albenga, Italy). The species was identified by Dr. Gemma Bramleyand a voucher specimen is deposited at Kew Herbarium (K) (Kew,Surrey, U.K.).

Extraction and Isolation of Ursolic and Oleanolic Acids Mixture[236]

For the isolation of leaf surface mixture of UA and OA, fresh aerial parts of Salvia Corrugata Vahl (2.6 kg) were immersed in CH_2Cl_2 for 20s to obtain only the external secreted material mixed with cuticular components, thereby avoiding extraction of components inside the cell wall. After filtration, the extraction solvent was removed under reduced pressure. The exudate (25 g, 0.96% wt/wt of fresh plant) was chromatographed in portions of 1.0 g on Sephadex LH-20 columns (53 × 2.5 cm), using $CHCl_3$/MeOH (7:3) as eluent. The eluate fractions (20 mL each) were combined according to TLC to obtain four main fraction groups (I-IV): group I (up to 140 mL) (waxy inactive compounds), group II (from 140 to 160 mL), group III (from 160 to 200 mL), group IV (from 200 to 260 mL). Group II was evaporated, washed with hexane and crystallized from EtOH and then from MeOH to yield a product which was identified as a crystalline mixture of UA and OA (4.2 g).

REACTIONS

Synthesis of 2, 2-*bis*(hydroxymethyl)propan-1-ol mono-stearate (4) and 2,2-*bis*(hydroxylmethyl)-1,3-propanediol mono-stearate (5)

Synthesis of acyl chloride (3)

In a 25 mL two-necked flask equipped with magnetic stirrer, condenser and nitrogen valve, stearic acid (1.00 g, 3.54 mmol) and fresh distillate thionyl chloride (1.73 g, 14.5 mmol, 1.05 mL) were mixed at 0°C. After stirring for 2 h at 70°C, the excess of $SOCl_2$ was removed under reduced pressure, providing **3** as yellow oil which crystallizes by cooling down (1.08 g, 3.56 mmol, 100%).

FTIR (film, cm^{-1}): 2925 and 2854 (CH_3CH_2), 1802 (C=O).

^{1}HNMR (300 MHz, $CDCl_3$): δ ppm = 0.88 (t, 3H, *J* = 7 Hz), 1.26 (s, 28H), 1.71 (m, 2H), 2.88 (t, 2H, *J*= 7 Hz).

^{13}CNMR (75.5 MHz, $CDCl_3$): δ ppm= 14.13 (*C*H_3), 22.71, 25.07, 28.43, 29.07, 29.33, 29.38, 29.53, 29.61 e 29.66 (9 *C*H_2), 29.68 and 29.70 (6 *C*H_2overlapped), 47.13 (*C*H_2C=O), 173.90 (*C*=O).

Synthesis of 2,2-bis(hydroxymethyl)propan-1-ol mono-stearate (4)

In a 25 mL flask flamed under nitrogen 2,2-bis(hydroxymethyl)propan-1-ol (**1**) (111.4 mg, 0.927 mmol), *N,N'*-dimethylaminopyridine (DMAP) (203.9 mg, 1.67 mmol), stearic acid chloride (**3**) (666.5 mg, 2.20 mmol, 743.0 μL), and freshly distilled pyridine on KOH were introduced. The reaction mixture was kept under stirring at 50°C for 24 h. At the end of the time, the white suspension in brown solution was transferred to a separator funnel and hydrolyzed with H_2O (20 mL). The water phase was extracted with dichloromethane (DCM) (2 x 15 mL) and the combined organic phases were dried over Na_2SO_4. After evaporation of the solvent at reduced pressure, a pyridine odorous residue (668.5 mg) was obtained. It was analyzed by TLC eluted both with petroleum ether/diethyl ether (Et_2O)/AcOH/methanol (MeOH) = 6/3/0.2/1 mixture (System B) and with a petroleum ether/Et_2O/AcOH = 7/3/0.2 (System A) to evaluate its composition. The crude was then chromatographed on silica gel column to separate the stearates. In fractions eluted with petroleum ether/ Et_2O 1/1, the *tri*-stearate was collected as white solid (158.0 mg, 0.172 mmol, 18.6%).

FTIR (KBr, cm^{-1}): 2955, 2917, 2849 (CH_3CH_2), 1722 (C=O).

^{1}HNMR (300 MHz, $CDCl_3$): δ ppm = 0.81 (t, 9H, *J* = 7.4 Hz, C*H*$_3$ stearate), 0.94 (s, 3H, C*H*$_3$*core*), 1.19 (br s, 84H, C*H*$_2$ stearate), 1.54 (m, 6H, C*H*$_2$ stearate), 2.24 (t, 6H, *J* = 8.2 Hz, C*H*$_2$C=O stearate), 3.93 (s, 6H, C*H*$_2$O).

^{13}CNMR (75.5 MHz, $CDCl_3$):δ ppm = 13.10 (*C*H_3 stearate), 13.18 (*C*H_3*core*), 21.70, 23.94, 27.92, 27.95, 28.00, 28.09, 28.17, 28.28, 28.38, 28.45, 28.50, 28.63, 28.68, 37.32 (*Ccore*), 64.64 (*C*H_2O *core*), 172.52 (*C*=O esters).Anal. Calcd. for $C_{58}H_{114}O_6$: C, 77.06; H, 12.50. Found: C, 77.46; H, 12.23.

In fractions eluted with Et_2O 100%, the *di*-stearate was collected as white solid (247.0 mg, 0.38 mmol, 40.8%).

FTIR (KBr, cm^{-1}): 3431 (OH), 2955, 2917, 2850 (CH_3CH_2), 1736 (C=O).

^{1}HNMR (300 MHz, $CDCl_3$): δ ppm = 0.88 (t, 6H, *J* = 8.2 Hz, C*H*$_3$ stearate), 0.96 (s, 3H, C*H*$_3$*core*), 1.25 (br s, 56H, C*H*$_2$ stearate), 1.62 (m, 4H , C*H*$_2$ stearate), 2.33

(t, 4H, *J* = 8.2 Hz, C*H*$_2$C=O stearate), 3.39 (s, 2H, C*H*$_2$OH), 4.03 (s, 4H, C*H*$_2$O), 1H, O*H*, not detected.

^{13}CNMR (75.5 MHz, CDCl$_3$): δ ppm = 14.13 (*C*H$_3$ stearate), 16.82 (*C*H$_3$*core*), 22.70, 25.00, 29.18, 29.27, 29.38, 29.48, 29.62, 29.67, 29.71, 31.94, 34.28 (*C*H$_2$ stearate, 5 overlapped), 40.34 (*Ccore*), 64.61 (*C*H$_2$OH), 65.89 (*C*H$_2$O), 174.19 (*C*=O esters).Anal. Calcd. for $C_{41}H_{80}O_5$: C, 75.40; H, 12.35. Found: C, 75.46; H, 12.22.

In the fractions eluted with Et$_2$O/MeOH 95/5, the *mono*-stearate of interest (**4**) was collected as white solid (158.4 mg, 0.41 mmol, 44.2%).

FTIR (KBr, cm^{-1}): 3412, 3271 (OH), 2955, 2918, 2849 (CH_3CH_2), 1722 (C=O).

^{1}HNMR (300 MHz, CDCl$_3$): δ ppm = 0.84 (s, 3H, C*H*$_3$*core*), 0.88 (t, 3H, *J* = 8.3 Hz, C*H*$_3$ stearate), 1.26 (br s, 28H, C*H*$_2$ stearate), 1.64 (m, 2H, C*H*$_2$ stearate), 2.36 (t, 2H, *J* = 8.2 Hz, C*H*$_2$C=O stearate), 2.70 (t, 2H, *J* = 6 Hz, O*H*), 3.54 (m, 4H, J_{vic} = 6 Hz, J_{gem} = 11 Hz, C*H*$_2$OH), 4.21 (s, 2H, C*H*$_2$O).

^{13}CNMR (75.5 MHz, CDCl$_3$): δ ppm = 14.13 (*C*H$_3$ stearate), 16.85 (*C*H$_3$ *core*), 22.70, 25.06, 29.18, 29.25, 29.37, 29.46, 29.61, 29.65, 29.71, 31.94, 34.35 (*C*H$_2$ stearate, 5 overlapped), 40.82 (*C core*), 66.37 (*C*H$_2$O), 67.88 (*C*H$_2$OH), 175.07 (*C*=O ester).Anal. Calcd. for $C_{23}H_{46}O_4$: C, 71.45; H, 11.99. Found: C, 77.48; H, 12.13.

Synthesis of 2,2-bis(hydroxylmethyl)-1, 3-propanediol mono-stearate (5)

In a 25 mL flask flamed under nitrogen 2,2-*bis*(hydroxymethyl)-1,3-propanediol (**2**) (189.4 mg, 1.24 mmol), *N,N'*-dimethylaminopyridine (DMAP) (272.7 mg, 2.23 mmol), stearic acid chloride (**3**) (1.08 mg, 3.57 mmol) and freshly distilled pyridine on KOH (7.7 mL) were introduced. The reaction was kept under stirring at 50°C for 24 h. At the end of the time the white suspension in brown solution is transferred to a separator funnel and hydrolyzed with H_2O (20 mL). Waters were extracted with dichloromethane (DCM) (2 x 15 mL). The combined organic extracts were washed with H_2O to remove pyridine as much as possible and dried over Na_2SO_4. After evaporation of the solvent, a residue smelling of pyridine (1.34 mg) was obtained and was analyzed by TLC eluted both with petroleum ether/Et$_2$O/AcOH/MeOH = 6/3/0.2/1 mixture and with a petroleum ether/Et$_2$O/AcOH = 7/3/0.2 to evaluate its composition. The crude was then chromatographed on silica column to separate the stearates. The polyesters are eluted in the head fractions, while from the fractions eluted with Et$_2$O/MeOH 90/10 the *mono*-stearate of interest (**5**) was collected as a white solid (328.9 mg) which, analyzed at the NMR resulted in containing traces residual of other esters. Further silica gel column

was necessary to allow isolating the pure compound **5** as a pale yellow solid (228.4 mg, 0.567 mmol, 45.8%) from fractions eluted with Et_2O/ MeOH 80/20.

FTIR (KBr, cm^{-1}): 3433 (OH), 2918, 2850 (CH_3CH_2), 1735(C=O).

^{1}HNMR (300 MHz, $CDCl_3$): δ ppm = 0.89 (t, 3H, *J* = 7.0 Hz, C*H*$_3$), 1.25 (br s, 28H, C*H*$_2$ stearate), 1.62 (m, 2H, C*H*$_2$ stearate), 2.37 (m, 2H, C*H*$_2$C=O stearate), 3.64 (s, 6H, C*H*$_2$OH), 4.17 (s, 2H, C*H*$_2$O), 3H, O*H*, not detected.

^{13}CNMR (75.5 MHz, $CDCl_3$): δ ppm = 14.13 (*C*H_3 stearate), 22.71, 25.02, 29.19, 29.28, 29.38, 29.49, 29.68, 29.72, 31.94, 34.29 (*C*H_2 stearate, 6 overlapped), 45.37 (*C core*), 62.84 (*C*H_2O), 63.37 (*C*H_2OH), 174.98 (*C*=O ester).Anal. Calcd. for $C_{23}H_{46}O_5$: C, 68.61; H, 11.52. Found: C, 68.93; H, 11.23.

Synthesis of compound 6

In a 100 mL one-neck flask equipped with magnetic stirrer, **1** (1.3g, 0.010 mol), *p*-toluenesulfonic acid (TsOH) (0.060g, 0.315mmol) and anhydrous tetrahydrofuran (THF) (20mL) were introduced. The suspension was added dropwise with benzaldehyde (1.21 g, 0.0115 mol, 1.16 mL) and allowed to react for 16 h at room temperature. The reaction was then neutralized with aqueous ammonia and the mixture was concentrated under reduced pressure to give a residue which was dissolved in dichloromethane (DCM) and washed three times with water. The organic phase was dried overnight on Na_2SO_4. After removal of the solvent under reduced pressure, an oil was obtained and was crystallized from toluene/*n*-hexane to give **6** as white solid (1.52 g, 7.29 mmol, 73%).

FTIR (KBr, cm^{-1}): 3486 and 3413 (OH), 3041 (CH benzene).

^{1}HNMR (300 MHz, $CDCl_3$): *δ* ppm = 0.76 (s, 3H), 2.39 (s, 1H, O*H*), 3.62 (d, 2H, *J* = 12 Hz, C*H*$_2$O dioxane), 5.42 (s, 2H, C*H*$_2$OH), 4.03 (d, 2H, *J* = 12 Hz, C*H*$_2$O dioxane), 5.42 (s, 1H, C*H*benzylidene), 7.33-7.39 (m, 3H, C*H*= phenyl), 7.45-7.48 (m, 2H, C*H*= phenyl).

^{13}CNMR (75.5 MHz, $CDCl_3$): *δ* ppm = 16.93 (*C*H_3), 34.90 (*C core*), 65.46 (*C*H_2OH), 73.31 (*C*H_2O dioxane), 101.78 (*C*H benzylidene), 126.06 (*C*H= phenyl), 126.30 (*C*H= phenyl), 128.98 (*C*H= phenyl), 138.17 (*C*phenyl).

Synthesis of compound 6 and the flopped attempt performed to restore the OH groups

A sample of **6** (1.05 g, 5.05 mmol), **3** (1.54 g, 5.08 mmol) and anhydrous pyridine (2 mL) were introduced at 0°C into a two-necks flask flamed under nitrogen and allowed to reach room temperature. After 2 h from a FTIR analysis, the disappearance of C=O peak of the stearic acid chloride at 1802 cm^{-1} was checked and

appearance of the ester peak at 1736 cm^{-1} was observed. Then, the reaction mixture was hydrolyzed with H_2O (20 mL) and the waters were extracted with DCM (3 x 15 mL). The combined organic phases were dried on Mg_2SO_4. After evaporation of the solvent at reduced pressure at dark, pyridine smelling residue was obtained and was filtered on a silica plug (h = 10 cm; ø = 2 cm) washing with petroleum ether (25 mL + 25 mL) and then with EtOAc/petroleum ether 1/1 (50 mL).After evaporation of the solvents an orange oil which was crystallized from petroleum ether was obtained. The crystallized solid was filtered, washed several times with water to remove the residual pyridine and recrystallized from methanol (MeOH) to obtain **7** as off white or tan solid (1.70 g, 3.71 mmol, 73.4%).

FTIR (KBr, cm^{-1}): 3063 and 3028 (CH phenyl), 2912 and 2849 (CH_3CH_2), 1736 (C=O).

^{1}H NMR (300 MHz, $CDCl_3$): δ ppm = 0.80 (s, 3H, C*H*$_3$ *core*), 0.88 (t, 3H, *J*= 7 Hz, C*H*$_3$ stearate), 1.25 (br s, 28H, C*H*$_2$ stearate), 1.63 (m, 2H, C*H*$_2$ stearate), 2.34 (t, 2H, *J* = 7 Hz, C*H*$_2$C=O stearate), 3.67 (d, 2H, *J*= 12 Hz, C*H*$_2$O dioxane), 4.06 (d, 2H, *J* = 12 Hz, C*H*$_2$O dioxane), 4.38 (s, 2H, C*H*$_2$O *core*), 5.42 (s, 1H, C*H* benzylidene).

^{13}CNMR (75.5 MHz, $CDCl_3$): δ ppm = 14.12 (*C*H$_3$ stearate), 17.21 (*C*H$_3$ *core*), 22.70, 25.00, 29.21, 29.28, 29.37, 29.48, 29.62, 29.70, 31.94, 33.68 (*C*H$_2$ stearate, 6 overlapped), 34.36 (*C core*), 66.38 (*C*H$_2$OC=O), 73.38 (*C*H$_2$O dioxane), 102.05 (*C*H benzylidene), 126.15 (*C*H= phenyl), 128.32 (*C*H= phenyl), 129.05 (*C*H= phenyl), 138.38 (*C*phenyl), 173.82 (*C*=O ester).

About the second step reported in the above Scheme we remember (see main test) that unfortunately, when **7** was subjected to deprotection reaction by catalytic hydrogenation (Pd / C 10 %) with H_2 at 1.5 torr in EtOH at 100% at room temperature, we achieved a solid which after purification by crystallization had FT-IR and NMR spectra identical to those of precursor **6**. Other attempts to restore the OH groups performing other procedure such as using acids resins were unsuccessful.

Synthesis of Dendrons 8-11

p-Toluenesulfonate of 4- (N, N'-dimethylamino) pyridinium (DPTS)

In a one-necked flask equipped with a magnetic stirrer, TsOH monohydrate (3.23 g; 17 mmol) was dried by distillation in anhydrous benzene (30 mL), then a solution of DMAP (2.08 g; 17 mmol) in benzene (20 mL) was slowly dripped into the

reaction flask maintaining vigorous stirring, with the formation of a white precipitate which is filtered and washed with pentane. The crude salt was dissolved in the minimum amount of CH_3Cl and crystallized by addition of CCl_4. The white solid was filtered and brought to constant weight at reduced pressure (4.23g; 14mmoli; 82%).M.p. =172-174°C(litt.[221]165°C).FTIR(KBr,cm^{-1}):1218(S=O).^{1}HNMR(CD_3OD,δppm): 2.35 (s, 3H), 3.21 (s, 6H), 6.94-7.23 (m, 4H), 7.68-8.09 (m, 4H).^{13}C NMR:21.49,40.41, 108.40, 127.14, 130.02, 140.15, 141.87, 143.82, 159.25.

Synthesis of compound 8

In a 100 mL one-neck flask equipped with magnetic stirrer, acetone (56 mL), 2,2-*bis*(hydroxymethyl) propanoic acid (10.00 g, 74.56 mmol), 2,2-Dimethoxypropane (15.08 mL, 12.77 g, 122.59 mmol) and TsOH (0.2330 g, 1.21 mmol) were inserted. The reaction mixture was kept under stirring at room temperature for 2 h, then NH_3 solution was added in EtOH 1/1 (2 mL) observing the formation of a colorless oil. After removal of the solvent under reduced pressure, formation of crystals was observed to give a fine white solid. This residue was dissolved in DCM (100 mL) and EtOAc (150 mL), the solution was washed with H_2O (2 x 40 mL). The organic phase was dried over Na_2SO_4 then evaporated under reduced pressure to give **8** as white solid (8.72 g, 50.6 mmol, 67%),m.p. = 122-125°C.

FTIR (KBr, cm^{-1}): 3500-2400 (OH), 1722 (C=O).

^{1}H NMR (300 MHz, $CDCl_3$):δ ppm = 1.20 (s, 3H), 1.42 (s, 3H), 1.45 (s, 3H), 3.68 (d, 2H, *J* = 12 Hz), 4.20 (d, 2H, *J* = 12 Hz), 10.15 (s, 1H, O*H*).

^{13}CNMR (75.5 MHz, $CDCl_3$): δ ppm = 18.39, 21.96, 25.12, 41.70, 65.81, 98.29, 180.17.

Synthesis of 9

In a 100 mL three-necks flask equipped with magnetic stirrer, condenser and nitrogen valve,2,2-*bis*(hydroxymethyl) propanoic acid (4.50 g, 33.6 mmol) and KOH (2.18 g, 38.9 mmol) were dissolved in DMF (25 mL). The reaction mixture was stirred for 1 h at 100°C, and then benzyl bromide (5 mL, 40.9 mmol) was added. After stirring for 15 h at 100°, the solvent was removed under reduced pressure and the residue dissolved inDCM (100 mL) and washed with H_2O (2 x 25 mL). The organic extracts were dried over Na_2SO_4 and then evaporated under reduced pressure to give **9** as an oil, which was crystallized from DCM/$_n$-hexane = 1/1 as white crystals (6.42 g, 28.6 mmoli, 85%), m.p. = 88-90°C.

FTIR (KBr, cm^{-1}):3512 (OH), 3365 (OH), 1720 (C=O).

^{1}H NMR (300 MHz, $CDCl_3$): δ ppm = 1.09 (s, 3H), 2.99 (s, 2H), 3.72 (d, 2H, *J* = 11.2 Hz), 3.92 (d, 2H, *J* = 11.2 Hz), 5.19 (s, 2H), 7.35 (m, 5H).

^{13}CNMR (300 MHz, $CDCl_3$): δ ppm = 17.16, 49.31, 66.63, 67.76, 127.66, 128.28, 128.63, 133.30, 175.72.

Synthesis of 10

In a 100 mL one-neck flask equipped with magnetic stirrer and nitrogen valve, **8** (7.32 g, 42.0 mmol), **9** (4.49 g, 20.0 mmol), DPTS (2.36 g, 8.0 mmol), DCM (70 mL) and finally *N*,*N'*-dicyclohexylcarbodiimide (DCC) (10.02 g, 50.0 mmol) were introduced. The reaction mixture was kept under stirring at room temperature in nitrogen stream for 15 h, then the precipitated *N*,*N'*-dicyclohexylurea (DCU) was removed by filtration and washed with DCM (3 x 5 mL). Evaporated the solvent, the residue was solved with EtOAc and the insoluble fraction (DPTS) was filtered and washed with EtOAc. The filtrate and washings were combined and chromatographed on silica gel column using apetroleum ether/EtOAc = 3/2 as eluent to give **10** as colourless viscous oil (10.00 g, 22.4 mmol, 97%).

FTIR (film, cm^{-1}): 1737 (C=O).

^{1}H NMR (300 MHz, $CDCl_3$): δ ppm = 1.09 (s, 6H), 1.31 (s, 3H), 1.34 (s, 6H), 1.41 (s, 6H), 3.58 (d, 4H, *J* = 12 Hz), 4.11 (d, 4H, *J* = 12 Hz), 4.34 (s, 2H), 4.35 (s, 2H), 5.16 (s, 2H), 7.26-7.35 (m, 5H).

^{13}CNMR (75.5 MHz, $CDCl_3$): δ ppm = 17.73, 18.48, 22.28, 24.96, 42.03, 46.84, 65.36, 65.92, 65.96, 66.98, 98.11, 128.23, 128.42, 128.64, 135.48, 172.42, 173.54.

Synthesis of 11

A 100 mL two-necked flask equipped with a magnetic stirrer containing a solution of **10** (6.05 g, 11.3 mmol) in EtOAc (50 mL) and Pd/C 10% (0.61 g) was connected to a hydrogenation burette system. The reaction mixture was kept under stirring under a slight hydrogen pressure for 6 h. After hydrogen adsorption ceased, the catalyst was removed by filtration on silica gel short column and the filtrate was evaporated under reduced pressure to give **11** as colorless viscous oil (5.05 g, 9.4 mmol, 84%).

FTIR (film, cm^{-1}):3500-2400 (OH),1736 (C=O).

^{1}H NMR (300 MHz, $CDCl_3$): δ ppm= 1.16 (s, 6H), 1.32 (s, 3H), 1.37 (s, 6H), 1.42 (s, 6H), 3.64 (d, 4H, *J* = 12 Hz), 4.17 (d, 4H, *J* = 12 Hz), 4.34 (s, 4H).

^{13}C NMR: (75.5 MHz, $CDCl_3$): δ ppm= 14.12, 18.50, 22.28, 24.91, 42.06, 46.54, 65.13, 65.92, 65.96, 98.25, 173.54, 177.36.

Synthesis of second and third generation acetonide protected C-18 dendrimers 13, 15, 17, 19 and 21.

Esterification reaction of 4 with 11 (12)

A sample of **4** (54.1 mg, 0.1399 mmol) was introduced into a flask flamed under nitrogen and was dissolved in DCM (1.5 mL). Then **11** (131.14 mg, 0.293 mmol) and DPTS (16.47 mg, 0.056 mmol) were introduced. The clear solution was added with *N,N'*-dicyclohexylcarbodiimide (DCC) (72.14 mg, 0.3497 mmol) by noticing immediate precipitation of *N,N'*-dicyclohexylurea (DCU) and the suspension was kept under stirring for 24 h at r.t. At the end of the time, the white suspension was filtered and the DCU was washed carefully with DCM (2 x 5 mL). The obtained solution was evaporated under reduced pressure. The residue was solved with ethyl acetate (EtOAc) (10 mL) and the insoluble portion re-filtered and washed with EtOAc (2 x 5 mL). The new solution was evaporated to give a residue (202.9 mg) which was purified by chromatography column, isolating **12** in the fractions eluted with petroleum ether/ethyl acetate (EtOAc) 1/1 as colorless resin (171.0 mg, 0.137 mmol, 98.3%).

FTIR (KBr, cm^{-1}): 2991, 2927, 2855 (CH_3CH_2), 1739 (C=O esters).

^{1}H NMR (300 MHz, $CDCl_3$): δ ppm = 0.88-1.18 (m, 6H, C*H*$_3$ *core* and C*H*$_3$ stearate), 1.26-1.31 (m, 46H, C*H*$_3$D1, D2 and C*H*$_2$ stearate), 1.35 and 1.36 (s, 12H, C*H*$_3$acetonide), 1.37 and 1.41 (s, 12H, C*H*$_3$acetonide), 1.62 (m, 2H, C*H*$_2$ stearate), 2.32 (two intersected triplets, 2H, *J* = 6.4 Hz, C*H*$_2$C=O stearate), 3.62 (d, 8H, *J* = 12.0 Hz, C*H*$_2$O dioxane), 4.01-4.10 (m, 4H, C*H*$_2$O *core*), 4.15 (d, 8H, *J* = 12.0 Hz, C*H*$_2$O dioxane), 4.32 (s, 2H, C*H*$_2$O *core*), 4.35 (br s, 8H, C*H*$_2$O D1).

^{13}C NMR (75.5 MHz, $CDCl_3$):δ ppm = 14.11 (*C*H$_3$ stearate), 17.06 (*C*H$_3$ *core*), 17.74 (*C*H$_3$ D1), 18.51 (*C*H$_3$ D2), 21.50-22.85 (more signals, *C*H$_3$ acetonide), 22.67 (*C*H$_2$ stearate), 24.71-26.08 (more signals, *C*H$_3$ acetonide), 24.98 (*C*H$_2$ stearate), 29.17, 29.26, 29.34, 29.46, 29.68, 31.91, 34.22 (14 *C*H$_2$ stearate, 7 overlapped), 38.88 and 40.19 (*C core*), 42.07 (*C* D2), 47.01 (*C* D1), 63.95-66.80 (*C*H$_2$O *core* e *C*H$_2$O D1, D2), 98.10 e 98.21 (*C*acetonide), 172.10-174.25 (*C*=O esters). Anal. Calcd. for $C_{65}H_{110}O_{22}$: C, 62.78; H, 8.92. Found: C, 62.44; H, 9.00.

Esterification reaction of 4 with 8 (14)

A sample of **4** (60.3 mg, 0.156 mmol), **8** (57.1 mg, 0.327 mmol), DPTS (18.4 mg, 0.0624 mmol) and DCM (3 mL) were introduced into a flask previously flamed under nitrogen. The clear solution was added with DCC (80.5 mg, 0.390 mmol) by noticing instant precipitation (DCU) and the suspension was kept under stirring for 24 h at r.t. Then the white suspension was filtered and washed carefully with DCM (3 x 5 mL). The residue obtained after evaporation of solvent under reduced pressure was solved with EtOAc (10 mL) and the insoluble portion filtered again and washed with EtOAc (3 x 15 mL). The new solution was evaporated to give a spongy residue (148.5 mg) which was purified by chromatography column, isolating the compound of interest **14** in fractions eluted with the mixture petroleum ether/EtOAc 1/1 ascolorless resin (95.3 mg, 0.136 mmol, 87.4%).

FTIR (KBr, cm^{-1}): 2926, 2853 (CH_3CH_2), 1737 (C=O esters).

^{1}H NMR (300 MHz, $CDCl_3$): δ ppm = 0.88 (t, 3H, *J* = 7.4 Hz, C*H*$_3$ stearate), 0.98 and 1.07 (s, 3H, C*H*$_3$ *core*), 1.14 and 1.16 (s, 6H, C*H*$_3$ D1), 1.26 (br s, 28H, C*H*$_2$ stearate), 1.36 and 1.37 (s, 6H, C*H*$_3$acetonide), 1.42 and 1.43 (s, 6H, C*H*$_3$acetonide), 1.61 (m, 2H, C*H*$_2$ stearate), 2.32 (two intersected triplets, 2H, *J* = 7.0 Hz, C*H*$_2$C=O stearate), 3.64 and 3.66 (d, 4H, *J* = 12.0 Hz, C*H*$_2$O dioxane), 4.04, 4.06 and 4.07 (s, 4H, C*H*$_2$O *core*), 4.12 (s, 2H, C*H*$_2$O *core*), 4.18 (d, 4H, *J* = 12.0 Hz, C*H*$_2$O dioxane).

^{13}C NMR (75.5 MHz, $CDCl_3$):δ ppm = 14.12 (*C*H$_3$ stearate), 16.90 and 18.37 (*C*H$_3$ *core*), 17.03 and 18.53 (*C*H$_3$ D1), 21.28 and 21.90 (*C*H$_3$ acetonide), 22.69 (*C*H$_2$ stearate), 24.68 (*C*H$_2$ stearate), 24.94 (*C*H$_3$ acetonide), 29.17, 29.27, 29.37, 29.48, 29.70, 31.93, 34.15 (*C*H$_2$ stearate, 7 overlapped), 39.13 and 40.43 (*C core*), 42.19 and 42.30 (*C* D1), 64.88-67.29 (*C*H$_2$O *core* and *C*H$_2$O D1), 98.12 and 98.20 (*C*acetonide), 173.32-174.47 (*C*=O esters). Anal. Calcd. for $C_{39}H_{70}O_{10}$: C, 67.02; H, 10.09. Found: C, 66.95; H, 9.82.

Esterification of 15 with 11 (16)

In flask flamed under nitrogen, **15** (87.3 mg, 0.141 mmol), (264.4 mg, 0.592 mmol) and DPTS (32.2 mg, 0.113 mmol) were introduced and dissolved in DCM (7.3 mL). The clear solution was added with DCC (145.5 mg, 0.705 mmol) by noticing instant precipitation (DCU) and the suspension was kept under stirring for 24 h at r.t. At the end of the time the white suspension was filtered. The solid was washed with DCM (3 x 5 mL) and the resulting solution was evaporated under reduced pressure. The residue was then re-suspended in EtOAc (10 mL), the insoluble portion filtered and

washed with EtOAc (3 x 5 mL). The new solution was evaporated to give a spongy residue (389.9 mg) which was purified by chromatography column, isolating the compound of interest **16** in fractions eluted with petroleum ether/EtOAc 1/1 and EtOAc as resin (225.4 mg, 0.0966 mmol, 68.5%).

FTIR (KBr, cm^{-1}): 2991, 2928, 2856 (CH_3CH_2), 1738 (C=O esters).

^{1}H NMR (300 MHz, $CDCl_3$): δ ppm = 0.88 (t, 3H, *J* = 7.4 Hz, C*H*$_3$ stearate), 1.07 (s, 3H, C*H*$_3$ *core*), 1.13 (s, 6H, C*H*$_3$ D1), 1.14 (s, 12H, C*H*$_3$ D2), 1.16 (s, 24H, C*H*$_3$ D3), 1.25-1.33 (m, 28H, C*H*$_2$ stearate), 1.35 and 1.36 (s, 24H, C*H*$_3$acetonide), 1.42 (s, 24H, C*H*$_3$acetonide), 1.60 (m, 2H, C*H*$_2$ stearate), 2.32 (t, 2H, *J* = 7.2Hz, C*H*$_2$C=O stearate), 3.61-3.65 (m, 16H, *J* = 12.0 Hz, C*H*$_2$O dioxane), 3.90-4.10 (m, 4H, C*H*$_2$O *core*), 4.15-4.19 (m, 16H, *J* = 12.0 Hz, C*H*$_2$O dioxane), 4.33-4.37 (m, 26H, C*H*$_2$O D1, D2 + C*H*$_2$O *core*).

^{13}C NMR (75.5 MHz, $CDCl_3$): δ ppm = 14.12 (*C*H$_3$ stearate), 17.54 (*C*H$_3$ *core*), 17.72 (*C*H$_3$ D1), 18.47 (*C*H$_3$ D2), 18.53 (*C*H$_3$ D3), 21.33-22.43 (more signals, *C*H$_3$acetonide), 22.68 (*C*H$_2$ stearate), 24.80 (*C*H$_2$ stearate), 24.80-26.97 (more signals *C*H$_3$ acetonide), 29.18, 29.27, 29.35, 29.49, 29.69, 31.92, 34.29 (*C*H$_2$ stearate, 7 overlapped), 38.96 (*C core*), 42.05 and 42.15 (*C* D3), 46.96 (*C* D2), 48.08 (*C*D1), 64.05-65.98 (*C*H$_2$O *core* + *C*H$_2$O D1, D2, D3), 98.18 and 98.27 (*C*acetonide), 171.92-174.92 (*C*=O esters). Anal. Calcd. for $C_{117}H_{190}O_{46}$: C, 60.24; H, 8.21. Found: C, 59.88; H, 8.23.

Esterification of 5 with 8 (18)

In a flask flamed under nitrogen, **5** (252 mg, 0.626 mmol), **8** (343.4 mg, 1.97 mmol) and DPTS (110.6 mg, 0.376 mmol) were introduced and dissolved in DCM (10 mL). The clear solution was added with DCC (484.3 mg, 2.35 mmol) by noticing immediately precipitated (DCU) and the suspension was kept under stirring for 24 h at r.t. Then the white suspension was filtered and the solid was washed with DCM (3 x 30 mL). The solution was evaporated under reduced pressure and the residue was taken up with EtOAc (30 mL). The insoluble portion was filtered and washed with EtOAc (3 x 30 mL). The new solution was evaporated to give a spongy residue (618.5 mg) which was purified by chromatography column, isolating the compound of interest **18** in the fractions eluted with petroleum ether/EtOAc 1/1 as colorless resin (353.6 mg, 0.406 mmol). Isolated yield: 64.5%.

FTIR (KBr, cm^{-1}): 2992, 2927, 2856 (CH_3CH_2), 1741 (C=O esters).

^{1}H NMR (300 MHz, $CDCl_3$): δ ppm = 0.88 (t, 3H, *J* = 7.2 Hz, C*H*$_3$ stearate), 1.14 (s, 9H, C*H*$_3$ D1), 1.26 (s, 28H, C*H*$_2$ stearate), 1.35 (s, 9H, C*H*$_3$acetonide), 1.42 (s, 9H, C*H*$_3$acetonide), 1.58 (m, 2H, C*H*$_2$ stearate), 2.32 (t, 2H, *J* = 7.4 Hz, C*H*$_2$C=O stearate), 3.64 (d, 6H, *J* = 11.9 Hz, C*H*$_2$O acetonide), 4.18 (d, 6H, *J* = 11.9 Hz, C*H*$_2$O acetonide), 4.25 (s, 6H, C*H*$_2$O *core*), 4.28 (s, 2H, C*H*$_2$O *core*).

^{13}C NMR (75.5 MHz, $CDCl_3$): δ ppm = 14.13 (*C*H_3 stearate), 18.45 (*C*H_3 D1), 21.59 (*C*H_3 acetonide), 22.71 (*C*H_2 stearate), 25.65 (*C*H_3 acetonide), 29.17-29.72 (*C*H_2 stearate), 31.96 (*C*H_2 stearate), 33.99 (*C*H_2 stearate), 42.26 (C D1), 43.10 (*C core*), 61.90 (*C*H_2O *core*), 66.08 (*C*H_2O D1), 98.18 (*C*acetonide), 173.57 (*C*=O esters). Anal. Calcd. for $C_{47}H_{82}O_{14}$: C, 64.80; H, 9.49. Found: C, 65.01; H, 9.57.

Esterification of 19 with 11 (20)

In a flask flamed under nitrogen, **19** (284.6 mg, 0.39 mmol), **11** (1.08 mg, 2.43 mmol) and DPTS (136.1 mg, 0.46 mmol) were introduced and dissolved in DCM (27 mL) and DMF (1 mL). The clear solution was added with DCC (596.0 mg, 2.89 mmol) by noticing instant precipitation (DCU). The suspension was kept under stirring for 24 h at r.t. then the white suspension was filtered, the solid was washed with DCM (3 x 20 mL) and the resulting solution was evaporated under reduced pressure. The residue was then re-suspended in EtOAc (30 mL) and the insoluble portion was filtered and washed with EtOAc (3 x 20 mL). The new solution was evaporated to give a residue (1.87 mg) which was purified by chromatography column, isolating the compound of interest **20** in the fractions eluted with EtOAc 100% as viscous resin (450.6 mg, 0.136 mmol, 35.3%).

FTIR (KBr, cm^{-1}): 2928, 2856 (CH_3CH_2), 1739 (C=O esters).

^{1}H NMR (300 MHz, $CDCl_3$): δ ppm = 0.88 (t, 3H, *J* = 7.1 Hz, C*H*$_3$ stearate), 1.12 (s, 36H, C*H*$_3$ D3), 1.14 (s, 18H, C*H*$_3$ D2), 1.19 (s, 9H, C*H*$_3$ D1), 1.26 (s, 28H, C*H*$_2$ stearate), 1.36 (s, 36H, C*H*$_3$acetonide), 1.42 (s, 36H, C*H*$_3$acetonide), 1.61 (m, 2H, C*H*$_2$ stearate), 2.33 (t, 2H, *J* = 7.4 Hz, C*H*$_2$C=O stearate), 3.63 (d, 24H, *J* = 11.7 Hz, C*H*$_2$O acetonide), 4.15 (d, 24H, *J* = 11.7 Hz, C*H*$_2$O acetonide), 4.33 (m, 44H, C*H*$_2$O stearate + *core*).

^{13}C NMR (75.5 MHz, $CDCl_3$): δ ppm = 14.13 (*C*H_3 stearate), 17.48 (*C*H_3 D1), 17.72 (*C*H_3 D2), 18.46 (*C*H_3 D3), 21.45-22.22 (more signals, *C*H_3 acetonide), 22.70 (*C*H_2 stearate), 24.87 (*C*H_2 stearate), 25.03-25.76 (more signals, *C*H_3 acetonide), 29.19-30.93 (*C*H_2stearate, some peaks overlapped), 31.94 (*C*H_2 stearate), 34.06 (*C*H_2 stearate), 42.07 (*C* D2), 42.16 (*C* D3), 46.88 and 46.99 (*C* D1), 48.62 (*C core*), 64.90-66.04 (*C*H_2O *core* and *C*H_2O D1, D2), 98.14 and 98.25 (*C*acetonide), 172.33, 173.52 and

173.62 (*C*=O esters). Anal. Calcd. for $C_{164}H_{262}O_{68}$: C, 59.30; H, 7.95. Found: C, 59.70; H, 8.00.

General procedure for the removal of acetonide protections to prepare C-18 polyhydroxylated dendrimers 12, 14, 16, 18 and 20

In a one-neck flask equipped with magnetic stirrer and $CaCl_2$ valve a sample of **12** (172.8 mg, 0.139 mmol) in MeOH (2.6 mL), **14** (95.3 mg, 0.14 mmol) in MeOH (1.5 mL), **16** (225.4 mg, 0.0966 mmol) in MeOH (3.6 mL), **18** (353.6 mg, 0.41 mmol) in MeOH (5.6 mL) or **20** (450.6 mg, 0.136 mmol) in MeOH (11 mL) and Dowex acid resins (one or two spatula) were introduced. The suspensions were kept under stirring for 24 h at r.t. In the case of preparation of **13**, at the end of time, the resins were filtered and washed with MeOH (10 mL). The solution was evaporated under reduced pressure to give a pink oil which was treated with Et_2O to give a white solid which was left in Et_2O extraction for the night. The powdery solid was separated from the solvent by centrifugation at 3500 r.p.m. for ten min, washed with Et_2O and dried under reduced pressure (31.7 mg, DCU) while from the ether phase, after evaporation **13** was obtained. In the other cases the resins were filtered on a silica gel plug (ø = 4 mm, h = 2 cm), washed with MeOH (15-40 mL) and evaporated under reduced pressure to obtain the compounds **15**, **17**, **19** and **21**.

*Second generation C-18 polyhydroxylated dendrimer **13***. Viscous yellow oil (148.0 mg, 0.137 mmol, 98.2%).

FTIR (KBr, cm^{-1}): 3418 (OH), 2927, 2854 (CH_3CH_2), 1733 (C=O esters).

^{1}H NMR (300 MHz, $CDCl_3$): δ ppm = 0.88 (t, 3H, *J* = 7.2 Hz, C*H*$_3$ stearate), 0.97 (s, 3H, C*H*$_3$ *core*), 1.07 (s, 6H, C*H*$_3$D1), 1.25-1.43 (br s, 40H, C*H*$_3$ D2 and C*H*$_2$ stearate), 1.63 (m, 2H, C*H*$_2$ stearate), 2.33 (t, 2H, *J* = 7 Hz, C*H*$_2$C=O stearate), 3.30-4.60 [m, 38H (16H, C*H*$_2$OH D2 + 8H, O*H* + 6H, C*H*$_2$O *core* + 8H, C*H*$_2$O D1)].

^{13}C NMR (75.5 MHz, $CDCl_3$): δ ppm = 14.13 (*C*H$_3$ stearate), 16.83 (CH$_3$ *core*), 17.19 (*C*H$_3$ D2), 18.13 (*C*H$_3$ D1), 22.70 (*C*H$_2$ stearate), 24.97 (*C*H$_2$ stearate), 29.19, 29.28, 29.37, 29.50, 31.93, 34.15 (*C*H$_2$ stearate, 8 overlapped), 40.14 (*C core*), 46.71 (*C* D1), 49.77 (*C* D2), 64.94-67.80 (*C*H$_2$O *core* + *C*H$_2$O D1 + *C*H$_2$OH), 175.11 (*C*=O esters). Anal. Calcd. for $C_{53}H_{94}O_{22}$: C, 58.76; H, 8.75. Found: C, 59.00; H, 9.03.

*First generation C-18 polyhydroxylated dendrimer **15***. Viscous resin (87.0 mg, 0.141 mmol, 100%).

FTIR (KBr, cm^{-1}): 3399 (OH), 2922, 2852 (CH_3CH_2), 1733 (C=O esters).

^{1}H NMR (300 MHz, $CDCl_3$): δ ppm = 0.88 (t, 3H, *J* = 6.9 Hz, C*H*$_3$ stearate), 0.97 (s, 3H, C*H*$_3$ *core*), 1.07 and 1.10 (s, 6H, C*H*$_3$D1), 1.26 (br s, 28H, C*H*$_2$ stearate), 1.63 (m, 2H, C*H*$_2$ stearate), 2.33 (t, 2H, *J* = 8 Hz, C*H*$_2$C=O stearate), 3.80 (m, 8H, *J* = 11 Hz, C*H*$_2$OH D1), 3.90-4.20 (m, 6H, C*H*$_2$O *core*), 4H, O*H*, not detected.

^{13}C NMR (75.5 MHz, $CDCl_3$): δ ppm = 14.12 (*C*H$_3$ stearate), 16.92 (*C*H$_3$ *core*), 17.04 (*C*H$_3$ D1), 22.70 (*C*H$_2$ stearate), 24.94 (*C*H$_2$ stearate), 29.18, 29.28, 29.37, 29.49, 29.68, 29.70, 31.93, 34.19 (*C*H$_2$ stearate, 6 overlapped), 38.96 e 40.10 (*C core*), 49.75 and 49.85 (*C* D1), 65.19 (*C*H$_2$O *core*), 66.93 (*C*H$_2$OH), 173.79, 174.19, 175.28 and 175.60 (*C*=O esters). Anal. Calcd. for $C_{33}H_{62}O_{10}$: C, 64.05; H, 10.10. Found: C, 64.00; H, 10.42.

*Third generation C-18 polyhydroxylated dendrimer **17***. Pink crystalline solid (194.4 mg, 0.097 mmol, 100%).

FTIR (KBr, cm^{-1}): 3419 (OH), 2927, 2855 (CH_3CH_2), 1732 (C=O esters).

^{1}H NMR (300 MHz, DMSO-*d6*): δ ppm = 0.85 (t, 3H, *J* = 7.1 Hz, C*H*$_3$ stearate), 0.96 (s, 3H, C*H*$_3$ *core*), 1.01 and 1.02 (s, 24H, C*H*$_3$ D3), 1.15 and 1.16 (s, 12H, C*H*$_3$ D2), 1.19 (s, 6H, C*H*$_3$ D1), 1.23 (m, 28H, C*H*$_2$ stearate), 1.51 (m, 2H, C*H*$_2$ stearate), 2.30 (t, 2H, *J* = 7 Hz, C*H*$_2$C=O stearate), 3.45 (AA'BB' system, 32H, *J* = 11.9 Hz, C*H*$_2$OH), 3.90-4.20 (m, 30H, C*H*$_2$O *core* + C*H*$_2$O D1, D2), 4.38 (br s, 16H, O*H*).

^{13}C NMR (75.5 MHz, DMSO-*d6*): δ ppm = 13.85 (*C*H$_3$ stearate), 16.63 (*C*H$_3$ *core* + *C*H$_3$ D1, D2, D3), 22.00 (*C*H$_2$ stearate), 24.37 (*C*H$_2$ stearate), 28.61-28.94 (*C*H$_2$ stearate), 31.20 (*C*H$_2$ stearate), 33.26 (*C*H$_2$ stearate), 45.55 (*C* D1), 46.21 (*C* D2), 50.17 (*C* D3), 63.59 (*C*H$_2$OH), 64.56 (*C*H$_2$O D1), 64.78 (*C*H$_2$O D2), 171.73-174.08 (*C*=O esters), (*C* and *C*H$_2$O *core* not detected). Anal. Calcd. for $C_{93}H_{158}O_{46}$: C, 55.51; H, 7.91. Found: C, 55.16; H, 8.23.

*First generation C-18 polyhydroxylated dendrimer **19***. Pink resin (284.6 mg, 0.379 mmol, 95.1%).

FTIR (KBr, cm^{-1}): 3422 (OH), 2920, 2851 (CH_3CH_2), 1733 (C=O esters).

^{1}H NMR (300 MHz, $CDCl_3$): δ ppm = 0.88 (t, 3H, *J* = 6.4 Hz, C*H*$_3$ stearate), 1.12 (s, 9H, C*H*$_3$ D1), 1.26 (s, 28H, C*H*$_2$ stearate), 1.63 (m, 2H, C*H*$_2$ stearate), 2.33 (t, 2H, *J* = 7.6 Hz, C*H*$_2$C=O stearate), 3.69 (m, 12H, C*H*$_2$OH D1), 4.19 (m, 8H, C*H*$_2$O *core*), 6H, O*H*, not detected.

^{13}C NMR (75.5 MHz, $CDCl_3$):δ ppm = 14.13 (*C*H$_3$ stearate), 17.20 (*C*H$_3$ D1), 22.70 (*C*H$_2$ stearate), 24.91 (*C*H$_2$ stearate), 29.17-29.72 (*C*H$_2$ stearate, some signals overlapped), 31.93 (*C*H$_2$ stearate), 34.19 (*C*H$_2$ stearate), 37.13 (*C core*), 49.38 and 49.99

(*C* D1), 65.77-67.64 (*C*H_2O *core* and *C*H_2O D1), 173.64, 173.70, 175.11 and 175.13 (*C*=O esters). Anal. Calcd. for $C_{38}H_{70}O_{14}$: C, 60.78; H, 9.40. Found: C, 61.06; H, 9.23.

*Third generation C-18 polyhydroxylated dendrimer **21***. Glassy pink solid (390.1 mg; 0.136 mmol, 100%).

FTIR (KBr, cm^{-1}): 3404 (OH), 2926, 2854 (CH_3CH_2), 1733 (C=O esters).

^{1}H NMR (300 MHz, $CDCl_3$): δ ppm = 0.81 (t, 3H, *J* = 6.9 Hz, C*H*$_3$ stearate), 0.99 (s, 36H, C*H*$_3$ D3), 1.00 (s, 18H, C*H*$_3$ D2), 1.01 (s, 9H, C*H*$_3$ D1), 1.18-1.24 (s, 28H, C*H*$_2$ stearate), 1.55 (m, 2H, C*H*$_2$ stearate), 2.28 (t, 2H, *J* = 7.4 Hz, C*H*$_2$C=O stearate), 3.61-3.78 (m, 48H, C*H*$_2$OH), 4.10-4.39 (m, 44H, C*H*$_2$O D1, D2 + *core*), 24H, O*H*, not detected.

^{13}C NMR (75.5 MHz, $CDCl_3$):δ ppm = 14.13 (*C*H_3 stearate), 17.13 (*C*H_3 D3), 17.44 (*C*H_3 D1), 18.01 (*C*H_3 D2), 22.69 (*C*H_2 stearate), 24.87 (*C*H_2 stearate), 29.19-29.71 (*C*H_2 stearate, some peaks overlapped), 30.93 (*C*H_2 stearate), 31.93 (*C*H_2 stearate), 42.00 (*C* D1), 46.68 (*C* D2), 49.00 (*C core*), 49.96 (*C* D3), 65.00-67.03 (*C*H_2O *core* and *C*H_2O D1, D2 e *C*H_2OH), 175.01 (*C*=O esters). Anal. Calcd. for $C_{128}H_{214}O_{68}$: C, 54.11; H, 7.59. Found: C, 54.46; H, 7.23.

Esterification of G4OH with $^{\alpha}$N-BOC-$^{\omega'}$N-nitro-L-arginine (22a), $^{\alpha}$N,$^{\varepsilon}$N-di-BOC-L-lysine (22b), $^{\alpha}$N-BOC-sarcosine (22c) and N,N'-dimethylglycine (22d)

Synthesis of N-BOC amino acids 22b and 22c

General Procedure

A solution of the amino acid and base in the proper solvent system was cooled to 0°C and treated with di-*tert*-butylcarbonate (1.1 equiv./amino group). The mixture was left overnight at room temperature under magnetic stirring. The disappearance of amino acid was checked by TLC using EtOAc containing a spatula tip of ninhydrin as the eluent. The mixture was concentrated at reduced pressure to half the volume, cooled to 0°C and acidified with 10% aq. $KHSO_4$ to pH = 2, extracted with EtOAc and dried (Na_2SO_4). The removal of the solvents at reduced pressure afforded the desired BOC protected amino acid.

*$^{\alpha}$N,$^{\varepsilon}$N-di-BOC-L-Lysine (**22b**).* Resin (mixture of rotamers), 93% isolated yield.

FTIR (KBr, cm^{-1}): 3500-2400 (OH), 3374 (NH), 1713 (C=O acid + carbamate), 1529 (NH).

^{1}H NMR (300 MHz, $CDCl_3$,):δ ppm = 1.45 (s, 18H, C*H*$_3$ BOC), 1.30-2.00 (m, 6H, $^{\beta}$C*H*$_2$$^{\gamma}$C*H*$_2$$^{\delta}$C*H*$_2$), 3.11 (m, 2H, $^{\varepsilon}$C*H*$_2$NHBOC), 4.11-4.38 (m, 1H, $^{\alpha}$C*H*NHBOC), 4.70 and 6.30 (m, 1H, $^{\varepsilon}$N*H*), 5.27 (d, *J* = 7.9 Hz, 1H, $^{\alpha}$N*H*), 8.50 (br, 1H, O*H*).

^{13}C NMR (75.5 MHz, $CDCl_3$):δ ppm = 22.42 (*C*H_2), 28.35 (*C*H_3BOC), 28.42 (*C*H_3BOC), 29.45 (*C*H_2), 32.10 (*C*H_2), 40.13 (major) and 41.24 (*C*H_2NH), 53.24 (major) and 54.58 (*C*HNH), 79.34 (major) and 80.86 (*C* BOC), 79.95 (major) and 81.48 (*C* BOC), 155.79 (major) and 156.88 (*C*=O carbamate), 156.33 (major) and 158.16 (*C*=O carbamate), 176.27 (*C*=O acid). NMR data were consistent with those of the literature.

*$^{\alpha}$N-BOC-Sarcosine (**22c**)[2]*.Glassy off white solid (mixture of rotamers),m.p. = 88-90°C.

FTIR (KBr, cm^{-1}): 3500-2400 (OH), 1764 (C=O acid), 1751 (C=O carbamate).

^{1}H NMR (300 MHz, $CDCl_3$): δ ppm = 1.44 and 1.47 (two signals, 9H, C*H*$_3$ BOC), 2.94 (s, 3H, C*H*$_3$N), 3.95 and 4.03 (two signals, 2H, C*H*$_2$N).

^{13}CNMR (300 MHz, $CDCl_3$): δ ppm = 28.25 and 28.32, 35.56 and 35.64, 50.20 and 50.78, 80.67, 155.63 and 156.43, 175.03 and 175.13.NMR data were consistent with those of the literature.

Synthesis of α-bromoacetic acid (23) [225a]

In a two-necked flask equipped with a magnetic stirrer and condenser, AcOH (10.49 g, 0.1750 mmol, 10.0 mL), acetic anhydride (Ac_2O) (2 mL) and anhydrous pyridine (10 μL) were added and brought to boiling. Then the heat source was removed and Br_2 solution (100 μL) was added dropwise. After heating again, further 3.6 mL of Br_2 were added and the solution was kept under stirring and refluxing until became colorless. After cooling water (1 mL) was added. The solution was evaporated to reduced pressure to remove HBr. The residue was subjected to vacuum distillation by collecting **23** in the fractions distillated at 95-97°C (10 Torr) as pale brown oil which solidified cooling to low melting crystals (m.p. = 48°C, lit. [66b]: m.p. = 50°C, 7.85 g, 0.0560 mmol, 32%). Anal. Calcd. For $C_2H_3BrO_2$: C, 17.29; H, 2.18; Br, 57.51%. Found: C, 17.45; H 2.52; Br, 57.16.

FTIR (KBr, cm^{-1}): 3395, 3011 (OH), 2957, 2917, 2856, 2685, 2574, 2484, 1726 (C=O), 1712 899, 875.

^{1}H NMR (300 MHz, $CDCl_3$): δ ppm = 3.98 (s, 2H, C*H*$_2$Br), 10.32 (s, 1H, O*H*).

^{13}C NMR (75.5 MHz, $CDCl_3$): δ ppm = 26.04, 171.88.

Functionalization of G4OH with 23 (24)

In a flask flamed under nitrogen, dendrimer **G4OH** (177.6 mg, 0.0332 mmol) solved in DCM (1.5 mL) and DMF (2.0 mL) was introduced and was added with **23** (46.5 mg, 0.3347 mmol, 20% mol/OH free, 1.05 equiv.) and DPTS (18.6 mg, 0.0631 mmol). Then dicyclohexylcarbodiimide (DCC) (82.2 mg, 0.3984 mmol) solved in DCM (1.5 mL) was added. The total volume of solvent was 5.0 mL. Immediately a precipitated (DCU) was visible and the suspension was kept under stirring for 24 h. At the end of the time the white suspension was filtered, the solid was washed with DCM (15 x 2.0 mL) and the solution was evaporated under reduced pressure to give a residue which was solved with acetone and filtered on a cotton plug to eliminate DCU residual traces. After evaporation an orange resin was obtained. It was submitted to cycles of washing/decantation/separation of solvent using two times petroleum ether and one time petroleum ether/Et_2O 1/1 to remove DMF and small molecules and finally brought to constant weight (262.4 mg). For further purification, the obtained resin was dissolved in acetone again and left to -4°C to promote the precipitation of DPTS residue and the centrifuged. The solvent was evaporated at reduced pressure to provide **24** as pale yellow viscous resin (216.3 mg, 0.0330 mmol, containing 10 bromoacetyl (AcBr) units and 38 residual OH groups as estimated by ^{1}H NMR spectrum, 99%. As reported in results and discussion section, the number of AcBr units of the products obtained varied from preparation to preparation, however, was in the range from 9-11.Anal. Calcd. for$C_{250}H_{382}Br_{10}O_{148}$: C, 45.81; H, 5.87; Br, 12.19%. Found: C, 46.02; H 6.06; Br, 11.96.

FT IR (KBr, cm^{-1}): 3404 (OH), 2931, 2855 (CH_3 and CH_2), 1736 (C=O esters), 1672, 1648, 1565.

^{1}H NMR (300 MHz, $CDCl_3$): δ ppm = 1.08, 1.11, 1.20, 1.26, 1.29, 1.34 and 1.43 (seven signals, 138H, C*H*$_3$G4), 3.67 (m, 76H, C*H*$_2$OH), 3.89 (s, 20H, C*H*$_2$Br), 4.27 [m, 148H (110H, C*H*$_2$O G4, 38H, O*H*)].

Substitution reaction of bromine with N,N'-dimethylamine (25)

In a one-neck flask compound **24** (216.3 mg, 0.0330 mmol) having on the periphery 10 brome acetyl units was solved in acetone (3.0 mL). Separately in a backer, dimethylamine hydrochloride [(20 equiv./AcBr unit), (578.0 mg, 6.6 mmol)] and solid NaOH 1/1 (164.0 mg, 6.6 mmol) were suspended in acetone (2.5 mL). Then some drops of water were added and the suspension was stirred until all the solid disappeared and

the characteristic smell of free amine was perceived. The heterogeneous solution was then transferred to the reaction flask and the clear and odorless solution was left under stirring for 1 h at room temperature then was evaporated at reduced pressure obtaining a solid residue that was solved in chloroform. The organic solution was washed with water (3 x 15 mL) and then dried on $MgSO_4$ dry overnight. After removal of solvent the DMG-modified dendrimer **25** was obtained as white glassy solid (215.5 mg, 0.0329 mmol, containing 10 DMG units and 38 residual OH groups as estimated by ^{1}H NMR spectrum, 99%). Anal. Calcd. for$C_{270}H_{442}N_{10}O_{148}$: C, 52.33; H, 7.19; N, 2.26%. Found: C, 52.65; H 7.16; N, 1.96.

FTIR (KBr, cm^{-1}): 3393 (OH), 2934, 2851 (CH_3 and CH_2), 1737 (C=O esters), 1651, 1626, 1575.

^{1}H NMR (300 MHz, $CDCl_3$): δ ppm = 1.09, 1.11, 1.13, 1.20, 1.26, 1.29, 1.34 and 1.42 (eight signals, 138H, C*H*$_3$G4)], 3.01 (s, 60H, C*H*$_3$NC*H*$_3$ DMG), 3.61-3.89 (m, 76H, C*H*$_2$OH), 4.13 and 4.18 (two broad signals, 20H, C*H*$_2$N DMG), 4.26 [m, 148H (110H, C*H*$_2$O G4 + 38H, O*H*)].

^{13}C NMR, DEPT-135 (75.5 MHz, $CDCl_3$): δ ppm = 17.12-18.39 (*C*H_3 G4), 46.69 (*C*H_3N*C*H_3 DMG), 53.83 (*C*H_2N DMG), 66.04-69.53 (*C*H_2O G4).

Functionalization of 25 with$^{\alpha}$N-BOC-$^{\omega'}$N-nitro-L-arginine (22a), $^{\alpha}$N, $^{\varepsilon}$N-di-BOC-L-lysine (22b) and $^{\alpha}$N-BOC-sarcosine (22c) (26)

In a flask flamed under nitrogen, the DMG-modified dendrimer **25** (102.2 mg, 0.0165 mmol) solved in hot DMF (1 mL) was introduced and was added with **22a** (77.5 mg, 0.2426 mmol), **22b** (84.0 mg, 0.2426 mmol), **22c** (31.4 mg, 0.1658 mmol) and DPTS (36.4 mg, 0.1238 mmol). Then dicyclohexylcarbodiimide (DCC) (160.0 mg, 0.7753 mmol) solved in DCM (3 mL) was added. An additional 1 mL was added and the total volume of solvents was 5 mL. Immediately a precipitated of dicyclohexylurea (DCU) was visible and the suspension was kept under stirring for 24 h. At the end of the time the white suspension was filtered, the solid was washed with DCM (5 x 3 mL). The organic solution was evaporated and the residue solved in EtOAc (20 mL). The separated solid was filtered, washed with EtOAc (3 x 15 mL), the solvent was evaporated to give a glassy solid which was submitted to a silica gel column separation using mixture petroleum ether/EtOAc with increasing gradient of EtOAc and then acetone 100% as eluent collecting compound **26** in the acetone 100% fraction as off white spongy solid (134.0 mg, 0.0777 mmol, containing ten DMG units, eighteen $^{\alpha}$N-BOC-$^{\omega'}$N-nitro-L-arginine units, fifthteen $^{\alpha}$N,$^{\varepsilon}$N-di-BOC-L-lysine units and five $^{\alpha}$N-

BOC-sarcosine units without any OH residual as estimated by ^{1}H NMR spectrum, (74%). Anal. Calcd. For $C_{748}H_{1269}N_{135}O_{328}$: C, 51.63; H, 7.35; N, 10.87%. Found: C, 52.00; H 7.36; N, 10.96.

FTIR (KBr, cm^{-1}): 3364 (NH + OH), 2977, 2931, 2865, 2781 (CH_3 and CH_2), 1740 (C=O esters), 1712 and 1692 (C=O carbamate), 1628 (NH), 1523 (NO_2), 1367 (NO_2).

^{1}H NMR (300 MHz, $CDCl_3$): δ ppm = 1.12, 1.17 and 1.26 (three signals, 138H, C*H*$_3$G4), 1.43 and 1.45 (two signals, 477H, C*H*$_3$BOC), 1.00-2.00 [m, 162H (72H, C*H*$_2$C*H*$_2$Arg + 90H, C*H*$_2$C*H*$_2$C*H*$_2$ Lys)], 2.89, 2.91, 2.93, 2.96, 2.98 and 3.09 [six signals, 75H (60H, C*H*$_3$NC*H*$_3$ DMG + 15H, C*H*$_3$N sarcosine)], 3.00-3.18 (m, 30H, $^{\varepsilon}$C*H*$_2$NHBOC Lys), 3.18-3.54 (br m, 36H, $^{\delta}$C*H*$_2$NH Arg), 3.94, 3.98 and 4.04 (three signals, 10H, C*H*$_2$N sarcosine), 4.11, 4.12 and 4.14 (three signals, 20H, C*H*$_2$N DMG), 4.26 [m, 219H(186H, C*H*$_2$O G4 + 18H, $^{\alpha}$C*H*NHBOC Arg + 15H, $^{\alpha}$C*H*NHBOC Lys), 102H not detected (15H, $^{\alpha}$N*H* Lys, 15H, $^{\varepsilon}$N*H* Lys 36H, $^{\omega}$N*H*$_2$Arg, 18H, $^{\alpha}$N*H* Arg, and 18H, $^{\delta}$N*H* Arg)].

Functionalization of 25 with $^{\alpha}$N-BOC-Sarcosine (22c) (27)

In a flask flamed under nitrogen, a sample of **25** with an estimated DMG content of 9 units and 39 free OH groups (328.8 mg, 0.053 mmol) solved in DCM was introduced and was added with **22c** (100.8 mg, 0.5327 mmol, 26% mol/OH free) and DPTS (29.6 mg, 0.1000 mmol). Then DCC (130.8 mg, 0.6339 mmol) solved in DCM was added. The total volume of solvent was 5.0 mL. Immediately a precipitated (DCU) was visible and the suspension was kept under stirring for 24 h. At the end of the time the white suspension was filtered, the solid was washed with DCM (5 x 5.0 mL), the solvent removed and the residue solved in EtOAc. The separated DPTS/DCU mixture was filtered, washed with EtOAc (5 x 5.0 mL) and the solvent evaporated again. The spongy solid achieved was solved in DCM, washed with water (3 x 15.0 mL) and the organic phase was dried on $MgSO_4$ overnight. Once evaporated at reduced pressure the solvent **27** was obtained as off white spongy solid (205.5 mg, 0.0281 mmol, containing seven DMG units, eight BOC-sarcosine units and 33 residual OH groups as estimated by ^{1}H NMR spectrum, 21%). Anal. Calcd. for$C_{322}H_{525}N_{15}O_{169}$: C, 52.91; H, 7.24; N, 2.87%. Found: C, 53.15; H 7.56; N, 2.96.

FTIR (KBr, cm^{-1}): 3399 (OH), 2977, 2930, 2851 (CH_3 and CH_2), 1736 (C=O esters), 1699 shoulder (C=O carbamate), 1653.

^{1}H NMR (300 MHz, $CDCl_3$): δ ppm = 1.08, 1.11, 1.16, 1.26, 1.29 and 1.35 (six signals, 138H, C*H*$_3$G4), 1.42 and 1.47 (two signals, 72H, C*H*$_3$BOC), 2.93, 2.95 and 2.99 [three signals, 66H (42H, C*H*$_3$NC*H*$_3$ DMG + 24H, C*H*$_3$N sarcosine)], 3.55-3.88 (m, 66H, C*H*$_2$OH), 3.97, 3.99 and 4.04 (three signals, 16H, C*H*$_2$N sarcosine), 4.13 and 4.18 (two signals, 14H, C*H*$_2$N DMG), 4.27[m, 153H (120H, C*H*$_2$O G4 + 33H, O*H*)].

Functionalization of 27 with a mixture $^{\alpha}$N-BOC-$^{\omega'}$N-nitro-L-arginine (22a) and $^{\alpha}$N,$^{\varepsilon}$N-di-BOC-L-lysine (22b)(28)

In a flask flamed under nitrogen, the DMG-BOC-sarcosine modified dendrimer **27** (205.5 mg, 0.0281 mmol) solved in DCM (3 mL) was introduced and was added with **22a** (160.3 mg, 0.5020 mmol), **22b** (173.9 mg, 0.502 mmol) and DPTS (56.1 mg, 0.1905 mmol). Then DCC (246.2 mg, 1.1930 mmol) solved in DCM (4 mL) was added. DMF (1 mL) was also added to obtain a homogeneous solution. Immediately a precipitated (DCU) was visible and the suspension was kept under stirring for 24 h. At the end of the time the white suspension was filtered, the solid was washed with DCM (10 x 3 mL), the solvent evaporated and the residue solved in EtOAc. The separated DPTS/DCU mixture was filtered, washed with EtOAc (3 x 10 mL) and the solvent evaporated again. The spongy solid achieved was suspended in Et_2O and kept under stirring for the night to remove unreacted DCC which was eliminated with ethereal washings. The solid residue was then solved in DCM, the organic phase was washed with water (3 x 15.0 mL) and then dried on $MgSO_4$ overnight. Once evaporated at reduced pressure the solvent **28** was obtained as off white spongy solid (339.7 mg, 0.01953 mmol, containing seven DMG units, eight BOC-sarcosine units, sixteen BOC-lysine and BOC-arginine units and only one residual OH group as estimated by ^{1}H NMR spectrum, 70%). Anal. Calcd. for$C_{754}H_{1277}N_{127}O_{329}$: C, 52.09; H, 7.40; N, 10.23%. Found: C, 52.38; H 7.56; N, 10.36.

FTIR (KBr, cm^{-1}): 3364 (NH + OH), 2978, 2931, 2865, 2785 (CH_3 and CH_2), 1738 (C=O esters), 1712 and 1696 (C=O carbamate), 1628 (NH), 1523 (NO_2), 1367 (NO_2).

^{1}H NMR (300 MHz, $CDCl_3$): δ ppm = 1.00-2.00 [more signals, 298H (138H, C*H*$_3$G4 + 64H, C*H*$_2$C*H*$_2$Arg + 96H, C*H*$_2$C*H*$_2$C*H*$_2$ Lys], 1.42 (s, 504H, C*H*$_3$BOC), 2.89 and 2.96 [two signals, 66H (42H, C*H*$_3$NC*H*$_3$ DMG + 24H, C*H*$_3$N sarcosine)], 3.08 (m, 32H, $^{\varepsilon}$C*H*$_2$NHBOC Lys), 3.20-3.50 (very broad signal, 32H, $^{\delta}$C*H*$_2$NH Arg), 3.62 and 3.64 [two br s, 18H (2H, C*H*$_2$OH + 16H, C*H*$_2$N sarcosine)], 4.12 (s, 14H, C*H*$_2$N DMG), 4.26 [m, 217H (64H, C*H*$_2$O G4 + 16H, $^{\alpha}$C*H*NHBOC Arg + 16H, $^{\alpha}$C*H*NHBOC Lys +

1H, O*H*)], 4.85 (broad singlet, 16H, $^{\alpha}$N*H* Lys), 5.38 (d, 16H, $^{\alpha}$N*H* Arg), 5.60 (very broad singlet 16H, $^{\varepsilon}$N*H* Lys), 7.40-9.00 [broad signals, 48H (16H, $^{\delta}$N*H* Arg + 32H, $^{\omega}$NH_2Arg)].

General procedure for the removal of protecting groups from 26 and 28

In a flask previously flamed under nitrogen the catalyst Pd/C 10% (153.5-339.6 mg) was suspended in MeOH/HCOOH 8.8% (7-15 mL) and then the BOC and nitro protected dendrimer **26** or **28** (0.0088-0.0195 mmol) dissolved in MeOH/HCOOH 8.8% (4-9 mL) was added under agitation. The suspension was kept under stirring for 24h at r.t. Then the catalyst was filtered on a short silica plug and was washed carefully with MeOH (10-20 mL). The obtained solution was evaporated under reduced pressure to obtain the desired product as oil which was solidified with acetone treatments. The compound deprived of NO_2 group and obtained as salt of formic acid was only investigated with FTIR and submitted to reaction for removing BOC groups without further purifications. So, it was solved in MeOH (3-8 mL) and inserted in a one-neck flask equipped with magnetic stirrer and a $CaCl_2$ valve. An excess of acetyl chloride (113-253 μL) was added and the mixture was allowed to stir at r.t. for 24-48 h. The solution was then evaporated under reduced pressure to give a resinous material which was dissolved in MeOH and precipitated in acetone. The precipitate recovered by centrifugation at 3500 rpm for 10 minutes was brought to constant weight, obtaining the desired unprotected cationic dendrimers as hydrochlorides which no longer have carbamate bands in the FTIR spectra.

*Dendrimer **29** (81 HCl)*.Slightly hygroscopic, off white spongy solid (110.3 mg, 0.0077 mmol, 88% overall yield). Anal. Calcd. for$C_{483}H_{944}N_{117}Cl_{81}O_{186}$: C, 40.74; H, 6.68; Cl, 20.17; N, 11.51%. Found: C, 41.11; H 6.56; Cl, 19.96; N, 11.63.

FTIR (KBr, cm^{-1}): 3435 (NH_3^+), 2930, 1739 (C=O esters), 1630 (NH).

^{1}H NMR (300 MHz, DMSO-*d6*): δ ppm =1.00-2.00 [more broad signals, 300H, (138H, CH_3G4 + 90H, CH_2CH_2CH_2 Lys + 72H, CH_2CH_2Arg)], 2.75 (m, 30H, C$H_2^{\varepsilon}NH_3^+$ Lys), 3.10-3.30 (broad signal, 36H,CH_2^{δ}NH Arg), 3.43-3.50 (broad signals, 15H, C$H_3NH_2^+$ sarcosine), 3.74 (s, 60H, (CH_3)$_2$NH$^+$ DMG), 3.99 [m, 33H, C*H*NH_3^+ (18H, Arg + 15H, Lys), 4.10-4.90 [m, 216H (20H, CH_2NH$^+$ DMG + 10H, C$H_2NH_2^+$ sarcosine + 186H, CH_2O G4)], 8.09, 8.24, 8.83 and 9.15 [four broad signals, 254H (54H, NH_3^+Arg + 36H, $^{\omega'}NH_2^+$Arg + 36H, $^{\omega}NH_2$Arg + 18H$^{\delta}$*NH*Arg + 45H, $^{\alpha}NH_3^+$Lys + 45H $^{\varepsilon}NH_3^+$Lys + 10H, NH$^+$ DMG + 10H, NH_2^+ sarcosine)].

*Dendrimer **30** (79 HCl).* Slightly Hygroscopic, off white spongy solid (250.7 mg, 0.01798 mmol, 92% overall yield). Anal. Calcd. for$C_{474}H_{924}N_{111}Cl_{79}O_{185}$: C, 40.84; H, 6.68; Cl, 20.09; N, 11.15%. Found: C, 41.20; H 6.86; Cl, 20.08; N, 10.96.

FTIR (KBr, cm^{-1}): 3431 (NH_3^+ + OH), 2934, 1741 (C=O esters), 1630 (NH).

^{1}H NMR (300 MHz, DMSO-*d6*): δ ppm =1.00-2.00 [more broad signals, 298H, (138H, C*H*$_3$G4 + 96H, C*H*$_2$C*H*$_2$C*H*$_2$ Lys + 64H, C*H*$_2$C*H*$_2$Arg)], 2.76 (m, 32H, C*H*$_2^{\varepsilon}NH_3^+$ Lys), 3.10-3.30 (m, 32H,C*H*$_2^{\delta}$NH Arg), 3.47 (br s, 24H, C*H*$_3NH_2^+$ sarcosine), 3.50 (br s, 2H, C*H*$_2$OH), 3.76 (s, 42H, (C*H*$_3$)$_2NH^+$ DMG), 4.01 (m, 32H, C*H*NH_3^+Arg + Lys), 4.10-4.50 [m, 215H (14H, C*H*$_2NH^+$ DMG + 16H, C*H*$_2NN_2^+$ sarcosine + 184H, C*H*$_2$O G4 + 1H, O*H*)], 8.08, 8.23, 8.81 [three broad signals, 247H (48H, *NH*$_3^+$Arg + 32H, $^{\omega'}$*NH*$_2^+$Arg + 32H, $^{\omega}$*NH*$_2$Arg + 16H$^{\delta}$*NH*Arg + 48H, $^{\alpha}$*NH*$_3^+$Lys + 48H $^{\varepsilon}$*NH*$_3^+$Lys + 7H, NH^+ DMG + 16H, *NH*$_2^+$ sarcosine)].

Preparation of amino acids-modified dendrimers

Typical procedure for esterification reactions of the poly-hydroxylated dendrimer scaffolds.

In a flask flamed under nitrogen the substrates to be functionalized by esterification reactions (**13**, **17**, **21**, **40** or **41**), amino acids (**22a**, **22b**, **22c**) or α-bromoacetic acid (**23**) and DPTS were dissolved in the appropriate solvent. Then to the clear solution, DCC dissolved in DCM, was added and the obtained suspension was kept under stirring for 24 h at r.t.

*Functionalization reactions of **13**, **17** and **21**.*

The solid was filtered and washed with DCM (3 x 5 mL), the obtained solution was evaporated and the residue was re-suspended in EtOAc. The insoluble portion was filtered again and washed with EtOAc. The new solution was evaporated to give a resinous residue.

*Functionalization reactions of **40** and **41**.*

The solid was filtered and washed with DCM (3 x 5 mL). The organic solution was transferred in separator funnel and washed with water (3 x 20 mL) then the water phase was re-extracted with DCM (3 x 20 mL). The organic phases were dried on

$MgSO_4$ overnight and evaporated at reduced pressure to obtain a spongy solid which was treated with petroleum ether to render it dusty and was left stirring overnight. After decanting, the solid was separated from the solvent and dried to constant weight to give hetero dendrimers **41 or 42**.

Synthesis of N,N'-dimethylamine-modified dendrimer 40

In a one-neck flask compound **39** (451.4 mg, 0.1315 mmol) was solved in acetone (6 mL). Separately in a backer, dimethylamine hydrochloride (33 equiv.) and solid NaOH (33 equiv.) were suspended in acetone (15 mL). Then 6/7 drops of water were added and the suspension was stirred until all the solid disappeared and the characteristic smell of free amine was perceived. The solution was then transferred to the reaction flask and the clear and odorless solution was left under stirring for 5h at room temperature then was evaporated at reduced pressure obtaining a solid residue that was solved in chloroform. The organic solution was washed with water three times and then dried on $MgSO_4$ dry overnight. The amphiphilic third generation dendrimer **40** having five peripheral *N,N'*-dimethylglycine (DMG) units and 19 residual OH groups as estimated by ^1H NMR spectrum was obtained as pale yellow glassy solid, (340.7 mg, 0.1047 mmol). Yield = 80%.

General procedure for the removal of protecting groups from 31, 32, 35, 36 and 42.

In a flask previously flamed under nitrogen the catalyst Pd/C 10 % (82-646 mg) was suspended in MeOH/HCOOH 8.8 % (5-30 mL) and then the protected dendrimer **31, 32, 35, 36 or 42** (0.0127-0.0774 mmol) solved in MeOH/HCOOH 8.8 % (3-18 mL) was added under agitation. The suspension was kept under stirring for 24 h at r.t. Then the catalyst was filtered on a silica gel plug and was washed carefully with MeOH (15-35 mL). The obtained solutions were evaporated under reduced pressure to obtain the desired products deprived of NO_2 group and as formic acid salts which were submitted to reaction for removing BOC groups without further purification. Each sample was dissolved in MeOH (3-13 mL) and inserted in a one-neck flask equipped with magnetic stirrer and a $CaCl_2$ valve. An excess of acetyl chloride (41-438 μL) was added and the mixture was allowed to stir at r.t. for 24-48 h. The solutions were then evaporated under reduced pressure to give pink resins which were dissolved in MeOH and precipitated in acetone. The precipitates recovered by centrifugation at 3500 rpm for 10 minutes were brought to constant weight, obtaining the desired unprotected cationic dendrimers as

hydrochloride.

Physical Characterization

Determination of molecular weights of dendrimers

Molecular weights of dendrimers in the form of hydrochlorides were obtained by volumetric titrations with $HClO_4$ in acetic acid (AcOH).

Preparation of titrating solution

To a solution of $HClO_4$ 70% (1.4 mL) in 80 mL of acetic acid (AcOH), 3.0 mL of acetic anhydride (Ac_2O) was added to give a colourless solution which was left stirring at room temperature for one night. The yellow solution was then brought to 100 mL with AcOH and standardized with anhydrous potassium phthalate.

Preparation of the indicator solution

The indicator solution was prepared by dissolving quinaldine red (100.0 mg) in AcOH (50.0 mL).

Preparation of mercury acetate solution

Mercuric acetate (1.5 g) was dissolved in hot AcOH (25 mL). The colourless solution was allowed to cool to room temperature. A sample of the dendrimer (10.0-30.0 mg) was dissolved in AcOH (5.0 mL), treated with 2-4.0 mL of a solution of mercury acetate (1.50 g) in AcOH (25.0 mL), added with a few drops of a solution of quinaldine red (100.0 mg) in AcOH (25.0 mL) and titrated with a standardized 0.17-0.18 N solution of $HClO_4$ in AcOH. The very sharp end points were detected by observing the disappearance of the red colour or its change to yellow and in some case the appearance of a fine white precipitate.

Potentiometric titrations of dendrimers

Potentiometric titrations to determine the buffer capacity [$\beta = dc_{(HCl)}/d(pH)$]and then the average buffer capacity [$\beta_{av} = dV_{(HCl)}/d(pH)(1)$] of dendrimers in the form of hydrochlorides were performed at room temperature. The dendrimer (20-30 mg) was dissolved in Milli-Q water (30.0 mL) then was treated with standard 0.1 N NaOH (1-1.5 mL, pH = 10-12). The clear solution was subjected to potentiometric titration by adding

0.2 mL samples of standard 0.1 N HCl up to total 3.0 mL and measuring the corresponding pH values.

Dynamic light scattering (DLS) and zeta potential

The hydrodynamic size (diameter) of the amino acids-modified dendrimers was measured in batch mode at 25°C in a low volume quartz cuvette (pathlength 10 mm) using a Malvern Zetasizer Nano ZS instrument with back scattering detector (173°, 633 nm laser wavelength). Dendrimer samples were prepared at a concentration of 1 mg/mL in PBS and filtered through a 0.02 μm filter. A minimum of twelve measurements per sample were made. Hydrodynamic size is reported as the intensity-weighted average (Int-Peak). The Zeta Potential was measured at 25°C in deionized water. An applied voltage of 100 V was used. Samples were loaded into pre-rinsed folded capillary cells and a minimum of twelve measurements were made per sample.

***"In vitro"* toxicity evaluation**

Cell culture

B14 cells (Cricetulus griseus, ATCC, CCL- 14.1, Sigma-Aldrich Inc.) were grown in High glucose DMEM medium with 10% (v/v) fetal bovine serum (FBS) and 4 mM glutamine; BRL 3A (Rattus norvegicus, ATCC, CRL-1442, Sigma-Aldrich Inc.) in Ham's F12 medium with 10% (v/v) FBS and 2 mM glutamine, all media were supplemented with 0.1% (w/v) penicillin and 0.1% (w/v) streptomycin. The cells were maintained in culture flasks in a 37° C humidified atmosphere of 5% CO_2/95% air (incubator) and passaged every 2–3 days. Cells were harvested and used in experiments after obtaining 80–90% confluence. The number of viable cells was determined by trypan blue exclusion on a haemocytometer. Then cells were suspended in media in a concentration of 1.0 x 10^{-5} cells per mL and plated in flat bottom 96-well plates. Plates with cells were incubated 24 h at a 37° C in a humidified atmosphere of 5% CO_2 to allow adherence of the cells before the administration of dendrimers.

MTT assay

Cytotoxicity of dendrimers was assayed with MTT (3-(4, 5-dimethylthiazol-2-yl)-2,5-diphenyltetrazoliumbromide). After 24 h incubation when cells attached on 96-well plates they were treated with concentration range from 0.5 to 20 μM dendrimers. After 24 h incubation, a 20 μL solution of MTT in PBS (5 mg/mL) was added to each well. Four hours later the medium was removed and the formazan precipitate dissolved

in DMSO for absorbance measurement at 580 nm and reference 700 nm. The cell viability (%) was related to the control wells containing untreated cells with fresh cell culture medium and was calculated according to the following:

Cell viability (%) = absorption test / absorption control ×100%. All dates are presented as the mean of three measurements (± SD).

Preparation of G4 and G5 Dendriplexes 50-55

General procedure

A solution of dendrimers **44-49**[205] (N= 58-136) in dry MeOH (2.0 mg/mL) was added with the UOA mixture (9 equiv.). The solution was kept under vigorous magnetic stirring at room temperature for 72 h in the dark. Then after removal of the solvent at reduced pressure the obtained white solids were suspended in DCM for a night to wash away the free UOA. After decanting the solid, dichloromethane was separated and evaporated to obtain a white solid which by IR analysis appeared to be the UOA mixture not complexed by dendrimers. The solid was brought to constant weight and then dissolved in MeOH/H_2O and precipitated in acetone in a centrifuge tube. After two cycles of centrifugation (3400 rpm) and washings with acetone, the wet solids were brought to dry and constant weight under reduced pressure and then stored on P_2O_5 in a dryer.

Complex G4[Arg(36)OH(12)UOA(6)] ***(50)***

Slightly hygroscopic yellowish glassy solid [6 units of UOA mixture per dendrimer mol (51.4 mg, 0.0031mmol, yield: 90%). FTIR (KBr): 3411 (OH and NH_3^+), 1742 (C=O ester), 1662 (NH). ^{1}H-NMR (300 MHz, CD_3OD,δ, ppm): 0.75-0.97 [several s, 132H, C$\underline{H}_3$ and $\underline{H}$ (C(5)) of triterpenoids], 1.07-2.38 [m, 414H (C$\underline{H}_3$ofdendrimer + C$\underline{H}_2$C$\underline{H}_2$Arg + C$\underline{H}$ and C$\underline{H}_2$ of triterpenoids)], 3.20-3.40 (m, 72H, C$\underline{H}_2$NH Arg), 3.85 (br, 24H, C$\underline{H}_2$OH), 4.05-4.62 [m, 198H (C$\underline{H}_2$O of dendrimer + C$\underline{H}$$NH_3^+$ Arg)], 5.22 (m, 6H, C$\underline{H}$ of triterpenoids), the signals for two C$\underline{H}$ of triterpenoids (12 H) are undetectable while the signal for one C$\underline{H}$ is hidden under solvent peak.

Complex G4[ArgGly(29)OH(19)UOA(7)] ***(51)***

Slightly hygroscopic yellowish glassy solid [7 units of UOA mixture per dendrimer mol (12.5 mg, 0.00074mmol, yield: 46%). FTIR (KBr): 3431 (OH and NH_3^+), 1747 (C=O ester), 1637 (NH). ^{1}H-NMR (300 MHz, CD_3OD, δ, ppm): 0.74-0.99 [several s, 154H, C$\underline{H}_3$ and $\underline{H}$ (C(5)) of triterpenoids], 1.11-2.37 [m, 408H (C$\underline{H}_3$ofdendrimer + C$\underline{H}_2$C$\underline{H}_2$Arg + C$\underline{H}$ and C$\underline{H}_2$ of triterpenoids)], 2.85 (m, 7H, C$\underline{H}$ of triterpenoids), 3.15 (m, 7H, C$\underline{H}$ of triterpenoids), 3.20-3.40 (m, 58H, C$\underline{H}_2$NH Arg), 3.64 (br t, 38H, C$\underline{H}_2$OH), 3.90-4.40 [m, 235H (C$\underline{H}_2$O of dendrimer + C$\underline{H}$$NH_3^+$ Arg + C$\underline{H}_2$NH Gly)], 5.22 (q, 7H, C$\underline{H}$ of triterpenoids), the signal for one C$\underline{H}$ of triterpenoids (7 H) is hidden under solvent peak.

Complex G4[Arg(16)Lys(19)OH(13)UOA(4)] ***(52)***

Slightly hygroscopic off white glassy solid [4 units of UOA mixture per dendrimer mol (27.0 mg, 0.0018mmol, yield: 90%).FTIR (KBr): 3431 (OH and NH_3^+), 1747 (C=O ester), 1631 (NH). ^{1}H-NMR (300 MHz, CD_3OD, δ, ppm): 0.78-0.99 [several s, 88H, C$\underline{H}_3$ and $\underline{H}$ (C(5)) of triterpenoids], 1.00-2.40 [m, 404H (C$\underline{H}_3$ofdendrimer + C$\underline{H}_2$C$\underline{H}_2$Arg + C$\underline{H}_2$C$\underline{H}_2$C$\underline{H}_2$Lys + C$\underline{H}$ and C$\underline{H}_2$ of triterpenoids)], 2.94-3.17 [m, 46H (C$\underline{H}_2$$NH_3^+$ Lys + C$\underline{H}$ of triterpenoids)], 3.30-3.50 (m, 32H, C$\underline{H}_2$NH Arg), 3.54-3.82 (m, 26H, C$\underline{H}_2$OH) 4.10-4.50 [m, 195H (C$\underline{H}_2$O of dendrimer + C$\underline{H}$$NH_3^+$ Lys + C$\underline{H}$$NH_3^+$ Arg)], 4.59-4.71 (dd, 4H, C$\underline{H}$ of triterpenoids), 5.22 (q, 4H, C$\underline{H}$ of triterpenoids).

Complex G5[Arg(66)OH(30)UOA(3)] ***(53)***

Slightly hygroscopic off white fluffy solid [3 units of UOA mixture per dendrimer mol (44.2 mg, 0.0016mmol, yield: 100%). FTIR (KBr): 3392 (OH and NH_3^+), 1743 (C=O ester), 1663 (NH).^{1}H-NMR (300 MHz, CD_3OD, δ, ppm): 0.78-0.97 [several s, 66H, C$\underline{H}_3$ and $\underline{H}$ (C(5)) of triterpenoids], 1.00-2.30 [m, 612H (C$\underline{H}_3$ofdendrimer + C$\underline{H}_2$C$\underline{H}_2$Arg + C$\underline{H}$ and C$\underline{H}_2$ of triterpenoids)], 3.27 (m, 132H, C$\underline{H}_2$NH Arg), 3.68-3.74 (br, 60H, C$\underline{H}_2$OH), 4.04-4.63 [m, 384H (C$\underline{H}_2$O of dendrimer + C$\underline{H}$$NH_3^+$ Arg)], 5.22 (q, 3H, C$\underline{H}$ of triterpenoids), the signals for two C$\underline{H}$ of triterpenoids (6 H) are undetectable while the signal for one C$\underline{H}$ is hidden under solvent peak.

Complex G5[ArgGly(52)OH(44)UOA(12)] ***(54)***

Slightly hygroscopic off white fluffy solid [12 units of UOA mixture per dendrimer mol (16.1 mg, 0.00051mmol, yield: 57%). FTIR (KBr): 3431 (OH and NH_3^+), 1739 (C=O ester), 1637 (NH). ^{1}H-NMR (300 MHz, CD_3OD/DMSO-d_6, δ, ppm):

0.76-0.99 [several s, 264 H, C$\underline{H}_3$ and $\underline{H}$ (C(5)) of triterpenoids], 1.10-2.36 [m, 754H (C$\underline{H}_3$ofdendrimer + C$\underline{H}_2$C$\underline{H}_2$Arg + C$\underline{H}$ and C$\underline{H}_2$ of triterpenoids)], 2.83 (m, 12H, C$\underline{H}$ of triterpenoids), 3.12 (m, 12H, C$\underline{H}$ of triterpenoids), 3.31 (m, 104H, C$\underline{H}_2$NH Arg), 3.62 (m, 88H, C$\underline{H}_2$OH), 3.90-4.40 [m, 461H (C$\underline{H}_2$O of dendrimer + C$\underline{H}$NH$_3^+$ Arg + C$\underline{H}_2$NH Gly)], 5.22 (q, 12H, C$\underline{H}$ of triterpenoids), the signal for one C$\underline{H}$ of triterpenoids (12 H) is hidden under solvent peak.

Complex G5[Arg(38)Lys(30)OH(28)UOA(8)] ***(55)***

Slightly hygroscopic pale yellow fluffy solid [8 units of UOA mixture per dendrimer mol (20.5 mg, 0.00070mmol, yield: 64%).FTIR (KBr): 3431 (OH and NH_3^+), 1747 (C=O ester), 1635 (NH). ^{1}H-NMR (300 MHz, CD_3OD, δ, ppm): 0.75-0.98 [several s, 176 H, seven C$\underline{H}_3$ and $\underline{H}$ (C(5)) of triterpenoids], 1.00-2.40 [m, 790 H (C$\underline{H}_3$of dendrimer + C$\underline{H}_2$C$\underline{H}_2$Arg + C$\underline{H}_2$C$\underline{H}_2$C$\underline{H}_2$Lys + C$\underline{H}$ and C$\underline{H}_2$ of triterpenoids)], 2.95-3.16 [m, 76H (C$\underline{H}_2$NH$_3^+$ Lys + C$\underline{H}$ of triterpenoids)], 3.38 (m, 76H, C$\underline{H}_2$NH Arg), 3.68 (m, 56H, C$\underline{H}_2$OH), 4.10-4.50 [m, 390 H (C$\underline{H}_2$O of dendrimer + C$\underline{H}$NH$_3^+$ Lys + C$\underline{H}$NH$_3^+$ Arg)], 4.58-4.70 (dd, 8H, C$\underline{H}$ of triterpenoids), 5.22 (q, 8H, C$\underline{H}$ of triterpenoids).

Physical characterization

Potentiometric Titrations of Dendriplexes 50-55

Potentiometric titrations to determine the buffer capacity [$\beta = dc_{(HCl)}/d(pH)$] and then the average buffer capacity [$\overline{\beta} = dV_{(HCl)}/d(pH)(1)$] of dendriplexes in the form of hydrochlorides were performed at room temperature with a Hanna Microprocessor Bench pH Meter. The dendrimer (20-30 mg) was dissolved in Milli-Q water (30 mL) then was treated with standard 0.1 N NaOH (1-1.5 mL, pH = 10-12). The solution was potentiometrically titrated by adding 0.2 mL samples of standard 0.1 N HCl up to total 3.0 mL and measuring the corresponding pH values.

Dynamic Light Scattering (DLS) and Zeta potential

The hydrodynamic size (diameter) of all dendriplexes prepared was measured in batch mode at 25°C in a low volume quartz cuvette (pathlength 10 mm) using a Malvern Zetasizer Nano ZS instrument with back scattering detector (173°, 633 nm laser wavelength). Dendriplexes samples were prepared at a concentration of 1 mg/mL

in PBS and filtered through a 0.02 μm filter. A minimum of twelve measurements per sample were made. Z average diameter, derived from a cumulants analysis of the measured correlation curve, is reported as the intensity-weighted average (Int-Peak) hydrodynamic radius. The Zeta Potential was measured at 25°C in deionized water. An applied voltage of 100 V was used. Samples were loaded into pre-rinsed folded capillary cells and a minimum of twelve measurements were made per sample.

"*In Vitro*" Ursolic and Oleanolic Acids Release from Dendriplexes 50-55

The "*in vitro*" release behavior of the mixture UOA from dendriplexes **50-55** was evaluated performing the dialysis bag diffusion technique using 20% ethanol in phosphate buffer saline (PBS) as dissolution medium. The dialysis bags (MWCO = 3.5kDa) were pre-swelled in milli-Q water for 12 h before use.

A sample of each dendriplex 50-55 (10 mg) was dissolved in 1 mL of 0.1 mol/L PBS (pH = 7.4) containing 20% of ethanol. Each obtained solution was placed into a dialysis bag and both ends were sealed. Then each bag was individually immersed in a beaker containing 100 mL of 0.1 mol/L PBS (pH = 7.4) and ethanol (20%). In parallel, a release study of free UA and OA mixture from the dialysis bag was performed under the same condition. The mixture (1 mg) was suspended in 1 mL of 0.1 mol/L PBS and ethanol (60%) and placed in a dialysis bag which was immersed in a beaker containing 100mL of 0.1 mol/L PBS (pH = 7.4) and ethanol (20%). The dialysis was carried out at 37°C, and the quantity of drugs released was analysed by HPLC as described in the following paragraph at various time points (1, 2, 5, 24 and 48 h) during the dialysis process.

HPLC Analysis

A Shimadzu LC-2010 C system equipped with a UV detector was used to perform the analyses of UOA mixture concentration. For the separation of drugs a Hypersil C_{18} column (5 μm particle size, 150 mm x 4.6 mm) was used. Mobile phase was composed of methanol and water (90/10, V/V). The flow rate was set at 1 mL/min and temperature at 25°C. The UV absorbance was determined at 210 nm. The concentration of the UA and OA mixture released was analysed on the bases of a free UOA calibration curve.

CONCLUSIONS

The aim of the research topic of this thesis was to design and synthesize amphiphilic hydrophilic not PAMAM dendrimers nanocarriers for biomedical applications. So in the first part,versatile and reliable protocols for the step-wise synthesis of five amino acids-modified amphiphilic dendrimers characterized by having hydrolysable neutral inner scaffolds of the ester-type already adopted by us but as novelty it was also built on a tetra functional *core* and in addition, a C-18 hydrocarbon chain directly linked to the *core* molecules was combined. This new feature resulted in a more favourable Hydrophilic-Lipophilic Balance (HLB) that it is known to promote an easier cross over of the biological membranes to soften the crown cationic nature, to reduce cytotoxicity levels and to confer a higher drug loading capacity (DL%). The preliminary cytotoxicity tests showed that these new C18-equipped dendrimers are significantly less toxic than others that do not contain the hydrocarbon chain and much less cytotoxic than PEI25K. The peripheral amino acids appropriately selected contribute to a proper and not too marked cationic character necessary for tha interaction with genetic materials, drugs, negative charged membrane lipids and for an appropriate buffer capacity. A third generation amphiphilic hetero dendrimer, which thanks to an assortment of four different peripheral amino, includes two kinds of primary amino groups, secondary and tertiary and the precious guanidine residue, has been successfully obtained.

In the second part,six dendrimer-based prodrugs were synthesized for the safe and effective administration of a mixture of two triterpenoid acids extracted and isolated from Salvia Corrugata Vahl. They were achieved by a physical incorporation of the triterpenoid acids which were successfully complexed by polycationic polyester-based amino acids modified dendrimers thanks to electrostatic and hydrogen bond interactions. These prepared hydrophilic complexes are water soluble thus allowing the incorporated UA and OA mixture to be well dispersed in water with an obviously better bioavailability and an increased pharmacokinetic. They have a peripheral polycationic character due to the presence of amino acids including arginine, which is well known promote interactions with membrane lipids for enhances cellular uptake. The obtained dendriplexes embody all the prerogatives to be considered as new attractive, promising and versatile DDSs.

REFERENCES

1. W. C. Zamboni, V. Torchilin, A. K. Patri, J. Hrkach, S. Stern, R. Lee, A. Nel, N. J. Panaro, and P. Grodzinski, *Clin.Cancer Res.*, **2012**; *18 (12)*, 3229-3241.
2. S. Bamrungsap, Z. Zhao, T. Chen, L. Wang, C. Li, T. Fu, and W. Tan, *Nanomedicine (Lond)*, **2012**; *7 (8)*, 1253-1271.
3. P. Couvreur, C. Vauthier, *Pharm. Res.*, **2006**; *23(7)*, 1417-1450.
4. T. L. Doane, C. Burda, *Chem. Soc. Rev.* **2012**; *41 (7)*, 2885-2911.
5. X. Ma, H. Yu, *J. Biol. Med.*, **2006**; *79 (3-4)*, 85-94.
6. A. Gupta, P. Avci, M. Sadasivam, R. Chandran, N. Parizotto, D. Vecchio, W. C. de Melo, T. Dai, L. Y. Chiang, M. R. Hamblin, *Biotechnol. Adv.*, **2012**; *31 (5)*, 607-631.
7. A. Juarranz, P. Jaen, F. Sanz-Rodriguez, J. Cuevas, S. Gonzalez, *Clin. Transl. Oncol.*, **2008**; *10 (3)*, 148-154.
8. J. R. Heath, M. E. Davis, *Annu. Rev. Med.*, **2008**; *59*, 251-265.
9. K. K. Jain, *BMC. Med,*. **2010**; *8*, 83.
10. Z. Gao, L. Zhang, Y. Sun, *J.Control Release* **2012**; *162(1)*, 45-55.
11. N. T. Huynh, E. Roger, N. Lautram, J. P. Benoit, C. Passirani, *Nanomedicine (Lond)*, **2010**; *5 (9)*, 1415-1433.
12. C. L. Waite, C. M. Roth, *Crit. Rev. Biomed. Eng.*, **2012**; *40 (1)*, 21-41.
13. M. Wang, M. Thanou, Pharmacol. Res., **2010**; *62 (2)*, 90-99.
14. S. E. Gratton, P. A. Ropp, P. D. Pohlhaus, J. C. Luft, V. J. Madden, M. E. Napier, J. M. Desimone, *Proc. Natl. Acad. Sci. U.S.A*, **2008**; *105 (33)*, 11613-11618.
15. Q. Mu, G. Jiang, et al., *Chem. Rev.*, **2014**; *114 (15)*, 7740-7781
16. R. Prado-Gotor, E. Grueso, *Phys. Chem.*, **2011**; *13 (4)*, 1479-1489.
17. H.S. Park, S.H. Nam, et al., *Sci. Rep.*, **2016**; *6*, 27407.
18. J. McMillan, E. Batrakova, et al., *Prog. Mol. Biol. Transl.*, **2011**; *104*, 563-601.
19. C. Buzea, I.I. Pacheco, et al., *Biointerphases*, **2007**; *2 (4)*, MR17-71.
20. C. Bantz, O. Koshkina, et al., R. Zellner, *ed. Beilstein J. Nanotechnol.*, **2014**; *5*, 1774-1786.
21. R. Khanbabaie, M. Jahanshahi, *Curr. Neuropharmacol.*, **2012**; *10 (4)*, 370-392.
22. G.H. Son, B.J. Lee, et al., *J. Pharmaceut. Invest.*, **2017**; https://doi.org/10.1007/s40005-017-0320-1.
23. S. Mura, J. Nicolas, et al., *Nat. Mater.*, **2013**; *12*, 991-1003.
24. J. Siepmann, A. Göpferich, *Adv. Drug Deliv. Rev.*, **2001**; *48 (2-3)*, 229-247.
25. S. Khatak, H. Dureja, *Recent patents on Nanotechnology*, **2015**; *9*, 150.
26. W. Mehnert, K. Mäder, *Adv. Drug Deliv. Rev.*, **2012**; *47 (2-3)*, 165-196.
27. R.H. Müller, K. Mäder, S. Gohla, *European J. Pharmaceutics and Biopharmaceutics*, **2000**; *50 (1)*, 161-177
28. A. Zeb, O.S. Qureshi, H.S. Kim, et al., *J. Pharm. Pharmacol.*, **2017**; *69 (8)*, 955-966.
29. R.H. Müller, M. Radtke, S.A. Wissing, *Int. J. Pharm.*, **2002**; *242*, 121-128.
30. O.S. Qureshi, H.S. Kim, A. Zeb, et al., *J. Microencapsul.*, **2017**; *34 (3)*, 250-261.
31. L. Battaglia, M. Gallarate, E. Peira, et al., *J. Pharm. Sci.*, **2014**; *103 (7)*, 2157-2165.

32. H. Yuan, J. Miao, Y-Z. Du, J. You, F-Q. Hu, S. Zeng, *Int. J. Pharm.*, **2008**; *348 (1-2)*,137-145.
33. D. Kakkar, S. Dumoga, R. Kumar, K. Chuttani, A.K. Mishra, *Med. Chem. Commun.*, **2015**; *6 (8)*, 1452-1463.
34. M.N. Patel, S. Lakkadwala, M.S. Majrad, et al., *AAPS Pharm. Scitech.*, **2014**; *15 (6)*, 1498-1508.
35. M. Uner, G. Yener, *Int. J. Nanomedecine*, **2007**; 2, 289-300
36. R.H. Müller, C.M. Keck, *J. Biotechnol.*, **2004**; *113*, 151-170
37. H. Khodabandehloo, et al., *Iran J. Cancer Prev.*, **2016**; *9 (2)*:e3966
38. A.S. Vanniasinghe, V. Bender, N. Monolios, *Semin. Artritis Reum.*, 2009; 39, 182-196.
39. A. Himanshu, P. Sitasharan, A.K. Singhai, *IJPLS*, **2011**; *2 (7)*, 945-951.
40. U. Bulbake, S. Doppalapudi, N. Kommineni, W. Khan, Pharmaceutics **2017**; *9 (2)* doi: 10.3390/pharmaceutics9020012.
41. J.P. Rao, K.E. Geckerler, *Prog. Polym. Sci.*, **2011**; *36 (7)*, 887-913.
42. S. Bamrungsap, Z. Zhao, T. Chen, et al., *Nanomedecine*, **2012**; *7 (8)*, 1253-1271.
43. V. Sanna, N. Pala, M. Sechi, *International Journal of Nanomedecine*, **2014**; *9*, 467-483.
44. M. Rawat, D. Singh, S. Saraf, *Biol. Pharm. Bull.*, **2006**; *29 (9)*, 1790-1798.
45. N.S. Rejinold, K.P. Chennazhi, S.V. Nair, H. Tamura, R. Jayakumar, *Carbohydr. Polym.*, **2011**; *83*, 776-786.
46. A. Martinem, I. Iglesias, R. Lozano, J.M. Teijon, M.D. Blanco, *Carbohydr. Polym.*, **2011**; *83*, 1311-1321.
47. G.K. Saraog, P. Gupta, U.D. Gupta, N.K. Jain, G.P. Agrawal, *Int. J. Pharm.*, **2010**; *385*, 143-149.
48. X. Wang, Y. Wang, Z.G. Chen, D.M. Shin, *Cancer Res. Treat.*, **2009**; *41 (1)*, 1-11.
49. F. Kratz, *J. Control Release*, **2008**; *132 (3)*, 171-183.
50. M.J. Hawkins, P. Soon-shiong, N. Desai, *Adv. Drug Deliv. Rev.*, **2008**; *60 (8)*, 876-885.
51. B. Brissault, A. Kichler, C. Guis, C. Leborgne, O. Danos, H. Cheradame, *Bio- conjugate Chem.*, **2003**, *14*, 581-7.

52. G.D. Jones, A. Langsjoen, M.M.C. Neumann, J. Zomlefer, *J. Org. Chem.*, **1944**, *9*, 125-47.

53. M. Neu, D. Fischer, T. Kissel, *J. Gene Med.*, **2005**, *7*, 992-1009.

54. K. Luby-Phelps, P.E. Castle, D.L. Taylor, F. Lanni, *Proc. Natl. Acad. Sci. U.S.A.*, **1987**, *84*, 4910-3.
55. J. Suh, H.J. Paik, B.W. Hwang, *Bioorganic Chemistry*, **1994**, *22*, 318-27.

56. I. M. Klotz, A. R. Sloniewsky, *Biochem. Biophys. Res. Commun.*, **1968**, *31*, 421-6.
57. W. T. Godbey, K. K. Wu, A. G. Mikos, *J. Biomed. Mater. Res.*, **1999**, *45*, 268- 275.
58. D. Fischer, Y. Li, B. Ahlemeyer, J. Krieglstein, T. Kissel, *Biomaterials*, **2003**, *24*, 1121-1131.

59. D. Fischer, T. Bieber, Y. Li, H. P. Elsasser, T. Kissel, *Pharm. Res.*, **1999**, *16*, 1273-1279.
60. D. Goula, C. Benoist, S. Mantero, G. Merlo, G. Levi, B. A. Demeneix, *Gene Ther.*, **1998**, *5*, 1291-1295.
61. S. M. Zou, P. Erbacher, J. S. Remy, J. P. Behr, *J. Gene Med.*, **2000**, *2*, 128-134.

62. L. Wightman, R. Kircheis, V. Rossler, S. Carotta, R. Ruzicka, M. Kursa, E. Wagner, *J. Gene Med.,* **2001**, *3,* 362-72.
63. H. Lv, S. Zhang, B. Wang, S.Cui, J. Yan, *J .Control. Rel.,* **2006**, *114,* 100-109.

64. Y. H. Kim, J. H. Park, M. Lee, Y. H. Kim, T. G. Park, S. W. Kim, *J. Control. Rel.,* **2005**, *103,* 209-219.
65. S. Han, R. I. Mahato, S. W. Kim, *Bioconj. Chem.,* **2001**; *12,* 337-345.
66. U. Kedar, P. Phutane, S. Shidhaye, V. Kadam, *Nanomedecine ,* **2010**; 6, 714-729.
67. A. Gothwal, Khan, U. Gupta, *Pharm. Res.,* **2016**; *33 (1),* 18-39.
68. G. Riess, *Prog. Polym. Sci.,* **2003**; *28,* 1107-1170.
69. Y. Zhang, T. Jing, R.X. Zhuo, *Colloids Surf B Biointerfaces,* **2005**; *44 (2-3),* 104-109.
70. H. Uchino, Y. Matsumura, T. Negishi et al., *Br. J. Cancer,* **2005**; *93 (6),* 678-687.
71. L. Zhang, Y. He, G. Ma, C. Song, H. Sun, *Nanomedecine,* **2012**; *8 (6),* 925-34.

72. Y. Li, P. Li, M. Jin, C. Jiang, Z. Gao, *Int. J. Mol. Sci.,* **2014**; *15 (12),* 23571-88.

73. D. Kim, ES Lee, KT Oh, ZG Gao, YH Bae, *Small,* **2008**; *4 (11),* 2043-50.

74. S. Svenson, *Dendrimers Kirk-Othmer Encyclopedia of Chemical Technology, fifth ed.* **2007**, *26,* 786-812.

75. S. Svenson, D.A. Tomalia , *Adv. Drug Deliv.,* **2005**; *57,* 2106-2129.

76. E. R. Gillies, J.M.J. Fréchet, *Drug Discov. Today,* **2005** ; *10,* 35-42.

77. D.A. Tomalia, *Prog. Polym. Sci.,* **2005**; *30,* 294-324.

78. U. Gupta, H.B. Agashe, A. Asthana, N.K. Jain, *Biomacromol.,* **2006**; *7,* 649-658.

79. Y. Cheng, J. Wang, T. Rao, X. He, T. Xu, *Front. Biosci.,* **2008**; *13,* 1447-1471.

80. Y. Li, Y. Cheng, T. Xu, *Curr. Drug Discov. Technol.,* **2007**; *4,* 246-254.
81. D. G. Shcharbin, B. Klajnert, M. Bryszewska, *Biochemistry (Moscow),* **2009**;

74, 1070-1079.

82. D. A. Tomalia, H. Baker, J. Dewald, M. Hall, G. Kallos, S. Martin, J. Roeck, J. Ryder, P. Smith, *Polym. J.,* **1985**; *17,* 117–32.
83. J. Haensler, F. C. Szoka Jr., *Bioconjugate Chem,* **1993**; *4,* 372–9.

84. J. F. Kukowska-Latallo, A. U. Bielinska, J. Johnson, R. Spindler, D. A. Tomalia, J. R. Baker Jr., *Proc. Natl. Acad. Sci. U.S.A.,* **1996**; *93,* 4897–4902.
85. A. U. Bielinska, C. Chen, J. Johnson, J. R. Baker Jr., *Bioconjugate Chem,* **1999**; *10,* 843–850.
86. T. Sato, T. Ishii, Y. Okahata, *Biomaterials,* **2001**; *22,* 2075–2080.

87. J. H. Lee, Y. B. Lim, J. S. Choi, Y. Lee, T. I. Kim, H. J. Kim, J. K. Yoon, K. Kim, J. S. Park, *Bioconjugate Chem.,* **2003**; *14,* 1214–1221.
88. T. I. Kim, H. J. Seo, J. S. Choi, H. S. Jang, J. Baek, K. Kim, J. S. Park, *Biomacromolecules,* **2004**; *5,* 2487–2492.
89. M. Tang, C. T. Redemann, F. C. Szoka Jr., *Bioconjugate Chem.,* **1996**; *7,* 703– 714.
90. J. S. Choi, K. Nam, J. Y. Park, J. B. Kim, J. K. Lee, J. S. Park, *J. Controlled Re lease,* **2004**; *99,* 445–456.

91. T. I. Kim, J. U. Baek, J. K. Yoon, J. S. Choi, K. Kim, J. S. Park, *Bioconjugate Chem.*, **2007**; *18*, 309–317.
92. K. Kono, H. Akiyama, T. Takahashi, T. Takagishi, A. Harada, *Bioconjugate Chem.*, **2005**; *16*, 208–214.
93. D. Luo, K. Haverstick, N. Belcheva, E. Han, W. M. Saltzman, *Macromolecules,*

2002; *35*, 3456-3462.

94. Zhang Xue-Quing, Wang Xu-Li, Huang Shi-Wen, Zhuo Ren-Xi, Liu Zhi-Lan, Mao Hai-Quan, K. W. Leong, *Biomacromolecules*, **2005**, *6*, 341-350.

95. Yanming Wang, Weiling Kong, Yu Song, Yajun Duan, Lianyong Wang, G. Steinhoff, Deling Kong, Yaoting Yu, *Biomacromolecules*, **2009**, *10*, 617-622.
96. H. Yoo, R. L. Juliano, *Nucleic Acids Res.*, **2000**; *28*, 4225–4231.
97. L. M. Shewaye, T. Hsieh-Chih, *Colloids and sufaces B:Biointerfaces,* **2015**;

135, 253-260.

98. L. M. Shewave, A. D. Tilahun, C. Hsiao-Ying, T. Hsien-Chih, *The J. of Physical Chem.B,* **2016**; *120*, 123-130.
99. J. F. Kukowska-Latallo, K. A. Candido, Z. Y. Cao, S. S. Nigavekar, I. J. Ma- joros, T. P. Thomas, L. P. Balogh, M. K. Khan, J. R. Baker, *Cancer Res.*, **2005**; *65*, 5317.
100. I. J. Majoros, T. P. Thomas, C. B. Metha, J. R. Baker, *J. Med. Chem.*, **2005**, *48*, 5892.
101. Y. Zhang, T. P. Thomas, K. H. Lee, M. Li, H. Zong, A. M. Desai, A. Kotlyar,

B. Huang, M. M. Banaszak Holl, J. R. Baker Jr., *Biorg. And Med. Chem.,* **2011**,

19, 2557-2564.

102. G. Yu, L. Zhihong, X. Xiaodong, W. Chaoqun, Y. Jiali, M. Fan, J. Biyu, C. Jianzhong, S. Jingwei, C. Haijun, J. Lee, *European J. of Pharm. Science*, **2015**; *70*, 55-63.
103. H. Zong, D. Shah, C. Selwa, R. E. Tsuchida, R. Rattan, J. Mohan, B. A. Stein, J.

B. Otis, S. N. Goonewardena, *Chemistry Open*, **2015**; *4*, 335-341.

104. E. Buhleier, W. Wehner, F. Voegtle, *Synthesis*, **1978**; *155*, 8.

105. V. A. Kabanov, V. G. Sergeyev, O. A. Pyshkina, A. A. Zinchenko, A. B. Zezin,

J. G. H. Joosten, J. Brackman, K. Yoshikawa, *Macromolecules*, **2000**; *33*, 9587– 9593.

106. R. G. Denkewalter, J. Kolc, W. J. Lukasavage, *U.S. Patent,* **1981**; *4*, *289*, 872.

107. R. G. Denkewalter, J. Kolc, W. J. Lukasavage, *U.S. Patent,* **1981**; *4*, *289*, 872.

108. P. L. Hermonat, J. G. Quirk, B. M. Bishop, L. Han, *FEBS Lett.*, **1997**, *407*, 78-84.
109. M. Arruebo, R. Fernandez-Pachero, M.R. Ibarra, J. Santamaria, *NanoToday*, **2007**; *2*, 22-32.
110. T. Neuberger, B. Schopf, H. Hofmann, M. Hofmann, B. Von Rechenberg, *J. M.M. M.*, **2005**; 293, 483-496.
111. A.K. Bajpai, R. Gupta, *J. Mater Sci. Mater Med.*, **2011**; *22*, 357-369
112. Q. Tong, H. Li, W. Li, H. Chen, X. Shu, X. Lu, G. Wang, *J. Nanosci Nanotechnol.*, **2011**;

11, 3651-3658
113. B. Gaibre, M.S. Khil, D.R. Lee, H.Y. Kim, *Int. J. Pharm.,* **2009**; *365*, 180-189.
114. J.L. Arias, M. Lopez-Viota, A.V. Delgado, M.A. Ruiz, *Colloids Surf. B. Biointerfaces,* **2010**; *77*, 111-116.
115. M.Y. Hua, H.W. Yang, C.K. Chuang, R. Y. Tsai, W.J. Chen et al., *Biomaterials,* **2010**; *31*, 7355-7363.

116. Z.P. Xu, Q.H. Zeng, G.Q. Lu, A. Yu, *Chem. Engin. Sci.,* **2006**; *61(3)*, 1027-40.

117. P.Ma, H. Xiao, C. Li, Y. Dai, Z. Cheng, Z. Hou, J. Lin, *Materials Today,* **2015**; *18 (10)*, 554-564.

118. D. Dhamecha, S. Jalalpure, Kiran et al., *Pharmacological Research,* **2016** ; *113 (part A)*, 547-556.

119. Z. Xing, Z. Liu, Y. Zu, Y. Fu, *Applied Surface Science,* **2010**; *256 (12)*, 3917-3920.

120. M.A. Safwat, G.M. Soliman, D. Sayed, M.A. Attia, *Int. J. Pharm.,* **2016**; *513 (1-2)*, 648-658.
121. M. Singh et al., *Nanomedecine: Nanotechnology, Biology and Medecine,* **2015**; *11 (8)*, 2083-2098.

122. J.C. Echeverria, J. Estella, V. Barbaria, J. Musgo, J.J. Garrido, *J. Non-Cryst. Solids,* **2010**; *356*, 378-382.

123. A. Fidalgo, T.M. Lopez, L.M. Ilharco, *J. Sol-Gel Sci. Technol,* **2009**; *49*, 320-328.

124. M. Prokopowicz, *J. Sol-Gel Sci Technol.,* **2010**; *53*, 525-533.

125. K. Czarnobaj, J. Lukasiak, *J. Mater Sci Mate Med,* **2007**; *18*, 2041-2044.

126. K. Czarnobaj, W. Sawicki, *Pharm. Dev. Technol.,* **2011**; (doi: 10.3109/10837450.2011.572894).

127. U. Maver, A. Godec, M. Bele, O. Planinsek, M. Gaberscek, S. Srcic, J. Jamnik, *Int. J. Pharm.,* **2007**; *330*, 164-174.

128. K. Czarnobaj, J. Czarnobaj, *J. Biomed. Mater. Res. B Appl. Biomater,* **2008**; *87*, 114-120.

129. M.S. Ahola, E.S. Sailynoja, M.H. Raitavuo, M.M. Vaahtio, J.I. Salonen, A.U. Yli-Urpo, *Biomaterials,* **2001**; *22*, 2163-2170.

130. I.I. Slowing, J.L. Vivero-Escoto, C-W. Wu, V.S. Lin, *Adv. Drug Deliv. Rev.,* **2008**; *60 (11)*, 1278-1288.

131. Y. Li, N. Li, W. Pan, Z. Yu, L. Yang, B. Tang, *ACS Appl. Mater. Interfaces,* **2017**; *9 (3),* 2123-2129.

132. Y. Wang, Q. Zhao, N. Han, et al., *Nanomedecine,* **2015** ; *11 (2),* 313-327.

133. L. Wei, N. Hu, Y. Zhang, *Materials,* **2010**; *3*, 4066-4079.

134. Q. He, Y. Gao, L. Zhang, Z. Zhang, F. Gao, X. Ji, Y. Li, J. Shi, *Biomaterials,* **2011**; *32*, 7711-7720.

135. Z. Li, K. Su, B. Cheng, Y. Deng, *J. Colloid Interface Sci,* **2010**; **342**, 607-613.

136. R.F. Popovici, E.M. Seftel, G.D. Mihai, E. Popovici, V.A. Voicu, *J. Pharm. Sci.*, **2011**; *100*, 704-714.

137. S. Iijima, *Nature,* **1991**; *354 (6348)*, 56-58.

138. A. Bianco, *Expert Opin. Drug Deliv.,* **2004**; *1 (1),* 57-65.

139. P.A. Martins-Júnior , C.E. Alcântara, R.R. Resende, A.J. Ferreira, *J. Dent. Res.*, **2013**; *92 (7)*, 575-583.

140. S.Y. Madani, N. Naderi, O. Dissanayake, A. Tan, A.M. Seifalian, *Int. J. Nanomedecine,* **2011**; *6,* 2963-2979.

141. C.M. Ng, H-S. Loh, K. Muthoosamy, N. Sridewi, S. Manickam, *Int. J. Nanomedecine,* **2016**; *11*, 1607-1614.

142. E. Pérez-Herrero, A. Fernandez-Medarde, *Eur. J. Pharm. Biopharm.*, **2015** ; *93*, 52-79.

143. S. Vardharajula, S.Z. Ali, P.M. Tiwari, et al., *Int. J. Nanomedecine,* **2012**; *7*, 5361-5374.

144. K. Shiba, M. Yudasaka, S. Iijima, *Nihon Rinsho,* **2006**; *64*, 239-246.

145. M. Manchester, P. Singh, *Adv. Drug Deliv. Rev.*, **2006**; *58 (14)*, 1505-1522.

146. K.Cho, X. Wang, S. Nie, Z. Chen, D. M-Shin, *Clinical Cancer Research,* **2008**; *14 (5),* doi: 10.1158/1078-0432.

147. P. Singh, D. Prasuhn, R.M. Yeh, et al., *J. Control Release,* **2007**; *120 (1-2)*, 41-50.

148. Y. Ma, R.J. Nolte, J.J. Cornelissen, *Adv. Drug Deliv. Rev.*, **2012**; *64 (9)*, 811-825.

149. J.K. Pokorski, N.F. Steinmetz, *Mol. Pharm.,* **2011**; *8 (1),* 29-43.

150. J. Cao, R.H. Guenther, T.L. Sit, C.H. Opperman, S.A.Lommel, J.A. Willoughby, *Small.*, **2014**; *10 (24)*, 5126-5136.

151. S. Honarbakhsh, R.H. Guenther, J.A. Willougby, S.A. Lommel, B. Pourdeyhimi, *Adv. Healthc. Mater.*, **2013**; *2 (7)*, 1001-1007.

152. F. Danhier, O. Feron, V. Preat, *Journal of Controlled Release*, **2010**; *148 (2)*, 135-146.

153. H. Maeda, *Adv. Enzyme Regul.*, **2001**; *41*, 189-207.

154. V. Torchilin, *Adv. Drug Deliv. Rev.*, **2011**; *63 (3)*, 131-135.

155. H. F. Dvorak, J. A. Nagy, J. T. Dvorak, and A. M. Dvorak, *Am. J. Pathol.*, **1988**; *1*, 133.

156. J. A. Nagy, A. M. Dvorak, and H. F. Dvorak, *Cold Spring Harb.Perspect.Med.*, **2012**; *2*, 2.

157. H. Pelicano, D.S. Martin, R.H. Xu, P. Huang, *Oncogene*, **2006**; *25*, 4633-46.

158. M.B.Yatvin, W. Kreutz, B.A. Horwitz, M. Shinitzky, *Science*, **1980**; *210*, 1253-5.

159. T. Sun, Y.S. Zhang, B. Pang, D.C. Hyun, M. Yang, Y. Xia, *Angew Chem. Int. Ed.*, **2014**; *53 (46)*, 12320-12364.

160. Y. Patil, T. Sadhukha, L. Ma, J. Panyam, *J. Control Release*, **2009**; *136 (1)*, 21-29.

161. P.P. Deshpande, S. Biswas, V.P. Torchilin, *Nanomedecine*, **2013**; *8 (9)*, 1509-1528.

162. T.M. Allen, *Nat. Rev. Cancer*, **2002**; *2 (10)*, 750-763.

163. K.F. Pirollo, E.H. Chang, *Trends Biotechnol.*, **2008**; *26 (10)*, 552-558.

164. G. Tiwari, R. Tiwari, B. Sriwastawa, L. Bhati, S. Pandey, P. Pandey, S. K. Bannerjee, *Int. J. Pharm. Investig.*, **2012**; *2 (1)*, 2-11.

165. L.M. Ensign, R. Cone, J. Hanes, *Adv. Drug Deliv. Rev.*, **2012**; *64*, 557-570.

166. N. Gulati, H. Gupta, *Recent Pat. Drug Deliv. Formul.*, **2011**; *5 (2)*, 133-45.

167. C. Tissot, M. Beghetti, *Vasc. Health Risk Manag.*, **2009**; 5, 325-331.

168. M. R. Prausnitz, R. Langer, *Nat. Biotechnol.*, **2008** ; *26 (11)*, 1261-1268.

169. M. V. Walter, M. Malkoch, *Chem. Soc. Rev.*, **2012**; *41*, 4593–4609.

170. A. Carlmark, E. Malström, M. Malkoch, *Chem. Soc. Rev.*, **2013**, *42*, 5858-5879.

171. N. Feliu, M. V. Walter, M. I. Montañez, A. Kunzmann, A. Hult, A. Nyström,

M. Malkoch, B. Fadeel, *Biomaterials,* **2012**; *33*, 1970-1981.

172. H. Ihre, O. L. P. De Jesus, J. M. J. Fréchet, *J. Am. Chem. Soc.,* **2001**; *123*, 5908– 5917.
173. M. Malkoch, E. Malmström, A. Hult, *Macromolecules,* **2002**; *35,* 8307–8314.

174. C. J. Hawker, J. M. J. Fréchet, *J. Am. Chem. Soc.*, **1990**; *112*, 7638–7647.

175. Ihre et al, *J. Am. Chem. Soc.,* **1996**; *118,* 6388-6395.

176. K. L. Wooley, C. J. Hawker, J. M. J. Fréchet, *Angew. Chem., Int. Ed. Engl.*,

1994; *33*, 82–85.

177. Z. F. Xu, M. Kahr, K. L. Walker, C. L. Wilkins, J. S. Moore, *J. Am. Chem. Soc.,*

1994;*116*, 4537–4550.

178. H. Ihre, A. Hult, J. M. J. Fréchet, I. Gitsov, *Macromolecules,* **1998**; *31*, 4061- 4068.
179. H. C. Kolb, M. G. Finn, K. B. Sharpless, *Angew. Chem., Int. Ed.,* **2001**; *40*, 2004–2021.
180. P. Wu, A. K. Feldman, A. K. Nugent, C. J. Hawker, A. Scheel, B. Voit, J. Pyun,

J. M. J. Fréchet, K. B. Sharpless, V. V. Fokin, *Angew. Chem. Int. Ed.,* **2004**; *43*, 3928–3932.

181. P. Antoni, D. Nyström, C. J. Hawker, A. Hult, M. Malkoch, *Chem. Commun.,*

2007; 2249-2251.

182. A. Carlmark, A. C. Hawker, B. A. Hulta, M. Malkoch, *Chem. Soc. Rev.,* **2009**;

38, 352-362.

183. E. R. Gillies, J. M. J. Fréchet, *J. Am. Chem. Soc.,* **2002**; *124*, 14137-14146.

184. A. P. Goodwin, S. S. Lam, J. M. J. Fréchet, *J. Am. Chem. Soc.,* **2007**, *129*, 6994-6995.
185. I. Gitsov, K. L. Wooley, J. M. J. Fréchet, *Angew. Chem*., **1992**, *104*, 1282–1285 (see also *Angew. Chem., Int. Ed. Engl.*, **1992**, *1231* , 1200-1282).
186. I. Gitsov, K. L. Wooley, C. J. Hawker, J. M. J. Fréchet, *Polym. Prepr.,* **1991**,

32, 631-632.

187. I. Gitsov, K. L. Wooley, C. J. Hawker, P. T. Ivanova, J. M. J. Fréchet, *Macro- molecules,* **1993**, *26,* 5621-5627.
188. A. Wuersch, M. Moeller, T. Glauser, L. S. Lim, S. B. Voytek, J. L. Hedrick, C.

W. Frank, J. G. Hilborn, *Macromolecules,* **2001**, *34*, 6601-6615.

189. T. Glauser, C. M. Stancik, M. Moeller, S. Voytek, A. P. Gast, J. L. Hedrick,

Macromolecules, **2002**, *35*, 5774-5781.

190. L. A. Connal, R. Vestberg, C. J. Hawker, G. G. Qiao, *Adv. Funct. Mater.*, **2008**, *18*, 3706-3714.

191. P. Lundberg, M. V. Walter, M. I. Montanez, D. Hult, A. Hult, A. Nyström, M.Malkoch,

Polym. Chem., **2011**, *2*, 394-402.
192. L. Jianfeng, J. Xutao, G. Yubo, A. Sai, K. Yuyang, Ma. Haojun, H. Xi, J. Chen, *Bioconjugate Chem*., **2015**, *26*, 418-426
193. A. Zhang, L. Shu, Z. Bo, A. D. Schlüter, *Macromol. Chem. Phys*., **2003**, *204*, 328–339.
194. M. Trollsas, J. L. Hedrick, D. Mecerreyes, P. Dubois, R. Jerome, H. Ihre, A. Hult, *Macromolecules,* **1997**, *30*, 8508-8511.
195. B. Atthoff, M. Trollsås, H. Claesson J. L. Hedrick, *Macromol. Chem. Phys*., **1999**, *200*, 1333-1339.
196. X. Zeng, Y. Zhang, Z. Wu, P. Lundberg, M. Malkoch, A. M. Nyström, *J.Polym. Sci.*, Part A: *Polym. Chem*., **2011**, *50*, 280-288.
197. H. Altin, I. Kosif, R. Sanyal, *Macromolecules*, **2010**, *43*, 3801-3808.
198. M. I. Montanez, Y. Hed, S. Utsel, J. Ropponen, E. Malmström, L. Wagberg, A. Hult, M. Malkoch, *Biomacromolecules,* **2011**, *12*, 2114-2125.
199. P. Liu, *Surf. Rev. Lett.*, **2005**, *12*, 619-622.
200. P. Liu, *Appl. Clay Sci*., **2007**, *35*, 11-16.
201. P. Liu, L. Zhang, *Surf. Rev. Lett*., **2007**, *14*, 1025-1032.
202. R. B. Soumya, L. Liu, H. Sheardown, A. Adronov, *Macromolecules,* **2008**, *41*, 2567-2576.
203. R.B. Soumya, H. Sheardown, A. Adronov, *Macromolecules,* **2008**, *41*, 4817- 4823.
204. S. Alfei, S. Castellaro, G. B. Taptue, *Org. Commun.,* **2017**, *10*, 144-177.
205. S. Alfei, S. Castellaro, *Macromol. Res.*, **2017**, *25(12)*, 1172-1186.
206. I. Nakase, H. Akita, K. Kogure, A. Gräslund, U. Langel, H. Harashima, S. Futaki, *Efficient Acc. Chem. Res.*, **2012**, *45*, 1132-1139.
207. I. Nakase, G. Tanaka, S. Futaki, *Mol. BioSyst.*, **2013**, *9*, 855-861.
208. C. Liu,X. Liu, P. Rocchi, F. Qu, J. L. Iovanna, L. Peng, *Bioconj. Chem.,* **2014**, *25*, 521-532.
209. X. Liu, C. Liu, J. Zhou, C. Chen, and F. Qu, J. J. Rossi, P. Rocchi, L. Peng, *Nanoscale,* **2015**, *7*, 3867-3875.
210. J. B. Kim, J. S. Choi, K. Nam, M. Lee, J. S. Park, J. K. Lee, *J. Control Release*, **2006**, *114*, 110-117.
211. T. Kim, C. Z. Bai, K. Nam, J. Park, *J. Control Release*, **2009**, *136*, 132-139.
212. A. Smith, P. Nobmann, G. Henehan, P. Bourke, J. Dunne, *Carbohydrate Research,* **2008**, *343*, 2557-2566.
213. E. C. Gleeson, Z. J. Wang, W. R. Jackson, A. J. Robinson, *J. Org. Chem.,* **2015**, *80*, 7205-7211.
214. Y. Chen, D. Cun, P. Quan, X. Liu, W. Guo, L. Peng, L. Fang, *Pharm. Research,* **2014**, *31*, 1907-1918.
215. M. R. Rodriguez, *J. of Carbohydrate Chem.,* **2005**, *24*, 41-54.
216. M. T. Richer, C. Paquot, *Oleagineux (Paris)*, **1969**, *24*, 413-416.

217. J. C. Dyke, K. J. Knight, H. Z.hou, C. K. Chiu, C. C. Ko, W. You, *J. Mater. Chem*., **2012**, *22*, 22888-22898.
218. B. F. Stimmel, C. G. King, *J. of Am. Chem. Soc*., **1934**, *56*, 1724-1725.

219. J. C. Dyke, K. J. Knight, H. Z.hou, C. K. Chiu, C. C. Ko, W. You, *J. Mater. Chem*., **2012**, *22*, 22888-22898.

220. B. F. Stimmel, C. G. King, *J. of Am. Chem. Soc*., **1934**, *56*, 1724-1725.

221. J. Moore, S. I. Stupp, *Macromolecules,* **1990**, *23*, 65-70.

222. W. Liang, J.K.W. Lam, *Molecular Regulation of Endocytosis. Dr. Brian Ceresa (Ed)* **2012**, 429-456

223. C. Sunshine, D.Y. Peng, J.J. Green, *Mol. Pharm.,* **2012**; *9*, 3375

224. B. Zhang, X. Ma, M. Sui, et al., *Chin. J. Polym. Sci.,* **2015**; *33*, 908

225. a) S. Natelson, S. Gottfried, Organic Synth., **1943**; *23*, 37. b) T.J. Logan, K.R. Hill, N.W. Standish, *J. Org. Chem.,* **1960**; *25*,1312.

226. L. Tasic, R.J. Abraham, R. Rittner, *Magn. Reson. Chem.,* **2002**; *40*, 449-454

227. A.I. Vogel, Of Amines (including quaternary ammonium salts), in *Elementary Practical Organic Chemistry. Part III. Quantitative Organic Analysis,* ed by Longman, London, **1958**, 702.

228. Y. Kim, S.C. Zimmerman, *Curr. Opin. Chem. Biol.,* **1998**, *2*, 733-742.

229. J.M. Benns, J.S. Choi, R.I. Mahato, J.S. Park, S.W. Kim, *Bioconj. Chem.,* **2000**; *11*, 637.

230. S.Y. Gwang, M.B. Yun, C. Hye, K. Bokyung, S.C. Insung, S.C. Joon, *Bioconj. Chem.*, **2011**; *22*, 1046.
231. N. Heigl, S. Bachmann, C. H. Petter, M. Marchetti-Deschmann, G. Allmaier, G. K. Bonn,

C. W. Huck, *Anal. Chem.,* **2009**; *81*, 5655.

232. Y. Zeng, Y. Kurokawa, T. T. Win-Shwe, Q. Zeng, S. Hirano, Z. Zhang, H. Sone, *J.*

Toxicol. Sci., **2016**; *41*, 351.

233. M.A. Dobrovolskaia, A. K. Patri, J. Simak, J. B. Hall, J. Semberova, S. H. De Paoli

Lacerda, S. E. McNeil, Nanoparticle size and surface charge determine effects of PAMAM

dendrimers on human platelets in vitro. *Molecular Pharmaceutics,* **2012**, *9*, 382-393.

234. T. Strasak, J. Maly, D. Wrobel, M. Maly, R. Herma, J. Cermak, M. Mullerova, et al., *RSC*

Adv., **2017**; *7*, 18724.

235. S.Shi, C.F. Guo, B. Kan, S.Z. Fu, X.H. Wang, et al., *BMC Biotechnology,* **2009**; *9*, 1.

236. A. Bisio, G. Romussi, E. Russo, S. Cafaggi, A.M. Schito, B. Repetto, N. De Tommasi, *J. Agric. Food Chem.,* **2008**, *56*, 10468-10472.

237. L. Fernandez, *J. Supramol. Chem.,* **2006**, *18*, 633-643.

238. M. Santo, M.A. Fox, *Phys. Org. Chem.,* **1999**, *12*, 293-307.

239. Y. Cheng, Z. Xu, M. Ma, T. Xu, *J. Pharm. Sci.,* **2008**, 97, 123-143.

240. O.M. Milhem, C. Myles, N.B. Mckeown, D. Atwood, A. D'Emanuele, *Int. J. Pharm.,* **2000**, *197*, 239-241.

241. P. Kolhe, E. Misra, R.M. Kannan, S. Kannan, M. Lieh- Lai, *Int. J. Pharm.,* **2003**; 259, 143-160.

242. L.J. Twyman, A. E. Beezer, R. Esfand, M.J. Hardy, J.C. Mitchell, *Tetrahedron Lett.,* **1999**, *40*, 1743-1746.

243. Y. Gao, Z. Li, X. Xie, C. Wang, J. You, F. Mo, B. Jin, J. Chen, J. Shao, et al., *Eur. J. Pharm. Sci.,* **2015**; *70*, 55-63.

244. W. Seebacher, N. Simic, R. Weis, R. Saf, O. Kunert, *Magn. Reson. Chem.* **2003**; *41*, 636-638.

245. F.Von Seel, in "Grundlagen der analyischen Chemie, Vol. 82", ed. By G. Geier, *Verlarg Chemie, Weinheim,* **1970**, 962.

246. L. Aravindran, K.A. Bicknell, G. Brooks, V.V. Khutoryanskiya, A.C.Williams, *Int. J. Pharm.,* 2009; 378, 201-210

247. J.Q. Wang, W.W.Mao, L.L. Lock, J.B. Tang, M.H. Sui, W.L. Sun, et al., *ACS Nano.,* **2015**; *9*, 7195-7206

248. H.Yu, Z.Cui, P. Yu, C. Guo, B. Feng, et al., *Adv. Funct. Mater.,* **2015**, *25*, 2489-2500.